INTERNATIONAL REVIEW OF CELL AND MOLECULAR BIOLOGY

Front Cover Photography: Oleg L. Serov, Natalia M. Matveeva and Anna A. Khabarova

Academic Press is an imprint of Elsevier
525 B Street, Suite 1900, San Diego, CA 92101-4495, USA
225 Wyman Street, Waltham, MA 02451, USA
32 Jamestown Road, London NW1 7BY, UK
Radarweg 29, PO Box 211, 1000 AE Amsterdam, The Netherlands

First edition 2011

British Library Cataloguing in Publication Data
A catalogue record for this book is available from the British Library

Library of Congress Cataloging-in-Publication Data
A catalog record for this book is available from the Library of Congress

For information on all Academic Press publications
visit our website at elsevierdirect.com

ISBN: 978-0-12-386035-4

PRINTED AND BOUND IN USA
11 12 13 14 10 9 8 7 6 5 4 3 2 1

Contributors

Jürgen Bernhagen
Institute of Biochemistry and Molecular Cell Biology, RWTH Aachen University, Aachen, Germany

Richard Bucala
Department of Medicine, Yale University School of Medicine, New Haven, Connecticut, USA

Gerrit Grieb
Department of Medicine, Yale University School of Medicine, New Haven, Connecticut, USA; Institute of Biochemistry and Molecular Cell Biology; and Department of Plastic Surgery and Hand Surgery, Burn Center, Medical Faculty, RWTH Aachen University, Aachen, Germany

Soichi Inagaki
Graduate School of Biological Sciences, Nara Institute of Science and Technology, Takayama, Ikoma, Nara, Japan

Yukihiro Kabeya
Center for Frontier Research, National Institute of Genetics, Yata, Mishima, Shizuoka, Japan

Anna A. Khabarova
Institute of Cytology and Genetics, Academy of Sciences of Russia, Siberian Branch, Novosibirsk, Russia

Akira Kikuchi
Department of Biochemistry, Graduate School of Medicine, Osaka University, Osaka, Japan

Tatjana Kleine
Lehrstuhl für Molekularbiologie der Pflanzen, Department Biologie I, Ludwig-Maximilians-Universität München (LMU), Planegg-Martinsried, Germany

Dario Leister
Lehrstuhl für Molekularbiologie der Pflanzen, Department Biologie I, Ludwig-Maximilians-Universität München (LMU), Planegg-Martinsried, Germany

Shinji Matsumoto
Department of Biochemistry, Graduate School of Medicine, Osaka University, Osaka, Japan

Natalia M. Matveeva
Institute of Cytology and Genetics, Academy of Sciences of Russia, Siberian Branch, Novosibirsk, Russia

Shin-ya Miyagishima
Center for Frontier Research, National Institute of Genetics, Yata, Mishima, Shizuoka, Japan

Hiromitsu Nakanishi
Satellite Venture Business Laboratory, Shinshu University, Tokida, Ueda, Nagano, Japan

Norbert Pallua
Department of Plastic Surgery and Hand Surgery, Burn Center, Medical Faculty, RWTH Aachen University, Aachen, Germany

Akira Sato
Department of Biochemistry, Graduate School of Medicine, Osaka University, Osaka, Japan

Oleg L. Serov
Institute of Cytology and Genetics, Academy of Sciences of Russia, Siberian Branch, Novosibirsk, Russia

Guy Steffens
Institute of Biochemistry and Molecular Cell Biology, RWTH Aachen University, Aachen, Germany

Piero A. Temussi
Department of Chemistry, Universita di Napoli Federico II, via Cinthia, Napoli, Italy; and National Institute for Medical Research, The Ridgeway, London, United Kingdom

Masaaki Umeda
Graduate School of Biological Sciences, Nara Institute of Science and Technology, Takayama, Ikoma, Nara, Japan

Hideki Yamamoto
Department of Biochemistry, Graduate School of Medicine, Osaka University, Osaka, Japan

CHAPTER ONE

Circulating Fibrocytes—Biology and Mechanisms in Wound Healing and Scar Formation

Gerrit Grieb,[*,†,‡] Guy Steffens,[†] Norbert Pallua,[‡] Jürgen Bernhagen,[†] *and* Richard Bucala[*]

Contents

Abstract

Fibrocytes were first described in 1994 as fibroblast-like, peripheral blood cells. These bone marrow-derived mesenchymal progenitor cells migrate into regions of tissue injury. They are unique in their expression of hematopoietic and monocyte lineage markers and extracellular matrix proteins. Several studies have focused on the specific role of fibrocytes in the process of wound repair and tissue regeneration. We discuss herein the biology and mechanistic action of fibrocytes in wound healing, scar formation, and maintenance of tissue integrity. Fibrocytes synthesize and secrete different cytokines, chemokines, and growth factors, providing a wound milieu that supports tissue repair.

* Department of Medicine, Yale University School of Medicine, New Haven, Connecticut, USA
† Institute of Biochemistry and Molecular Cell Biology, RWTH Aachen University, Aachen, Germany
‡ Department of Plastic Surgery and Hand Surgery, Burn Center, Medical Faculty, RWTH Aachen University, Aachen, Germany

International Review of Cell and Molecular Biology, Volume 291
ISSN 1937-6448, DOI: 10.1016/B978-0-12-386035-4.00001-X

They further promote angiogenesis and contribute to wound closure via pathways involving specific cytokines, leukocyte-specific protein-1, serum amyloid P, and adenosine A_{2A} receptors. Fibrocytes are involved in inflammatory fibrotic processes in such diseases as systemic fibrosis, atherosclerosis, asthma, hypertrophic scarring, and keloid formation. Accumulating literature has emphasized the important role of fibrocytes in wound healing and fibrosis. Detailed mechanisms nevertheless remain to be investigated to elucidate the full therapeutic potential of fibrocytes in the treatment of fibrosing disorders and the enhancement of tissue repair.

Key Words: Fibrocytes, Wound healing, Scar formation, Hypertrophic scarring, Keloid.

1. Introduction

Fibrocytes were first described in 1994 as fibroblast-like, peripheral blood cells that migrate into regions of tissue injury (Bucala et al., 1994). There is now a wealth of data about fibrocyte biology, indicating that these cells are involved in inflammatory fibrotic processes occurring in diseases such as systemic fibrosis, atherosclerosis, airway remodeling in asthma, interstitial pulmonary fibrosis, the stromal response to tumor invasion, hypertrophic scarring, and keloid formation (Bucala, 2007; Bellini and Mattoli, 2007). Fibrocytes secrete a unique complement of cytokines and chemokines that differs from that of monocytes, macrophages, T lymphocytes, dendritic cells, fibroblasts, and endothelial cells (Pilling et al., 2009). They express different fibroblast proteins such as vimentin, collagen I and III, fibronectin, the hematopoietic stem cell marker (CD34), and the leukocyte common antigen (CD45) (Bucala et al., 1994). Further, fibrocytes exhibit cytoplasmic extensions that are intermediate in size between classical pseudopodia and microvilli (Bucala et al., 1994). Approximately 0.5% of nonerythrocytic cells in the peripheral blood are fibrocytes, and in culture, they can differentiate from $CD14^+$ cells into a phenotype with wound-healing potential. It was demonstrated that fibrocytes are able to migrate to wounds in response to secondary lymphoid chemokine (SLC), which is a ligand for the chemokine receptor CCR7 (Abe et al., 2001). Additional chemokine receptors on the fibrocyte cell surface also have been identified, such as CCR3, CCR5, CCR7, and CXCR4, which are likely involved in fibrocyte signaling and trafficking pathways (Abe et al., 2001). Pilling et al. identified additional surface receptors such as CD10, CD11a,b,c, CD13, CD18, CD29, CD32a,b, CD43, CD45, CD49e, CD68, CD81, CD105, CD164, Coll I, III, IV, pro-Coll I, Lamin B, leukocyte-specific protein-1 (LSP-1), Mac2, S100, 25F9, and P-4-H (Pilling et al., 2009).

Moreover, recent clinical data suggest that the enumeration of circulating fibrocytes may serve as a biomarker for disease in different fibrotic disorders such as asthma, pulmonary fibrosis, atherosclerosis, nephrogenic systemic fibrosis (NSF), and hypertrophic scarring or keloid formation (Galan et al., 2006; Herzog and Bucala, 2010). A greater understanding of the mediators that influence fibrocyte biology may offer new opportunities for therapeutic manipulation of fibrocytes in these fibrotic disorders. In this chapter, we focus on the cellular and molecular biology of fibrocytes in wound healing, scar formation, hypertrophic scarring, and keloid formation and review the current literature.

2. Fibrocytes in Wound Healing

2.1. Biology of wound healing

For successful healing, wound tissue has to progress through four stages: hemostasis, inflammation, proliferation, and remodeling (Ayello and Cuddigan, 2004). In the following sections, we discuss these four phases of acute wound healing.

2.1.1. Hemostasis

At the onset of tissue injury, capillary blood enters the wound bed (Diegelmann and Evans, 2004), but this is followed by a requirement to reduce continuous blood loss (Molnar, 2006). Humoral and cellular components such as fibrinogen and platelets stem blood loss and additionally provide signals that contribute to the earliest phases of wound healing (Sheffield and Smith, 2002). Fibrinogen is activated in response to exposed epithelium to form fibrin meshes that trap platelets, which adhere to the ruptures blood vessels, preventing further blood loss (Sheffield and Smith, 2002). In addition, as platelets come into contact with damaged extracellular matrix (ECM) components, they release coagulation factors, leading to the formation of blood clots with the injured tissue (Diegelmann and Evans, 2004). Very rapidly, various growth factors and chemokines such as platelet-derived growth factor (PDGF), vascular endothelial growth factor (VEGF), and transforming growth factor β (TGF-β) are released (Abe et al., 2001; Bauer et al., 2005; Cullum et al., 2001). This phase is called hemostasis and under normal circumstances occurs over a period of minutes to hours.

2.1.2. Inflammation

The subsequent inflammatory phase is characterized by the invasion of phagocytic neutrophils in the wound area (Enoch et al., 2006), usually within the first 24 h after injury. Neutrophils phagocytose foreign particles, bacteria, and necrotic cell components (Mathieu, 2002) and release

chemotactic factors that attract monocytes to egress from blood vessels and enter injured tissue (Diegelmann and Evans, 2004). These cells, now rather macrophages than monocytes (Bellingan et al., 1996), are essential for further wound healing due to their contribution to angiogenesis, matrix deposition, and epithelialization (Byrne and Owen, 2002). A distinct "cocktail" of chemokines secreted by macrophages attracts different fibroblasts to migrate from the surrounding undamaged ECM into the wound site (Diegelmann and Evans, 2004). The inflammatory phase typically lasts for several days.

2.1.3. Proliferation

Besides the involvement of fibrocytes, the fibroblast is a very dominant cell in the wound area during the proliferative phase (Bauer et al., 2005). Fibroblast proliferation is oxygen dependent, and thus a sufficient peripheral oxygen partial pressure is necessary for adequate wound healing (Gordillo and Sen, 2003). Fibrocytes, like fibroblasts, have the ability to produce collagen, which is a major component of the ECM (Enoch et al., 2006). Newly formed blood vessels enter the collagenous network via angiogenesis to form highly vascularized, "granulation tissue" (Sheffield and Smith, 2002). Growth factors stimulate endothelial cells in the nearby healthy tissue to release different proteases such as matrix metalloproteinases (MMPs) into the wound area (Ulrich et al., 2005). MMPs digest the basement membrane, allowing endothelial cells to escape from their parent vessel (Bauer et al., 2005). The cells elongate and form a new capillary sprout extending away from the original vessel (Diegelmann and Evans, 2004). This formation of new blood vessels from preexisting ones is called angiogenesis. Vasculogenesis, in contrast, is defined as the formation of new blood vessels by differentiation of endothelial progenitor cells (EPCs) (Velazquez, 2007) and also contributes to enhanced blood vessel growth during the wound-healing process (Tepper et al., 2005). Some distinct factors have been proposed to play a major role in EPC mobilization and recruitment to the hypoxic and injured site. These are the cognate and noncognate ligands to CXCR4, that is, CXCL12 (also termed SDF-1α) (Ceradini et al., 2004) and macrophage migration inhibitory factor (MIF) (Grieb et al., 2010b). The extension of blood vessels into the injured tissue allows nutrients and oxygen to be transported further into the wound region (Sheffield and Smith, 2002). Thus, cells as fibroblasts, fibrocytes, and macrophages migrate further into the wound, moving the whole "wound-healing machinery" further into the injured area. After completion, blood vessels are networked over the entire wound site (Diegelmann and Evans, 2004). Fibroblasts generally differentiate further into myofibroblasts and generate a tensile strength across the wound, leading to contraction and further closure of the wound (Bauer et al., 2005). Fibroblasts continue to secrete growth factors such as TGF-β, PDGF, and VEGF (Lerman et al., 2003), which

activate the migration and proliferation of keratinocytes, creating the epithelial layer that covers the top of the wound (Sheffield and Smith, 2002). This is accompanied by a constant transition from the proliferative phase into the remodeling phase of the wound-healing process.

2.1.4. Remodeling

The remodeling phase can last for several months or even years (Sheffield and Smith, 2002). During this period, collagen cross-linking is enhanced and the ECM remodeled into a more mature structure with greater integrity. Due to myofibroblast contraction, complete wound closure occurs and the wound strength is increased from 20% normal tensile strength at 3 weeks after injury to about 80% within 2 years (Natarajan et al., 2000).

2.2. Regulatory role of fibrocytes during wound healing

Fibrocytes secrete a combination of chemokines, cytokines, and growth factors that create a milieu favorable for a wound to heal (Chesney and Bucala, 1997). Over time, the initially expressed hematopoietic stem cell marker, CD34, decreases during the wound-healing process (Blakaj and Bucala, 2009) (Fig. 1.1). This phenomenon appears together with the increased production of propyl-4-hydroxlase, an enzyme that is important

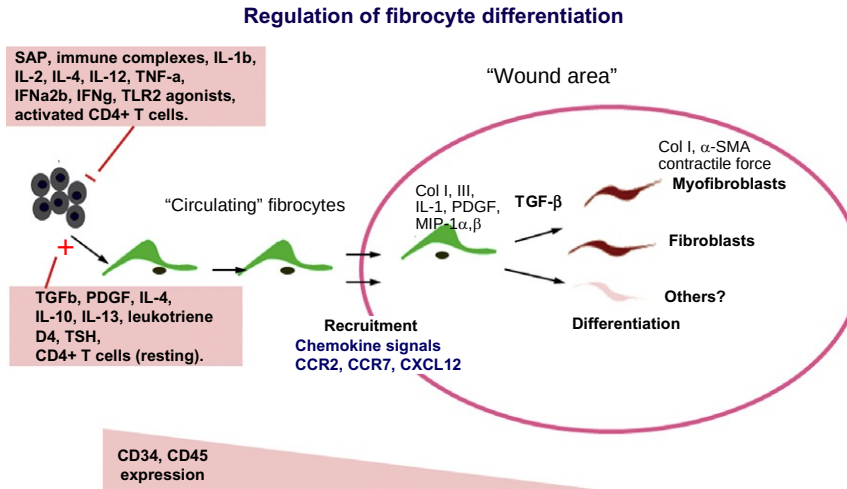

Figure 1.1 As monocytic progenitors, circulating fibrocytes are recruited via different chemokine signals to the wound area. The differentiation of the circulating progenitors into mature cells is stimulated or decreased by various factors. In wounds, the hematopoietic marker CD34 and the leukocyte common antigen CD45 are downregulated as fibrocytes differentiate.

stabilization of collagen triple helices (Aiba and Tagami, 1997). Different researchers hypothesize that CD34 expression may reflect the actual inflammatory state of the wound, which is downregulated upon fibrocytes differentiation into more mature connective tissue cells (Aiba and Tagami, 1997). CD45, which is also known as the leukocyte common antigen, demonstrates a similar downregulation as fibrocytes differentiate (Mori et al., 2005) (Fig. 1.1). This transition of fibrocytes appears also in the context of increased expression of TGF-β in the wound (Aiba and Tagami, 1997), which is well known to play an important role in tissue repair and fibrosis. TGF-β1 accelerates fibrocyte differentiation to cells that are phenotypically similar to fibroblasts and myofibroblasts (Abe et al., 2001) (Fig. 1.1). In addition, fibrocytes secrete other cytokines as well as type I collagen during the inflammatory and proliferative phase of the wound-healing process. High levels of IL-1 were observed to induce the fibrocyte secretion of TNF-α, M-CSF, IL-6, IL-10, MIP-1α, and MIP-β (Chesney et al., 1998). Fibrocytes also are potent antigen-presenting cells capable of initiating T-cell immunity, and they express the surface proteins required for antigen presentation, including the class II major histocompatibility complex molecules HLA-DP, HLA-DQ, and HLA-DR, and the costimulatory molecules CD80 and CD86 (Chesney et al., 1997). The adhesion molecules CD11a, CD54, and CD58 are expressed as well (Chesney et al., 1997). In addition, human fibrocytes can induce a tetanus toxoid-specific T-cell response that is equipotent to that of dendritic cells and significantly greater than that initiated by blood monocytes (Chesney et al., 1997). This effect was confirmed in *in vivo* studies, which showed that antigen-pulsed fibrocytes migrate to regional lymph nodes to prime naïve T cells (Chesney et al., 1997). Thus fibrocytes exhibit a high antigen presenting capability, which supports their role in fibrotic responses associated with inflammation, such as granulomas, or in the autoimmune disease scleroderma.

Fibrocytes also promote angiogenesis, which is a prerequisite for the development of new granulation tissue during the proliferative phase of wound repair (Blakaj and Bucala, 2009). Fibrocytes promote different aspects of blood vessel growth and have been shown to be involved in the proteolysis of the basement membrane by secreting EMC degrading enzymes such as matrix metalloproteinase 9 (MMP-9) and allowing endothelial cells to escape their parent vessel (Bauer et al., 2005). Fibrocytes release different growth factors as VEGF, bFGF, and PDGF and influence the proliferation, migration, and tube formation of endothelial cells *in vitro*. In addition, studies using a Matrigel implant model confirmed the pro-angiogenic action of fibrocytes *in vivo* (Hartlapp et al., 2001).

During the remodeling phase of tissue repair, there is wound contracture that occurs by the action of myofibroblasts. Fibrocytes also can express α-smooth muscle actin (α-SMA) under the influence of TGF-β1 and contract collagen gels *in vitro* (Abe et al., 2001) (Fig. 1.1). These observations

were confirmed *in vivo*, indicating that fibrocytes can further differentiate into a myofibroblast phenotype and actively participate in wound contracture and tissue remodeling (Mori et al., 2005).

Fibrocytes were first identified in mice with surgically implanted wound chambers (Bucala et al., 1994). Within 2 days of implantation into the subdermis, the exudative fluid that collected within these silastic chambers contained an adherent cell population in which approximately 10% of the cells were $CD34^+$ and Col I^+, and spindle-shaped. These cells thus were termed "fibrocytes" to denote their connective tissue and blood-borne characteristics (Bucala et al., 1994). Fibrocytes also can be isolated from a $CD14^+$-enriched mononuclear cell population from the peripheral blood (Abe et al., 2001). This provides easy isolation of fibrocytes for further experiments or phenotypic analysis in different disease states (Quan and Bucala, 2007).

By labeling fibrocytes *ex vivo* with the fluorescent dye PKH-26 and administering these cells into mice, Abe et al. visualized the homing of fibrocytes into the wound area (Abe et al., 2001). To verify that fibrocytes indeed develop in the bone marrow, Mori et al. used an *in vivo* model of sex-mismatched bone marrow chimera mice (Mori et al., 2005). In this study, whole male bone marrow was transplanted into female mice that had received prior lethal irradiation. Further analysis of mouse wounded tissue by *in situ* hybridization showed that both circulating fibrocytes and fibrocytes isolated from the wound area were cells from the male donor, thus confirming the hematopoietic origin of fibrocytes (Mori et al., 2005). These observations were confirmed by Fathke et al., who transplanted bone marrow from enhanced green fluorescent protein (EGFP) transgenic mice into wild-type mice. In the skin, diverse $EGFP^+$, bone marrow-derived cells were identified, and these cells further showed a strong expression for CD45 and a typical fibrocyte morphology (Fathke et al., 2004).

2.3. Regulation of fibrocyte trafficking and differentiation

Fibrocytes undergo regulation by different soluble mediators. The profibrotic cytokines IL-4, IL-13, and PDGF promote the differentiation of $CD14^+$ precursors into fibrocytes (Shao et al., 2008). In contrast, proinflammatory cytokines such as IL-12 and IFN-γ and also SAP and aggregated IgG inhibit the further differentiation of $CD14^+$ precursors into fibrocytes (Pilling et al., 2003, 2006; Shao et al., 2008) (Fig. 1.1). Further, fibrocyte differentiation into mature mesenchymal cells is stimulated by TGF-β (as discussed above) and endothelin-1 (ET-1), which is a mediator of endothelial homeostasis (Schmidt et al., 2003). In addition, fibrocytes also may acquire the characteristics of a fat cell when cultured under appropriate adipogenic conditions, emphasizing the potential of these cells to differentiate into different mesenchymal cell types (Hong et al., 2005).

LSP-1 is a protein involved in leukocyte chemotaxis that also plays a role in the wound-healing process and fibrocyte biology (Blakaj and Bucala, 2009). Both fibrocytes and leukocytes express LSP-1; fibroblasts, in contrast, do not. However, LSP-1 expression is more upregulated in fibrocytes than it is in leukocytes (Yang et al., 2005). In LSP-$1^{-/-}$ knock-out mice, collagen synthesis, reepithelialization, and angiogenesis are enhanced and wound healing is accelerated. Further, the number of circulating fibrocytes was found to be higher than in the wild-type animals; thus, the acceleration in wound repair or in fibrotic responses can at least partly be attributed to higher fibrocyte levels (Wang et al., 2007, 2008).

Adenosine and the adenosine A_2 receptor play an important role in wound repair in diabetic animals (Montesinos et al., 1997). Katebi et al. proposed a function of the adenosine A_{2A} receptor in the proliferation and differentiation of mouse bone marrow-derived mesenchymal stem cells (BM-MSCs) (Katebi et al., 2009). Interestingly, there is less fibrocyte accumulation in the dermis of bleomycin-treated mice of scleroderma after blockade or genetic deletion of adenosine A_{2A} receptors (Katebi et al., 2008). Whether this effect reflects increased recruitment or survival of mature fibrocytes in the injured tissue or is based on the increased maturation of fibrocyte precursors remains to be determined. Nevertheless, the adenosine A_{2A} receptor might represent a potential therapeutic target for fibrotic diseases (Blakaj and Bucala, 2009).

SAP is a member of the pentraxin family of acute phase proteins and has a negative regulatory influence on fibrocyte differentiation (Pilling et al., 2003). When administered 7 days after a dermal wound, SAP administration decreased wound closure and resulted in a decreased number of myofibroblasts in the wound bed, most likely by inhibiting fibrocyte differentiation into myofibroblasts (Naik-Mathuria et al., 2008). Thus, SAP might be of therapeutic value in certain circumstances of aberrant wound healing.

3. Fibrocytes and Hypertrophic Scarring

3.1. Hypertrophic scarring—Causes and mechanisms

3.1.1. Composition and structure of the ECM of hypertrophic scars

In hypertrophic scars that occur after burn injury, the ECM differs both qualitatively and quantitatively from that present in the skin of normotrophic scars (Scott et al., 2000). The overall collagen content is increased in hypertrophic scars, but the proportion of collagen on a dry-weight basis is actually 30% lower than in mature scars or normal dermis (Scott et al., 1996). This difference can be explained by the increased content of proteoglycan and glycoproteins. Collagen in postburn hypertrophic scarring consists primarily of type I collagen, whereas in normal dermis, higher portions of type III

collagen are found. The physical properties of hypertrophic scars are a consequence of the disordered organization of the narrower collagen fibrils, which are arranged chaotically. By contrast, in normal dermis and normotrophic scars, the fibers are bundled and run parallel to the surface (Linares et al., 1972). This disorganization of collagen in the hypertrophic scar may be the result of a higher relative amount of proteoglycans and glycoproteins. In addition, hypertrophic scars contain more water and more fibronectin (Scott et al., 1994). The relative hardness and inelasticity of hypertrophic scars may be explained by the low content of elastin in the ECM. In addition, the glycoproteins in hypertrophic scars differ qualitatively: dermatan sulfate, one of the major glycosaminoglycans in normal dermis, is absent and chondroin sulfate, which is usually barely detectable in normal scars, is prominent in hypertrophic scars (Alexander and Donoff, 1980). Further, there are abnormally high levels of biglycan and versican in hypertrophic scars (Scott et al., 1995, 1996). Thus, aberrant proteoglycan metabolism might therefore be an important factor in the development and persistence of hypertrophic scars.

3.1.2. Dysregulation of apoptosis in hypertrophic scars

Normal wound healing requires the coordinated action of neutrophils, macrophages, lymphocytes, endothelial cells, fibroblasts, and fibrocytes. This deposition of new matrix materials leads progressively to the next steps of wound healing and to the maturation of the scar. Thus, repair involves a transition from a highly cellular and vascular tissue to a relatively acellular and avascular scar. In this context, apoptosis plays an important role in removing effete cells and reducing overall cell numbers (Desmouliere et al., 1997). Apoptosis also is critical for the removal of infiltrating inflammatory cells and in downregulating fibroblast responses and collagen deposition as the scar becomes more mature (Greenhalgh, 1998). Failure in the downregulatory action of apoptosis can result in prolonged inflammation, sustained matrix deposition, and hypertrophic scarring.

3.1.3. Inflammation in hypertrophic scars

Due to the association of tissue injury with acute inflammation, polymorphonuclear leukocytes (PMNs) are attracted by different chemokines and chemotactic signals (Martin, 1997). Increased numbers of PMN are found in early wound healing and are usually eliminated after a few days (Savill et al., 1989). The relatively short lifespan of PMNs, however, is increased severalfold when these cells are recruited into inflamed tissue (Witko-Sarsat et al., 2000). PMN numbers then steadily decline as a result of apoptosis, and apoptotic PMNs are detected and ingested by macrophages. Spontaneous apoptosis thus plays an essential role at the end of the inflammatory phase, which has been well demonstrated in the porcine skin wound-healing model (Wang et al., 2001). Macrophages retrieved from rat wounds also have been shown to ingest not only apoptotic but also living PMN

(Meszaros et al., 1999). Overall, these experimental studies support the concept that neutrophil apoptosis plays a major role in the decline of inflammation during wound repair. The pathological scar formation that occurs after burn injury also has been closely related to protracted inflammation (Tredget, 1999; Tredget et al., 1997). Bacterial infection also enhances the life span of PMN, and its contribution to prolonging inflammation may additionally lead to hypertrophic scarring (Deitch et al., 1983).

3.1.4. Delayed apoptosis in hypertrophic scars

One of the main characteristics of hypertrophic scars is tissue contraction, which is partially due to an increased number of myofibroblasts in the wound bed (Desmouliere et al., 2005). Myofibroblasts secrete ECM proteins and promote the contraction of granulation tissue through the expression of α-SMA and thus are believed to be essential for wound closure. Increased numbers of myofibroblasts are found in hypertrophic scars (Nedelec et al., 1998, 2000). Delayed apoptosis of myofibroblasts has long been suggested as a major component of the genesis of hypertrophic scars. The *Bcl-2* proto-oncogene, whose protein product protects cells from apoptosis, is upregulated in hypertrophic scars (Moulin et al., 2004). Further, the transcription factor p53, which is a major regulator in apoptosis, is downregulated in hypertrophic scars. Recently, it also has been demonstrated that fibroblasts from normal healing wounds show higher rates of apoptosis than those from a hypertrophic scar (Moulin et al., 2004). Linge et al. could show that hypertrophic scar fibroblasts show resistance to a specific apoptosis form induced by the contraction of collagen lattices. This phenomenon depended on the activity of cell surface tissue transglutaminase (Linge et al., 2005). Briefly summarized, these studies indicate that delayed disappearance of fibroblasts and myofibroblasts can result in pathological and hypertrophic scar formation.

3.1.5. Increased levels of TGF-β and CTGF in hypertrophic scars

TGF-β1 is involved in numerous proliferative, inductive, and regulatory processes (Leask and Abraham, 2004). Three isoforms (β1, β2, and β3) exist in mammals, and of these, the functional properties of TGF-β1 have been studied the most intensively.

In wound healing, TGF-β1 influences ECM deposition, tissue remodeling, angiogenesis, and reepithelialization (Liu et al., 2004), and it also was one of the first cytokines described to induce inflammatory cell recruitment. The inflammatory phase of the wound-healing process is thought to be initiated in part by secreted TGF-β1 and other growth factors from platelets. TGF-β1 is chemotatically active and mitogenic and regulates the production of ECM components, not only by promoting their production but also by reducing the expression of MMPs. TGF-β1 is considered one of the most prominent profibrotic growth factors in wound healing (Scott et al., 2000), and it is known to be overexpressed in hypertrophic scars

(Tredget, 1999; Tredget et al., 1997). Further, experimental neutralization of TGF-β1 in the wound environment in rats, mice, and pigs results in scarless healing (Ferguson and O'Kane, 2004). Downregulation of TGF-β1 expression in rat wounds leads to decreased inflammatory infiltrate, faster epithelialization and less scarring, thus affirming the central role of TGF-β1 in wound healing and scar formation (Liu et al., 2004).

Another important growth factor involved in pathological scar formation is connective tissue growth factor (CTGF). Different studies have shown that, while the stimulation of ECM synthesis by TGF-β1 is not shared by factors such as epidermal growth factor (EGF), fibroblast growth factor (FGF), and PDGF, CTGF mediates many of the downstream effects of TGF-β1 on fibroblasts (Grotendorst, 1997). CTGF is a 38-kDa heparin-binding protein that was first identified in the medium of cultured human umbilical vein endothelial cells (HUVECs). It stimulates the mitosis, chemotaxis, and proliferation of fibroblasts (Frazier et al., 1996), as well as the production of the ECM compounds as collagen I, integrin, and fibronectin (Brigstock, 2003).

CTGF is overexpressed in different fibrotic skin disorders such as localized skin sclerosis, systemic sclerosis, scar tissue, and keloids (Igarashi et al., 1996). Further studies have shown that CTGF is overexpressed in the fibrotic lesions of atherosclerosis and in renal and hepatic fibrosis (Moussad and Brigstock, 2000). In these diseases, a high level of CTGF in proliferative areas can be found (Brigstock, 2003) and there is a correlation between high levels of TGF-β1 and CTGF (Moussad and Brigstock, 2000).

Interestingly, in a pig skin wound-healing model, TGF-β1 expression peaked earlier than the CTGF expression did (Wang et al., 2000, 2001). This sequential expression of the two growth factors was interpreted as a specific feature of a growth factor cascade in which TGF-β1 initiated repair and CTGF was required later during the wound-healing process. This model is also consistent with various studies, suggesting that the profibrotic properties of TGF-β1 occur via the induction of CTGF, which then stimulates fibroblast and ECM production (Brigstock, 2003).

In fibroblasts from hypertrophic scars, CTGF mRNA levels were reported to be 20-fold increased when compared to normal fibroblasts (Colwell et al., 2005). A high CTGF transcriptional response to TGF-β1 stimulation also is a characteristic of hypertrophic scar fibroblasts. Overall, these data support the conclusion that both TGF-β1 and CTGF play an important major role in pathological scar formation (Colwell et al., 2005).

3.2. Role of fibrocytes in hypertrophic scars

3.2.1. Hypertrophic scars are associated with circulating fibrocytes

During wound healing, dermal fibroblasts migrate from surrounding tissue into the injured region. After severe burn wounding, such migration may be made physically impossible by the sheer distance of the uninjured tissue.

Severe burn wounds nevertheless can be associated with the excessive deposition of ECM in the dermis and the formation of hypertrophic scars or keloids (Scott et al., 2000; Tredget et al., 1997). Thus, an outstanding question has been to address the source(s) of the large numbers of activated cells that are recruited into the burn injured tissue.

Several studies now have shown that circulating fibrocytes play a role in postburn hypertrophic scarring (Yang et al., 2002, 2005). As described above, these cells, which constitute 0.5% of nonerythrocytic blood cells and exhibit fibroblast-like characteristics, can be recruited from the peripheral blood into injured tissue (Bucala et al., 1994; Quan et al., 2004). Yang et al. isolated fibrocytes from the peripheral blood mononuclear cell (PBMC) fraction of burn patients and analyzed their ability to produce collagen I when compared to healthy controls (Yang et al., 2002). These authors were able to show that burn patient PBMCs developed more efficiently into fibrocytes than the corresponding cell fraction from healthy donors. In addition, the percentage of collagen I^+ fibrocytes was significantly larger in burn patients than in controls ($p < 0.001$) (Yang et al., 2002). The percentage of collagen I^+ fibrocytes was even more highly increased in those patients suffering from a burn wound covering more than 30% of the total body surface area. Further, a correlation was found between the ability of PBMCs to develop into fibrocytes and the serum concentration of TGF-β1 of the same patients. These burn-induced circulating fibrocytes were also found to be derived from a $CD14^+$ mononuclear cell subpopulation (Yang et al., 2002). Taken together, these data suggest that the fibrocyte differentiation is upregulated in burn patients. An increase in the TGF-β serum concentration thus appears to stimulate the differentiation of a $CD14^+$ mononuclear cell precursor population into collagen producing fibrocytes that likely play an important role in tissue repair from burn injury.

3.2.2. LSP-1, a potential fibrocyte marker

Although fibrocytes and fibroblasts share such common characteristics as a spindle-shaped appearance and the ability to synthesize collagen and other ECM molecules, their tissue origins appear distinct, with fibrocytes originating in bone marrow progenitors and fibroblasts from mature tissues (Yang et al., 2005). When examined under an electron microscope, mature fibrocytes are characterized by an elongated body and fiber-like projections (Bucala, 2007). Fibroblasts, in contrast, show a rather smooth cell body with ruffled borders and a single fiber at the cell body's end. As discussed above, fibrocytes are characterized by the expression of collagen I, fibronectin, CD11b, CD34, and CD45 while in the peripheral blood, wound regions, and areas of tissue remodeling (Quan et al., 2004). These surface markers are not unique to fibrocytes but are expressed on other cells as well. CD34 is

expressed on stem cells, EPCs, and can be detected in the microvasculature (Grieb et al., 2010a,b; Simons et al., 2011). In addition, the typical fibrocyte markers of CD34 and CD45 may be downregulated over time in culture or as a result of fibrocyte maturation (Phillips et al., 2004). In an attempt to establish more stably expressed markers of fibrocytes, Yang et al. extracted and examined proteins of fibrocytes, fibroblasts, and nonadherent lymphocytes (Yang et al., 2005). These experiments revealed that the LSP-1 is more highly expressed in fibrocytes from burn patients than in nonadherent lymphocytes or fibrocytes from healthy controls. Since LSP-1 is completely absent in fibroblasts, dual staining for procollagen I and LSP-1 may be considered for identifying fibrocytes both in culture and in hypertrophic scars (Yang et al., 2005).

LSP-1 is an intracellular F-actin-binding protein with a molecular weight of 52 kDa. It is expressed in B and T cells, as well as in macrophages and neutrophils (Jongstra-Bilen et al., 2000). Mouse and human LSP-1 share equal expression patterns and exhibit a high sequence identity. LSP-1 has two putative Ca^{2+}-binding motifs and is present in three different cell compartments. About 25% is integrated in the plasma membrane, 15% is in the cytoskeleton, and 60% is in the cytosol (Jongstra-Bilen et al., 1992). LSP-1 mediates the Ca^{2+}-dependent regulation of an anti-IgM apoptotic response (Jongstra-Bilen et al., 1999), and it appears to control cytoskeletal architecture and mobility. LSP-1 is overexpressed in leukemia, where it has been implicated in increased cell adhesion and inhibition of neutrophil migration, leading to recurrent infection (Miyoshi et al., 2001). Accordingly, LSP-1 may play a role in the regulation of fibrocyte motility as the increased binding of fibrocytes to newly formed matrix compounds might inhibit their own migration and affect the secretion of collagen. Irrespective of its precise function, LSP-1 may serve as a relatively stable marker of fibrocytes in different physiologic and pathologic contexts (Bucala, 2007).

3.2.3. Increased numbers of circulating fibrocytes in postburn hypertrophic scars

By employing a double staining methodology for LSP-1 and procollagen I, Yang et al. investigated the number of fibrocytes in postburn hypertrophic scars in comparison to mature scars (Yang et al., 2005). Procollagen I staining was found extensively in both hypertrophic and mature scar; however, the number of spindle-shaped and procoallagen I^+/LSP-1^+ dual-labeled cells were significantly higher in hypertrophic scars than in mature scars. In normal skin, a fibrocyte population of about 0.45% (of procoallagen I^+/LSP-1^+ dual labeled cells per high-power field) was observed, which is comparable to the fibrocyte content of a mature scar. In a hypertrophic scar, on the other hand, a fibrocyte population of 0.81% was observed (Bucala, 2007).

3.2.4. Interaction of fibrocytes with endothelial cells and fibroblasts

Fibrocytes interact functionally with several other cell types (Abe et al., 2001; Bucala et al., 1994), which may additionally contribute to hypertrophic scarring and keloid formation. An interaction between fibrocytes and tissue fibroblasts, which are rich producers of collagen, appears likely. Compared to fibroblasts, fibrocytes produce lower amounts of collagen *in vitro*, as assessed by the assay for hydroxyproline content in conditioned medium (Bucala, 2007). Interestingly, the medium of cultured fibrocytes from burn patients when added to dermal fibroblasts increases markedly the hydroxyproline synthesis of these cells. Such an effect was not observed for medium obtained from the fibrocytes of healthy controls. These findings raise the possibility that an important role for fibrocytes in wound healing and scar formation is the upregulation of dermal fibroblast activity rather than in the direct deposition of ECM compounds (Wang et al., 2007).

3.2.5. Role of fibrocytes in burn scar formation

A model for the role of fibrocytes in burn injury and scar formation may be envisioned as follows: thermal trauma activates circulating fibrocytes and their progenitors by various inflammatory mechanisms. Fibrocytes (and their progenitors) traffic into the areas of injured tissue, where they differentiate further and contribute to ECM production by secreting collagen, fibronectin, and vimentin. They promote angiogenic responses by the regulated release of VEGF, bFGF, and PDGF. By the localized secretion of the profibrotic factors, TGF-β1 fibrocytes activate local fibroblasts to upregulate matrix protein production and further promote wound repair. Under the reciprocal influence of TGF-β1 and other growth factors, some fibrocytes may also differentiate into α-SMA-expressing myofibroblasts, thus contributing to wound closure, scar formation, and tissue remodeling (Fig. 1.1).

4. Conclusions

Since the initial description of fibrocytes more than 15 years ago, our collective knowledge of fibrocyte biology has increased significantly as well as the breadth of pathologic conditions in which these cells play a role. In wound healing or tissue regeneration, fibrocytes have been demonstrated to produce a profile of chemokines, cytokines, and growth factors that are required for optimal wound healing and regeneration. Further, their involvement in wound closure, angiogenesis, and antigen presentation has been established. The regulation of fibrocyte function by different cytokines and chemokines, the proteins LSP-1 and SAP, and the adenosine A_{2A}

receptor have also been defined. As more detailed information about fibrocyte mobilization, trafficking signals, and differentiation emerge in the contexts of wound healing, hypertrophic scarring, and keloid formation, we anticipate that there will be new avenues for therapeutic intervention.

ACKNOWLEDGMENTS

G. G. was supported by the "START" program of the RWTH Aachen University and travel funds from the "Deutsche Forschungsgemeinschaft (DFG)" (GR 3724/1-1). J. B. was supported by the Interdisciplinary Center of Clinical Research (IZKF Aachen/K1-4).

REFERENCES

Abe, R., Donnelly, S.C., Peng, T., Bucala, R., Metz, C.N., 2001. Peripheral blood fibrocytes: differentiation pathway and migration to wound sites. J. Immunol. 166, 7556–7562.

Aiba, S., Tagami, H., 1997. Inverse correlation between CD34 expression and proline-4-hydroxylase immunoreactivity on spindle cells noted in hypertrophic scars and keloids. J. Cutan. Pathol. 24, 65–69.

Alexander, S.A., Donoff, R.B., 1980. The histochemistry of glycosaminoglycans within hypertrophic scars. J. Surg. Res. 28, 171–181.

Ayello, E.A., Cuddigan, J.E., 2004. Conquer chronic wounds with wound bed preparation. Nurse Pract. 29, 8–25, quiz 26–7.

Bauer, S.M., Bauer, R.J., Velazquez, O.C., 2005. Angiogenesis, vasculogenesis, and induction of healing in chronic wounds. Vasc. Endovasc. Surg. 39, 293–306.

Bellingan, G.J., Caldwell, H., Howie, S.E., Dransfield, I., Haslett, C., 1996. In vivo fate of the inflammatory macrophage during the resolution of inflammation: inflammatory macrophages do not die locally, but emigrate to the draining lymph nodes. J. Immunol. 157, 2577–2585.

Bellini, A., Mattoli, S., 2007. The role of the fibrocyte, a bone marrow-derived mesenchymal progenitor, in reactive and reparative fibroses. Lab. Invest. 87, 858–870.

Blakaj, A., Bucala, R., 2009. The role of fibrocytes in wound healing. Adv. Wound Care 1, 266–271.

Brigstock, D.R., 2003. The CCN family: a new stimulus package. J. Endocrinol. 178, 169–175.

Bucala, R., 2007. Fibrocytes: New Insights into Tissue Repair and Systemic Fibrosis. World Scientific, Hackensack, NJ, pp. 1–249.

Bucala, R., Spiegel, L.A., Chesney, J., Hogan, M., Cerami, A., 1994. Circulating fibrocytes define a new leukocyte subpopulation that mediates tissue repair. Mol. Med. 1, 71–81.

Byrne, H.M., Owen, M.R., 2002. Use of mathematical models to simulate and predict macrophage activity in diseased tissue. In: Burke, B., Lewis, C.E. (Eds.), The Macrophage. Oxford University Press, Oxford, UK, pp. 1–59.

Ceradini, D.J., Kulkarni, A.R., Callaghan, M.J., Tepper, O.M., Bastidas, N., Kleinman, M.E., et al., 2004. Progenitor cell trafficking is regulated by hypoxic gradients through HIF-1 induction of SDF-1. Nat. Med. 10, 858–864.

Chesney, J., Bucala, R., 1997. Peripheral blood fibrocytes: novel fibroblast-like cells that present antigen and mediate tissue repair. Biochem. Soc. Trans. 25, 520–524.

Chesney, J., Bacher, M., Bender, A., Bucala, R., 1997. The peripheral blood fibrocyte is a potent antigen-presenting cell capable of priming naive T cells in situ. Proc. Natl. Acad. Sci. USA 94, 6307–6312.

Chesney, J., Metz, C., Stavitsky, A.B., Bacher, M., Bucala, R., 1998. Regulated production of type I collagen and inflammatory cytokines by peripheral blood fibrocytes. J. Immunol. 160, 419–425.

Colwell, A.S., Phan, T.T., Kong, W., Longaker, M.T., Lorenz, P.H., 2005. Hypertrophic scar fibroblasts have increased connective tissue growth factor expression after transforming growth factor-beta stimulation. Plast. Reconstr. Surg. 116, 1387–1390 discussion 1391–1392.

Cullum, N., Nelson, E.A., Fletcher, A.W., Sheldon, T.A., 2001. Compression for venous leg ulcers. Cochrane Database Syst. Rev. 2, CD000265.

Deitch, E.A., Wheelahan, T.M., Rose, M.P., Clothier, J., Cotter, J., 1983. Hypertrophic burn scars: analysis of variables. J. Trauma 23, 895–898.

Desmouliere, A., Badid, C., Bochaton-Piallat, M.L., Gabbiani, G., 1997. Apoptosis during wound healing, fibrocontractive diseases and vascular wall injury. Int. J. Biochem. Cell Biol. 29, 19–30.

Desmouliere, A., Chaponnier, C., Gabbiani, G., 2005. Tissue repair, contraction, and the myofibroblast. Wound Repair Regen. 13, 7–12.

Diegelmann, R.F., Evans, M.C., 2004. Wound healing: an overview of acute, fibrotic and delayed healing. Front. Biosci. 9, 283–289.

Enoch, S., Grey, J.E., Harding, K.G., 2006. Recent advances and emerging treatments. BMJ 332, 962–965.

Fathke, C., Wilson, L., Hutter, J., Kapoor, V., Smith, A., Hocking, A., et al., 2004. Contribution of bone marrow-derived cells to skin: collagen deposition and wound repair. Stem Cells 22, 812–822.

Ferguson, M.W., O'Kane, S., 2004. Scar-free healing: from embryonic mechanisms to adult therapeutic intervention. Philos. Trans. R. Soc. Lond. B Biol. Sci. 359, 839–850.

Frazier, K., Williams, S., Kothapalli, D., Klapper, H., Grotendorst, G.R., 1996. Stimulation of fibroblast cell growth, matrix production, and granulation tissue formation by connective tissue growth factor. J. Invest. Dermatol. 107, 404–411.

Galan, A., Cowper, S.E., Bucala, R., 2006. Nephrogenic systemic fibrosis (nephrogenic fibrosing dermopathy). Curr. Opin. Rheumatol. 18, 614–617.

Gordillo, G.M., Sen, C.K., 2003. Revisiting the essential role of oxygen in wound healing. Am. J. Surg. 186, 259–263.

Greenhalgh, D.G., 1998. The role of apoptosis in wound healing. Int. J. Biochem. Cell Biol. 30, 1019–1030.

Grieb, G., Groger, A., Piatkowski, A., Markowicz, M., Steffens, G.C., Pallua, N., 2010a. Tissue substitutes with improved angiogenic capabilities: an in vitro investigation with endothelial cells and endothelial progenitor cells. Cells Tissues Organs 191, 96–104.

Grieb, G., Piatkowski, A., Simons, D., Hörmann, N., Dewor, M., Steffens, G., et al., 2010b. Macrophage migration inhibitory factor is a potential inducer of endothelial progenitor cell mobilization after flap operation. Surgery, doi:10.1016/j.surg.2010.10.008.

Grotendorst, G.R., 1997. Connective tissue growth factor: a mediator of TGF-beta action on fibroblasts. Cytokine Growth Factor Rev. 8, 171–179.

Hartlapp, I., Abe, R., Saeed, R.W., Peng, T., Voelter, W., Bucala, R., et al., 2001. Fibrocytes induce an angiogenic phenotype in cultured endothelial cells and promote angiogenesis in vivo. FASEB J. 15, 2215–2224.

Herzog, E.L., Bucala, R., 2010. Fibrocytes in health and disease. Exp. Hematol. 38, 548–556.

Hong, K.M., Burdick, M.D., Phillips, R.J., Heber, D., Strieter, R.M., 2005. Characterization of human fibrocytes as circulating adipocyte progenitors and the formation of human adipose tissue in SCID mice. FASEB J. 19, 2029–2031.

Igarashi, A., Nashiro, K., Kikuchi, K., Sato, S., Ihn, H., Fujimoto, M., et al., 1996. Connective tissue growth factor gene expression in tissue sections from localized scleroderma, keloid, and other fibrotic skin disorders. J. Invest. Dermatol. 106, 729–733.

Jongstra-Bilen, J., Janmey, P.A., Hartwig, J.H., Galea, S., Jongstra, J., 1992. The lymphocyte-specific protein LSP1 binds to F-actin and to the cytoskeleton through its COOH-terminal basic domain. J. Cell Biol. 118, 1443–1453.

Jongstra-Bilen, J., Wielowieyski, A., Misener, V., Jongstra, J., 1999. LSP1 regulates anti-IgM induced apoptosis in WEHI-231 cells and normal immature B-cells. Mol. Immunol. 36, 349–359.

Jongstra-Bilen, J., Misener, V.L., Wang, C., Ginzberg, H., Auerbach, A., Joyner, A.L., et al., 2000. LSP1 modulates leukocyte populations in resting and inflamed peritoneum. Blood 96, 1827–1835.

Katebi, M., Fernandez, P., Chan, E.S., Cronstein, B.N., 2008. Adenosine A2A receptor blockade or deletion diminishes fibrocyte accumulation in the skin in a murine model of scleroderma, bleomycin-induced fibrosis. Inflammation 31, 299–303.

Katebi, M., Soleimani, M., Cronstein, B.N., 2009. Adenosine A2A receptors play an active role in mouse bone marrow-derived mesenchymal stem cell development. J. Leukoc. Biol. 85, 438–444.

Leask, A., Abraham, D.J., 2004. TGF-beta signaling and the fibrotic response. FASEB J. 18, 816–827.

Lerman, O.Z., Galiano, R.D., Armour, M., Levine, J.P., Gurtner, G.C., 2003. Cellular dysfunction in the diabetic fibroblast: impairment in migration, vascular endothelial growth factor production, and response to hypoxia. Am. J. Pathol. 162, 303–312.

Linares, H.A., Kischer, C.W., Dobrkovsky, M., Larson, D.L., 1972. The histiotypic organization of the hypertrophic scar in humans. J. Invest. Dermatol. 59, 323–331.

Linge, C., Richardson, J., Vigor, C., Clayton, E., Hardas, B., Rolfe, K., 2005. Hypertrophic scar cells fail to undergo a form of apoptosis specific to contractile collagen-the role of tissue transglutaminase. J. Invest. Dermatol. 125, 72–82.

Liu, W., Wang, D.R., Cao, Y.L., 2004. TGF-beta: a fibrotic factor in wound scarring and a potential target for anti-scarring gene therapy. Curr. Gene Ther. 4, 123–136.

Martin, P., 1997. Wound healing—aiming for perfect skin regeneration. Science 276, 75–81.

Mathieu, D., 2002. Hyperbaric oxygen therapy in the management of non-healing wounds. In: Bakker, D.J., Cramer, F.S. (Eds.), Hyperbaric Surgery. Best Publishing Company, Flagstaff, AZ, pp. 317–339.

Meszaros, A.J., Reichner, J.S., Albina, J.E., 1999. Macrophage phagocytosis of wound neutrophils. J. Leukoc. Biol. 65, 35–42.

Miyoshi, E.K., Stewart, P.L., Kincade, P.W., Lee, M.B., Thompson, A.A., Wall, R., 2001. Aberrant expression and localization of the cytoskeleton-binding pp 52 (LSP1) protein in hairy cell leukemia. Leuk. Res. 25, 57–67.

Molnar, J.A., 2006. Overview of nutrition and wound healing. In: Molnar, J.A. (Ed.), Nutrition and Wound Healing. CRC Press, Boca Raton, FL, pp. 1–14.

Montesinos, M.C., Gadangi, P., Longaker, M., Sung, J., Levine, J., Nilsen, D., et al., 1997. Wound healing is accelerated by agonists of adenosine A2 (G alpha s-linked) receptors. J. Exp. Med. 186, 1615–1620.

Mori, L., Bellini, A., Stacey, M.A., Schmidt, M., Mattoli, S., 2005. Fibrocytes contribute to the myofibroblast population in wounded skin and originate from the bone marrow. Exp. Cell Res. 304, 81–90.

Moulin, V., Larochelle, S., Langlois, C., Thibault, I., Lopez-Valle, C.A., Roy, M., 2004. Normal skin wound and hypertrophic scar myofibroblasts have differential responses to apoptotic inductors. J. Cell. Physiol. 198, 350–358.

Moussad, E.E., Brigstock, D.R., 2000. Connective tissue growth factor: what's in a name? Mol. Genet. Metab. 71, 276–292.

Naik-Mathuria, B., Pilling, D., Crawford, J.R., Gay, A.N., Smith, C.W., Gomer, R.H., et al., 2008. Serum amyloid P inhibits dermal wound healing. Wound Repair Regen. 16, 266–273.

Natarajan, S., Williamson, D., Stiltz, A.J., Harding, K., 2000. Advances in wound care and healing technology. Am. J. Clin. Dermatol. 1, 269–275.

Nedelec, B., Dodd, C.M., Scott, P.G., Ghahary, A., Tredget, E.E., 1998. Effect of interferon-alpha2b on guinea pig wound closure and the expression of cytoskeletal proteins in vivo. Wound Repair Regen. 6, 202–212.

Nedelec, B., Ghahary, A., Scott, P.G., Tredget, E.E., 2000. Control of wound contraction. Basic and clinical features. Hand Clin. 16, 289–302.

Phillips, R.J., Burdick, M.D., Hong, K., Lutz, M.A., Murray, L.A., Xue, Y.Y., et al., 2004. Circulating fibrocytes traffic to the lungs in response to CXCL12 and mediate fibrosis. J. Clin. Invest. 114, 438–446.

Pilling, D., Buckley, C.D., Salmon, M., Gomer, R.H., 2003. Inhibition of fibrocyte differentiation by serum amyloid P. J. Immunol. 171, 5537–5546.

Pilling, D., Tucker, N.M., Gomer, R.H., 2006. Aggregated IgG inhibits the differentiation of human fibrocytes. J. Leukoc. Biol. 79, 1242–1251.

Pilling, D., Fan, T., Huang, D., Kaul, B., Gomer, R.H., 2009. Identification of markers that distinguish monocyte-derived fibrocytes from monocytes, macrophages, and fibroblasts. PLoS One 4, e7475 [Electronic Resource].

Quan, T.E., Bucala, R., 2007. Culture and analysis of circulating fibrocytes. Methods Mol. Med. 135, 423–434.

Quan, T.E., Cowper, S., Wu, S.P., Bockenstedt, L.K., Bucala, R., 2004. Circulating fibrocytes: collagen-secreting cells of the peripheral blood. Int. J. Biochem. Cell Biol. 36, 598–606.

Savill, J.S., Wyllie, A.H., Henson, J.E., Walport, M.J., Henson, P.M., Haslett, C., 1989. Macrophage phagocytosis of aging neutrophils in inflammation. Programmed cell death in the neutrophil leads to its recognition by macrophages. J. Clin. Invest. 83, 865–875.

Schmidt, M., Sun, G., Stacey, M.A., Mori, L., Mattoli, S., 2003. Identification of circulating fibrocytes as precursors of bronchial myofibroblasts in asthma. J. Immunol. 171, 380–389.

Scott, P.G., Ghahary, A., Chambers, M.M., Tredget, E.E., 1994. Biological basis of hypertrophic scarring. Adv. Struct. Biol. 3, 157–202.

Scott, P.G., Dodd, C.M., Tredget, E.E., Ghahary, A., Rahemtulla, F., 1995. Immunohistochemical localization of the proteoglycans decorin, biglycan and versican and transforming growth factor-beta in human post-burn hypertrophic and mature scars. Histopathology 26, 423–431.

Scott, P.G., Dodd, C.M., Tredget, E.E., Ghahary, A., Rahemtulla, F., 1996. Chemical characterization and quantification of proteoglycans in human post-burn hypertrophic and mature scars. Clin. Sci. 90, 417–425.

Scott, P.G., Ghahary, A., Tredget, E.E., 2000. Molecular and cellular aspects of fibrosis following thermal injury. Hand Clin. 16, 271–287.

Shao, D.D., Suresh, R., Vakil, V., Gomer, R.H., Pilling, D., 2008. Pivotal Advance: Th-1 cytokines inhibit, and Th-2 cytokines promote fibrocyte differentiation. J. Leukoc. Biol. 83, 1323–1333.

Sheffield, P.J., Smith, A.P.S., 2002. Physiological and pharmacological basis of hyperbaric oxygen therapy. In: Bakker, D.J., Cramer, F.S. (Eds.), Hyperbaric Surgery. Best Publishing Company, Flagstaff, AZ, pp. 63–109.

Simons, D., Grieb, G., Hristov, M., Pallua, N., Weber, C., Bernhagen, J., et al., 2011. Hypoxia-induced endothelial secretion of macrophage migration inhibitory factor and role in endothelial progenitor cell recruitment. J. Cell. Mol. Med. 15, 668–678.

Tepper, O.M., Capla, J.M., Galiano, R.D., Ceradini, D.J., Callaghan, M.J., Kleinman, M.E., et al., 2005. Adult vasculogenesis occurs through in situ recruitment, proliferation, and tubulization of circulating bone marrow-derived cells. Blood 105, 1068–1077.

Tredget, E.E., 1999. Pathophysiology and treatment of fibroproliferative disorders following thermal injury. Ann. N. Y. Acad. Sci. 888, 165–182.

Tredget, E.E., Nedelec, B., Scott, P.G., Ghahary, A., 1997. Hypertrophic scars, keloids, and contractures. The cellular and molecular basis for therapy. Surg. Clin. North Am. 77, 701–730.

Ulrich, D., Lichtenegger, F., Unglaub, F., Smeets, R., Pallua, N., 2005. Effect of chronic wound exudates and MMP-2/-9 inhibitor on angiogenesis in vitro. Plast. Reconstr. Surg. 116, 539–545.

Velazquez, O.C., 2007. Angiogenesis and vasculogenesis: inducing the growth of new blood vessels and wound healing by stimulation of bone marrow-derived progenitor cell mobilization and homing. J. Vasc. Surg. 45 (Suppl. A), A39–A47.

Wang, J.F., Olson, M.E., Reno, C.R., Kulyk, W., Wright, J.B., Hart, D.A., 2000. Molecular and cell biology of skin wound healing in a pig model. Connect. Tissue Res. 41, 195–211.

Wang, J.F., Olson, M.E., Reno, C.R., Wright, J.B., Hart, D.A., 2001. The pig as a model for excisional skin wound healing: characterization of the molecular and cellular biology, and bacteriology of the healing process. Comp. Med. 51, 341–348.

Wang, J., Jiao, H., Stewart, T.L., Shankowsky, H.A., Scott, P.G., Tredget, E.E., 2007. Fibrocytes from burn patients regulate the activity of fibroblasts. Wound Repair Regen. 15, 113–121.

Wang, J., Jiao, H., Stewart, T.L., Shankowsky, H.A., Scott, P.G., Tredget, E.E., 2008. Increased severity of bleomycin-induced skin fibrosis in mice with leukocyte-specific protein 1 deficiency. J. Invest. Dermatol. 128, 2767–2776.

Witko-Sarsat, V., Rieu, P., Descamps-Latscha, B., Lesavre, P., Halbwachs-Mecarelli, L., 2000. Neutrophils: molecules, functions and pathophysiological aspects. Lab. Invest. 80, 617–653.

Yang, L., Scott, P.G., Giuffre, J., Shankowsky, H.A., Ghahary, A., Tredget, E.E., 2002. Peripheral blood fibrocytes from burn patients: identification and quantification of fibrocytes in adherent cells cultured from peripheral blood mononuclear cells. Lab. Invest. 82, 1183–1192.

Yang, L., Scott, P.G., Dodd, C., Medina, A., Jiao, H., Shankowsky, H.A., et al., 2005. Identification of fibrocytes in postburn hypertrophic scar. Wound Repair Regen. 13, 398–404.

CHAPTER TWO

New Insights into the Mechanism of Wnt Signaling Pathway Activation

Akira Kikuchi, Hideki Yamamoto, Akira Sato, *and* Shinji Matsumoto

Contents

Department of Biochemistry, Graduate School of Medicine, Osaka University, Osaka, Japan

International Review of Cell and Molecular Biology, Volume 291
ISSN 1937-6448, DOI: 10.1016/B978-0-12-386035-4.00002-1

Abstract

Wnts compromise a large family of secreted, hydrophobic glycoproteins that control a variety of developmental and adult processes in all metazoan organisms. Recent advances in the Wnt-signal studies have revealed that distinct Wnts activate multiple intracellular cascades that regulate cellular proliferation, differentiation, migration, and polarity. Although the mechanism by which Wnts regulate different pathways selectively remains to be clarified, evidence has accumulated that in addition to the formation of ligand–receptor pairs, phosphorylation of receptors, receptor-mediated endocytosis, acidification, and the presence of cofactors, such as heparan sulfate proteoglycans, are also involved in the activation of specific Wnt pathways. Here, we review the mechanism of activation in Wnt signaling initiated on the cell-surface membrane. In addition, the mechanisms for fine-tuning by cross talk between Wnt and other signaling are also discussed.

Key Words: Wnt, Signal pathways, β-Catenin, Receptor, Endocytosis, Phosphorylation, Cross talk.

1. Introduction

Wnts constitute a large family of cysteine-rich secreted ligands that are essential for a wide array of developmental and physiological processes (Logan et al., 2004). At least 19 Wnt members have been found in humans and mice, and they exhibit unique expression patterns and distinct functions during development. Wnts control various cellular functions including proliferation, differentiation, death, migration, and polarity, by activating multiple intracellular signaling cascades, including the β-catenin-dependent and -independent pathways (Fig. 2.1). Wnts have been divided classically into two distinct types based on their ability to induce transformation of the mouse mammary epithelial cell line C57MG (Wong et al., 1994). Highly transforming members include Wnt1, Wnt3, Wnt3a, and Wnt7a, and intermediately transforming or nontransforming members include Wnt2, Wnt4, Wnt5a, Wnt5b, Wnt6, Wnt7b, and Wnt11.

In humans and mice, the 10 members of the Frizzled (Fz) family comprise a series of seven-pass transmembrane receptors that have been

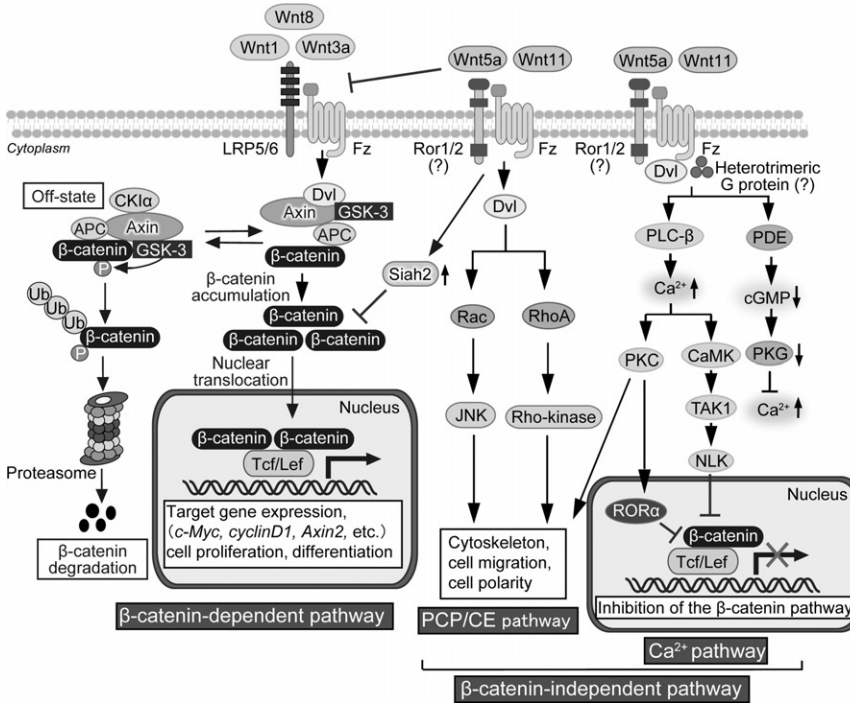

Figure 2.1 Multiple Wnt signaling pathways. Wnt regulates at least three distinct intracellular signaling pathways: the β-catenin pathway, the planar cell polarity (PCP)/convergent extension (CE) pathway, and the Ca^{2+} pathway. See details in the text. APC, adenomatous polyposis coli; CaMK, Ca^{2+}/calmodulin-dependent kinase; cGMP, cyclic guanosine monophosphate; CKIα, casein kinase Iα; Dvl, dishevelled; Fz, Frizzled; GSK-3, glycogen synthase kinase-3; JNK, c-Jun N-terminal kinase; LRP5/6, low-density lipoprotein receptor-related protein 5/6; NLK, Nemo-like kinase; PDE, phosphodiesterases; PKC, protein kinase C; PKG, protein kinase G; RORα, retinoic acid-related orphan nuclear receptor; Ror1/2, receptor tyrosine kinase-like orphan receptor 1/2; TAK1, TGF-β activated kinase1; Tcf/Lef, T-cell factor/lymphoid enhancer-binding factor; Ub, ubiquitin.

identified as Wnt receptors (Schulte, 2010; Wang et al., 2006). In addition to Fz proteins, single-pass transmembrane proteins, such as low-density lipoprotein receptor-related protein 5 (LRP5), LRP6, receptor tyrosine kinase (RTK)-like orphan receptor 1(Ror1), Ror2, and receptor-like tyrosine kinase (Ryk), have been shown to function as coreceptors for Wnt signaling (Fradkin et al., 2009; Green et al., 2008; Kikuchi et al., 2007, 2009; MacDonald et al., 2009; Nishita et al., 2010a). Therefore, it has been assumed traditionally that the binding of different Wnts to their specific receptors selectively triggers different outcomes via distinct intracellular

pathways. However, it has been suggested that in addition to the specific combination of Wnt ligands and receptors, phosphorylation of receptors (MacDonald et al., 2009; Niehrs et al., 2010b), endocytosis of the Wnt/receptor complex (Kikuchi et al., 2009), generation of phospholipids (Pan et al., 2008), extracellular and intracellular acidification (Cruciat et al., 2010; Niehrs et al., 2010a), and binding of Wnt to heparan sulfate proteoglycans (HSPGs; Lin, 2004) are involved in the selective activation of the Wnt signaling pathway. Further, there is increasing evidence that Wnt components are shared by other signaling pathways and that cross talk of Wnt signaling occurs with multiple pathways. This review highlights new insight into the mechanism of Wnt signaling pathway activation.

2. Wnt Regulates Multiple Pathways

2.1. β-Catenin-dependent pathway

The intracellular signaling pathway activated by Wnts was originally identified as the β-catenin-dependent pathway, which is highly conserved among various species (Kikuchi et al., 2009; Logan et al., 2004; MacDonald et al., 2009) (Fig. 2.1). In this text, the β-catenin-dependent pathway is often referred to as the β-catenin pathway. β-Catenin was found as a cadherin-binding protein involved in the regulation of cell to cell adhesion and is now known to function as an important mediator of Wnt signaling. In the absence of Wnt stimulation, cytoplasmic β-catenin levels are low because β-catenin is ubiquitinated and degraded in the proteasome (Aberle et al., 1997). Axin acts as a scaffold protein to degrade β-catenin by forming a complex with glycogen synthase kinase-3 (GSK-3), β-catenin, adenomatous polyposis coli (APC) gene product, and casein kinase 1α (CK1α), and β-catenin is efficiently phosphorylated by CK1α and GSK-3 and ubiquitinated in the Axin complex (Hino et al., 2003; Ikeda et al., 1998; Kishida et al., 1998; Kitagawa et al., 1999; Liu et al., 2002). At low levels of β-catenin, the transcription factor T-cell factor (Tcf)/lymphoid enhancer-binding factor (Lef) binds to Groucho, which recruits histone deacetylase (HDAC) to mediate transcriptional repression (Hurlstone et al., 2002). When Wnts, such as Wnt1, Wnt3a, and Wnt8, bind to cell-surface coreceptors consisting of Fz and LRP5/6, cytoplasmic β-catenin is stabilized and enters into the nucleus. In the nucleus, β-catenin associates with the basal transcriptional machinery, such as TATA box binding protein (TBP), and with transcriptional coactivators such as CREB-binding protein (CBP)/p300 and Brg1. By binding to Tcf/Lef, β-catenin displaces Groucho to stimulate the transcription of target genes, including *c-Myc*, *cyclinD1*, and *Axin2* (Hurlstone et al., 2002). This pathway regulates mainly cellular proliferation and differentiation.

2.2. β-Catenin-independent pathway

Some Wnts, such as Wnt5a and Wnt11, activate a β-catenin-independent pathway that primarily modulates cell movement, as initially observed during embryogenesis (Kikuchi et al., 2008, 2011; Veeman et al., 2003) (Fig. 2.1). There are at least two pathways in the β-catenin-independent pathway. The planar cell polarity (PCP) pathway, which was originally identified in *Drosophila*, is mediated by Fz and dishevelled (Dvl) and activates small GTP-binding proteins (G proteins), including Rac and Rho, and protein kinases, such as c-Jun N-terminal kinase (JNK) and Rho-associated kinase (Rho-kinase), thereby regulating tissue polarity and cell migration (Zallen, 2007). Experiments performed in *Xenopus* and zebrafish embryonic systems also confirm that Wnt5a or Wnt11 signaling regulates cell migration and polarity, including convergent extension (CE) movement (Veeman et al., 2003). Therefore, it seems that the PCP pathway coordinates the cytoskeleton. In mammals, knockout mice of Wnt5a show the PCP phenotype in the cochlea, including shortness of the cochlea duct and a discontinuous additional row of outer hair cells (Qian et al., 2007), and Wnt5a activates Rac to stimulate cell migration (Kikuchi et al., 2008, 2011).

Another β-catenin-independent pathway, the Ca^{2+} pathway, can increase the intracellular Ca^{2+} concentration and activate calcium/calmodulin-dependent protein kinase (CaMK) II and protein kinase C (PKC; Veeman et al., 2003) (Fig. 2.1). Injection of Wnt5a or Wnt11 mRNA into zebrafish or *Xenopus* embryos doubled the frequency of calcium transients (Sheldahl et al., 1999; Slusarski et al., 1997). Dvl also showed a modest ability to activate Ca^{2+} signaling in Ca^{2+} flux, classical PKC (cPKC), and CaMKII assays. PKCδ, a novel PKC (nPKC), has been shown to form a complex with Dvl and to be required to translocate Dvl to the cell membrane in response to *Xenopus* Fz7, which is a possible receptor for Wnt11 (Kinoshita et al., 2003). PKCδ was also found to be required for proper CE movement. In mammalian cells, Wnt5a also elicits an intracellular release of Ca^{2+}, thereby activating PKC, CaMKII, and calpain to regulate cellular functions including cell migration (Ishitani et al., 2003; O'Connell et al., 2009; Weeraratna et al., 2002). It is not clear how the β-catenin-independent pathway induces intracellular Ca^{2+} mobilization. One possible mechanism is via heterotrimeric G proteins. Phospholipase C-β (PLC-β) may generate inositol 1,4,5 triphosphate (IP3) in response to these Wnts because rat Fz2 leads to activation of Ca^{2+} transients in zebrafish embryos through pertussis toxin-sensitive heterotrimeric G proteins (Slusarski et al., 1997). Stimulation of heterotrimeric G proteins is also associated with the activation of increased activity of cGMP-sensitive phosphodiesterases (PDEs). PDE inhibitors suppress the Ca^{2+} transient induced by Fz2 in zebrafish embryos, suggesting that PDEs function downstream of Fz2 (Ahumada et al., 2002). Although whether specific G proteins couple to Wnt–Ca^{2+} signaling remains to

be clarified, these studies support the hypothesis that Fz2 functions as a G protein-coupled receptor (GPCR), which mediates Ca^{2+} release in the β-catenin-independent pathway.

2.3. Inhibition of the β-catenin-dependent pathway by Wnt5a

Wnt5a, a representative ligand that activates the β-catenin-independent pathway, was shown to inhibit the β-catenin pathway (Kikuchi et al., 2011) (Fig. 2.1). Initial evidence was provided using *Xenopus* embryos, in which Wnt5a suppressed axis duplication induced by the expression of Xwnt-8, which activates the β-catenin pathway (Torres et al., 1996). Several possible mechanisms have been proposed for the inhibitory action of Wnt5a on the β-catenin pathway. First, Wnt5a has been demonstrated to inhibit the β-catenin pathway by affecting receptors (Sato et al., 2010). Because Wnt5a inhibits the binding of Wnt3a to Fz2, Wnt5a may compete with Wnt3a for binding to Fz, thereby suppressing the β-catenin pathway. Second, Wnt5a was shown to induce the expression of Siah2, which is an ubiquitin E3 ligase involved in the degradation of β-catenin (Topol et al., 2003). Therefore, Wnt5a signaling might affect β-catenin stability. Third, it was shown that Wnt5a inhibits β-catenin-dependent gene expression downstream of β-catenin probably through the activation of Nemo-like kinase (NLK) or retinoic acid-related orphan nuclear receptor (RORα; Ishitani et al., 1999, 2003; Lee et al., 2010; Mikels et al., 2006). In the former case, Wnt5a activates CaMK through the activation of TGF-β activated kinase (TAK), thereby activating NLK, which phosphorylates and inhibits the β-catenin-dependent transcriptional activity of Tcf. In the latter case, Wnt5a activates PKCα, leading to the phosphorylation of RORα, which inhibits the recruitment of coactivators, such as p300 and CBP, to the promoter region of β-catenin-dependent Tcf-target genes. Thus, it is likely that Wnt5a negatively regulates the β-catenin pathway by multiple steps at the cell surface, in the cytoplasm, and in the nucleus.

3. Wnt Proteins Have Unique Properties

Wnt proteins contain a signal sequence followed by a highly conserved distribution of cysteine residues. An active Wnt protein was difficult to purify, and this difficulty was because of its biochemical characteristics. At present, it is possible to purify Wnt3a and Wnt5a to near homogeneity from conditioned medium (Kishida et al., 2004; Kurayoshi et al., 2007; Mikels et al., 2006; Sato et al., 2010; Willert et al., 2003). Conditioned media (CM) containing Wnt1, Wnt2b, Wnt7a, and Wnt11 have been reported (Bradley et al., 1995; Hirabayashi et al., 2004; Hwang et al., 2004; Nakagawa et al., 2003;

Pandur et al., 2002). Wnt1 CM induces the transformation of C57MG cells, Wnt2b CM stimulates the proliferation of retinal cells, Wnt7a CM induces differentiation of chondrocytes and neuroprogenitor cells, and Wnt11 CM triggers differentiation to cardiac muscle cells. However, these Wnt proteins have not yet been purified. Clarification of the biological activities of purified Wnt proteins is important for understanding the mechanistic details of Wnt signaling.

3.1. Posttranslational glycosylation of Wnt proteins

Molecules that are secreted from cells are often posttranslationally modified. Experiments using tunicamycin (an inhibitor of N-linked glycosylation) have shown that Wnt1, Wnt3a, Wnt5a, Wnt5b, Wnt6, and Wnt7b enter the endoplasmic reticulum (ER) and are glycosylated (Smolich et al., 1993) (Fig. 2.2A). Wnt3a is glycosylated at N87 and N298 and is sensitive to *N*-glycosidase F and endoglycosidase H, suggesting that Wnt3a is modified with high mannose or hybrid-type *N*-glycans (Komekado et al., 2007). Wnt5a is suggested to be modified with *N*-glycans on at least three of N114, N120, N311, and N325 (Kurayoshi et al., 2007). Mutations of these asparagine residues to glutamine impair the secretion of Wnt3a and Wnt5a. Therefore, glycosylation plays an important role in their secretion. However, when purified Wnt3a and Wnt5a are deglycosylated *in vitro*, the unglycosylated forms of Wnt3a and Wnt5a retain their signaling capabilities, suggesting that glycosylation is not necessary for their actions after secretion (Komekado et al., 2007; Kurayoshi et al., 2007). It is unclear whether each Wnt is secreted to the apical or basolateral membrane side of polarized epithelial cells. Because glycosylation is involved in the delivery of proteins to appropriate subcellular destinations (Vagin et al., 2009), it would be important to examine roles of glycosylation in the polarized secretion of Wnt.

3.2. Posttranslational lipidation of Wnt proteins

The hydrophobic characteristics of Wnt could be based on posttranslational modifications by lipids. One of the reasons for the difficulty of purifying Wnts is their insolubility because of their hydrophobicity. Wnt3a is modified with palmitate at Cys77 and palmitoleic acid at Ser209 (Takada et al., 2006; Willert et al., 2003), and Wnt5a is modified at least with palmitate at Cys104 (Kurayoshi et al., 2007) (Fig. 2.2B). These cysteine and serine residues are basically conserved among Wnt family proteins although there are some exceptions, but whether other Wnts are modified with palmitates is not known. Palmitoleic acid attachment at Ser209 is essential for the secretion of Wnt3a (Takada et al., 2006). However, palmitoylation at Cys77 is not essential for the secretion of Wnt3a, rather it is involved in its activities (Komekado et al., 2007;

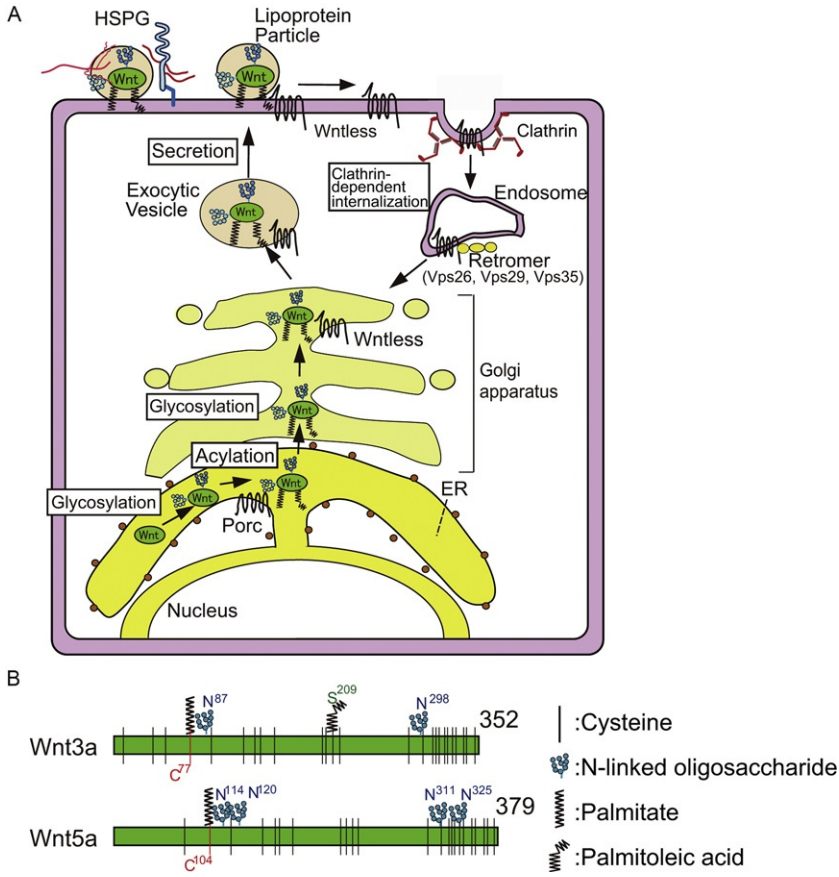

Figure 2.2 Posttranslational modifications of Wnt and its trafficking. (A) Regulation of intracellular and extracellular trafficking of Wnt. Wnts enter into the ER, where initial glycosylation and acylation occur. Wnts are transported to the Golgi complex, where they interact with Wntless (Wls), which supports the transport of Wnts from the *trans*-Golgi network (TGN) to the plasma membrane. After Wnts are secreted from the cell surface as a mature and active form, Wnts associated with HSPGs or other extracellular matrix components are transported to target cells. After the release of Wls, Wls is internalized through clathrin-mediated endocytosis and transported back to the TGN through a retromer-dependent trafficking step. Porc, Porcupine; HSPG, heparan sulfate proteoglycan. (B) Structures and posttranslational modifications of Wnt3a and Wnt5a. Amino acids that are modified posttranslationally are indicated.

Willert et al., 2003). By removing palmitoylation at Cys77, Wnt3a does not bind to its receptors, Fz8 and LRP6, or soluble Frizzled-related protein2 (sFRP2), and does not induce the internalization of LRP6 and, therefore, loses the ability to induce the accumulation of β-catenin (Komekado et al., 2007). Wnt5a defective in palmitoylation at Cys104

is secreted but neither binds to Fz5 nor induces the internalization of Fz5, and, therefore, lacks the abilities to inhibit Tcf activity and to stimulate cell migration (Kurayoshi et al., 2007).

Wingless (Wg), an ortholog of Wnt1 in *Drosophila*, has conserved Cys93 and Ser239 (Franch-Marro et al., 2008). Without palmitoylation at Cys93, Wg fails to be secreted and accumulates in the ER. A mutation of Wg with Ser239 changed to Ala is secreted but shows poor signaling activity. These results suggest that the roles of lipidation are different between mammalian Wnts and *Drosophila* Wg.

Porcupine (Porc), a protein with structural similarities to membrane-bound *O*-acyltransferase in *Drosophila*, has been suggested to be a membrane-bound acyltransferase (Hofmann, 2000; Nusse, 2003) (Fig. 2.2A). It has been reported that *Drosophila porc* is required for Wg-producing cells to generate the fully functional protein signal (van den Heuvel et al., 1993) and for secreting Wg (Tanaka et al., 2000). Four different types of mouse *Porc* (Mporc A, B, C, and D) are generated from a single gene by alternative splicing (Tanaka et al., 2000). NIH3T3 cells express multiple types of *Mporc* mRNA, suggesting that alternative splicing can occur in a single cell. Although there is no direct evidence showing that Porc acylates Wnt3a, expression of Porc increases the hydrophobicity of Wnt3a in cultured mammalian cells and chick neural tube (Galli et al., 2007; Komekado et al., 2007), and Porc is required for Ser209-dependent lipid modification (Takada et al., 2006). It remains to be clarified whether Porc is directly responsible for the attachment of the two different lipids or whether additional acyltransferases are involved. In addition, how different posttranslational modifications, glycosylation and lipidation, of Wnt are interdependent and whether this process is similarly regulated in all Wnts is an important topic for furthering the understanding of the biochemical characteristics of Wnt proteins.

3.3. Wntless and intracellular trafficking of Wnts

Wntless (Wls; also Eveness interrupted or sprinter) was identified as a component required for the secretion of Wg and Wnt (Banziger et al., 2006; Bartscherer et al., 2006) (Fig. 2.2A). Wls is a seven-pass membrane protein and is evolutionally conserved in a number of species from *Caenorhabditis elegans* (*C. elegans*) and *Drosophila* to mouse and human. A Wls loss-of-function mutation in *Drosophila* was rescued by providing Wg-producing cells, and secretion of Wnt3a was impaired but that of tumor necrosis factor (TNF) or Hedgehog was not in Wls-depleting mammalian cells. Therefore, Wls could be specifically required for Wnt secretion. Wnt1, Wnt3a, and Wnt5a form a complex with Wls. Although Wnt3a mutant that lacks palmitoylation or glycosylation still binds to Wls (Banziger et al., 2006; Komekado et al., 2007), Wnt3a that lacks palmitoleic acid modification does not (Coombs et al., 2010), suggesting that acylation of Wnt3a at

Ser209 is required for binding to Wls. These findings are consistent with the observation that mutation of Wnt3a at Ser209 failed to be secreted (Takada et al., 2006). Wls is localized at the plasma membrane, the Golgi complex, and in the cytoplasm, and in the absence of Wls, Wg accumulates predominantly in the Golgi (Bartscherer et al., 2006; Port et al., 2008). Therefore, it is likely that Wls facilitates the Golgi exit of Wnt and Wg, possibly by binding to Wnt and Wg and concentrating them in vesicles destined for delivery to the plasma membrane. However, another *Drosophila* Wnt, WntD (Wnt inhibitor of dorsal), has conserved Cys51 but not the serine residue corresponding to Ser209 of Wnt3a and is considered not to be modified with lipids (Ching et al., 2008). WntD is secreted outside of WntD-expressing cells in the wing disk of a *wls* homozygous mutant (Ching et al., 2008). However, a dominant-negative form of Rab1, a small G protein that regulates the transport of intracellular vesicles from the ER to the Golgi complex, suppresses WntD secretion. Therefore, WntD could be sorted to an alternative secretory route, independently of Wls.

Gpr177, a mouse ortholog of *Drosophila Wls*, is expressed during formation of the embryonic axis, and its disruption exhibits defects in establishment of the body axis, a phenotype resembling of a knockout of Wnt3 (Fu et al., 2009). It was also shown that the regulatory region of *Gpr177* contains seven potential Lef/Tcf binding sites and that they are responsible for β-catenin-dependent transcription (Fu et al., 2009). Therefore, *Gpr177* might be a direct target of the β-catenin pathway and involved in the secretory process in a feedback regulatory manner.

Retromer was originally identified in yeast as a protein complex involved in retrograde transport from the endosomes to the *trans*-Golgi network (TGN; Bonifacino et al., 2008). The retromer complex comprises a sorting nexin (snx) dimer that mediates membrane attachment and a cargo recognition trimer composed of Vps35, Vps29, and Vps26 (Bonifacino et al., 2008). Because mutations in Vps35 or its knockdown reduced Wnt gradient formation and the expression of Wnt target genes in *C. elegans* and mammalian cultured cells, the retromer complex was found to be important for Wnt signaling in Wnt-producing cells, suggesting that intracellular recycling factors are necessary for Wnt secretion (Coudreuse et al., 2006) (Fig. 2.2A). Because the absence of Vps35 or Vps26 function in *C. elegans*, *Drosophila*, or cultured mammalian cells reduced Wls levels, it is conceivable that retromer is responsible for routing Wls into a retrograde trafficking pathway that transports transmembrane proteins from the endosomes to the TGN (Port et al., 2008, 2010). When retromer is absent, Wls is trapped in the endosomes and finally degraded in the lysosomes. Therefore, the target of retromer in Wnt-producing cells is Wls. Taken together, Wls functions to facilitate maturation, sorting, and secretory processes of Wnts.

3.4. Extracellular trafficking and stabilization of Wnt

How Wnts with hydrophobic properties can spread in an aqueous environment remains elusive. Several possible mechanisms have been proposed, especially using *Drosophila* embryos: (i) Wnt might be distributed by direct transfer from cell to cell through binding to HSPGs, (ii) Wnt could be secreted on membranous lipoprotein particles, and (iii) the lipid modification of Wnt could be masked inside micelle-like aggregates. Although other mechanisms have been reported, it seems likely that the tissue type and its developmental status influence which mechanisms are used and to what extent.

Once secreted, Wnt interacts with glycosaminoglycans (GAGs) in the extracellular matrix and binds tightly to the cell surface (Bradley et al., 1990; Reichsman et al., 1996) (Fig. 2.2A). HSPGs are cell-surface and extracellular matrix macromolecules that are composed of a core protein modified with covalently linked GAG chains. Studies in *Drosophila* and vertebrates have demonstrated the critical roles of HSPGs in several growth factor signaling activities during development (Couchman, 2003; Lin, 2004). The functions of HSPGs in Wg signaling were first revealed by the identification of *sugarless* (*sgl*) and *sulfateless* (*sfl*) in *Drosophila*. *Sgl* and *Sfl* encode UDP-glucose dehydrogenase and *N*-sulfotransferase, respectively, and their mutants are defective in GAG biosynthesis and HS modification. *Sgl* and *Sfl* mutant embryos exhibit phenotypes similar to Wg mutant and lead to reduced extracellular Wg protein levels and to the reduced expression of a target gene (*Distalless*) in wing imaginal discs. Other GAG biosynthetic mutants showed the accumulation of Wg in the cell front and also reduced target gene expression (Takei et al., 2004). It has been demonstrated that HSPG core proteins are also involved in Wg signaling (Lin, 2004). As HSPGs, *Dally* and *Dlp*, two *Drosophila* glypicans (GPCs), which are attached to the cell surface by means of a glycosylphosphatidylinositol (GPI) anchor, function in Wg signaling. Double knockdown for *Dally* and *Dlp* shows more severe Wg phenotypes in embryos than single knockdowns for either of them (Baeg et al., 2001). Overexpression of Dlp has been reported to increase extracellular Wg protein levels by binding to Wg, thereby inhibiting its signaling (Baeg et al., 2004). These results suggest that HSPGs have positive and negative roles in Wg signaling. Wg can be transported by passive diffusion through the extracellular space by attaching to HSPGs (Belenkaya et al., 2004; Tabata et al., 2004). However, it was difficult to show that HSPGs affect the extracellular distribution of endogenous Wnt in mammalian tissues, rather they were shown to maintain the solubility of Wnt, thus stabilizing their activity (Fuerer et al., 2010). Therefore, the roles of HSPGs are not only to concentrate Wnt at the cell surface but also to prevent them from aggregating and inactivating in the extracellular environment.

It is also possible that Wnt is secreted and spread by being attached to membranous vesicles. In *Drosophila*, Wg derived from wing disk was found to be copurified with lipoprotein particles (Panakova et al., 2005). Larvae with reduced lipoprotein particles (siRNA against lipophorin) showed a narrow expression of *Distalless* in wing porch. In mammals, Wnt3a was released from mouse fibroblasts by the presence of lipoproteins in the culture medium, and the release occurred through high-density lipoprotein (HDL) particles specifically (Neumann et al., 2009). Lipoprotein particles are large, globular complexes composed of a central core of hydrophobic lipids that are associated with apoproteins and surrounded by a monolayer of membrane phospholipids. Wnt3a was active under these conditions, and Wnt3a mutant that lacks palmitate was not associated with lipoproteins. The lipid modification of Wnt3a could be important for targeting Wnt3a to phospholipids of lipoproteins. These results suggest that lipoprotein particles act as machinery for the efficient intercellular movement and stabilization of Wnt3a/Wg.

One of the simplest models is the formation of micelle-like multimers of Wnt. Wnt might form multimers, thereby overcoming their hydrophobicity. Direct evidence for this model has not been reported for Wnt, although the hydrophobic modification of Hedgehog is arranged in a way that the multimers become soluble in a polar medium (Zeng et al., 2001).

4. Cell-Surface Receptors Function in a Context-Specific Manner

4.1. Receptors that regulate Wnt signaling

4.1.1. Frizzled (Fz)

The Fz family belongs to the superfamily of GPCR and has been found in many animal species (Fig. 2.3A). Fzs are seven-pass transmembrane proteins that act as receptors for secreted Wnts (Schulte, 2010; Wang et al., 2006). All Fzs (there are 10 Fzs in humans and mice) share the following structural similarities: a signal peptide sequence at the amino terminus, a conserved region of 120 amino acids in the extracellular domain containing 10 invariantly spaced cysteine residues (called the cysteine-rich domain—CRD), a seven-pass transmembrane region, in which the transmembrane segments are well conserved, and a cytoplasmic domain with little homology among members of the family. The CRD has been shown to be necessary and sufficient for Wnt ligand binding to the surface of expressing cells (Dann et al., 2001).

Although how Fzs mediate Wnt signaling has not yet been elucidated, the binding of Fz and Dvl could be important. Dvl is a critical component of the Wnt signaling pathway to regulate both the β-catenin-dependent and -independent pathways and contains three highly conserved domains: a

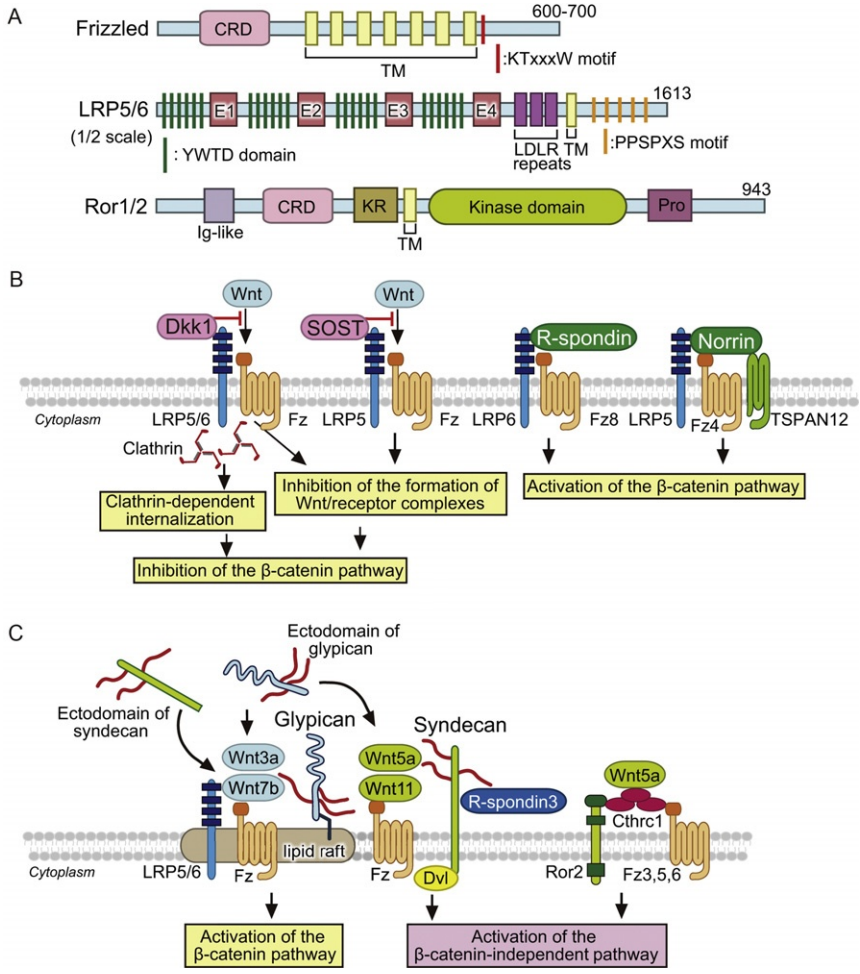

Figure 2.3 Cell surface molecules that regulate Wnt signaling. (A) Schematic presentation of the domain structure of Fz, LRP5/6, and Ror1/2. (B) Ligands that are structurally unrelated to Wnts. Dkk1, SOST, R-spondin, and Norrin interact with Fzs and LRP5/6 or TSPAN12, thereby regulating the β-catenin pathway positively or negatively. (C) Cell surface HSPGs that regulate Wnt signaling. Glypican and syndecan bind to Wnt and concentrate it on the cell surface making it bind to receptors efficiently. CRD, cysteine-rich domain; Cthrc1, collagen triple helix repeat containing 1; Dkk1, Dickkopf 1; E1–4, EGF-like repeats 1–4; Ig-like, immunoglobulin like domain; KR, Kringle domain; LDLR, low-density lipoprotein receptor; Pro, proline-rich domain; TM, transmembrane domain; TSPAN12, tetraspanin 12.

DIX domain, a PDZ domain, and a DEP domain (Wharton, 2003). Although a cytoplasmic domain has little homology among the Fz family members, it contains a small region with a very high level of homology among them. The highest level of homology is confined to the first 25 residues of the N-terminal region of the C-terminal tail. Studies in *Xenopus* embryos have shown that the KTxxxW motif, which is located in two amino acids C-terminal to the seventh transmembrane domain, is necessary for the activation of the β-catenin pathway and for membrane relocalization and phosphorylation of Dvl (Umbhauer et al., 2000). In fact, chemical-shift perturbation NMR spectroscopy revealed that the 12-amino acid peptide containing this sequence of Fz7 binds directly to the PDZ domain of Dvl (Wong et al., 2003) with a K_d of approximately 10^{-5} M. This relatively weak interaction between this Fz7 peptide and the Dvl PDZ domain suggests that other regions of Dvl are required for signal transduction between Fz and Dvl. In addition, mutation of the KTxxxW motif or in the first or the third loop of human Fz5 abolished binding to Dvl and signaling (Cong et al., 2004). Although the DEP domain of Dvl does not bind to the Fz7 peptide, the DEP domain plays a role in the membrane localization of the protein (Axelrod et al., 1998; Boutros et al., 1998). Therefore, signal transduction between Fz and Dvl may require the membrane-targeting function of the DEP domain to bring the two proteins into close proximity to one another.

The following evidence supports the notion that Fzs are coupled with trimeric G proteins. The Wnt-stimulated pathway is sensitive to inactivation by pertussis toxin, an ADP-ribosyltransferase that inactivates only members of the Gi/Go family of G proteins (Liu et al., 1999; Slusarski et al., 1997). β_2-Adrenergic receptor (β_2AR)/RFz1 and β_2AR/RFz2 chimeras, in which the extracellular domain of β_2AR is fused to the transmembrane and cytoplasmic domains of Fzs, display a GTP-dependent and agonist-specific shift in receptor affinity, which demonstrates the direct receptor-G protein interaction (Liu et al., 1999). The *Drosophila* homolog of human Go is essential in the activation of the β-catenin and PCP pathways (Katanaev et al., 2005). Thus, heterotrimeric G proteins might be coupled with Wnt signaling, but direct experimental proof is still lacking (Schulte, 2010).

4.1.2. LRP5/6 and Arrow

LRP5, LRP6, and Arrow, which are type I single-pass transmembrane proteins, are a subfamily of the LDL receptor family, whose members play diverse roles in metabolism and development (Herz et al., 2002) (Fig. 2.3A). These receptors have a long extracellular domain (~1400 amino acids) containing YWTD domains, EGF-like repeats, and LDL receptor repeats, and a short intracellular domain (~200 amino acids) comprising five PPSPXS repeats and juxtaposed casein kinase phosphorylation sites (MacDonald et al., 2009; Niehrs et al., 2010b).

The roles of Arrow and LRP6 in Wnt signaling were discovered via genetic studies. *Drosophila* mutants lacking *arrow* phenotypically resemble the Wg mutant but not the PCP phenotypes (Wehrli et al., 2000), suggesting that Arrow specifically activates the β-catenin pathway. Mutant mice lacking *Lrp6* exhibit combined phenotypes similar to those caused by mutations of several individual Wnt genes (Pinson et al., 2000). Although LRP5 is expressed during embryogenesis, mice deficient in *Lrp5* do not show any developmental abnormality but exhibit a low bone mass formation and decreased osteoblast formation and function only postnatally (Kato et al., 2002). It is believed that LRP5 and LRP6 activate the β-catenin pathway because expression of LRP5 and LRP6 in mammalian cultured cells increases the ability of Wnt to enhance β-catenin-dependent transcriptional activity. However, it was also reported that overexpression of the extracellular domain of LRP6 inhibits the β-catenin-independent pathway by binding to Wnt5a and that the phenotypes by deletion of LRP6 in mice and *Xenopus* embryos are rescued by the additional deletion of Wnt5a (Bryja et al., 2009). These results suggest that the extracellular domain of LRP6 behaves as a physiologically relevant inhibitor of the β-catenin-independent pathway during *Xenopus* and mouse development *in vivo*.

A LRP6 mutant lacking the intracellular domain is completely inactive and it blocks Wnt and Fz signaling in a dominant-negative manner (Tamai et al., 2004). Conversely, LRP5/6 mutants that lack the extracellular domain activate the β-catenin pathway constitutively in mammalian cells (Liu et al., 2003; Mao et al., 2001a,b) and *Xenopus* embryos (Tamai et al., 2004), suggesting the extracellular domain autoinhibits receptor signaling. In *Drosophila* although a similar truncated form of Arrow does not activate Wg signaling in *Drosophila*, a chimera containing the intracellular domain of Arrow fused to the C-terminus of DFz2 activates Wg target genes (Tolwinski et al., 2003). These results indicate that misexpression of truncated Arrow from a single-copy transgene is not sufficient to bypass the other branch of Wg signaling. How LRP6 mediates the Wnt signal to activate the β-catenin pathway is discussed in the following session.

4.1.3. Ror1/2

Ror, which is a single-pass transmembrane protein with a tyrosine kinase domain, also functions as a coreceptor in Wnt signaling (Green et al., 2008; Nishita et al., 2010a) (Fig. 2.3A). The Ror family of RTKs, which consists of two structurally related proteins, Ror1 and Ror2, is characterized by an extracellular CRD, a membrane proximal Kringle (KR) domain, and intracellular cytoplasmic tyrosine kinase and proline-rich domains (Forrester et al., 1999). Ror2 is expressed primarily in neural crest-derived cells and mesenchymal cells during mouse embryogenesis and plays crucial roles in developmental morphogenesis (Matsuda et al., 2001). Ror2-deficient mice exhibit skeletal, genital, cardiovascular, and respiratory

abnormalities, presumably because of partly disrupted CE movements during gastrulation (Oishi et al., 2003). The phenotypes of Wnt5a knockout mice are similar to those of mice lacking Ror2 compared with those lacking Fzs, indicating that Ror2 could be more closely involved in specific activation of Wnt5a signaling. Importantly, mutations in human *ROR2* or *WNT5a* lead to Robinow syndrome, which is characterized by short stature, rib fusions, genital hypoplasia, cardiac malformations, and facial clefting (Person et al., 2010; van Bokhoven et al., 2000). These results strongly support the idea that Ror2 mediates Wnt5a and β-catenin-independent signaling.

Ror2 by itself or in combination with Fzs can mediate diverse Wnt5a signaling activities. Wnt5a, Fzs (Fz5, Fz6, or Fz7), and Ror2 have been indeed shown to form a ternary complex (Nishita et al., 2010b; Yamamoto et al., 2008b). The extracellular domain of Ror2 associates with Wnt5a (Mikels et al., 2006). It has also been reported that although both Wnt5a and Wnt3a bind to Ror2, only Wnt5a induces the dimerization of Ror2 (Liu et al., 2008a). In response to Wnt5a, Ror2 stimulates cell migration by binding to filamin A and inhibits the β-catenin pathway in mammalian cells (Mikels et al., 2006; Nishita et al., 2006). In *Xenopus*, Wnt5a and Ror2 regulate CE through the activation of Cdc42 and JNK, which enhances the expression of paraxial protocadherin (Schambony et al., 2007). CAM-1, the *C. elegans* ortholog of Ror2, has been implicated in cell migration, asymmetric cell division, and axonal extension during embryogenesis (Forrester et al., 1999). It has been noted that tyrosine kinase domain is required for Wnt5a-induced formation of invadopodia but not for Wnt5a-induced cell migration and filopodia formation (Nishita et al., 2010a). Although Ror1, which is another member of the Ror family, has been less investigated, it could be another Wnt5a receptor considering the finding that Wnt5a binds to Ror1 and induces its phosphorylation (Fukuda et al., 2008; Grumolato et al., 2010).

4.1.4. Ryk

Ryk and its *Drosophila* (Derailed, Drl) and worm (LIN-18) orthologs are the single-pass transmembrane proteins with an extracellular Wnt-binding WIF (a secreted Wnt inhibitor) domain, a putative tetrabasic cleavage site, an intracellular domain bearing the RTK-related catalytic domain, and a C-terminal PDZ-binding domain (Fradkin et al., 2009). In the *Drosophila* embryonic nervous system, Derailed is expressed in the anterior-most of two commissures and controls the trajectories of axons that cross the ventral midline (Bonkowsky et al., 1999). DRL binds WNT5, and *drl* mutants display improper axonal guidance across the midline similar to that observed in *Wnt5* mutants (Yoshikawa et al., 2003). In *Xenopus* embryos, Ryk forms a complex with Wnt11 and Fz7 to cause the β-arrestin-2-mediated endocytosis of Dvl, which is necessary for CE (Kim et al., 2008). In mammals,

Wnt5a has been shown to simultaneously increase axon growth and induce repulsive axon guidance through Ryk (Li et al., 2009).

Conversely, it was reported that although Wnt5a expression is low in adult spinal cord, the level of Wnt5a increases in reactive astrocytes around the injury site following a spinal cord injury (Miyashita et al., 2009). Damaged cortical spinal tracts also showed the increase in Ryk expression (Liu et al., 2008b). In rats with thoracic spinal cord contusion, intrathecal administration of a neutralizing antibody to Ryk resulted in significant axonal growth of the corticospinal tract and enhanced functional recovery. Because Wnt5a inhibits the neurite growth of postnatal cerebellar neurons by activating RhoA/Rho-kinase *in vitro* (Miyashita et al., 2009), reexpression of the embryonic repulsive cues, such as Wnt5a and Ryk, in adult tissues might contribute to the failure of axon regeneration in the central nervous system.

These results suggest that Ryk mediates the β-catenin-independent pathway. However, mammalian Ryk also forms a complex with Fz8 and Wnt1, and Wnt1 and Wnt3a activate the β-catenin pathway in Ryk-expressing cells (Lu et al., 2004a). The WIF domain interacts with the CRD of Fz8, and these two proteins form a ternary complex with Wnt1, and Ryk and Dvl interact with each other. Wnt3a-dependent neuronal extension from the dorsal root ganglion requires Ryk, and knockdown of Ryk reduces the Wnt1-dependent Tcf activation in HEK293T cells. Therefore, Ryk may mediate multiple Wnt signaling pathways in a context-dependent manner. However, it is not clear how Ryk activates the intracellular signaling cascade after binding to Wnts.

4.1.5. Protein tyrosine kinase 7

Protein tyrosine kinase 7 (PTK7) is a single-pass transmembrane protein containing extracellular immunoglobulin domains and an intracellular tyrosine kinase homology domain, although the kinase domain lacks the DFG triplet motif (Lu et al., 2004b). Deletion or disruption of PTK7 generates comparable effects as core *PCP* genes and Wnt5a-like craniorachischisis (Lu et al., 2004b; Paudyal et al., 2010; Shnitsar et al., 2008). In *Xenopus* embryos, PTK7 recruits Dvl to the plasma membrane which requires its kinase domain, and PTK7 is necessary for Fz7-dependent phosphorylation of Dvl. A kinase motif deletion mutant of PTK7 inhibits neural crest migration (Shnitsar et al., 2008). Although these results implicate that PTK7 is involved in the Wnt5a/β-catenin-independent pathway, it remains to be proved that Wnt5a binds directly to PTK7.

4.1.6. Tetraspanin

The tetraspanin family is characterized by the existence of common four-pass transmembrane domains with two extracellular regions that are distinguished from other four-pass transmembrane domain proteins (Serru et al., 2000). Among tetraspanin family members, TSPAN12 is expressed in the

retinal vasculature, and loss of *Tspan12* reduces intraretinal capillaries (Junge et al., 2009), which was observed in *Fz4*, *Lrp5*, and *Norrin* mutant mice (Xia et al., 2008; Xu et al., 2004). TSPAN12 binds to Fz4 and promotes multimerization of Fz4 cooperatively with Norrin (see Section 4.2.4), thereby activating the β-catenin pathway (Junge et al., 2009). Although TSPAN12 is required for Norrin signaling but not for Wnt3a signaling, it is likely that receptor oligomerization including Fz4 clustering plays roles in the activation of the β-catenin pathway (Bilic et al., 2007).

4.1.7. Vangl

Van Gogh (also known as Vang or Strabismus) is a four-pass transmembrane protein and a core PCP component in *Drosophila* (Zallen, 2007), and the protein functions as a binding protein to the CRD of Fz in a cell–cell contact region to establish proper PCP along proximo-distal axis in developing wing epithelia (Wu et al., 2009b). There are two vertebrate orthologs, Vang like 1 and 2 (Vangl1 and Vangl2). Mutations in human *VANGL1* and *VANGL2* have been identified in neural-tube defects, which are typical phenotypes resulting from the disruption of CE (Lei et al., 2010). It has been shown that *Vangl2* interacts genetically with *Wnt5a* (Qian et al., 2007). Further, Wnt5a induces a complex formation between Ror2 and Vangl2 and phosphorylation of Vangl2 through CK1δ (Gao et al., 2011). The phosphorylation is important functionally because the phosphorylation site mutants of Vangl2 could not rescue CE failure in zebrafish. Vangl2 has also been reported to be required with Fz3 for Wnt5a-stimulated outgrowth and anterior–posterior guidance of commissural axons (Shafer et al., 2011). Vangl2 promotes PCP signaling by antagonizing Dvl1-mediated feedback inhibition in growth cone guidance. Although there are no data showing that Wnt5a binds to Vangl2, Vangl2 might act as a cofactor in Wnt5a/β-catenin-independent signaling.

4.2. Ligands that regulate signaling by binding to Wnt receptors other than Wnts

Our knowledge of ligands involved in the Wnt signaling pathway has expanded considerably, and it was found that proteins structurally unrelated to Wnts can also regulate Wnt signaling pathways (Hendrickx et al., 2008).

4.2.1. Dickkopf (Dkk)

The Dkk family comprises four members (Dkk1–Dkk4), which antagonize Wnt signaling (Niehrs, 2006). Dkks contain two characteristic cysteine-rich domains (CRD-1 and CRD-2) separated by a linker region of variable length (Glinka et al., 1998). CRD-2, in particular, is highly conserved among all members of the family and contains 10 conserved cysteine residues. The characteristic developmental function of Dkk1 is its head-inducing activity.

Dkk1 is expressed in the anterior endomesoderm of the Spemann organizer of *Xenopus* embryos (Glinka et al., 1998). Dkk1-knockout mice lack anterior head structures, indicating that Dkk-1 is essential for head formation (Mukhopadhyay et al., 2001).

Dkk1 prevents activation of the Wnt signaling pathway by binding to LRP5/6 (Bafico et al., 2001; Mao et al., 2001a) (Fig. 2.3B). The C-terminal domains of Dkk1 and Dkk2, which contain the CRD-2 region, are necessary and sufficient for association with LRP6 (Li et al., 2002). There are two possible mechanisms by which Dkk1 might inhibit the β-catenin pathway. One possibility is that Dkk1 prevents the formation of Wnt/Fz/LRP6 complexes on the cell surface by binding to LRP6 (Semënov et al., 2001, 2008). In this scenario, Dkk1 does not induce the internalization of endogenous LRP6 but does inhibit β-catenin signaling. Another possibility is that Dkk1 induces rapid endocytosis of LRP6, and internalized LRP6 is localized with clathrin (Mao et al., 2001a; Sakane et al., 2010; Yamamoto et al., 2008a). Knockdown of clathrin blocks Dkk1-induced internalization of LRP6 and the Dkk1-dependent inhibition of Wnt3a-induced β-catenin accumulation, although it does not affect the Wnt3a-dependent accumulation of β-catenin (Yamamoto et al., 2008a). At present, the reasons for the discrepancy between these studies are not known.

4.2.2. SOST/Sclerostin

SOST is a secreted protein that shares 36% identity with WISE, which binds to LRP6 and activates or inhibits Wnt signaling in a context-dependent manner (Itasaki et al., 2003) (Fig. 2.3B). A loss of function of the *SOST* gene is linked to sclerostenosis, an autosomal recessive craniotubular hyperostosis (Beighton et al., 1976). This disease is characterized by generalized overgrowth of bone tissue, mostly manifested in cranial bones and in the diaphysis of tubular bones. SOST expression is confined specifically to osteoblasts and osteocytes postnatally (Winkler et al., 2003), and an increased rate of bone formation and elevated levels of alkaline phosphatase and osteocalcin are associated with *SOST* mutation carriers. A loss of SOST function results in phenotypes related to excessive LRP5 function. These results imply that SOST may antagonize LRP5 function.

Consistent with this idea, SOST inhibits ectopic axis duplication and Xnr3 expression induced by Xwnt-8 in *Xenopus* embryos, and it also inhibits Wnt1-induced Tcf activation in mammalian cells (Semënov et al., 2005). Further, SOST binds to both LRP5 and LRP6 and disrupts the Fz–LRP6 complex formed in the presence of Wnt1, thereby inhibiting the β-catenin pathway (Li et al., 2005; Semënov et al., 2005). Thus, SOST acts as an antagonist for Wnt signaling by binding to LRP5 and LRP6 like Dkk1. From these characteristics of SOST, it may be possible to develop medicines that block the actions of SOST for the treatment of osteoporosis.

4.2.3. R-spondin

R-spondin was originally identified as a human protein of unknown function containing a leading signal peptide, a cysteine-rich region with two furin-like domains, one thrombospondin type I domain, and a C-terminal region with positively charged amino acids (Chen et al., 2002; Hendrickx et al., 2008) (Fig. 2.3B). There are four related genes in this family, *R-spondin1–4*, in the human and mouse genomes. No orthologs of this gene were found in *Drosophila* and *C. elegans*, suggesting that R-spondins are expressed in vertebrates (Kamata et al., 2004; Kazanskaya et al., 2004). Expression of R-spondin1 throughout development is similar to that of Wnt1 or Wnt3a, and R-spondin1 expression is reduced in *Wnt1* or *Wnt3a* knockout mice (Kamata et al., 2004), suggesting that its expression is under the control of Wnt signaling. R-spondin1 was also found to induce the proliferation of cells in intestinal crypt through the stabilization of β-catenin (Kim et al., 2005). R-spondin2 was expressed in the apical ectodermal ridge, and knockout mice for this gene, which die at birth, have limb patterning defects associated with altered β-catenin signaling (Hendrickx et al., 2008). *Xenopus* R-spondin2 was isolated during the screening of a Wnt activator from a *Xenopus* eye library and is required for Wnt-dependent myogenesis in *Xenopus* (Kazanskaya et al., 2004).

The R-spondin family exhibits synergistic activity regulating the β-catenin pathway with Wnt ligands, possibly through direct physical interaction in mammalian cells (Kim et al., 2005). In addition, R-spondin can interact with the extracellular domains of LRP6 or Fz8, although it fails to form a ternary complex with LRP6 and Fz8, unlike Wnt proteins (Nam et al., 2006). Importantly, in contrast to Wnt3a, R-spondin1 could not induce any β-catenin stabilization in fibroblast L cells, suggesting that R-spondin may activate the β-catenin pathway by a mechanism different from Wnt. It has been proposed that R-spondin1 competitively antagonizes Dkk1 through the interaction with Kremen, which was shown to bind to Dkk1 and to be involved in the actions of Dkk1 (Mao et al., 2002), thereby activating the β-catenin pathway (Binnerts et al., 2007). However, this possibility may be unlikely because Kremen is not an essential mediator for Dkk1 function according to the following reports. It was shown that Kremen is not universally required for Dkk1 function using knockout mice (Ellwanger et al., 2008). The knockdown of Kremen did not affect the internalization of LRP6 (Sakane et al., 2010). Moreover, Dkk1 mutants that do not bind to Kremen still antagonized Wnt3a-dependent Lef1 activity (Wang et al., 2008). Thus, the molecular mechanism by which R-spondin activates Wnt signaling remains to be clarified.

It was shown that R-spondin3 activates the β-catenin-independent pathway (Ohkawara et al., 2011). In this scenario, R-spondin3 binds to syndecan-4 (SDC4) and cooperates with Wnt5a and Fz7 to activate JNK in

Xenopus embryos through clathrin-mediated endocytosis (see Section 4.3). Thus, each R-spondin may have different actions on Wnt signaling.

4.2.4. Norrin

Norrin is a secreted protein with a cysteine-knot motif, which is encoded by the Norrie disease gene (Berger et al., 1992). Norrie disease is an X-linked congenital retinal dysfunction that, in most cases, presents with blindness at birth. Several *Norrin* gene mutations have been found in a number of patients with familial exudative vitreoretinopathy (FEVR), which is a developmental disorder characterized by incomplete vascularization of the peripheral retina (Pendergast et al., 1998). One autosomal dominant FEVR locus has been shown to correspond to the *Fz4* gene. Further, there is the similarity in vascular phenotypes caused by Norrin and Fz4 mutations in humans and mice.

As already discussed (see Section 4.1.6), phenotypes such as retinal vascular defects are also observed in mice lacking *TSPAN12* (Junge et al., 2009). Biochemical studies based on these observations have revealed that Norrin specifically binds to Fz4 but not to Fz8, and Norrin multimers cooperate with LRP5 and TSPAN12 to promote oligomerization of Fz4, thereby activating the β-catenin pathway (Junge et al., 2009; Xu et al., 2004) (Fig. 2.3B). Therefore, Norrin is not related to Wnt but acts as a ligand that binds to Fz4 and activates Wnt signaling, and Norrin-Fz4 signaling through LRP5 and TSPAN12 plays a central role in vascular development in the eye.

4.3. Modulation by HSPGs

As discussed in Section 3.4, HSPGs are important for concentrating and stabilizing Wnts on the cell surface. In addition, evidence has accumulated that HSPGs also play a role in Wnt signaling (Fig. 2.3C). To date, six GPCs, cell-surface HSPGs, have been identified in mammals (GPC1–6; Song et al., 2002). GPCs are linked to the exocytoplasmic surface of the plasma membrane through a covalent GPI linkage modified with heparan sulfates at the sites near to a GPI anchor. GPC3 knockout mice embryos exhibit a reduction in JNK activity (Song et al., 2005). GPC3 binds to Wnt5a and enhances Wnt5a-dependent JNK activation in mammalian mesothelioma cells, and interference with GPC3 expression disrupts gastrulation movements in zebrafish (De Cat et al., 2003; Song et al., 2005). Further, zebrafish Knypek (GPC4/6) binds to Dkk1 and potentiates the activity of Dkk1 to activate JNK in zebrafish (Caneparo et al., 2007). *Xenopus* GPC4 interacts with Wnt11 and enhances Wnt-stimulated cell migration in CE (Ohkawara et al., 2003). These results suggest that the GPC family serves as a selective regulator of Wnt signaling by potentiating the β-catenin-independent pathway. However, it has also been reported that GPC3 knockout mice embryos contain elevated levels of β-catenin in the cytoplasm and that

GPC3 binds to Wnt3a and Wnt7b and enhances the Wnt-dependent Tcf activities in hepatocellular carcinoma cell lines, suggesting that GPCs regulate the β-catenin pathway (Capurro et al., 2005).

A transmembrane type HSPG, syndecan (SDC), also regulates Wnt signaling. SDC1–4 have a region near the N-terminus that bears heparan sulfate chains and a transmembrane domain with a C-terminal cytoplasmic region (Bernfield et al., 1999; Couchman, 2003; Tkachenko et al., 2005). Some SDCs are also modified with chondroitin sulfates. Mice with mammary-gland-specific transgenic expression of Wnt1 develop mammary tumors, and SDC1 is required for Wnt1-induced tumorigenesis (Alexander et al., 2000), suggesting that SDC is involved in the regulation of the β-catenin pathway. In contrast, SDC4 was shown to bind to Fz7 and Dvl and regulate CE in *Xenopus* (Munoz et al., 2006). In addition, as discussed in Section 4.2.3, SDC4 interacts with R-spondin3 and is involved in CE in cooperation with Wnt5a and Fz7 in *Xenopus* embryos (Ohkawara et al., 2011). These results suggest that SDC is also involved in the regulation of the β-catenin-independent pathway. Therefore, whether the action of HSPG is positive or negative for β-catenin-dependent or -independent pathway might be dependent on types of cells and tissues.

It was found that GPCs are present in both lipid raft and nonlipid raft microdomains and that SDCs are predominantly in nonlipid rafts (Sakane et al., 2011). GPC4 in lipid raft microdomains activates Wnt3a-dependent activation of the β-catenin pathway, and GPC4 in nonlipid raft microdomains activates Wnt5a-dependent activation of the β-catenin-independent pathway. Therefore, the localization of GPCs in the plasma membrane microdomains might be also important for the selective activation of Wnt signaling.

It is known that the ectodomains of HSPGs are shed into the extracellular space (Bernfield et al., 1999). The SDC1 ectodomain was shown to activate the β-catenin pathway in cultured cells, and this may explain why the knockout of SDC1 suppresses Wnt1-induced mammary tumorigenesis (Alexander et al., 2000). It was also reported that GPC3 is subjected to endoproteolytic processing by convertases in CHO cells and that processed GPC3 modulates both the β-catenin-dependent and -independent pathways (De Cat et al., 2003). The GPC4 ectodomain showed inhibitory actions for both Wnt signaling pathways (Sakane et al., 2011). Taken together, the localization (lipid raft or nonlipid raft microdomains) and form (membrane anchored structure or soluble structure) of HSPGs could be important for the regulation of Wnt signaling.

Drosophila studies have provided interesting findings on the roles of HSPG. In the wing imaginal discs, Wg is found in specialized membrane vesicles called lipoprotein particles (see Section 3.4), which are thought to be derived from lipid raft microdomains (Panakova et al., 2005). Incorporation of Wg into lipoprotein particles requires HSPGs, suggesting that proteoglycans play a role in sorting Wg to specialized membrane

microdomains in Wg-producing cells or alternatively is involved in localizing Wg to distinct endocytic compartments in receiving cells. Overexpression of Dlp causes a decrease in extracellular Wg on the apical surface of Wg-expressing cells and an increase on the lateral surface of receiving cells, suggesting that Dlp plays a role in the delivery of Wg to the lateral surface of wing imaginal discs (Gallet et al., 2008). Whereas the absence of Dlp near the Wg-expressing cells increases Wg signaling, a defect in Dlp far from the Wg source decreases Wg signaling (Kirkpatrick et al., 2004; Kreuger et al., 2004). Thus, Dlp appears to have dual functions in Wg signaling. These suggest that Wg may be secreted apically in the disk epithelium and is then endocytosed with receptors and HSPGs. Once internalized, Dlp targets Wg by transcytosis to the lateral component, where it is stabilized and can spread away to activate long-range target genes.

It has been demonstrated that collagen triple helix repeat containing 1 (Cthrc1), a chordate-specific secreted glycoprotein, may be involved in specific activation of the PCP pathway (Yamamoto et al., 2008b) (Fig. 2.3C). When Cthrc1 is deleted in *Vangl2* heterozygous mice, significant PCP phenotypes are observed, indicating a genetic interaction between *Cthrc1* and the core *PCP* gene *Vangl2*. Expression of Cthrc1 stimulates Wnt3a- and Wnt5a-dependent Rho and Rac activities and suppresses Wnt3a-dependent Tcf transcriptional activity in HEK293 cells. In addition, Cthrc1 enhances the formation of a complex between Wnt (Wnt3a/5a), Fz (Fz3/5/6), and Ror2, whereas it does not influence the interaction of Wnt, Fz, and LRP6. These results suggest that Cthrc1 enhances selectively the interaction of Wnt with its receptors (Fz and Ror2). Such selective enhancement of a ligand–receptor interaction by a cofactor may be an important molecular basis of the specific activation of the β-catenin-dependent or -independent pathways among multiple Wnt signaling pathways.

5. How Do Multiple Wnts Activate a Specific Pathway Selectively?

5.1. Pairing of Wnt proteins and receptors

The Wnt–Fz ligand–receptor relationship was first characterized in *Drosophila* molecules. Two members of the Fz family, Dfz1 and Dfz2, bind to Wg with a K_d value of 10^{-8} and 10^{-9} M, respectively (Bhanot et al., 1996; Rulifson et al., 2000). *Drosophila* mutants lacking both *Dfz1* and *Dfz2*, but not mutants lacking either, have severely defective Wg signaling (Bhat, 1998; Kennerdell et al., 1998), providing evidence that Dfz1 and Dfz2 are partially redundant Wg receptors in many contexts. A *Dfz1* mutant but not a *Dfz2* mutant shows the PCP phenotypes, indicating that Dfz1 mainly

regulates the PCP pathway. However, ligand(s) that activate the PCP pathway have not yet been identified.

Although studies in *C. elegans*, *Xenopus*, and mammalian cells support the Wnt–Fz ligand–receptor relationship (He et al., 1997; Hsieh et al., 1999; Sawa et al., 1996), the specificity of the Wnt–Fz interaction remains largely unknown, particularly in vertebrates, because of the large numbers of Wnts and Fzs. Accumulated results do not provide evidence of simple, specific interactions between Wnts and Fzs. Among the mammalian Fz family, Wnt3a signaling could be mediated through at least Fz3, Fz4, Fz5, and Fz8 but not Fz6 from assessment of the phosphorylation of dishevelled (Dvl ortholog) in *Drosophila* S2 cells (Takada et al., 2005). In this assay, Wnt5a also induces the phosphorylation of dishevelled through the same Fzs (Takada et al., 2005). Further, Fz7 is required for Wnt5a-induced Dvl polymerization and AP-1 activation in mouse fibroblast L cells (Nishita et al., 2010b). It has also been shown that Fz2 mediates a Wnt5a-dependent increase in intracellular calcium concentration in zebrafish embryos and differentiation of F9 teratocarcinoma cells into primitive endoderm (Liu et al., 1999). Further, Fz2 is required for Wnt5a-dependent activation of Rac in HeLaS3 cells (Sato et al., 2010) and Wnt5a-dependent expression of laminin γ2 in gastric cancer cells (Yamamoto et al., 2009). Therefore, it is suggested that Wnt5a regulates cellular functions by binding to several Fzs. Another ligand that activates the β-catenin-independent pathway, Wnt11, has been shown to be interacted with Fz7 genetically, functionally, and biochemically (Djiane et al., 2000; Kim et al., 2008; Witzel et al., 2006).

Unlike Fzs, Arrow and LRP6 appear to be specifically required for β-catenin signaling. In *Drosophila*, *arrow* mutants exhibit normal PCP (Wehrli et al., 2000). Similarly, in *Xenopus*, blocking LRP6 function has little effect on gastrulation movements (Semënov et al., 2001). Knockout mice of Ror2 show similar phenotypes to Wnt5a knockout mice, indicating that Ror2 is required for the β-catenin-independent pathway (Oishi et al., 2003). Wnt5a has a less affinity with LRP6 and a higher affinity with Ror2 rather than Wnt3a (Sato et al., 2010). Therefore, Fzs act as common receptors for both the β-catenin-dependent and -independent pathways, and LRP6 and Ror2 determine the specific pathways. Alternatively, Fz can bind to different Wnts and an individual Wnt can activate multiple receptors. Wnt signaling outcomes may be dictated largely by which Wnt receptor is expressed in a tissue.

5.2. Involvement of receptor clustering, phosphorylation, and phospholipids in Wnt signaling

As discussed in Section 4.1.2, LRP5 and LRP6 are key signaling receptors for the β-catenin pathway (MacDonald et al., 2009; Niehrs et al., 2010b). Wnt3a binds Fz and LRP6 (or LRP5) and recruits Dvl to the plasma

membrane. Dvl itself forms polymers and the DIX domain is required for Dvl polymerization, which increases its binding to Axin associated with GSK-3 and β-catenin (Kishida et al., 1999; Schwarz-Romond et al., 2007a, b) and promotes the oligomerization of LRP6, which is referred to as an LRP6 signalosome (Bilic et al., 2007). Polymerized LRP6 is phosphorylated by CK1γ at T1479 in the S/T cluster, and PPSP motifs are phosphorylated by GSK-3 (Fig. 2.4A). Phosphorylated LRP6 binds to Axin associated with GSK-3 and β-catenin, which is necessary for the stabilization of β-catenin (Cliffe et al., 2003; Davidson et al., 2005; MacDonald et al., 2008; Tamai et al., 2004; Zeng et al., 2005, 2008). The phosphorylation is a consequence but not the cause of oligomerization of LRP6 because a dominant-negative form of CK1γ did not affect LRP6 signalosome formation but blocks the phosphorylation (Bilic et al., 2007). GSK-3-dependent phosphorylation of β-catenin on the Axin complex is essential for the degradation of β-catenin (Ikeda et al., 1998; Kikuchi et al., 2009; Kishida et al., 1998). Although the mechanism by which the binding of LRP6 and Axin induces the stabilization of β-catenin is not clear, one possibility is that phosphorylated LRP6 directly binds to GSK-3 associated with Axin and suppresses GSK-3 activity (Mi et al., 2006; Wu et al., 2009a).

Phospholipids are generally known to be important for signal transduction. In Wnt signaling, Dvl binds to and activates phosphatidylinositol 4-kinase type IIα (PI4KIIα) and phosphatidyl-4-phosphate 5-kinase type I (PIP5KI), and Wnt3a stimulates the production of phosphatidylinositol 4,5-bisphosphate (PIP2), which depends on Fz and Dvl and enhances phosphorylation of LRP6 by an unknown mechanism (Pan et al., 2008) (Fig. 2.4A). Although it is not known whether the ternary complex of Dvl, PI4KIIα, and PIP5KI is formed on the plasma membrane, this complex would produce PIP2 through phosphatidylinositol 4-phosphate from phosphatidylinositol more efficiently.

It has been reported that APC membrane recruitment 1 (Amer1), a membrane-associated PIP2-binding protein, is necessary for the activation of the β-catenin pathway at the LRP6 receptor level (Tanneberger et al., 2011). Wnt3a induces the translocation of Amer1 to the plasma membrane in a PIP2-dependent manner and Amer1 binds CK1γ, recruits Axin and GSK-3 to the plasma membrane, and promotes the formation of a complex between Axin and LRP6. Therefore, Amer1 might act as a scaffold protein to stimulate phosphorylation of LRP6.

As compared with the β-catenin pathway, the cluster and phosphorylation of receptors in the β-catenin-independent pathway are not clear. However, it has been demonstrated that Wnt5a induces the phosphorylation of Ror2 at Ser864 by GSK-3 and that Axin is recruited to Ror2 in response to Wnt5a (Grumolato et al., 2010; Yamamoto et al., 2007). The $Ror2^{S864A}$ mutant impairs Wnt5a-dependent cell migration. Therefore, Wnt5a-dependent phosphorylation of Ror2 may be required for the

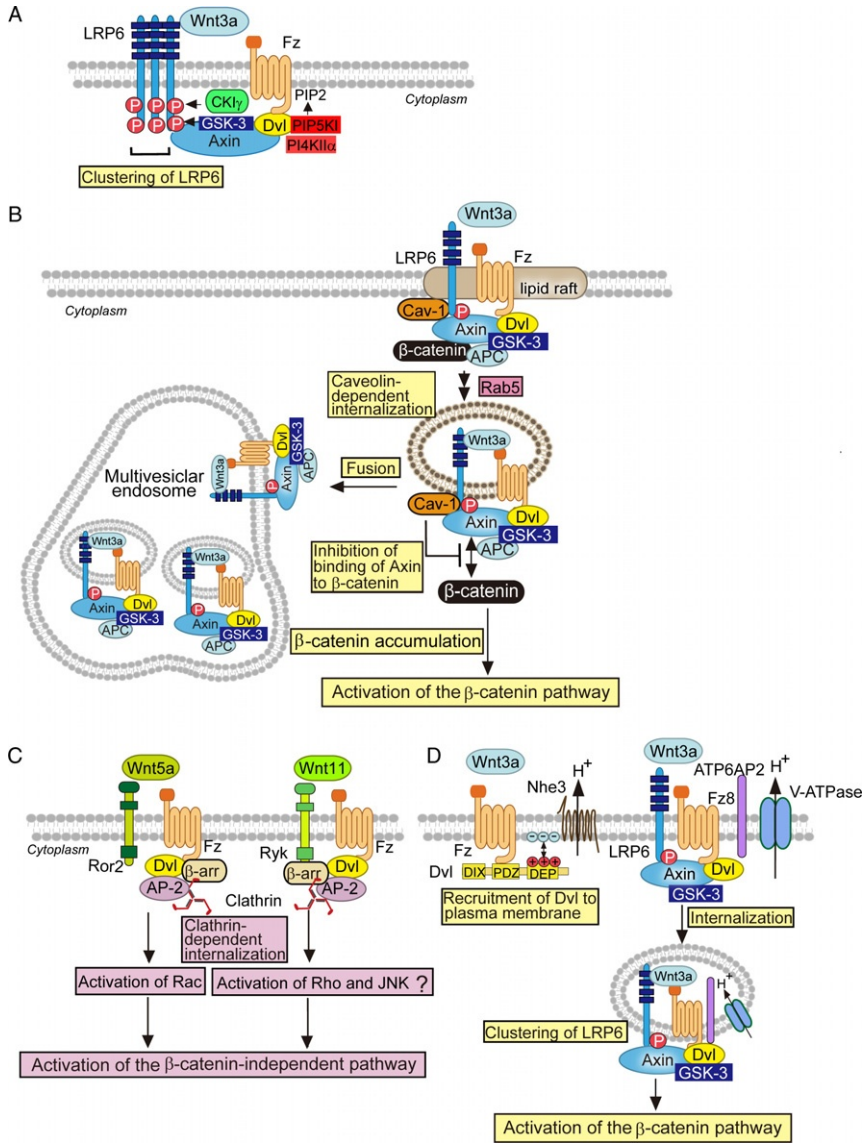

Figure 2.4 Selective activation mechanism of Wnt signaling. (A) Clustering of LRP6. After Wnt3a binds to Fz and LRP6, Dvl is translocated to the Wnt receptor complex. Dvl generates PtdIns(4,5)P2 (PIP2) by binding and activating PI4KIIα and PIP5KI and induces the recruitment of the Axin complex to the membrane. Phosphorylation of LRP6 by CK1γ and GSK-3 enhances the binding of the Axin complex to LRP6. Dvl and Axin oligomerize, and their oligomerization promotes the clustering of LRP6. (B) Activation of the β-catenin pathway by receptor-mediated endocytosis. After the Axin complex is translocated to the Fz and LRP6 complex in response to Wnt3a, the

activation of the β-catenin-independent pathway. These are analogous to the priming phosphorylation of LRP6 in the β-catenin pathway in response to Wnt3a.

It has been shown that the DEP domain of Dvl is required for its membrane targeting in *Xenopus* embryos (Rothbaher et al., 2000) and important for the PCP pathway in *Drosophila* ommatidium (Boutros et al., 1998). A polybasic stretch within the DEP domain binds to negatively charged acidic phospholipids, especially phosphatidic acid, and a DEP mutant in which the polybasic amino acid stretch was converted into a polyacidic stretch shows PCP defects in the *Drosophila* eye and wing but rescues Wg phenotypes in the β-catenin pathway (Simons et al., 2009). This is discussed in Section 5.6 again.

5.3. Endocytic routes of ligand–receptor complexes

It is becoming clear that endocytosis of the ligand–receptor complex is required for the regulation of Wnt signaling (Kikuchi et al., 2009). There are at least two routes, clathrin- and caveolin-mediated endocytosis (Sorkin et al., 2009). In clathrin-mediated endocytosis, the ligand–receptor complex is concentrated into "coated pits" on the plasma membrane, which are formed by the assembly of the cytosolic coat protein, clathrin (Traub, 2009). Coated pits are encapsulated by a polygonal clathrin coat and carry receptor–ligand complexes, including assembly protein adaptor protein-2

receptor complex may be internalized via caveolin-mediated route to stabilize β-catenin. Although the mechanism is unclear, it is suggested that β-catenin is released from Axin or phosphorylated LRP6 inhibits GSK-3, leading to the stabilization of β-catenin. Wnt3a also triggers the sequestration of GSK-3 into multivesicular endosomes to inhibit its activity and reduce the phosphorylation of β-catenin, leading to its stabilization. (C) Activation of the β-catenin-independent pathway by receptor-mediated endocytosis. Wnt5a induces the internalization of Fz and Ror2 in a clathrin-dependent manner, thereby activating Rac. Ryk interacts with β-arrestin-2 and promotes Wnt11-induced internalization of Fz7 and Dvl, leading to activation of the β-catenin-independent pathway in *Xenopus*. (D) Involvement of acidification in Wnt signaling. The Na^+/H^+ exchanger Nhe3 is involved in the recruitment of Dvl to plasma membrane by the formation of alkaline pH and a charge microenvironment at the plasma membrane. Dvl binds to Fz through its PDZ domain. In addition, the DEP domain binds directly to acidic phospholipids, which is dependent on local pH and charge. The Wnt and receptor complex is relocated to a subcellular compartment that is acidified by V-ATPase. The acid in microenvironment induces the phosphorylation of LRP6 and its clustering, and then leading to the clustering of LRP6. Afterward, the Wnt and receptor complex is internalized, resulting in activation of the β-catenin pathway. β-arr, β-arrestin; ATP6AP2, ATPase, H^+ transporting, lysosomal accessory protein 2; Cav-1, caveolin-1; PI4KIIα, phosphatidylinositol 4-kinase type IIα, PIP5KI, phosphatidyl-4-phosphate 5-kinase type I; V-ATPase, H^+-ATPase.

(AP-2), into the cell. In the late stages of the formation of clathrin-coated vesicles (CCVs), dynamin severs the invaginated CCVs. CCVs are uncoated after internalization from the plasma membranes and then fuse with the early endosomes. Early endosomes are multifunctional organelles that regulate membrane transport between the plasma membrane and various intracellular components (Zerial et al., 2001). After arriving at the early endosomes, uncoated vesicles are returned to the plasma membrane, transported to late endosomes and lysosomes for degradation, or connected to the TGN. Rab GTP-binding proteins, including Rab4, Rab5, Rab7, Rab9, and Rab11 exert a regulatory function in vesicle trafficking.

Nonclathrin-dependent endocytosis through lipid raft microdomains and the caveolar pathway has emerged as another important trafficking pathway (Lajoie et al., 2010; Razani et al., 2002). Caveolae are flask-shaped invaginations of the plasma membrane. The shape and structural organization of caveolae are conferred by caveolin, which binds directly to cholesterol. Caveolin self-associates to form a striated caveolin coat on the surface for the membrane invaginations. It is likely that caveolin-mediated endocytosis shares common features with clathrin-dependent endocytosis. Although the mechanism of caveolae formation is becoming clear, the trafficking pathway after the internalization of caveolae has not yet been clarified.

5.4. Roles of receptor-mediated endocytosis in the β-catenin-dependent pathway

LRP6 has been shown to form intracellular aggregates to be phosphorylated in response to Wnt3a (Bilic et al., 2007). These aggregates do not colocalize with endocytic markers except for caveolin. Consistent with this observation, it has been shown that LRP6 is internalized through a caveolin-mediated route in cultured cells in response to Wnt3a and that manipulations to inhibit caveolin-mediated endocytosis block Wnt3a-dependent β-catenin accumulation and Tcf transcriptional activation (Sakane et al., 2010; Yamamoto et al., 2006, 2008a) (Fig. 2.4B). Therefore, caveolin-mediated endocytosis is required for Wnt3a-dependent activation of the β-catenin pathway. However, inhibition of internalization of LRP6 does not suppress Wnt3a-dependent phosphorylation of LRP6, suggesting that phosphorylation of LRP6 is not sufficient for activation of the β-catenin pathway. It is likely that Wnt3a-dependent phosphorylation of LRP6 is independent of its internalization.

Rab5 is involved in the internalization of LRP6 to early endosome, and internalized LRP6 is recycled to the cell-surface membrane from recycling endosomes (Yamamoto et al., 2006). Although the precise mechanism by which caveolin-mediated endocytosis promotes the β-catenin pathway has been unclear, two models are proposed. When Axin binds to phosphorylated LRP6 upon stimulation with Wnt3a and the complex is internalized

with caveolin, caveolin acts on the Axin complex to dissociate β-catenin from Axin, thereby reducing the phosphorylation by GSK-3 (Yamamoto et al., 2006). Another model suggests that Wnt3a causes sequestration of GSK-3 into multivesicular endosomes to inhibit its activity, resulting in reduction in the phosphorylation of β-catenin, leading to its stabilization (Taelman et al., 2010).

It is known that mice lacking each of caveolin-1, caveolin-2, or caveolin-3 displayed no overt phenotypic abnormalities (Razani et al., 2002), that were different from the phenotypes of Wnt3a or β-catenin knockout mice, suggesting that the β-catenin pathway signaling during development does not critically depend on caveolin. Further, there is no caveolin ortholog in *Drosophila*. Therefore, other proteins may substitute for caveolin to activate the β-catenin pathway of Wnt/Wg signaling. Among the proteins in lipid raft microdomains, flotillin belongs to a larger class of integral membrane proteins and is expressed in a wide variety species from mammals to *Drosophila* (Morrow et al., 2005). In addition, flotillin is highly expressed in cells such as neurons that lack caveolin, suggesting that it may represent a functional analogue of caveolin in caveolin-negative cells. Therefore, it will be of interest to speculate whether flotillin is involved in the internalization of LRP6 and stabilization of β-catenin.

It has also been proposed that clathrin-mediated endocytosis is involved in activation of the β-catenin pathway. The inhibition of clathrin-mediated endocytosis with pharmacological reagents suppressed Wnt3a-induced β-catenin stabilization in mouse fibroblast L cells (Blitzer et al., 2006). Consistent with the positive role of clathrin in the β-catenin pathway, it was shown that β-arrestin, a clathrin adaptor, binds to Dvl and these proteins activate Wnt-dependent Tcf transcriptional activity synergistically (Chen et al., 2001). In addition, by knockdown of β-arrestin, Dvl fails to be phosphorylated and β-catenin fails to be stabilized in response to Wnt3a stimulation (Bryja et al., 2007). These results suggest that clathrin and β-arrestin play a role in the β-catenin pathway, but whether β-arrestin is involved in the endocytosis of Fz and LRP6 through clathrin remains to be clarified. Thus, there are contradictory reports on the role of endocytosis in the β-catenin pathway.

5.5. Involvement of clathrin-mediated endocytosis in the β-catenin-independent pathway

As compared with the controversial roles of endocytic pathways in the β-catenin pathway, the importance of endocytosis in the β-catenin-independent pathway is well documented. Because Fz belongs to the GPCR family (Schulte, 2010; Wang et al., 2006), β-arrestin is expected to be involved in the internalization of Fz. Wnt5a triggers internalization of Fz4, which requires the recruitment of Dvl2 and β-arrestin-2 to the plasma

membrane in HEK293 cells (Chen et al., 2003). Reduction of β-arrestin-2 in *Xenopus* embryos leads to defects in CE (Kim et al., 2007). Dvl2 also interacts with μ2-adaptin of AP-2, which is a clathrin-binding protein, and this interaction is required for the internalization of Fz4 (Yu et al., 2007).

It has also been demonstrated that Wnt5a induces the internalization of Fz2, Fz5, and Ror2 in a clathrin-dependent manner and that knockdown of Dvl2, β-arrestin-2, and Ror2 suppresses Wnt5a-dependent internalization of receptors and the activation of Rac (Sakane et al., 2011; Sato et al., 2010) (Fig. 2.4C). In addition, Ryk interacts with β-arrestin-2 and promotes Wnt11-induced internalization of Fz7 and Dvl in *Xenopus* (Kim et al., 2008). It is notable that Ryk plays a role in the activation of RhoA and JNK and is necessary for CE. Taken together, it is possible that Wnt5a and Wnt11 induce the internalization of Fzs with Ror2 or Ryk in cooperation with Dvl2 and β-arrestin-2 via a clathrin-mediated route, thereby activating the β-catenin-independent pathway. In addition, Wnt5a induces the internalization of Fz with SDC4 through a clathrin-mediated endocytic route, as discussed in Sections 4.2.3 and 4.3 (Ohkawara et al., 2011).

Taken together, the different endocytic routes could be important for deciding the activation of either the β-catenin-dependent or -independent pathway. It has been shown that TGF-β receptors also traffic to different endocytic pathways (Di Guglielmo et al., 2003). TGF-β Ser/Thr kinase receptors are internalized through the clathrin-mediated route as well as the caveolin-mediated route, with the former pathway facilitating Smad activation and the latter mediating receptor degradation. Therefore, it could be possible that distinct endocytic routes determine specifically the activation of one signaling pathway by a certain pair of Wnts and receptors.

5.6. Involvement of acidification in Wnt signaling

Intracellular pH is involved in various cellular functions including proliferation and differentiation. Evidence has accumulated that enzymes regulating acidification are implicated in Wnt signaling. Genome-wide RNAi library screening in *Drosophila* S2R+ cells demonstrated that Nhe2, a sodium/proton (Na^+/H^+) exchanger, is required for the recruitment of dishevelled to Fz (Simons et al., 2009). Overexpression and reduced expression of Nhe2 caused PCP phenotypes, such as chirality inversions, symmetrical cluster formation, and rotation defects of ommatidia (Simons et al., 2009). *Drosophila* Nhe2 has the highest sequence homology to human NHE3. These types of NHEs have been implicated in the formation of alkaline pH and charge microenvironments at the plasma membrane (Ro et al., 2004). Knockdown of NHE3 in HEK293 cells impaired Fz-mediated Dvl recruitment and the phenotypes were partially rescued by alkalinization treatment of the cells with NH_4Cl. As discussed in Section 5.2, it has been suggested that the polybasic stretch within the DEP domain binds to acidic and

negatively charged phospholipids. Therefore, it is conceivable that binding and surface recruitment of Dvl to Fz is pH- and charge-dependent. When local pH is lower, the lipid headgroups would be protonated, thereby losing negative charge, which induces the dissociation of Dvl from Fz and cell membrane (Fig. 2.4D).

Another genome siRNA screen for regulators of Wnt signaling in mammalian cells identified prorenin receptor (PRR), which is known as adenosine triphosphatase (ATPase), H^+-transporting, lysosomal, accessory protein 2 (ATP6AP2; Cruciat et al., 2010). PRR interacts with H^+-ATPase (V-ATPase), which is a multiprotein complex localized in intracellular organelles including the Golgi complex, endo- and exocytic vesicles, and lysosomes, and at the plasma membrane. Its main function is to pump protons and acidify vesicles, thereby promoting vesicular trafficking and endocytosis (Forgac, 2007). PRR also forms a complex with Fz8 and LRP6 and its knockdown or treatment with V-ATPase inhibitors inhibits Wnt3a-dependent phosphorylation of LRP6 and its internalization (Cruciat et al., 2010) (Fig. 2.4D). Therefore, PRR may act as an adaptor to bring Fz and LRP6 complexes in close proximity to V-ATPases. These manipulations also induced neural patterning defects in *Xenopus* embryos that are characteristics in Wnt-signal inhibition. PRR is conserved in *Drosophila* (dPRR), and depletion of dPRR suppressed not only Wg signaling but also PCP signaling (Buechling et al., 2010; Hermle et al., 2010). In addition, dPRR interacted with dFz1 and dFz2 biochemically, consistent with a role in both the β-catenin-dependent and -independent pathways. Taken together, the following model is conceivable. Upon stimulation with Wnt3a, V-ATPase and Na^+/H^+ exchanger are activated and pH of outside cell and inside cell across the plasma membrane decreases and increases, respectively. Extracellular acidification induces clustering of LRP6, and intracellular alkalization enhances the recruitment of Dvl to Fz, resulting in the phosphorylation of LRP6 on the cell-surface membrane. Then, the Wnt receptor complex is internalized and the β-catenin pathway is fully activated.

A study using various V-ATPase inhibitors revealed that acidification is involved in various aspects of Wnt signaling (Coombs et al., 2010). Using treatment with acidification inhibitors, *Xenopus* embryos lack dorsal structures, and activin-induced CE movement in animal cap is inhibited, which is consistent with the finding that acidification is required for both the β-catenin-dependent and -independent pathways. Interestingly, these phenotypes in *Xenopus* embryos are due to impairment of Wnt-producing cells not due to of Wnt-receiving cells. Acidification inhibitors increase the formation of a complex between Wnt3a and Wls and prevented the release of Wnt3a from the cell surface (Coombs et al., 2010). Therefore, vesicular acidification could be important not only for Wnt signal receiving but also for Wnt secretion.

6. Cross Talk Between Wnt Signaling Pathway and Other Pathways

It has become increasingly apparent that signal transduction pathways are not merely linear cascades and that they are organized into complex signaling networks that require high levels of regulation to generate precise and unique cellular responses. The initially simple Wg linear pathway described from *Drosophila* genetic studies has expanded into multiple pathways of Wnt signaling in vertebrates. During embryonic development, the complex and delicate interactions between Wnt signaling and other signaling pathways, including protein kinase A (PKA), TGF-β, Hippo, Notch, mTOR, and nuclear factor kappa B (NF-κB) pathways, are crucial for stem cell maintenance, body patterning, cell fate, and organogenesis. These signals are also important for adult tissue homeostasis, such as the proper growth and functioning of cells. Ongoing research in the signaling field is revealing many points of cross talk between Wnt signaling and other pathways (Jin et al., 2008; McNeill et al., 2010).

6.1. PKA signaling and Wnt signaling

PKA functions as a central player in signal transduction and cellular functions. The binding of agonists including prostaglandins (PGs), hormones, and neurotransmitters, to GPCRs leads to dissociation of the α and βγ subunits of trimeric G proteins, and then the α subunit binds and activates adenylate cyclase to produce cAMP.

PGs play critical roles in tumorigenesis. For example, it has been reported that PGE_2 activity phosphorylates and inhibits GSK-3, thereby stabilizing β-catenin and activating Tcf in HEK293 cells (Fujino et al., 2002). PGE_2 has been shown to stabilize β-catenin in DLD1 cells, a colon cancer cell line, through the activation of Gs (Castellone et al., 2005) (Fig. 2.5A). Gsα, a subunit of Gs, binds to the RGS domain of Axin, thereby releasing GSK-3 from β-catenin, while Gsβγ, another subunit of Gs, activates Akt, which leads to phosphorylation and inhibition of GSK-3. These actions might inhibit GSK-3-dependent phosphorylation of β-catenin, resulting in the stabilization of β-catenin. It has also been reported that free Gβγ recruits GSK-3 to the plasma membrane to promote the phosphorylation of LRP6 and subsequent activation of the β-catenin pathway, suggesting that Gβγ plays a role in GPCR-dependent activation of the β-catenin pathway (Jernigan et al., 2010). PGE_1 stabilizes β-catenin through a different mechanism in HEK293 cells (Hino et al., 2005). PKA is activated by PGE1 and phosphorylates β-catenin at Ser675, which

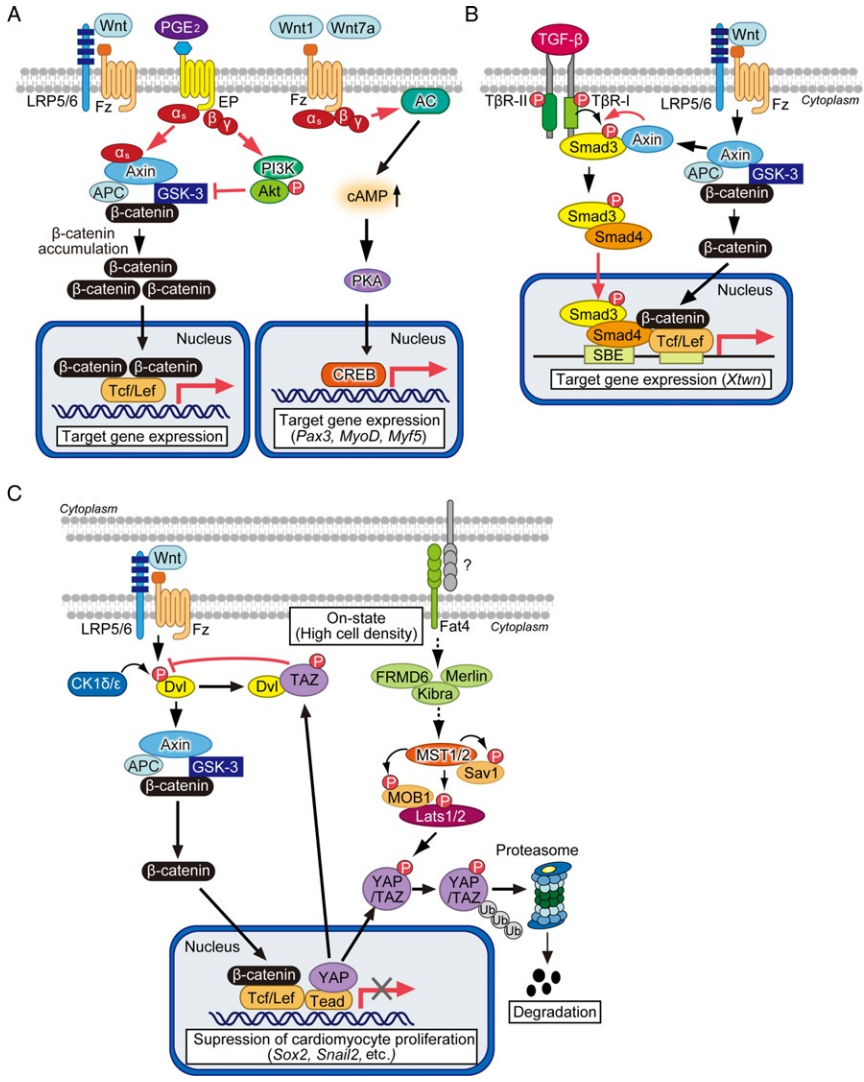

Figure 2.5 Cross talk between Wnt and other signaling pathways. (A) Cross talk between PKA signaling and Wnt signaling. PGE signaling stabilizes β-catenin by two mechanisms: one is to regulate Axin to release GSK-3 from β-catenin and another to activate Akt leading to phosphorylation and inhibition of GSK-3. Wnt1 and Wnt7a activate PKA to induce myogenesis during embryogenesis by activating PKA. (B) Cross talk between TGF-β signaling and Wnt signaling. β-Catenin cooperates with the Smad3/Smad4 complex in the nucleus to activate gene expression. Axin assists the phosphorylation of Smad3 induced by TGF-β signaling. (C) Cross talk between Hippo signaling and Wnt signaling. In a Hippo signaling active state, TAZ, which is translocated into the cytoplasm from the nucleus, targets Dvl and inhibits its signaling activity. Active Hippo signaling also suppresses the nuclear retention of Yap, which synergistically activates gene expressions with β-catenin in cardiomyogenesis.

inhibits the ubiquitination of β-catenin, thereby stabilizing β-catenin. This mechanism by which PGE_1 and PGE_2 activate the β-catenin pathway might be related to observations that a COX2 inhibitor, such as aspirin, that inhibits production of PGs suppresses the growth of colon cancer cells in which the β-catenin pathway is activated.

The binding of parathyroid hormone (PTH) to its receptor PTHR has been shown to induce the association between PTHR and LRP6 and lead to the phosphorylation of LRP6 at Ser1490 through PKA, thereby stabilizing β-catenin to promote osteoblast differentiation (Wan et al., 2008). PTH is also reported to inhibit GSK-3 through activation of PKA, leading to the stabilization of β-catenin in osteoblastic cell line Saos-2 (Suzuki et al., 2008). Taken together with the findings that the β-catenin pathway is important for osteogenesis (Harada et al., 2003), PTH/PKA signaling affects Wnt signaling at two different levels to promote bone formation.

There is an example indicating that Wnt signaling activates PKA signaling. Wnt1 and Wnt7a activate PKA to induce the myogenic determinant genes *Pax3*, *MyoD*, and *Myf5* during embryogenesis (Chen et al., 2005) (Fig. 2.5A). In this mechanism, Wnts activate Gs proteins and then activate PKA, which leads to the phosphorylation of transcription factor CREB, resulting in transcription activation by binding to genes containing cAMP-responsive elements. It has also been reported that LRP6 binds to the Gs heterotrimer and regulates the localization of Gαs to the plasma membrane (Wan et al., 2011). Further, a specific PKA phosphorylation of LRP6 at Thr1548 enhances the binding of Gαs to LRP6, its localization to the plasma membrane, and the production of cAMP in response to PTH (Wan et al., 2011). Therefore, PKA phosphorylation of LRP6 is critical for the activation of PKA signaling. It is intriguing to speculate that Wnt and PKA signals can regulate each other mutually.

6.2. TGF-β signaling and Wnt signaling

Cytokines of the TGF-β superfamily are dimeric proteins and TGF-βs are the prototype of the TGF-β superfamily (Massague, 1998). TGF-β acts as a potent growth inhibitors for most types of cells, induces the apoptosis of epithelial cells, and also stimulates the production of extracellular matrix proteins, thereby playing critical roles in embryonic development, adult homeostasis, and the pathogenesis of a variety of diseases. Upon binding of TGF-β to type I receptor (TβR-I) and type II receptor (TβR-II), both of which have an intracellular serine/threonine kinase domain, they form a hetero-tetramer complex (Wrighton et al., 2009). TβR-II transphosphorylates and activates TβR-I, and then TβR-I phosphorylates R-Smad such as Smad2 and Smad3. Activated R-Smads interact with a Co-Smad, Smad4, and the Smad complex accumulates into the nucleus where it induces the expression of various target genes.

Cross talk between the TGF-β and Wnt pathways was found in *Xenopus* Spemann's organizer (Nishita et al., 2000). *Xenopus Twin* (*Xtwn*) is expressed by either Nodal (one of TGF family) or Wnt signaling, and Wnt8-dependent expression of *Xtwn* requires the Smad binding sites *Xtwn* gene. The MH1 domain of Smad4 binds to the HMG box domain of Lef1, and β-catenin, Lef1, and Smad4 form a complex. The complex binds to adjacent regulatory region to express *Xtwn*. This cooperation is also observed in mammalian cells (Labbe et al., 2000; Nishita et al., 2000) (Fig. 2.5B). An inhibitory Smad, Smad7, has also been shown to be associated with β-catenin and Lef1 (Edlund et al., 2005). Smad7 is required for the TGF-β1-dependent accumulation of β-catenin and the interaction between β-catenin and Lef1. These results suggest that Wnt and TGF-β pathways cooperate synergistically in the nucleus. As another cross talk example, Axin, which is important for the degradation of β-catenin, interacts with Smad3 and facilitates the phosphorylation of Smad3 by TβR-I (Furuhashi et al., 2001) (Fig. 2.5B). Further, TGF-β-dependent transcription is enhanced by Axin, suggesting that Axin may function as an adaptor of Smad3 for efficient TGF-β signaling.

6.3. Hippo signaling and Wnt signaling

The Hippo pathway was identified as a signaling pathway to control organ size in *Drosophila* (Bao et al., 2011; Pan, 2010). Loss of *fat*, a protocadherin molecule, leads to tissue outgrowth and has been classified as a tumor suppressor gene originally. Subsequent genetic studies showed that fat regulates a kinase cascade, known as the Hippo pathway. The kinase cascade is composed of Hippo (the sterile 20-like kinase), which binds to Salvador (an adaptor protein), and Warts (the DBF family kinase), which forms a complex with Mob as tumor suppressor (MATS) (an adaptor protein). In this cascade, Hippo phosphorylates and activates Warts, and then Warts phosphorylate the transcriptional coactivator Yorkie. In the nucleus, Yorkie induces growth promoting and apoptosis-inhibiting genes. Because phosphorylated Yorkie is excluded from the nucleus, the Hippo pathway restricts cell proliferation and promotes cell death. As upstream molecules, Expanded, Merlin, and Kibra are identified and the complex acts downstream of the Fat/Dachsous complex and enhances Hippo activity. Fat and Dachsous are protocadherins that interact with each other.

Vertebrate homologues have been identified for most components of the *Drosophila* Hippo pathway (Bao et al., 2011). Merlin activates the Hippo pathway at high cell density. MST1/2 kinase (a Hippo ortholog) cooperates with MOB1 (a MATS ortholog) and Sav1/WW45 (a Salvador ortholog) to activate Lats1/2 kinase (a Warts ortholog), resulting in the phosphorylation of YAP or TAZ (a Yorkie ortholog). The phosphorylation of these transcriptional coactivators by Lats1/2 inhibits their nuclear localization.

Drosophila studies have shown that Wg is expressed by a mutant of *fat* and the overexpression of Yorkie in wing imaginal discs, suggesting that Hippo signaling affects Wg activity (Cho et al., 2006). In mammalian cultured cells, TAZ binds to Dvl in the cytosol, and this interaction inhibits Wnt3a-dependent phosphorylation of Dvl by CK1δ/ε, thereby suppressing the β-catenin pathway (Varelas et al., 2010) (Fig. 2.5C). Consistent with these observations, nuclear β-catenin is increased in embryos of *TAZ* mutant mice. This cross talk is also observed in *Drosophila*, in which ectopic expression of Yorkie suppresses expression of Wg target gene *Distalless* (*Dll;* Varelas et al., 2010). Another mechanism of this cross talk has been reported (Heallen et al., 2011). In mammalian cardiogenesis, Yap cooperates with β-catenin in the nucleus to activate *Sox2* and *Snail2* expression, which enhance cardiomyocyte proliferation, while the activation of Hippo signal induces phosphorylation and cytoplasmic translocation of Yap to inhibit the Yap- and β-catenin-interdependent transcriptional activation. Thus, direct communication between the Hippo and Wnt pathways might coordinately regulate morphogen signaling with tissue growth control in animals.

6.4. Notch signaling and Wnt signaling

The Notch signaling pathway is highly evolutionarily conserved. It controls cell fate determination and pattern formation in organ development in both invertebrates and vertebrates (Bray, 2006). Both Notch (receptor) and its ligands, Delta and Serrate (Jagged in mammals), are transmembrane proteins. The binding of ligands initiates proteolytic cleavages of Notch by ADAM family metalloproteases at an extracellular domain and by γ-secretases at the cytoplasmic domain, thereby releasing the Notch intracellular domain (Nicd). Nicd then translocates into the nucleus and interacts with the DNA-binding protein CSL to promote transcription by recruiting the coactivator Mastermind. Although members of Notch signaling components differ between species, the basic system is common throughout.

Cross talk between Wnt and Notch signaling has also been demonstrated in *Drosophila* (Axelrod et al., 1996). Ectopic bristle generation by ectopic overexpression of dishevelled was observed more frequently in Notch heterozygotes than in a wild-type, suggesting that Notch and dishevelled have opposing effects on bristle induction. The cytoplasmic C-terminal region of Notch interacts with the N-terminal region of dishevelled. In addition, colocalization of Notch and dishevelled is observed in *Drosophila* S2 cells in the presence of Delta-expressing cells. These results provide a model that dishevelled inhibits Notch functions by binding to its cytoplasmic region. It was also demonstrated that Notch and Wg signaling decreases and increases, respectively, the numbers of muscle and heart progenitors of *Drosophila* embryos (Carmena et al., 1998). Canoe, a PDZ domain-containing protein, binds to Notch and dishevelled and suppresses their signaling, thereby ensuring a fine-tuned regulation

(Carmena et al., 2006). Canoe may coordinate two pathways during progenitor specification. In mouse neural precursor cells, β-catenin associates with Nicd, and this association is enhanced in the presence of CBP/p300 and CBP/p300-associated protein (Shimizu et al., 2008). Nuclear-accumulated β-catenin induces antineurogenic *hes1* gene expression, thereby inhibiting neuronal differentiation.

Lef1 has been found to bind multiple sites in the Notch ligand *Delta-like1 (Dll1)* promoter, and the expression of Lef1 and β-catenin activates the expression of *Dll1* in the mouse presomitic mesoderm (PSM; Galceran et al., 2004). However, mouse embryos that develop in the absence of Notch activity show severely downregulated expression of the β-catenin pathway target gene *Axin2* in the PSM (Ferjentsik et al., 2009). Similarly, *Axin2* expression has been shown to be modulated in the *Notch* or *Dll1* mutant mouse (Aulehla et al., 2003). Therefore, the Notch and Wnt pathways regulate each other in a bidirectional manner in the PSM. Taken together, it is likely that there are multiple points of cross talk between Wnt and Notch signaling pathways to regulate cell differentiation.

6.5. mTOR signaling and Wnt signaling

The serine/threonine kinase mTOR is a key component of the mTORC1 complex, which has been implicated in sensing nutritional needs and integrating growth signals in both yeast and mammalian cells (Jorgensen et al., 2004; Schmelzle et al., 2000). mTOR phosphorylates and activates ribosomal subunit S6 kinase (S6K) to stimulate biogenesis and protein synthesis. mTOR is activated by small G protein Rheb, which is inhibited by the TSC1/2 complex that has a GAP activity for Rheb. Various growth factors, nutrients, and energy stresses determine the GAP activity of the TSC1/2 complex by activating protein kinases, including Akt/PKB, AMPK, and GSK-3.

Wnt1 and Wnt3a have been shown to phosphorylate S6K by activating mTOR in HEK293 cells, and Wnt10b also increases the cell size of bone marrow ST2 cells and induces the phosphorylation of S6K in the mandibular bone of Wnt10b transgenic mice (Inoki et al., 2006). The effects of Wnt signaling on mTOR signaling are independent of β-catenin. GSK-3 phosphorylates TSC2 at S1337 and S1341 after priming phosphorylation at S1345 by AMPK, thereby activating the GAP activity of TSC2. Further, TSC2 forms a complex with GSK-3, Axin, and Dvl, and Wnt stimulates the dissociation of TSC2 from GSK-3 and Axin but association of TSC2 and Dvl (Mak et al., 2003). These results suggest that Wnt signaling inhibits the GSK-3-dependent phosphorylation of TSC2, thereby activating mTOR signaling to increase protein synthesis and promote cell growth. Rapamycin inhibits mTOR and suppresses Wnt1-induced mammary tumor growth (Inoki et al., 2006). Therefore, rapamycin could have a therapeutic potential in treating diseases caused by Wnt-signal dysregulation.

6.6. NF-κB signaling and Wnt signaling

NF-κB signaling has critical roles in immunoresponses, including innate immunity, inflammation, dendric cell activation, and lymphocyte activation (Sun et al., 2008). In unstimulated cells, NF-κB proteins, which are transcription factors composed of two subunits (p65 and p50), are sequestered in the cytoplasm by the inhibitory protein IκB. A variety of stimuli, such as TNF-α, lypopolysaccharide, and interleukin-1, activate IκB kinase (IKK) to phosphorylate IκB, resulting in its ubiquitination and proteasomal degradation, which leads to the translocation of p65/p50 into the nucleus and the activation of target genes.

Cross talk between NF-κB signaling and Wnt signaling has been reported. In the nucleus of breast and colon cancer cells that express β-catenin aberrantly, the ability of NF-κB to bind DNA is suppressed by its association with β-catenin (Deng et al., 2002). Dvl also binds to and inhibits NF-κB activity in the nucleus, but this inhibition is not dependent on Wnt stimulation (Deng et al., 2002). Further, through screening deubiquinating enzymes involved in Wnt signal, CYLD, a negative regulator of NF-κB signaling, has been identified as an important regulator of the β-catenin pathway (Tauriello et al., 2010). In this scenario, after Wnt stimuli, Dvl is polymerized and conjugated with a Lys63-linked ubiquitin chain in the DIX domain by an unknown mechanism, leading to the enhancement of its signaling activity, while CYLD interacts with and disassembles the Lys63-linked ubiquitin chain of Dvl to regulate the signal downstream of Dvl.

In addition, the cross talk between NF-κB signaling and Wnt signaling has also been demonstrated in the β-catenin-independent pathway, mainly through Wnt5a actions. In endothelial cells, Wnt5a induces translocation of NF-κB into the nucleus through the Ca^{2+}/PKC pathway to cause inflammation (Kim et al., 2010). Wnt5a has been reported to be upregulated in several human inflammatory diseases, including macrophages exposed to microbes, rheumatoid arthritis, psoriasis, and atherosclerosis (Blumenthal et al., 2006; Christman et al., 2008; Romanowska et al., 2009; Sen et al., 2000). Therefore, it is likely that Wnt5a has positive roles in inflammatory situations, but its molecular mechanisms still remain unclear.

7. Concluding Remarks and Future Perspectives

This review focuses on how so-called Wnt signaling is activated selectively and how Wnt signaling and other signaling pathways are regulated mutually. Although our knowledge concerning Wnt signaling continues to increase, there are a number of critical issues that remain to be clarified. First, why are there so many Wnt ligands and receptors in genomes? The fact that

all animal species have kept a large numbers of Wnt and its receptor genes during evolution and that the phenotypes of knockout mice for individual Wnts or receptors are different suggests that they do not function redundantly, although some Wnt gene knockout mouse (Wnt2b, Wnt5b, Wnt6, Wnt8a, Wnt16) looks normal (van Amerongen et al., 2006). As to intracellular signaling pathways, the β-catenin pathway is fairly unique for Wnt signaling. The regulation of β-catenin phosphorylation by GSK-3 associated with Axin could be essential for the stability of β-catenin because the global inhibition of GSK-3 by EGF or insulin does not cause the stabilization of β-catenin. However, the β-catenin-independent pathway is not specific for Wnt signaling, because many ligands such as growth factors, cytokines, and hormones are able to activate Rho, Rac, PKC, and CaMK. Therefore, it seems to be unlikely that the activation itself of intracellular signaling pathways other than the β-catenin pathway is important in Wnt signaling. Rather, when, where, and how long the pathway is activated during prenatal and postnatal stages could be important for Wnt signaling. Thus, it is essential to clarify the spatiotemporal expression of genes and proteins of Wnts and their receptors. Expression of Wnts and receptors at the appropriate time and place can control the proper morphogenesis of tissues or organs. To regulate different genes in different ways could be better for development than to regulate a single gene in the same way in different tissues. Further, it is also important to understand how long Wnt signaling continues. Unlike other growth factor signaling pathways, including EGF, PDGF, and insulin, it has not yet been demonstrated that Wnt signaling stops quickly. To exert Wnt effects, Wnt signaling could continue for a long time by the adhesion of Wnt to the cell surface, and secreted inhibitory ligands suppress Wnt signaling at appropriate time.

Second, why is the specificity of Wnt and its receptor not so strict under *in vitro* experimental conditions? Based on *Drosophila* genetic studies, Wg, Fz, and Arrow have been identified as Wg signaling components. However, there have been relatively few reliable biochemical studies that address the binding of Wnt and Fz, and it is not clear to what extent specific Wnt and receptor pairings have distinct functions. In addition to LRP5/6, Ror1/2 and Ryk have been found to act as Wnt coreceptors. Because of unique biochemical properties of Wnt proteins, they bind to certain proteins in order to be solubilized in the extracellular space and interact with HSPGs on the cell surface. These characteristics of Wnt proteins make the analysis of binding of Wnts to receptors at the cellular level difficult. The presence of coreceptors and HSPGs and the posttranslational modification of Wnts might influence the responses that occur in the context of intact cells, tissues, and organs to determine the specificity of Wnt and receptors more clearly than we imagine.

Third, how is receptor-meditated endocytosis involved in the activation of Wnt signaling? In the MAP kinase pathways, β-arrestin acts as a multiple

endocytic adaptor and signal transducer (Lefkowitz et al., 2005). β-Arrestin binds to activated and phosphorylated seven transmembrane GPCRs and targets the receptors to clathrin-coated pits by binding to clathrin. β-Arrestin also interacts with other endocytic components, including the AP-2, small G protein ARF6 and its GDP/GTP exchange protein ARNO, and *N*-ethylmaleimide-sensitive fusion protein (NSF). Thus, β-arrestin is essential for the internalization of GPCRs. ERK1 and ERK2, MAP kinase members, are known to be regulated by upstream kinases MEK and Raf. JNK3, another MAPK, is phosphorylated and activated by MKK4 and ASK1. β-Arrestin acts as a scaffold protein that binds to all the component kinases of both the modules that activate ERKs and JNK3 to organize particular MAPK pathways with specificity and efficiency. Therefore, β-arrestin can activate MAPK pathways by mediating the endocytosis of receptors in clathrin-coated pits.

Because β-arrestin2 was required for the Wnt5a-dependent internalization of Fz and Rac activation (Sato et al., 2010), it is intriguing to speculate that β-arrestin2 binds to a GDP/GTP exchange protein of Rac in the β-catenin-independent pathway. The β-catenin pathway is unique in that Axin functions as a scaffold protein to regulate the stabilization of β-catenin. Several possible models indeed show how GSK-3-dependent phosphorylation of β-catenin on the Axin complex is influenced during the endocytic process.

Understanding of the whole picture of the specific activation mechanism of the Wnt signaling pathway would shed new light on the therapeutic usage of Wnts, their antagonists, or receptors as molecular targets because Wnt signaling pathways are involved in developmental stages, and misregulation of Wnt signals is involved in adult diseases, such as cancers, inflammatory diseases, and metabolic disorders.

ACKNOWLEDGMENTS

We thank all of our laboratory members for reading this chapter carefully. Studies in our laboratory were supported by Grants-in-Aid for Scientific Research and for Scientific Research on priority areas from the Ministry of Education, Science, and Culture, Japan.

REFERENCES

Aberle, H., et al., 1997. β-Catenin is a target for the ubiquitin–proteasome pathway. EMBO J. 16, 3797–3804.

Ahumada, A., et al., 2002. Signaling of rat Frizzled-2 through phosphodiesterase and cyclic GMP. Science 298, 2006–2010.

Alexander, C.M., et al., 2000. Syndecan-1 is required for Wnt-1-induced mammary tumorigenesis in mice. Nat. Genet. 25, 329–332.

Aulehla, A., et al., 2003. Wnt3a plays a major role in the segmentation clock controlling somitogenesis. Dev. Cell 4, 395–406.
Axelrod, J.D., et al., 1996. Interaction between Wingless and Notch signaling pathways mediated by dishevelled. Science 271, 1826–1832.
Axelrod, J.D., et al., 1998. Differential recruitment of Dishevelled provides signaling specificity in the planar cell polarity and Wingless signaling pathways. Genes Dev. 12, 2610–2622.
Baeg, G.H., et al., 2001. Heparan sulfate proteoglycans are critical for the organization of the extracellular distribution of Wingless. Development 128, 87–94.
Baeg, G.H., et al., 2004. The Wingless morphogen gradient is established by the cooperative action of Frizzled and heparan sulfate proteoglycan receptors. Dev. Biol. 276, 89–100.
Bafico, A., et al., 2001. Novel mechanism of Wnt signalling inhibition mediated by Dickkopf-1 interaction with LRP6/Arrow. Nat. Cell Biol. 3, 683–686.
Banziger, C., et al., 2006. Wntless, a conserved membrane protein dedicated to the secretion of Wnt proteins from signaling cells. Cell 125, 509–522.
Bao, Y., et al., 2011. Mammalian Hippo pathway: from development to cancer and beyond. J. Biochem. 149, 361–379.
Bartscherer, K., et al., 2006. Secretion of Wnt ligands requires Evi, a conserved transmembrane protein. Cell 125, 523–533.
Beighton, P., et al., 1976. The clinical features of sclerosteosis. A review of the manifestations in twenty-five affected individuals. Ann. Intern. Med. 84, 393–397.
Belenkaya, T.Y., et al., 2004. *Drosophila* Dpp morphogen movement is independent of dynamin-mediated endocytosis but regulated by the glypican members of heparan sulfate proteoglycans. Cell 119, 231–244.
Berger, W., et al., 1992. Mutations in the candidate gene for Norrie disease. Hum. Mol. Genet. 1, 461–465.
Bernfield, M., et al., 1999. Functions of cell surface heparan sulfate proteoglycans. Annu. Rev. Biochem. 68, 729–777.
Bhanot, P., et al., 1996. A new member of the *frizzled* family from *Drosophila* functions as a Wingless receptor. Nature 382, 225–230.
Bhat, K.M., 1998. *frizzled* and *frizzled 2* play a partially redundant role in wingless signaling and have similar requirements to wingless in neurogenesis. Cell 95, 1027–1036.
Bilic, J., et al., 2007. Wnt induces LRP6 signalosomes and promotes dishevelled-dependent LRP6 phosphorylation. Science 316, 1619–1622.
Binnerts, M.E., et al., 2007. R-Spondin1 regulates Wnt signaling by inhibiting internalization of LRP6. Proc. Natl. Acad. Sci. USA 104, 14700–14705.
Blitzer, J.T., et al., 2006. A critical role for endocytosis in Wnt signaling. BMC Cell Biol. 7, 28.
Blumenthal, A., et al., 2006. The Wingless homolog WNT5A and its receptor Frizzled-5 regulate inflammatory responses of human mononuclear cells induced by microbial stimulation. Blood 108, 965–973.
Bonifacino, J.S., et al., 2008. Retromer. Curr. Opin. Cell Biol. 20, 427–436.
Bonkowsky, J.L., et al., 1999. Axon routing across the midline controlled by the *Drosophila* Derailed receptor. Nature 402, 540–544.
Boutros, M., et al., 1998. Dishevelled activates JNK and discriminates between JNK pathways in planar polarity and *wingless* signaling. Cell 94, 109–118.
Bradley, R.S., et al., 1990. The proto-oncogene int-1 encodes a secreted protein associated with the extracellular matrix. EMBO J. 9, 1569–1575.
Bradley, R.S., et al., 1995. A soluble form of Wnt-1 protein with mitogenic activity on mammary epithelial cells. Mol. Cell. Biol. 15, 4616–4622.
Bray, S.J., 2006. Notch signalling: a simple pathway becomes complex. Nat. Rev. Mol. Cell Biol. 7, 678–689.

Bryja, V., et al., 2007. β-Arrestin is a necessary component of Wnt/β-catenin signaling *in vitro* and *in vivo*. Proc. Natl. Acad. Sci. USA 104, 6690–6695.
Bryja, V., et al., 2009. The extracellular domain of Lrp5/6 inhibits noncanonical Wnt signaling *in vivo*. Mol. Biol. Cell 20, 924–936.
Buechling, T., et al., 2010. Wnt/Frizzled signaling requires dPRR, the *Drosophila* homolog of the prorenin receptor. Curr. Biol. 20, 1263–1268.
Caneparo, L., et al., 2007. Dickkopf-1 regulates gastrulation movements by coordinated modulation of Wnt/β-catenin and Wnt/PCP activities, through interaction with the Dally-like homolog Knypek. Genes Dev. 21, 465–480.
Capurro, M.I., et al., 2005. Glypican-3 promotes the growth of hepatocellular carcinoma by stimulating canonical Wnt signaling. Cancer Res. 65, 6245–6254.
Carmena, A., et al., 1998. Combinatorial signaling codes for the progressive determination of cell fates in the *Drosophila* embryonic mesoderm. Genes Dev. 12, 3910–3922.
Carmena, A., et al., 2006. The PDZ protein Canoe/AF-6 links Ras-MAPK, Notch and Wingless/Wnt signaling pathways by directly interacting with Ras, Notch and Dishevelled. PLoS ONE 1, e66.
Castellone, M.D., et al., 2005. Prostaglandin E2 promotes colon cancer cell growth through a Gs-axin-β-catenin signaling axis. Science 310, 1504–1510.
Chen, W., et al., 2001. β-Arrestin1 modulates lymphoid enhancer factor transcriptional activity through interaction with phosphorylated dishevelled proteins. Proc. Natl. Acad. Sci. USA 98, 14889–14894.
Chen, J.Z., et al., 2002. Cloning and identification of a cDNA that encodes a novel human protein with thrombospondin type I repeat domain, *hPWTSR*. Mol. Biol. Rep. 29, 287–292.
Chen, W., et al., 2003. Dishevelled 2 recruits β-arrestin 2 to mediate Wnt5A-stimulated endocytosis of Frizzled 4. Science 301, 1391–1394.
Chen, A.E., et al., 2005. Protein kinase A signalling via CREB controls myogenesis induced by Wnt proteins. Nature 433, 317–322.
Ching, W., et al., 2008. Lipid-independent secretion of a *Drosophila* Wnt protein. J. Biol. Chem. 283, 17092–17098.
Cho, E., et al., 2006. Delineation of a Fat tumor suppressor pathway. Nat. Genet. 38, 1142–1150.
Christman 2nd, M.A., et al., 2008. Wnt5a is expressed in murine and human atherosclerotic lesions. Am. J. Physiol. Heart Circ. Physiol. 294, H2864–H2870.
Cliffe, A., et al., 2003. A role of Dishevelled in relocating Axin to the plasma membrane during Wingless signaling. Curr. Biol. 13, 960–966.
Cong, F., et al., 2004. Wnt signals across the plasma membrane to activate the β-catenin pathway by forming oligomers containing its receptors, Frizzled and LRP. Development 131, 5103–5115.
Coombs, G.S., et al., 2010. WLS-dependent secretion of WNT3A requires Ser209 acylation and vacuolar acidification. J. Cell Sci. 123, 3357–3367.
Couchman, J.R., 2003. Syndecans: proteoglycan regulators of cell-surface microdomains? Nat. Rev. Mol. Cell Biol. 4, 926–937.
Coudreuse, D.Y., et al., 2006. Wnt gradient formation requires retromer function in Wnt-producing cells. Science 312, 921–924.
Cruciat, C.M., et al., 2010. Requirement of prorenin receptor and vacuolar H^+-ATPase-mediated acidification for Wnt signaling. Science 327, 459–463.
Dann, C.E., et al., 2001. Insights into Wnt binding and signalling from the structures of two Frizzled cysteine-rich domains. Nature 412, 86–90.
Davidson, G., et al., 2005. Casein kinase 1γ couples Wnt receptor activation to cytoplasmic signal transduction. Nature 438, 867–872.

De Cat, B., et al., 2003. Processing by proprotein convertases is required for glypican-3 modulation of cell survival, Wnt signaling, and gastrulation movements. J. Cell Biol. 163, 625–635.
Deng, J., et al., 2002. β-Catenin interacts with and inhibits NF-κB in human colon and breast cancer. Cancer Cell 2, 323–334.
Di Guglielmo, G.M., et al., 2003. Distinct endocytic pathways regulate TGF-β receptor signalling and turnover. Nat. Cell Biol. 5, 410–421.
Djiane, A., et al., 2000. Role of frizzled 7 in the regulation of convergent extension movements during gastrulation in *Xenopus laevis*. Development 127, 3091–3100.
Edlund, S., et al., 2005. Interaction between Smad7 and β-catenin: importance for transforming growth factor β-induced apoptosis. Mol. Cell. Biol. 25, 1475–1488.
Ellwanger, K., et al., 2008. Targeted disruption of the Wnt regulator Kremen induces limb defects and high bone density. Mol. Cell. Biol. 28, 4875–4882.
Ferjentsik, Z., et al., 2009. Notch is a critical component of the mouse somitogenesis oscillator and is essential for the formation of the somites. PLoS Genet. 5, e1000662.
Forgac, M., 2007. Vacuolar ATPases: rotary proton pumps in physiology and pathophysiology. Nat. Rev. Mol. Cell Biol. 8, 917–929.
Forrester, W.C., et al., 1999. A *C. elegans* Ror receptor tyrosine kinase regulates cell motility and asymmetric cell division. Nature 400, 881–885.
Fradkin, L.G., et al., 2009. Ryks: new partners for Wnts in the developing and regenerating nervous system. Trends Neurosci. 33, 84–92.
Franch-Marro, X., et al., 2008. *In vivo* role of lipid adducts on Wingless. J. Cell Sci. 121, 1587–1592.
Fu, J., et al., 2009. Reciprocal regulation of Wnt and Gpr177/mouse Wntless is required for embryonic axis formation. Proc. Natl. Acad. Sci. USA 106, 18598–18603.
Fuerer, C., et al., 2010. A study on the interactions between heparan sulfate proteoglycans and Wnt proteins. Dev. Dyn. 239, 184–190.
Fujino, H., et al., 2002. Phosphorylation of glycogen synthase kinase-3 and stimulation of T-cell factor signaling following activation of EP_2 and EP_4 prostanoid receptors by prostaglandin E_2. J. Biol. Chem. 277, 2614–2619.
Fukuda, T., et al., 2008. Antisera induced by infusions of autologous Ad-CD154-leukemia B cells identify ROR1 as an oncofetal antigen and receptor for Wnt5a. Proc. Natl. Acad. Sci. USA 105, 3047–3052.
Furuhashi, M., et al., 2001. Axin facilitates Smad3 activation in the transforming growth factor β signaling pathway. Mol. Cell. Biol. 21, 5132–5141.
Galceran, J., et al., 2004. LEF1-mediated regulation of Delta-like1 links Wnt and Notch signaling in somitogenesis. Genes Dev. 18, 2718–2723.
Gallet, A., et al., 2008. Cellular trafficking of the glypican Dally-like is required for full-strength Hedgehog signaling and wingless transcytosis. Dev. Cell 14, 712–725.
Galli, L.M., et al., 2007. Porcupine-mediated lipid-modification regulates the activity and distribution of Wnt proteins in the chick neural tube. Development 134, 3339–3348.
Gao, B., et al., 2011. Wnt signaling gradients establish planar cell polarity by inducing Vangl2 phosphorylation through Ror2. Dev. Cell 20, 163–176.
Glinka, A., et al., 1998. Dickkopf-1 is a member of a new family of secreted proteins and functions in head induction. Nature 391, 357–362.
Green, J.L., et al., 2008. Ror receptor tyrosine kinases: orphans no more. Trends Cell Biol. 18, 536–544.
Grumolato, L., et al., 2010. Canonical and noncanonical Wnts use a common mechanism to activate completely unrelated coreceptors. Genes Dev. 24, 2517–2530.
Harada, S., et al., 2003. Control of osteoblast function and regulation of bone mass. Nature 423, 349–355.

He, X., et al., 1997. A member of the Frizzled protein family mediating axis induction by Wnt-5A. Science 275, 1652–1654.
Heallen, T., et al., 2011. Hippo pathway inhibits Wnt signaling to restrain cardiomyocyte proliferation and heart size. Science 332, 458–461.
Hendrickx, M., et al., 2008. Non-conventional Frizzled ligands and Wnt receptors. Dev. Growth Differ. 50, 229–243.
Hermle, T., et al., 2010. Regulation of Frizzled-dependent planar polarity signaling by a V-ATPase subunit. Curr. Biol. 20, 1269–1276.
Herz, J., et al., 2002. Lipoprotein receptors in the nervous system. Annu. Rev. Biochem. 71, 405–434.
Hino, S., et al., 2003. Casein kinase 1ε enhances the binding of Dvl-1 to Frat-1 and is essential for Wnt-3a-induced accumulation of β-catenin. J. Biol. Chem. 278, 14066–14073.
Hino, S., et al., 2005. Phosphorylation of β-catenin by cyclic AMP-dependent protein kinase stabilizes β-catenin through inhibition of its ubiquitination. Mol. Cell. Biol. 25, 9063–9072.
Hirabayashi, Y., et al., 2004. The Wnt/β-catenin pathway directs neuronal differentiation of cortical neural precursor cells. Development 131, 2791–2801.
Hofmann, K., 2000. A superfamily of membrane-bound *O*-acyltransferases with implications for Wnt signaling. Trends Biochem. Sci. 25, 111–112.
Hsieh, J.C., et al., 1999. Biochemical characterization of Wnt-frizzled interactions using a soluble, biologically active vertebrate Wnt protein. Proc. Natl. Acad. Sci. USA 96, 3546–3551.
Hurlstone, A., et al., 2002. T-cell factors: turn-ons and turn-offs. EMBO J. 21, 2303–2311.
Hwang, S.G., et al., 2004. Wnt-7a causes loss of differentiated phenotype and inhibits apoptosis of articular chondrocytes via different mechanisms. J. Biol. Chem. 279, 26597–26604.
Ikeda, S., et al., 1998. Axin, a negative regulator of the Wnt signaling pathway, forms a complex with GSK-3β and β-catenin and promotes GSK-3β-dependent phosphorylation of β-catenin. EMBO J. 17, 1371–1384.
Inoki, K., et al., 2006. TSC2 integrates Wnt and energy signals via a coordinated phosphorylation by AMPK and GSK3 to regulate cell growth. Cell 126, 955–968.
Ishitani, T., et al., 1999. The TAK1-NLK-MAPK-related pathway antagonizes signalling between β-catenin and transcription factor TCF. Nature 399, 798–802.
Ishitani, T., et al., 2003. The TAK1-NLK mitogen-activated protein kinase cascade functions in the Wnt-5a/Ca^{2+} pathway to antagonize Wnt/β-catenin signaling. Mol. Cell. Biol. 23, 131–139.
Itasaki, N., et al., 2003. Wise, a context-dependent activator and inhibitor of Wnt signalling. Development 130, 4295–4305.
Jernigan, K.K., et al., 2010. Gβγ activates GSK3 to promote LRP6-mediated β-catenin transcriptional activity. Sci. Signal. 3, ra37.
Jin, T., et al., 2008. Wnt and beyond Wnt: multiple mechanisms control the transcriptional property of β-catenin. Cell. Signal. 20, 1697–1704.
Jorgensen, P., et al., 2004. A dynamic transcriptional network communicates growth potential to ribosome synthesis and critical cell size. Genes Dev. 18, 2491–2505.
Junge, H.J., et al., 2009. TSPAN12 regulates retinal vascular development by promoting Norrin- but not Wnt-induced FZD4/β-catenin signaling. Cell 139, 299–311.
Kamata, T., et al., 2004. *R-spondin*, a novel gene with thrombospondin type 1 domain, was expressed in the dorsal neural tube and affected in *Wnts* mutants. Biochim. Biophys. Acta 1676, 51–62.
Katanaev, V.L., et al., 2005. Trimeric G protein-dependent frizzled signaling in *Drosophila*. Cell 120, 111–122.

Kato, M., et al., 2002. *Cbfa1*-independent decrease in osteoblast proliferation, osteopenia, and persistent embryonic eye vascularization in mice deficient in Lrp5, a Wnt coreceptor. J. Cell Biol. 157, 303–314.
Kazanskaya, O., et al., 2004. R-Spondin2 is a secreted activator of Wnt/β-catenin signaling and is required for *Xenopus* myogenesis. Dev. Cell 7, 525–534.
Kennerdell, J.R., et al., 1998. Use of dsRNA-mediated genetic interference to demonstrate that *frizzled* and *frizzled 2* act in the wingless pathway. Cell 95, 1017–1026.
Kikuchi, A., et al., 2007. Multiplicity of the interactions of Wnt proteins and their receptors. Cell. Signal. 19, 659–671.
Kikuchi, A., et al., 2008. Tumor formation due to abnormalities in the β-catenin-independent pathway of Wnt signaling. Cancer Sci. 99, 202–208.
Kikuchi, A., et al., 2009. Selective activation mechanisms of Wnt signaling pathways. Trends Cell Biol. 19, 119–129.
Kikuchi, A., et al., 2011. Wnt5a: its signalling, functions and implication in diseases. Acta Physiol. (Oxf.) doi: 10.1111/j.1748-1716.2011.02294.x.
Kim, K.A., et al., 2005. Mitogenic influence of human R-spondin1 on the intestinal epithelium. Science 309, 1256–1259.
Kim, G.H., et al., 2007. Essential role for β-arrestin 2 in the regulation of *Xenopus* convergent extension movements. EMBO J. 26, 2513–2526.
Kim, G.H., et al., 2008. Ryk cooperates with Frizzled 7 to promote Wnt11-mediated endocytosis and is essential for *Xenopus laevis* convergent extension movements. J. Cell Biol. 182, 1073–1082.
Kim, J., et al., 2010. Wnt5a induces endothelial inflammation via β-catenin-independent signaling. J. Immunol. 185, 1274–1282.
Kinoshita, N., et al., 2003. PKCδ is essential for Dishevelled function in a noncanonical Wnt pathway that regulates *Xenopus* convergent extension movements. Genes Dev. 17, 1663–1676.
Kirkpatrick, C.A., et al., 2004. Spatial regulation of Wingless morphogen distribution and signaling by Dally-like protein. Dev. Cell 7, 513–523.
Kishida, S., et al., 1998. Axin, a negative regulator of the Wnt signaling pathway, directly interacts with adenomatous polyposis coli and regulates the stabilization of β-catenin. J. Biol. Chem. 273, 10823–10826.
Kishida, S., et al., 1999. DIX domains of Dvl and axin are necessary for protein interactions and their ability to regulate β-catenin stability. Mol. Cell. Biol. 19, 4414–4422.
Kishida, S., et al., 2004. Wnt-3a and Dvl induce neurite retraction by activating Rho-associated kinase. Mol. Cell. Biol. 24, 4487–4501.
Kitagawa, M., et al., 1999. An F-box protein, FWD1, mediates ubiquitin-dependent proteolysis of β-catenin. EMBO J. 18, 2401–2410.
Komekado, H., et al., 2007. Glycosylation and palmitoylation of Wnt-3a are coupled to produce an active form of Wnt-3a. Genes Cells 12, 521–534.
Kreuger, J., et al., 2004. Opposing activities of Dally-like glypican at high and low levels of Wingless morphogen activity. Dev. Cell 7, 503–512.
Kurayoshi, M., et al., 2007. Post-translational palmitoylation and glycosylation of Wnt-5a are necessary for its signalling. Biochem. J. 402, 515–523.
Labbe, E., et al., 2000. Association of Smads with lymphoid enhancer binding factor 1/T cell-specific factor mediates cooperative signaling by the transforming growth factor-β and wnt pathways. Proc. Natl. Acad. Sci. USA 97, 8358–8363.
Lajoie, P., et al., 2010. Lipid rafts, caveolae, and their endocytosis. Int. Rev. Cell Mol. Biol. 282, 135–163.
Lee, J.M., et al., 2010. RORα attenuates Wnt/β-catenin signaling by PKCα-dependent phosphorylation in colon cancer. Mol. Cell 37, 183–195.

Lefkowitz, R.J., et al., 2005. Transduction of receptor signals by β-arrestins. Science 308, 512–517.
Lei, Y.P., et al., 2010. *VANGL2* mutations in human cranial neural-tube defects. N. Engl. J. Med. 362, 2232–2235.
Li, L., et al., 2002. Second cysteine-rich domain of Dickkopf-2 activates canonical Wnt signaling pathway via LRP-6 independently of dishevelled. J. Biol. Chem. 277, 5977–5981.
Li, X., et al., 2005. Sclerostin binds to LRP5/6 and antagonizes canonical Wnt signaling. J. Biol. Chem. 280, 19883–19887.
Li, L., et al., 2009. Wnt5a induces simultaneous cortical axon outgrowth and repulsive axon guidance through distinct signaling mechanisms. J. Neurosci. 29, 5873–5883.
Lin, X., 2004. Functions of heparan sulfate proteoglycans in cell signaling during development. Development 131, 6009–6021.
Liu, X., et al., 1999. Activation of a Frizzled-2/β-adrenergic receptor chimera promotes Wnt signaling and differentiation of mouse F9 teratocarcinoma cells via Gαo and Gαt. Proc. Natl. Acad. Sci. USA 96, 14383–14388.
Liu, C., et al., 2002. Control of β-catenin phosphorylation/degradation by a dual-kinase mechanism. Cell 108, 837–847.
Liu, G., et al., 2003. A novel mechanism for Wnt activation of canonical signaling through the LRP6 receptor. Mol. Cell. Biol. 23, 5825–5835.
Liu, Y., et al., 2008a. Wnt5a induces homodimerization and activation of Ror2 receptor tyrosine kinase. J. Cell. Biochem. 105, 497–502.
Liu, Y., et al., 2008b. Repulsive Wnt signaling inhibits axon regeneration after CNS injury. J. Neurosci. 28, 8376–8382.
Logan, C.Y., et al., 2004. The Wnt signaling pathway in development and disease. Annu. Rev. Cell Dev. Biol. 20, 781–810.
Lu, W., et al., 2004a. Mammalian Ryk is a Wnt coreceptor required for stimulation of neurite outgrowth. Cell 119, 97–108.
Lu, X., et al., 2004b. PTK7/CCK-4 is a novel regulator of planar cell polarity in vertebrates. Nature 430, 93–98.
MacDonald, B.T., et al., 2008. Wnt signal amplification via activity, cooperativity, and regulation of multiple intracellular PPPSP motifs in the Wnt co-receptor LRP6. J. Biol. Chem. 283, 16115–16123.
MacDonald, B.T., et al., 2009. Wnt/β-catenin signaling: components, mechanisms, and diseases. Dev. Cell 17, 9–26.
Mak, B.C., et al., 2003. The tuberin–hamartin complex negatively regulates beta-catenin signaling activity. J. Biol. Chem. 278, 5947–5951.
Mao, B., et al., 2001a. LDL-receptor-related protein 6 is a receptor for Dickkopf proteins. Nature 411, 321–325.
Mao, J., et al., 2001b. Low-density lipoprotein receptor-related protein-5 binds to Axin and regulates the canonical Wnt signaling pathway. Mol. Cell 7, 801–809.
Mao, B., et al., 2002. Kremen proteins are Dickkopf receptors that regulate Wnt/β-catenin signalling. Nature 417, 664–667.
Massague, J., 1998. TGF-β signal transduction. Annu. Rev. Biochem. 67, 753–791.
Matsuda, T., et al., 2001. Expression of the receptor tyrosine kinase genes, *Ror1* and *Ror2*, during mouse development. Mech. Dev. 105, 153–156.
McNeill, H., et al., 2010. When pathways collide: collaboration and connivance among signalling proteins in development. Nat. Rev. Mol. Cell Biol. 11, 404–413.
Mi, K., et al., 2006. The low density lipoprotein receptor-related protein 6 interacts with glycogen synthase kinase 3 and attenuates activity. J. Biol. Chem. 281, 4787–4794.
Mikels, A.J., et al., 2006. Purified Wnt5a protein activates or inhibits β-catenin-TCF signaling depending on receptor context. PLoS Biol. 4, 570–582.

Miyashita, T., et al., 2009. Wnt-Ryk signaling mediates axon growth inhibition and limits functional recovery after spinal cord injury. J. Neurotrauma 26, 955–964.
Morrow, I.C., et al., 2005. Flotillins and the PHB domain protein family: rafts, worms and anaesthetics. Traffic 6, 725–740.
Mukhopadhyay, M., et al., 2001. *Dickkopf1* is required for embryonic head induction and limb morphogenesis in the mouse. Dev. Cell 1, 423–434.
Munoz, R., et al., 2006. Syndecan-4 regulates non-canonical Wnt signalling and is essential for convergent and extension movements in *Xenopus* embryos. Nat. Cell Biol. 8, 492–500.
Nakagawa, S., et al., 2003. Identification of the laminar-inducing factor: Wnt-signal from the anterior rim induces correct laminar formation of the neural retina *in vitro*. Dev. Biol. 260, 414–425.
Nam, J.S., et al., 2006. Mouse cristin/R-spondin family proteins are novel ligands for the Frizzled 8 and LRP6 receptors and activate β-catenin-dependent gene expression. J. Biol. Chem. 281, 13247–13257.
Neumann, S., et al., 2009. Mammalian Wnt3a is released on lipoprotein particles. Traffic 10, 334–343.
Niehrs, C., 2006. Function and biological roles of the Dickkopf family of Wnt modulators. Oncogene 25, 7469–7481.
Niehrs, C., et al., 2010a. Trafficking, acidification, and growth factor signaling. Sci. Signal. 3, pe26.
Niehrs, C., et al., 2010b. Regulation of Lrp6 phosphorylation. Cell. Mol. Life Sci. 67, 2551–2562.
Nishita, M., et al., 2000. Interaction between Wnt and TGF-β signalling pathways during formation of Spemann's organizer. Nature 403, 781–785.
Nishita, M., et al., 2006. Filopodia formation mediated by receptor tyrosine kinase Ror2 is required for Wnt5a-induced cell migration. J. Cell Biol. 175, 555–562.
Nishita, M., et al., 2010a. Cell/tissue-tropic functions of Wnt5a signaling in normal and cancer cells. Trends Cell Biol. 20, 346–354.
Nishita, M., et al., 2010b. Ror2/Frizzled complex mediates Wnt5a-induced AP-1 activation by regulating Dishevelled polymerization. Mol. Cell. Biol. 30, 3610–3619.
Nusse, R., 2003. Wnts and Hedgehogs: lipid-modified proteins and similarities in signaling mechanisms at the cell surface. Development 130, 5297–5305.
O'Connell, M.P., et al., 2009. Wnt5A activates the calpain-mediated cleavage of filamin A. J. Invest. Dermatol. 129, 1782–1789.
Ohkawara, B., et al., 2003. Role of glypican 4 in the regulation of convergent extension movements during gastrulation in *Xenopus laevis*. Development 130, 2129–2138.
Ohkawara, B., et al., 2011. Rspo3 binds syndecan 4 and induces Wnt/PCP signaling via clathrin-mediated endocytosis to promote morphogenesis. Dev. Cell 20, 303–314.
Oishi, I., et al., 2003. The receptor tyrosine kinase Ror2 is involved in non-canonical Wnt5a/JNK signalling pathway. Genes Cells 8, 645–654.
Pan, D., 2010. The hippo signaling pathway in development and cancer. Dev. Cell 19, 491–505.
Pan, W., et al., 2008. Wnt3a-mediated formation of phosphatidylinositol 4,5-bisphosphate regulates LRP6 phosphorylation. Science 321, 1350–1353.
Panakova, D., et al., 2005. Lipoprotein particles are required for Hedgehog and Wingless signalling. Nature 435, 58–65.
Pandur, P., et al., 2002. Wnt-11 activation of a non-canonical Wnt signalling pathway is required for cardiogenesis. Nature 418, 636–641.
Paudyal, A., et al., 2010. The novel mouse mutant, *chuzhoi*, has disruption of Ptk7 protein and exhibits defects in neural tube, heart and lung development and abnormal planar cell polarity in the ear. BMC Dev. Biol. 10, 87.

Pendergast, S.D., et al., 1998. Familial exudative vitreoretinopathy. Results of surgical management. Ophthalmology 105, 1015–1023.
Person, A.D., et al., 2010. *WNT5A* mutations in patients with autosomal dominant Robinow syndrome. Dev. Dyn. 239, 327–337.
Pinson, K.I., et al., 2000. An LDL-receptor-related protein mediates Wnt signalling in mice. Nature 407, 535–538.
Port, F., et al., 2008. Wingless secretion promotes and requires retromer-dependent cycling of Wntless. Nat. Cell Biol. 10, 178–185.
Port, F., et al., 2010. Wnt trafficking: new insights into Wnt maturation, secretion and spreading. Traffic 11, 1265–1271.
Qian, D., et al., 2007. Wnt5a functions in planar cell polarity regulation in mice. Dev. Biol. 306, 121–133.
Razani, B., et al., 2002. Caveolae: from cell biology to animal physiology. Pharmacol. Rev. 54, 431–467.
Reichsman, F., et al., 1996. Glycosaminoglycans can modulate extracellular localization of the wingless protein and promote signal transduction. J. Cell Biol. 135, 819–827.
Ro, H.A., et al., 2004. pH microdomains in oligodendrocytes. J. Biol. Chem. 279, 37115–37123.
Romanowska, M., et al., 2009. Wnt5a exhibits layer-specific expression in adult skin, is upregulated in psoriasis, and synergizes with type 1 interferon. PLoS ONE 4, e5354.
Rothbaher, U., et al., 2000. Dishevelled phosphorylation, subcellular localization and multimerization regulate its role in early embryogenesis. EMBO J. 19, 1010–1022.
Rulifson, E.J., et al., 2000. Pathway specificity by the bifunctional receptor frizzled is determined by affinity for wingless. Mol. Cell 6, 117–126.
Sakane, H., et al., 2010. LRP6 is internalized by Dkk1 to suppress its phosphorylation in the lipid raft and is recycled for reuse. J. Cell Sci. 123, 360–368.
Sakane, H., et al., 2011. Localization of glypican-4 in different membrane microdomains is involved in the regulation of Wnt signaling. J. Cell Sci. in press.
Sato, A., et al., 2010. Wnt5a regulates distinct signalling pathways by binding to Frizzled2. EMBO J. 29, 41–54.
Sawa, H., et al., 1996. The *Caenorhabditis elegans* gene *lin-17*, which is required for certain asymmetric cell divisions, encodes a putative seven-transmembrane protein similar to the *Drosophila* frizzled protein. Genes Dev. 10, 2189–2197.
Schambony, A., et al., 2007. Wnt-5A/Ror2 regulate expression of XPAPC through an alternative noncanonical signaling pathway. Dev. Cell 12, 779–792.
Schmelzle, T., et al., 2000. TOR, a central controller of cell growth. Cell 103, 253–262.
Schulte, G., 2010. International Union of Basic and Clinical Pharmacology. LXXX. The class Frizzled receptors. Pharmacol. Rev. 62, 632–667.
Schwarz-Romond, T., et al., 2007a. The DIX domain of Dishevelled confers Wnt signaling by dynamic polymerization. Nat. Struct. Mol. Biol. 14, 484–492.
Schwarz-Romond, T., et al., 2007b. Dynamic recruitment of axin by Dishevelled protein assemblies. J. Cell Sci. 120, 2402–2412.
Semënov, M.V., et al., 2001. Head inducer Dickkopf-1 is a ligand for Wnt coreceptor LRP6. Curr. Biol. 11, 951–961.
Semënov, M., et al., 2005. SOST is a ligand for LRP5/LRP6 and a Wnt signaling inhibitor. J. Biol. Chem. 280, 26770–26775.
Semënov, M.V., et al., 2008. DKK1 antagonizes Wnt signaling without promotion of LRP6 internalization and degradation. J. Biol. Chem. 283, 21427–21432.
Sen, M., et al., 2000. Expression and function of wingless and frizzled homologs in rheumatoid arthritis. Proc. Natl. Acad. Sci. USA 97, 2791–2796.
Serru, V., et al., 2000. Sequence and expression of seven new tetraspans. Biochim. Biophys. Acta 1478, 159–163.

Shafer, B., et al., 2011. Vangl2 promotes Wnt/planar cell polarity-like signaling by antagonizing Dvl1-mediated feedback inhibition in growth cone guidance. Dev. Cell 20, 177–191.
Sheldahl, L.C., et al., 1999. Protein kinase C is differentially stimulated by Wnt and Frizzled homologs in a G-protein-dependent manner. Curr. Biol. 9, 695–698.
Shimizu, T., et al., 2008. Stabilized β-catenin functions through TCF/LEF proteins and the Notch/RBP-Jκ complex to promote proliferation and suppress differentiation of neural precursor cells. Mol. Cell. Biol. 28, 7427–7441.
Shnitsar, I., et al., 2008. PTK7 recruits dsh to regulate neural crest migration. Development 135, 4015–4024.
Simons, M., et al., 2009. Electrochemical cues regulate assembly of the Frizzled/Dishevelled complex at the plasma membrane during planar epithelial polarization. Nat. Cell Biol. 11, 286–294.
Slusarski, D.C., et al., 1997. Interaction of Wnt and a Frizzled homologue triggers G-protein-linked phosphatidylinositol signalling. Nature 390, 410–413.
Smolich, B.D., et al., 1993. *Wnt* family proteins are secreted and associated with the cell surface. Mol. Biol. Cell 4, 1267–1275.
Song, H.H., et al., 2002. The role of glypicans in mammalian development. Biochim. Biophys. Acta 1573, 241–246.
Song, H.H., et al., 2005. The loss of glypican-3 induces alterations in Wnt signaling. J. Biol. Chem. 280, 2116–2125.
Sorkin, A., et al., 2009. Endocytosis and signalling: intertwining molecular networks. Nat. Rev. Mol. Cell Biol. 10, 609–622.
Sun, S.C., et al., 2008. New insights into NF-κB regulation and function. Trends Immunol. 29, 469–478.
Suzuki, A., et al., 2008. PTH/cAMP/PKA signaling facilitates canonical Wnt signaling via inactivation of glycogen synthase kinase-3β in osteoblastic Saos-2 cells. J. Cell. Biochem. 104, 304–317.
Tabata, T., et al., 2004. Morphogens, their identification and regulation. Development 131, 703–712.
Taelman, V.F., et al., 2010. Wnt signaling requires sequestration of glycogen synthase kinase 3 inside multivesicular endosomes. Cell 143, 1136–1148.
Takada, R., et al., 2005. Analysis of combinatorial effects of Wnts and Frizzleds on β-catenin/armadillo stabilization and Dishevelled phosphorylation. Genes Cells 10, 919–928.
Takada, R., et al., 2006. Monounsaturated fatty acid modification of Wnt protein: its role in Wnt secretion. Dev. Cell 11, 791–801.
Takei, Y., et al., 2004. Three *Drosophila* EXT genes shape morphogen gradients through synthesis of heparan sulfate proteoglycans. Development 131, 73–82.
Tamai, K., et al., 2004. A mechanism for Wnt coreceptor activation. Mol. Cell 13, 149–156.
Tanaka, K., et al., 2000. The evolutionarily conserved *porcupine* gene family is involved in the processing of the Wnt family. Eur. J. Biochem. 267, 4300–4311.
Tanneberger, K., et al., 2011. Amer1/WTX couples Wnt-induced formation of PtdIns(4,5) P(2) to LRP6 phosphorylation. EMBO J. 30, 1433–1443.
Tauriello, D.V., et al., 2010. Loss of the tumor suppressor CYLD enhances Wnt/β-catenin signaling through K63-linked ubiquitination of Dvl. Mol. Cell 37, 607–619.
Tkachenko, E., et al., 2005. Syndecans: new kids on the signaling block. Circ. Res. 96, 488–500.
Tolwinski, N.S., et al., 2003. Wg/Wnt signal can be transmitted through arrow/LRP5,6 and Axin independently of Zw3/Gsk3beta activity. Dev. Cell 4, 407–418.
Topol, L., et al., 2003. Wnt-5a inhibits the canonical Wnt pathway by promoting GSK-3-independent β-catenin degradation. J. Cell Biol. 162, 899–908.

Torres, M.A., et al., 1996. Activities of the *Wnt*-1 class of secreted signaling factors are antagonized by the *Wnt*-5A class and by a dominant negative cadherin in early *Xenopus* development. J. Cell Biol. 133, 1123–1137.
Traub, L.M., 2009. Tickets to ride: selecting cargo for clathrin-regulated internalization. Nat. Rev. Mol. Cell Biol. 10, 583–596.
Umbhauer, M., et al., 2000. The C-terminal cytoplasmic Lys-thr-X-X-X-Trp motif in frizzled receptors mediates Wnt/β-catenin signalling. EMBO J. 19, 4944–4954.
Vagin, O., et al., 2009. Role of N-glycosylation in trafficking of apical membrane proteins in epithelia. Am. J. Physiol. Renal Physiol. 296, F459–F469.
van Amerongen, R., et al., 2006. Knockout mouse models to study Wnt signal transduction. Trends Genet. 22, 678–689.
van Bokhoven, H., et al., 2000. Mutation of the gene encoding the ROR2 tyrosine kinase causes autosomal recessive Robinow syndrome. Nat. Genet. 25, 423–426.
van den Heuvel, M., et al., 1993. Mutations in the segment polarity genes *wingless* and *porcupine* impair secretion of the wingless protein. EMBO J. 12, 5293–5302.
Varelas, X., et al., 2010. The Hippo pathway regulates Wnt/β-catenin signaling. Dev. Cell 18, 579–591.
Veeman, M.T., et al., 2003. A second canon. Functions and mechanisms of β-catenin-independent Wnt signaling. Dev. Cell 5, 367–377.
Wan, M., et al., 2008. Parathyroid hormone signaling through low-density lipoprotein-related protein 6. Genes Dev. 22, 2968–2979.
Wan, M., et al., 2011. LRP6 mediates cAMP generation by G protein-coupled receptors through regulating the membrane targeting of Gα(s). Sci. Signal. 4, ra15.
Wang, H.Y., et al., 2006. Structure–function analysis of Frizzleds. Cell. Signal. 18, 934–941.
Wang, K., et al., 2008. Characterization of the Kremen-binding site on Dkk1 and elucidation of the role of Kremen in Dkk-mediated Wnt antagonism. J. Biol. Chem. 283, 23371–23375.
Weeraratna, A.T., et al., 2002. Wnt5a signaling directly affects cell motility and invasion of metastatic melanoma. Cancer Cell 1, 279–288.
Wehrli, M., et al., 2000. *Arrow* encodes an LDL-receptor-related protein essential for Wingless signalling. Nature 407, 527–530.
Wharton, K.A.J., 2003. Runnin' with the Dvl: proteins that associate with Dsh/Dvl and their significance to Wnt signal transduction. Dev. Biol. 253, 1–17.
Willert, K., et al., 2003. Wnt proteins are lipid-modified and can act as stem cell growth factors. Nature 423, 448–452.
Winkler, D.G., et al., 2003. Osteocyte control of bone formation via sclerostin, a novel BMP antagonist. EMBO J. 22, 6267–6276.
Witzel, S., et al., 2006. Wnt11 controls cell contact persistence by local accumulation of Frizzled 7 at the plasma membrane. J. Cell Biol. 175, 791–802.
Wong, G.T., et al., 1994. Differential transformation of mammary epithelial cells by Wnt genes. Mol. Cell. Biol. 14, 6278–6286.
Wong, H., et al., 2003. Direct binding of the PDZ domain of Dishevelled to a conserved internal sequence in the C-terminal region of Frizzled. Mol. Cell 12, 1251–1260.
Wrighton, K.H., et al., 2009. Phospho-control of TGF-β superfamily signaling. Cell Res. 19, 8–20.
Wu, G., et al., 2009a. Inhibition of GSK3 phosphorylation of β-catenin via phosphorylated PPPSPXS motifs of Wnt coreceptor LRP6. PLoS ONE 4, e4926.
Wu, J., et al., 2009b. A quest for the mechanism regulating global planar cell polarity of tissues. Trends Cell Biol. 19, 295–305.
Xia, C.H., et al., 2008. A model for familial exudative vitreoretinopathy caused by LPR5 mutations. Hum. Mol. Genet. 17, 1605–1612.

Xu, Q., et al., 2004. Vascular development in the retina and inner ear: control by Norrin and Frizzled-4, a high-affinity ligand–receptor pair. Cell 116, 883–895.
Yamamoto, H., et al., 2006. Caveolin is necessary for Wnt-3a-dependent internalization of LRP6 and accumulation of β-catenin. Dev. Cell 11, 213–223.
Yamamoto, H., et al., 2007. Wnt5a modulates glycogen synthase kinase 3 to induce phosphorylation of receptor tyrosine kinase Ror2. Genes Cells 12, 1215–1223.
Yamamoto, H., et al., 2008a. Wnt3a and Dkk1 regulate distinct internalization pathways of LRP6 to tune the activation of β-catenin signaling. Dev. Cell 15, 37–48.
Yamamoto, S., et al., 2008b. Cthrc1 selectively activates the planar cell polarity pathway of Wnt signaling by stabilizing the Wnt–receptor complex. Dev. Cell 15, 23–36.
Yamamoto, H., et al., 2009. Laminin γ2 mediates Wnt5a-induced invasion of gastric cancer cells. Gastroenterology 137, 242–252.
Yoshikawa, S., et al., 2003. Wnt-mediated axon guidance via the *Drosophila* Derailed receptor. Nature 422, 583–588.
Yu, A., et al., 2007. Association of Dishevelled with the clathrin AP-2 adaptor is required for Frizzled endocytosis and planar cell polarity signaling. Dev. Cell 12, 129–141.
Zallen, J.A., 2007. Planar polarity and tissue morphogenesis. Cell 129, 1051–1063.
Zeng, X., et al., 2001. A freely diffusible form of Sonic hedgehog mediates long-range signalling. Nature 411, 716–720.
Zeng, X., et al., 2005. A dual-kinase mechanism for Wnt co-receptor phosphorylation and activation. Nature 438, 873–877.
Zeng, X., et al., 2008. Initiation of Wnt signaling: control of Wnt coreceptor Lrp6 phosphorylation/activation via frizzled, dishevelled and axin functions. Development 135, 367–375.
Zerial, M., et al., 2001. Rab proteins as membrane organizers. Nat. Rev. Mol. Cell Biol. 2, 107–117.

CHAPTER THREE

Role of Intercompartmental DNA Transfer in Producing Genetic Diversity

Dario Leister *and* Tatjana Kleine

Contents

Lehrstuhl für Molekularbiologie der Pflanzen, Department Biologie I, Ludwig-Maximilians-Universität München (LMU), Planegg-Martinsried, Germany

International Review of Cell and Molecular Biology, Volume 291
ISSN 1937-6448, DOI: 10.1016/B978-0-12-386035-4.00003-3

Abstract

In eukaryotic cells, genes are found in three compartments—the nucleus, mitochondria, and plastids—and extensive gene transfer has occurred between them. Most organellar genes in the nucleus migrated there long ago, but transfer is ongoing and ubiquitous. It now generates mostly noncoding nuclear DNA, can also disrupt gene functions, and reshape genes by adding novel exons. Plastid or nuclear sequences have also contributed to the formation of mitochondrial tRNA genes. It is now clear that organelle-to-nucleus DNA transfer involves the escape of DNA molecules from the organelles at times of stress or at certain developmental stages, and their subsequent incorporation at sites of double-stranded breaks in nuclear DNA by nonhomologous recombination. Intercompartmental DNA transfer thus appears to be an inescapable phenomenon that has had a broad impact on eukaryotic evolution, affecting DNA repair, gene and genome evolution, and redirecting proteins to different target compartments.

Key Words: Endosymbiosis, Horizontal gene transfer, Intercompartmental DNA transfer, NUMTs, NUPTs, Gene evolution, Genome evolution.

1. Introduction

Almost all genes in eukaryotic cells are found in the nucleus, but mitochondria and plastids also contain genomes, derived from their endosymbiont forebears (see Section 2.1). By comparison with their extant prokaryotic relatives, mitochondria and plastids contain far fewer genes, and this reflects an evolutionarily ancient relocation of genes from the organelles to the nucleus. Indeed, organelle-to-nucleus transfer of genetic material continues, mostly involving nonfunctional organellar DNA (orgDNA) (see Section 4). In this review, we summarize the impact of organelle-to-nucleus DNA transfer (see Sections 2 and 4) and other types of intercompartmental DNA migration (see Section 3) on gene and genome evolution (Fig. 3.1). Moreover, we present results obtained from genome analyses, and experimental efforts to reconstruct DNA transfer events (see Section 2.6), that help to clarify the mechanisms that underlie the relocation of DNA from one genetic compartment to another (see Section 5). We also discuss why certain organellar genes seem to be resistant to transfer (see Section 2.5).

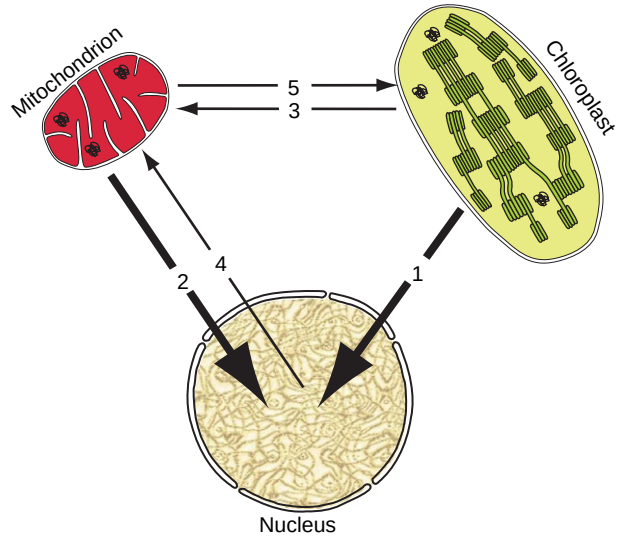

Figure 3.1 Overview of the known types of intercompartmental DNA transfer. (1) Plastid-to-nucleus; (2) mitochondrion-to-nucleus; (3) plastid-to-mitochondrion; (4) nucleus-to-mitochondrion; (5) mitochondrion-to-plastid. The thickness of the arrows indicates the (relative) quantitative significance of transfer events. Here, the photosynthetic version of a plastid, the chloroplast, is shown.

2. Gene Transfer from Organelles to the Nucleus

2.1. The origin of mitochondria and plastids

It is now widely accepted that mitochondria and plastids are of endosymbiotic origin, deriving from progenitors that resembled extant α-proteobacteria (Andersson et al., 2003; Gray et al., 1999) and cyanobacteria (Raven and Allen, 2003), respectively. The identity of the closest living relative of mitochondria among free-living α-proteobacteria is still disputed. Links have been demonstrated between mitochondria and organisms belonging to the order Rickettsiales (Andersson et al., 2003; Fitzpatrick et al., 2006), as well as to *Rhodospirillum rubrum* (Esser et al., 2004). Recently, it was proposed that mitochondria may have originated before the separation of Rickettsiaceae, Anaplasmataceae, and Rhodospirillaceae and that the possibility of genome chimerism must be considered in the analysis of the origin of mitochondria (Abhishek et al., 2011). Plastids, however, are most closely related to nitrogen-fixing unicellular cyanobacteria classified in subsection I, with the heterocyst-forming Nostocales as their nearest sister group (Deusch et al.,

2008; Falcon et al., 2010). The acquisition of mitochondria and plastids is thought to have taken place 1.5–2 (Brocks et al., 1999) and 1.2 billion years ago (Yoon et al., 2004), respectively.

The acquisition of a cyanobacterial symbiont by a eukaryotic host gave rise to "primary" plastids. Once established, primary plastids then spread from red and green algae to other eukaryotes by additional rounds of endosymbiosis between two eukaryotes. The resulting "secondary" and "tertiary" plastids display a very complex pattern of diversity and distribution because the plastids and their hosts can have different evolutionary histories (Keeling, 2010). For more details on specific aspects of secondary and tertiary endosymbiosis in plastid evolution, the reader is referred to a number of recent reviews (Gould et al., 2008; Green, 2011; Keeling, 2010; Kleine et al., 2009a).

In addition to fully fledged plastid organelles, numerous symbiotic partnerships demonstrate that endosymbiosis is a persistent driving force in evolution, and relevant cases of ongoing endosymbiotic relationships are presented in Gould et al. (2008). Symbiotic relationships between bacteria and eukaryotic organisms are widespread in nature, and the photosynthetic symbiosis between algal chloroplasts and sea slugs is a well-known example (Rumpho et al., 2000). Moreover, experimental infection of amoebae can result in the production of permanently infected clones (Jeon and Lorch, 1967), which might even require the presence of living endosymbionts for their survival (Jeon and Jeon, 1976). Recently, the potential of symbiotic relationships in the creation of organisms with specific new functions has begun to be exploited in synthetic biological networks (Chin, 2006). It is even possible to equip photosynthetic bacteria with the ability to invade the cytoplasm of mammalian cells, enabling further engineering and applications in synthetic biology (Agapakis et al., 2011).

Although mitochondria and plastids have retained the bulk of their prokaryotic biochemistry (Timmis et al., 2004), their genomes now encode only a small fraction of the organelles' proteins, ranging from 3 to 67 in mitochondria (Szklarczyk and Huynen, 2010) and from 15 to 209 in plastids (Keeling and Palmer, 2008). This situation is the result of both extensive horizontal (or lateral) gene transfer—more precisely endosymbiotic gene transfer (EGT) from the endosymbiont to the nucleus—and gene loss (Kleine et al., 2009a; Martin et al., 2002; Timmis et al., 2004). The EGT/gene loss resulted in progressive loss of the organelle's genetic autonomy and has led in extreme cases to the loss of the entire genome (in some hydrogenosomes and all mitosomes) (Szklarczyk and Huynen, 2010). Based on the residual gene complements in organelles from different species, it is thought that most plastid and mitochondrial genes were transferred in early, and perhaps rapid, migrations, whereas subsequent transfers have been highly discontinuous (Keeling and Palmer, 2008).

2.2. Endosymbiosis has shaped the nuclear genomes of eukaryotes

orgDNA was initially detected in the nuclear genome by hybridization experiments (Stern and Lonsdale, 1982; Tsuzuki et al., 1983). Subsequently, sequencing data directly demonstrated that certain sequences in the nuclear genome are almost identical to segments of mitochondrial (Arctander, 1995) or chloroplast (Baldauf and Palmer, 1990) DNA. The analysis of EGT and nuclear orgDNA (norgDNA) received a tremendous boost, as complete genome sequences of prokaryotes and eukaryotes became available. Quantitative estimates of the α-proteobacterial heritage based on a phylogenetic analysis of 144 completed genomes, including 11 α-proteobacterial genomes and those of the eukaryotes *Saccharomyces cerevisiae*, *Candida albicans*, *Plasmodium falciparum*, *Homo sapiens*, *Caenorhabditis elegans*, *Schizosaccharomyces pombe*, *Arabidopsis thaliana*, and *Drosophila melanogaster*, led to the identification of a set of 842 eukaryotic genes bearing an α-proteobacterial signature (Gabaldon and Huynen, 2007). In light of the weakness of both the phylogenetic signal and constraints on the incidence of gene loss, this number represents a minimal estimate of the protomitochondrial proteome (Boussau et al., 2004; Esser et al., 2007). Using the complete set of orthologous groups present in the α-proteobacterial ancestor in sequence-similarity searches against eukaryotic genomes, an upper bound of 1700 genes resulting from transfer from proteobacterial sources was found (Boussau et al., 2004). Mitochondrial proteins represent only a minority of the proteins of protomitochondrial descent (14–22% in human and 16–32% in yeast). Accordingly, it is estimated that around 70% and 60% of the total set of α-proteobacterial-derived proteins in human and yeast, respectively, are targeted to locations other than mitochondria (Gabaldon and Huynen, 2007).

Depending on the type of analysis, various estimates for the contribution of cyanobacterial EGT to nuclear genomes have been proposed. For the extremophilic red alga *Cyanidioschyzon merolae*, cyanobacterial EGT is thought to have contributed a minimum of 12% of the genes present in its reduced nuclear genome (Sato et al., 2005), whereas in the green alga *Chlamydomonas reinhardtii*, 3.5–6% of the protein-coding genes in the nuclear genome are of cyanobacterial origin, of which at least 44% code for plastid-targeted proteins and at least 47% are involved in metabolic processes (Moustafa and Bhattacharya, 2008). Of the 3576 nuclear genes in the glaucophyte *Cyanophora paradoxa*, 10.8% are of cyanobacterial origin and only a minor portion (one-ninth) of these have been recruited for nonplastid functions (Reyes-Prieto et al., 2006). Extensive analyses have been employed to assess the cyanobacterial heritage of the model flowering plant *A. thaliana* (Deusch et al., 2008; Martin et al., 2002) and of three other photosynthetic eukaryotes (Deusch et al., 2008). By comparing the genome

of *A. thaliana* with those of 3 cyanobacterial species, 16 other prokaryotes, and yeast, it has been extrapolated that the cyanobacterial endosymbiont contributed 18% (or 4500) of all nuclear genes in *A. thaliana*, with about one-half of these having been recruited for nonplastid functions (Martin et al., 2002). In a follow-up analysis by the same group, the genomes of *A. thaliana*, *Oryza sativa*, *C. reinhardtii*, and the red alga *C. merolae* were compared with 224 prokaryotic (including nine cyanobacterial) and 13 eukaryotic genomes. On average, about 14% of the proteins examined in each of the four photosynthetic eukaryotes were judged to be of cyanobacterial origin (Deusch et al., 2008). As in the earlier study (Martin et al., 2002), genes transferred to the nuclear genome encode proteins belonging to virtually all functional categories (Deusch et al., 2008).

Thus, although the precise magnitude of the cyanobacterial or proteobacterial heritage varies depending on organism and analytical method, it is obvious that EGT has played a significant role in shaping eukaryotic genomes, and during the early phase of organelle evolution, this transfer resulted in a massive relocation of genes from organelles to nucleus.

2.3. Recurrent and ongoing gene transfers

In animals, transfer of functional genes from mitochondria to the nucleus has entirely ceased (Boore, 1999). By contrast, in plants, transfer of organellar genes to the nucleus has continued up to the present day (Cullis et al., 2009; Knoop, 2004). It appears that many mitochondrial genes in angiosperms—especially those coding for ribosomal proteins—have been transferred to the nucleus many times independently (Adams and Palmer, 2003). For instance, complete loss of the mitochondrial *rps10* gene (26 times) or its transfer to the nucleus was observed frequently in a sample of 277 diverse angiosperms (Adams et al., 2000). Moreover, successful functional transfer of the *rps14* gene from the mitochondrion to the nucleus has occurred at least three times during the evolution of the Poales (Ong and Palmer, 2006). The transfers in Cyperaceae and Poaceae are relatively ancient, whereas the putative Joinvilleaceae transfer may be the most recent case of functional mitochondrion-to-nucleus transfer yet described (Ong and Palmer, 2006). In an extended study, DNAs from 280 genera of flowering plants were surveyed for the presence or absence of 40 mitochondrial protein genes by Southern hybridization (Adams et al., 2002). All 14 ribosomal protein genes and the succinate dehydrogenase genes *sdh3* and *sdh4* have been lost from the mitochondrial genome many times (6–42) during angiosperm evolution, whereas only two losses were detected among the other 24 genes, most of which represent respiratory genes (Adams et al., 2002).

Like these mitochondrial examples, the chloroplast gene for translation initiation factor 1 (*infA*) is strikingly mobile, according to a survey of more

than 300 angiosperms (Millen et al., 2001). In four species with nonfunctional chloroplast *infA* genes, transferred and expressed copies of the gene, complete with stretches coding for putative chloroplast transit peptides, were found in the nucleus (Millen et al., 2001). Within rosids, there have been independent transfers of *rpl22* from the plastid to the nucleus in Fabaceae and Fagaceae and a putative third transfer was observed in Passiflora; these shifts occurred approximately 56–58, 34–37, and 26–27 million years ago, respectively (Jansen et al., 2011). The high level of sequence divergence between the transit peptides of *infA* and *rpl22* strongly suggests that the nuclear *infA* and *rpl22* genes derived from four (in the case of *infA*) or three (in the case of *rpl22*) independent chloroplast-to-nucleus gene transfers during angiosperm evolution (Jansen et al., 2011; Millen et al., 2001).

2.4. Intermediate stages of organelle-to-nucleus gene transfer

Until functional organelle-to-nucleus transfer is successfully accomplished, both the organellar and nuclear genomes may contain a copy of the same gene, as exemplified by the *rps14* and *rps16* genes. Thus, nearly intact and expressed pseudogenes of *rps14* have persisted in the mitochondrial genomes of most lineages of the Poaceae and Cyperaceae (Ong and Palmer, 2006), whereas in *A. thaliana* and its close relatives, nucleus- and plastid-encoded *rps16* genes have coexisted for at least 126 million years (Roy et al., 2010). Moreover, *rps16* pseudogenes are often found in angiosperm plastid genomes—a fact which might be explained by the loss of its splicing capacity even when the gene is transcriptionally active (Roy et al., 2010). In rice, a comprehensive search for splinters of chloroplast DNA (cpDNA) in the nuclear genome revealed the coexistence of 53 known rice plastid genes with two or more intact nuclear counterparts (Akbarova et al., 2011). Moreover, copies of five genes that are still active in the plastid seem to be transcribed in the nucleus, representing an intermediate stage in an organelle-to-nucleus gene transfer process that continues at the present time (Akbarova et al., 2011).

2.5. Why have organelles retained genomes at all?

Several hypotheses attempt to explain why certain organellar genes have never been transferred to the nucleus. Widely discussed is the "hydrophobicity–importability" hypothesis, which postulates that the hydrophobicity of certain organellar proteins might interfere with their efficient retargeting to, and import into, the organelle (Daley and Whelan, 2005). Very hydrophobic proteins might also be misrouted to the endoplasmic reticulum (Vonheijne, 1986). This hypothesis is supported by the fact that the only

protein-coding genes found in every completely sequenced mitochondrial genome—*cox1* and *cob*, encoding cytochrome oxidase subunit 1 and apocytochrome *b*, respectively—code for the most hydrophobic proteins present in mitochondria (Adams and Palmer, 2003). Further, when synthesized in the cytosol, Cox2 and Cob could not be imported into mitochondria unless their hydrophobicity was reduced by mutations (Claros et al., 1995; Daley et al., 2002). In contrast, it was experimentally possible to express the hydrophobic D1 protein of photosystem II and the large subunit (RbcL) of the ribulose-bisphosphate carboxylase/oxygenase (RubisCO) equipped with chloroplast transit peptides from nucleus-encoded gene copies, demonstrating that at least these large hydrophobic proteins can be successfully retargeted to and imported into chloroplasts (Cheung et al., 1988; Kanevski and Maliga, 1994).

An alternative explanation for the retention of genomes by organelles is based on the fact that the genes still residing in the organelles have more in common than the hydrophobicity of their products. A core set of around 35 plastid genes is found in almost all photosynthetic organisms and these code for subunits of the bacterial-type RNA polymerase, RbcL, subunits of the 70S ribosome, the two photosystems, the cytochrome b_6/f complex and the ATP synthase, as well as rRNAs and tRNAs (Green, 2011). The "redox regulatory control" hypothesis (Allen, 1993) assumes that organelles need to retain control of the expression of genes encoding components of their electron transport chain in order to maintain redox balance. Thus, their synthesis can be regulated in such a way that the production of toxic reactive oxygen species can be largely avoided (Allen et al., 2005). Therefore, safe and efficient energy transduction might be critically dependent on rapid and efficient on-site regulation of certain organellar genes, and this would preclude their transfer to the nucleus. This idea is supported by the finding that, in parasitic plants, photosynthesis-related plastid genes, such as genes encoding photosystem subunits, are especially susceptible to loss or degradation to pseudogenes (Gao et al., 2010). For instance, the plastome of *Epifagus virginiana* has undergone extreme reduction and now comprises only 42 genes; strikingly, none of them is an intact photosynthetic or chlororespiratory gene (Depamphilis and Palmer, 1990).

2.6. Experimental reconstructions of gene transfer

2.6.1. Mitochondrion-to-nucleus gene transfer in yeast

The first successful experimental demonstration of DNA migration from organelles to the nucleus was accomplished in yeast (Thorsness and Fox, 1990). A yeast strain lacking endogenous mitochondrial DNA (mtDNA) and bearing the nuclear *uracil auxotrophy 3* (*ura3*) mutation was used to propagate the nuclear genetic marker *URA3* on recombinant plasmid DNA located in mitochondria. Because of the mitochondrial location of

the episomal *URA3* gene, the uracil auxotrophy (Ura^-) of this yeast strain was initially not complemented and the original strain could only grow on medium supplemented with uracil. However, upon subsequent propagation on Ura^- medium, several Ura^+ prototrophs were identified. The numbers of mutants obtained revealed that episomal DNA moves from mitochondria to the nucleus with a frequency of $\sim 2 \times 10^{-5}$ per cell per generation (Thorsness and Fox, 1990). When the plasmid was integrated into the mitochondrial chromosome, a lower frequency of migration ($\sim 5 \times 10^{-6}$ per cell per generation) was observed (Thorsness and Fox, 1993). Conversely, when selection conditions were set up to detect migration of DNA from the nucleus to mitochondria, it was estimated that nucleus-to-mitochondrion transfer occurs at least 100,000 times less frequently (Thorsness and Fox, 1990).

2.6.2. Plastid-to-nucleus gene transfer in tobacco

Escape of tobacco orgDNA and its uptake into the nucleus have also been experimentally demonstrated (Huang et al., 2003, 2004; Lloyd and Timmis, 2011; Sheppard et al., 2008; Stegemann and Bock, 2006; Stegemann et al., 2003). The earliest studies were based on the integration of marker genes into the plastid genome: an aminoglycoside resistance gene (*aadA*) conferring spectinomycin resistance to select for transplastomic lines and a kanamycin resistance gene (*neo*) designed for exclusive expression in the nucleus. Because—in analogy to the yeast experiments—the *neo* marker would be functional only in the nucleus, its relocation from plastids to the nucleus could be monitored by screening of cells or seedling progeny for kanamycin resistance. Sixteen of $\sim$250,000 seedlings tested contained the *neo* marker integrated into the nuclear genome, each time in a different location (Huang et al., 2003). The frequency of chloroplast-to-nucleus gene transfer was also measured in somatic tobacco cells; here, in 1 in 5 million somatic cells regenerated from leaf explants, the marker gene had translocated to the nucleus (Stegemann et al., 2003). In a refined genetic screen designed to select specifically for the activation of the originally plastid-localized *aadA* gene in the nuclear genome, a frequency of 3 in 10^8 cells of leaf explants was obtained (Stegemann and Bock, 2006). This demonstrates that DNA-mediated gene transfer from plastids to the nucleus and activation of the gene by suitable mutations or rearrangements in the nuclear genome occur with an unexpectedly high frequency. However, the estimation of the frequency of activation of recently transferred plastid genes is complicated by the fact that the pair of reporter genes used was arranged in the same transcriptional polarity, with the 35S-driven *neo* gene upstream of *aadA*. Therefore, transcriptional activation of *aadA* in the nucleus always involved partial deletion of *neo* sequences and capture of the 35S promoter, as demonstrated by sequencing of the rearranged loci (Stegemann and Bock, 2006). To overcome this problem, the reporter gene cassettes were arranged

in opposite directions (Lloyd and Timmis, 2011), but in this assay also, the 35S promoter was still implicated in all events leading to *aadA* activation, involving either duplication of the 35S promoter used for *neo* in reverse polarity upstream of *aadA* or recruitment of nuclear gene regulatory elements within the 35S promoter to enhance nuclear transcription from the *psbA* promoter, which is known to have weak nuclear activity (Cornelissen and Vandewiele, 1989). Accordingly, the value of one activation event per 2×10^8 cells observed here still overestimates the frequency of natural plastid gene activation in the nucleus.

2.7. Key events in organelle-to-nucleus gene transfer

2.7.1. Functional activation of organellar genes in the nucleus

In the majority of cases, orgDNA transferred to the nucleus is nonfunctional and its sequence decays rapidly and/or it is eliminated from the nuclear genome (Sheppard and Timmis, 2009). For a nuclear copy of an organellar gene to become functional, it must acquire additional genetic elements, including appropriate promoter and terminator sequences to drive its expression, and presequences in cases where the protein must be targeted to organelles (Martin and Herrmann, 1998). It is possible that some plastid promoters, like the *psbA* promoter (Cornelissen and Vandewiele, 1989), already show weak activity in the nucleus. In the experimental reconstruction of the translocation of plastid-localized marker genes into the nucleus of tobacco (see Section 2.6.2), one line was found to contain a 98-bp deletion that brought the 35S promoter closer to the *psbA* promoter and enhanced nuclear transcription from the *psbA* promoter, which was cointegrated in the nuclear DNA; polyadenylation was found to occur at two separate sites within the *psbA* untranslated region (Lloyd and Timmis, 2011). This supports earlier suggestions that the AT-rich nature of chloroplast noncoding regions may coincidentally provide abundant polyadenylation sites (Stegemann and Bock, 2006). Further, it has been shown that some organellar genes already contain N-terminal targeting sequence-like extensions which, upon transfer to the nucleus, could act as targeting signals to allow the gene product to be reimported into the original organelle. Examples include mitochondrial genes encoding ribosomal proteins whose N-terminal sequences have been shown by GFP fusion experiments to mediate import into mitochondria (Ueda et al., 2008a). Moreover, a dual targeting to the mitochondria and chloroplasts has been discovered in the *rps16* gene without an N-terminal extension (Ueda et al., 2008b). But a targeting signal can undoubtedly be acquired after integration into the nuclear chromosome. Two intriguing cases of insertion of an organellar gene into a preexisting gene for a mitochondrial protein and recruitment of its presequence have been described (Adams et al., 2000; Figueroa et al., 1999). Recently, in a large-scale analysis of gene structures and sequence

evolution in 77 cases of functional mitochondrial gene transfers, acquisition of a presequence from a preexisting gene for a mitochondrial protein was found to be quite common: 50% (21/42) of genes with a presequence had obtained it from another nuclear gene for a mitochondrial protein, 36% (15/42) possessed a presequence derived from an unknown source, and the others had acquired their presequences from genes coding for nonmitochondrial proteins (Liu et al., 2009). It is tempting to speculate that presequences of unknown origin are derived *de novo* upon association with the newly transferred genes, and several mechanisms for the acquisition of a targeting signal have been suggested (Adams and Palmer, 2003).

2.7.2. Evolution of novel transport machineries

If the product of a gene that has been transferred from an organelle to the nucleus is required in the organelle, mechanisms for its import are needed. Therefore, the genetic and biochemical transition from a bacterial endosymbiont to a fully integrated organelle required the evolution of novel transport machineries that facilitated the import of proteins into and across the double membrane of the ancestral endosymbiont (Dolezal et al., 2006; Gross and Bhattacharya, 2009; Reumann et al., 2005).

2.7.2.1. Import into mitochondria The mitochondrion predates the plastid and therefore was the first to evolve sophisticated machinery for targeting nucleus-encoded gene products back to this compartment (de Duve, 2007). Thereafter, the first algae independently developed a protein import apparatus to service the plastid (Bhattacharya et al., 2007).

Protein transport into mitochondria is mediated by four protein complexes that are embedded in the outer and inner membranes of mitochondria: TOM, TIM23, TIM22, and SAM (sorting and assembly machinery) complexes (Mokranjac and Neupert, 2009; Neupert and Herrmann, 2007). This protein transport system is shared by all eukaryotes, whether they possess mitochondria, hydrogenosomes, or mitosomes (Szklarczyk and Huynen, 2010). The central, and the only essential, component of the TOM complex is Tom40, a β-barrel protein which forms a translocation channel (Mokranjac and Neupert, 2009). The ancestry of Tom40 is controversial (Alcock et al., 2010). However, some evidence, such as its β-barrel structure—which is characteristic for bacterial outer-membrane proteins—suggests that Tom40 family members resemble YdeK, a bacterial protein export channel (Cavalier-Smith, 2006). The central translocase is the TIM23 complex: the membrane part of the complex consists of Tim17, Tim23, and Tim50, while the import motor is formed by Tim14, Tim16, Tim44, Mge1, and mtHsp70 (Mokranjac and Neupert, 2009). Tim17 and Tim23 family proteins share sequence similarity with OEP16, a channel-forming amino acid transporter in the outer envelope of chloroplasts, and contain a PRAT (preprotein and amino acid transporters) motif also found in LivH, a bacterial amino

acid transporter, representing a living link to the ancestral Tim23 (Rassow et al., 1999). In addition, bioinformatic analysis of extant α-proteobacteria, and experimental work on the model α-proteobacterium *Caulobacter crescentus*, have demonstrated that Tim44 and Tim14 have bacterial homologs, suggesting that at least a part of the TIM23 complex was derived from the endosymbiont (Clements et al., 2009). Together with the LivH amino acid transporter, these TIM23 homologs could have served as bacterial "pre-adaptations" when the need for protein import arose (Clements et al., 2009). Tim22, the central component of TIM22, is homologous to Tim17 and Tim23 (Rassow et al., 1999). The SAM complex is closely related in sequence and function to the bacterial Omp85 protein translocase (Dolezal et al., 2006).

Especially in the jakobids, which are free-living, heterotrophic flagellates, crucial evidence bearing on protein transport pathways has been retained. Thus, *Reclinomonas americana* possesses the most bacterial-like mitochondrial genome reported to date, with a total of 98 genes, of which 67 code for proteins (Gray et al., 2004). These include SecY, the core subunit of the translocon/SecY complex. In all bacteria, the SecY complex is the major route for transferring proteins across the inner membrane and assists in the assembly of hydrophobic proteins into the inner membrane (Rapoport, 2007). Because *R. americana* has a mitochondrial TIM machinery in addition to SecY, as determined by the analysis of expressed sequence tags, it was suggested that this species represents an evolutionary transition in which the ancestral and derived protein transport pathways coexist and could complement one another in the assembly of proteins into the mitochondrial inner membrane (Tong et al., 2011).

2.7.2.2. Import into chloroplasts In the case of plant chloroplasts, the import and processing machinery comprise the TIC–TOC (translocators of the inner and outer chloroplast membrane) complexes. An endosymbiont ancestry has been suggested for the outer-membrane channel protein Toc75, as well as for the inner chloroplast membrane proteins Tic20, Tic22, and Tic55, on the basis of their similarity to cyanobacterial proteins (Reumann and Keegstra, 1999). This finding was corroborated when, in addition to the *A. thaliana* and cyanobacterial genomes, the genomes of a red alga, a diatom and phylogenetically diverse plastids, were analyzed (Reumann et al., 2005). The high sequence variability between chloroplast and *Synechocystis* sp. PCC 6803 proteins suggests that the ancestral proteins had different physiological roles and were modified significantly to take over the novel function of precursor import (Reumann and Keegstra, 1999). Another view suggests that many TOC and TIC components possess a functional duality that might reflect conservation of ancestral pre-endosymbiotic properties (Gross and Bhattacharya, 2009).

Most of the remaining subunits seem to be of eukaryotic origin, recruited from preexisting nuclear genes. As indicated by their presence in the red alga *C. merolae*, Toc34 and Toc110 were the next subunits that joined the protein import complex, followed by the stromal processing peptidase, members of the Toc159 receptor family, Toc64, Tic40, and finally regulatory redox components Tic62, Tic32, and possibly Tic55 (Benz et al., 2009), all of which were probably required to increase the specificity and efficiency of precursor import (Reumann et al., 2005). Import-related components on the chloroplast stromal side, such as the molecular chaperones of the Hsp70 and Hsp100 family, and their attendant factors GrpE and DnaJ, are derived from the endosymbiont (McFadden and van Dooren, 2004).

However, the initial system for protein trafficking to the endosymbiont probably exploited the host endomembrane system (Bhattacharya et al., 2007). Indeed, some plastid protein import takes place independently of the TIC–TOC machinery, and the list of proteins imported via an alternative route is growing (Armbruster et al., 2009; Li and Chiu, 2010). It now includes embryo defective 1211, glycolate oxidase 2, and a putative glutathione *S*-transferase (Armbruster et al., 2009) and members of the canonical TIC–TOC complex like Tic32 (Nada and Soll, 2004).

Taken together, all evolutionary analyses indicate that the protein import machineries of mitochondria and plastids are mosaics of both endosymbiont- and host-cell-derived proteins (Dolezal et al., 2006; Reumann et al., 2005). But it remains unclear whether the development of protein import machineries was driven by the ancestral host cell, by the prokaryotic endosymbiont, or by both (Alcock et al., 2010; Gross and Bhattacharya, 2009).

2.8. Consequences of organelle-to-nucleus gene transfer

2.8.1. Cellular functions of mosaic origin

It was originally postulated that transfer of genes from the endosymbiont to the nucleus should always be accompanied by retargeting and import of its product into the original compartment: chloroplast or mitochondrion (Martin and Herrmann, 1998). However, this simple "gene transfer, protein re-import" model can no longer be upheld (Elias and Archibald, 2009), because (i) many products of transferred genes have acquired extraorganellar functions (Archibald, 2006; Deusch et al., 2008; Gabaldon and Huynen, 2003; Karlberg et al., 2000; Martin et al., 2002; Timmis et al., 2004) and (ii) numerous plastid- and mitochondrion-related processes involve proteins of diverse evolutionary origins (Atteia et al., 2009; Gabaldon and Huynen, 2007; Reumann et al., 2005; Reyes-Prieto and Bhattacharya, 2007; Richards et al., 2006; Suzuki and Miyagishima, 2010; Szklarczyk and Huynen, 2010; Tzin and Galili, 2010). Accordingly, the blending of nuclear and organellar gene products enabled the evolution of many new or modified metabolic pathways and control networks (Gould et al., 2008).

2.8.1.1. Extraorganellar functions of mosaic origin One example of extraorganellar functions of mosaic origin is glycolysis in the cytosol, which involves cyanobacterial- and proteobacterial-like enzymes (Martin and Schnarrenberger, 1997). Moreover, the majority of the products of genes of proteobacterial origin are not located in the mitochondrion. For instance, the enzymes of fatty acid oxidation are located in the peroxisome (Gabaldon et al., 2006), and enzymes involved in fructose and mannose metabolism are cytoplasmic (Gabaldon and Huynen, 2007). Further, phylogenetic analyses strongly suggest that several central components of the nuclear pore complex most probably have an endosymbiotic origin (Mans et al., 2004).

2.8.1.2. Organellar functions of mosaic origin Approximately 40% of the nucleus-encoded plastid proteome that is shared by the red alga *C. merolae* and *A. thaliana* does not derive from cyanobacteria but originates from genes of the ancestral eukaryotic host or various other bacterial lineages (Suzuki and Miyagishima, 2010). In consequence, organellar functions are also carried out by proteins of mosaic origin. For instance, although the photosynthetic machinery in chloroplasts, as well as the respiratory chain in mitochondria, is essentially very similar to the energy-generating systems in their prokaryotic relatives (Berry, 2003), even here a number of proteins do not have counterparts in prokaryotes (Gabaldon and Huynen, 2007; Nelson and Yocum, 2006; Scheller et al., 2001; Suzuki and Miyagishima, 2010). Additional examples for chloroplast functions of mosaic origin include the Calvin cycle (Martin and Schnarrenberger, 1997) and the heme biosynthesis pathway (Obornik and Green, 2005), which result from gene fusions, horizontal gene transfer, and endosymbiotic replacements.

Mitochondrial proteins represent only a minority (14–22% and 16–33%, respectively) of the proteins of proteobacterial descent in humans and yeast (Gabaldon and Huynen, 2003; Karlberg et al., 2000; Richly et al., 2003). Human mitochondrial protein complexes with at least three subunits, like the ATPase, 70S ribosome, and TIM complex, have counterparts in α-proteobacteria, but on average, only 30% of their subunits are of unequivocally endosymbiotic origin as the consequence of extensive eukaryotic inventions (Szklarczyk and Huynen, 2010). Remarkably, the degree of overlap between the human and yeast mitochondrial proteomes is rather modest: 312 (42%) of the yeast mitochondrial proteins have 400 (47%) orthologs in human mitochondria. This implies that protein gain, loss, and retargeting have mostly occurred in a lineage-specific manner, resulting in the metabolic differences encountered between human and yeast mitochondria (Gabaldon and Huynen, 2007). From an evolutionary standpoint, nuclear copies of organellar genes represent the raw material for evolutionary "tinkering" (Jacob, 1977) to create evolutionary innovation throughout the entire cell.

2.8.2. Anterograde and retrograde signaling

Because organellar multiprotein complexes are actually mosaics of subunits encoded by nuclear and organellar genes (see Section 2.8.1), mechanisms that coordinate gene expression in the organelle and nucleus are required to ensure appropriate and energy-saving assembly of such complexes. Consequently, mechanisms have evolved that provide for direct control of organellar gene expression (OGE) and their posttranslational modifications by nuclear genes (anterograde signaling) (Barkan and Goldschmidt-Clermont, 2000; Choquet and Wollman, 2002; Giege et al., 2005; Rochaix, 2001; Somanchi and Mayfield, 1999; Stern et al., 2010). These, in turn, rely on "retrograde" signaling from the organelle, which conveys information on its developmental and metabolic state to the nucleus, thus enabling nuclear gene expression (NGE) to be modified in accordance with the current status of the organelle (Kleine et al., 2009b; Pogson et al., 2008; Woodson and Chory, 2008). Whereas chloroplast-to-nucleus signaling has been extensively investigated in plants (Kleine et al., 2009b; Liu and Butow, 2006; Pogson et al., 2008; Rhoads and Subbaiah, 2007; Woodson and Chory, 2008), mitochondrial retrograde signaling has been studied predominantly in yeast (Liu and Butow, 2006) and relatively little is known about mitochondrion-to-nucleus signaling in plants (Rhoads and Subbaiah, 2007). The coordination of OGE and NGE directly at the transcript level represents a straightforward mechanism of control. In *A. thaliana*, the transcriptional coregulation of organellar and nuclear genes which code for proteins with similar functions, such as OGE or energy production, was dissected by analyzing 1300 transcription profiles encompassing eight different categories of environmental and genetic conditions (Leister et al., 2011). The tightest coregulation generally occurs for genes that are located in the same genetic compartment and code for products targeted to the same organelle (Fig. 3.2A). However, it also emerged that coregulation between genetic compartments is characteristic for chloroplasts and occurs at a basal level also for mitochondria (Fig. 3.2B). Moreover, in chloroplasts, nucleus–organelle coregulation can actually predominate over intracompartmental networks, as exemplified by the coexpression of nuclear and organellar photosynthesis genes under "general stresses" conditions (Fig. 3.2B).

3. DNA Transfer to Organelles

3.1. Transfer of plastid or nuclear DNA to mitochondria

In addition to organelle-to-nucleus transfer of DNA, incorporation of chloroplast or nuclear DNA into mitochondrial genomes has been observed (Fig. 3.1; Ellis, 1982; Kubo and Mikami, 2007; Pont-Kingdon et al., 1998).

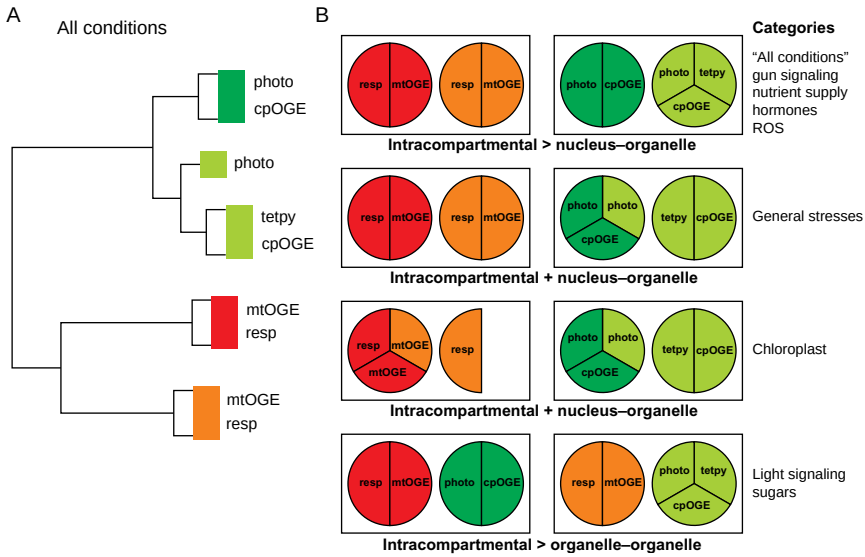

Figure 3.2 Different layers of transcriptional control regulate the expression of genes for organellar proteins. (A) Nearly 1300 ATH microarray-based transcriptional profiles of nuclear and organellar genes for mitochondrial and chloroplast proteins in the model plant Arabidopsis were analyzed (Leister et al., 2011). The perturbations considered and conditions imposed were assigned to eight major categories of environmental or genetic stimuli (see (B)), which are known or assumed to be relevant for cp and/or mt functions and retrograde signaling. The outcome of the hierarchical clustering of the expression profiles of gene sets over all conditions is shown. Light green and orange squares stand for nuclear genes encoding plastid and mitochondrial proteins, respectively; dark green and red squares for organellar genes for plastid or mitochondrial proteins, respectively. The genes were assigned to classes according to their function: photo, photosynthesis; cpOGE, chloroplast organellar gene expression; mtOGE, mitochondrial OGE; resp, respiration (mitochondrion); tetpy, tetrapyrrole biosynthesis (chloroplast). (B) A scheme detailing the similarities in the expression profiles of the different gene sets following exposure of plants to the eight different conditions summarized in (A). Highly coregulated gene sets ("intracompartmental" or "nucleus–organelle") are symbolized by sectors, moderately coregulated gene sets ("nucleus–organelle" or "organelle–organelle") are enclosed by boxes. The color code is as in (A). $x > y$ indicates that mode x of transcriptional coregulation prevails over mode y.

Chloroplast genes were first detected in mitochondria in 1982 and were dubbed "promiscuous DNA" (Ellis, 1982). It has been estimated that DNA transfer from plastids to mitochondria has been going on at least since the time of the last common ancestor of extant gymnosperms and angiosperms, about 300 million years ago (Wang et al., 2007). Because gene-coding regions constitute only between 7% and 17% of mitochondrial

genomes in angiosperms, it follows that the expansion of mitochondrial genomes has occurred mainly by the enlargement of intergenic regions (Kubo and Newton, 2008). Indeed, database searches have revealed that these regions contain between 1.6% (sugar beet; Satoh et al., 2004) and 8.8% (*Vitis vinifera*; Goremykin et al., 2009) cpDNA sequences and between 0.1% (maize; Clifton et al., 2004) and 13.4% (rice; Notsu et al., 2002) nuclear DNA sequences. In contrast, the mitochondrial genome of *Marchantia polymorpha* seems to lack sequences with homology to plastid or nuclear DNA (Oda et al., 1992). It is still not clear when and why plants accepted foreign DNA insertions into their mitochondrial genome (Knoop, 2004).

The only cpDNA sequences that have contributed to the transcribed fraction of mitochondrial genomes are tRNA genes (Sangare et al., 1989; Veronico et al., 1996). Consequently, the tRNA gene set present in the mitochondrial genomes of higher plants includes sequences of both proteobacterial and cyanobacterial origin. Six of the 22 tRNA genes identified in the *A. thaliana* chondriome appear to be derived from the plastid genome (Marienfeld et al., 1999). Moreover, the plastid-derived tRNA genes $tRNA^{His}$, $tRNA^{Met}$, $tRNA^{Asn}$, and $tRNA^{Trp}$ are present in all angiosperm chondriomes that have been sequenced (Knoop, 2004). Characteristic for such plastid-derived tRNA genes is their very high sequence similarity (95–100%) to the original plastid sequence (Veronico et al., 1996). However, not all plastid tRNA sequences transferred into the mitochondrion gave rise to functional tRNA genes. For instance, in the sunflower mitochondrial genome, a $tRNA^{Val}$ gene is part of a 417-bp insertion of plastid origin but the gene is not transcribed (Ceci et al., 1993).

It should be noted that a cpDNA sequence has also been reported to serve as the promoter for the gene for NADH dehydrogenase subunit 9 (*nad9*) in rice mitochondria (Nakazono et al., 1996). Further, at least five independent transfers of the *rbcL* gene to mitochondria have been detected (Cummings et al., 2003). Not surprisingly, the *rbcL* sequences found in mtDNAs represent pseudogenes, displaying insertions and/or deletions that disrupt the reading frame and a high rate of nonsynonymous substitutions (Cummings et al., 2003). Until recently, tRNA gene replacements and the recruitment of the chloroplast-derived promoter sequence for *nad9* were the only cases of DNA transfer known to have a direct impact on mitochondrial gene function. Nonetheless, plant mitochondrial genomes often contain open reading frames (ORFs) of unknown function, and one of these conserved ORFs corresponds to a functional *rpl10* gene (Kubo and Arimura, 2010), which is not found in most other mtDNAs. It turns out that the original mitochondrial *rpl10* gene has been lost in monocots and some lineages of Brassicaceae and was replaced by an extra copy of

the nuclear gene that normally encodes the chloroplast RPL10 protein (Kubo and Arimura, 2010).

Moreover, recombination/gene conversion between homologous chloroplast and mitochondrial genes can result in the formation of chimeric mitochondrial genes (Hao and Palmer, 2009). During angiosperm evolution, recurrent conversion of short patches of mitochondrial genes by chloroplast homologs appears to have taken place, and all nine putative conversion events involve the *atp1/atpA* gene encoding the α-subunit of ATP synthase, which is unusually well conserved between the two organelles. Remarkably, no evidence of gene conversion in the opposite direction could be identified (Hao and Palmer, 2009).

3.1.1. Constraints acting on nucleus-to-mitochondrion DNA transfer

In the mitochondrial genome of Oenothera, a 528-bp stretch with 91% homology to a nuclear 18S rRNA sequence and an ORF with high predicted sequence homology to reverse transcriptase have been identified (Schuster and Brennicke, 1987). The fraction of nuclear DNA incorporated into mtDNA can be as large as 13.4% (in rice; Notsu et al., 2002), but to our knowledge, no function has yet been reported for any of these nuclear DNA sequences in plant mitochondria. Moreover, experimental studies in yeast have demonstrated that the rate of gene transfer from nucleus to mitochondrion is five orders of magnitude lower than that for transfers in the opposite direction (Thorsness and Fox, 1990, 1993; see Section 2.6.1). This raises the question of why genetic material is so rarely transferred from the (animal) nucleus to mitochondria? In contrast to the diversity in size, structure, and gene content of mitochondrial genomes observed across diverse eukaryotic groups, those of multicellular animals (Metazoa) are considered to be largely uniform (Lang et al., 1999), and evidence for the presence of promiscuous DNA in animal mitochondrial genomes is scarce. Indeed, there is only one report of a potentially functional gene in the mitochondrion that may have been transferred from the nucleus—a *mutS* gene for mismatch repair in corals (Pont-Kingdon et al., 1998). One possible explanation for this is that the capacity to acquire and incorporate foreign DNA may depend on the ability to undergo homologous or nonhomologous recombination and the presence of endonuclease activity, that is, recombination may be more frequent in cnidarian mitochondria than in other animals (Shao et al., 2006). Accordingly, it was suggested that the absence of homologous recombination mechanisms in liverwort mitochondria is responsible for the uniformity of their mtDNA (Ohyama et al., 2009) and the absence of promiscuous DNA in the mitochondrial genome of Marchantia (Oda et al., 1992). Moreover, the vast majority of nuclear genes do not code for mitochondrial proteins and, therefore, transfer to the mitochondria would not serve a biological function (Adams and Palmer, 2003).

3.2. Transfer of mitochondrial or nuclear DNA to plastids

In contrast to the high plasticity of mitochondrial genomes in flowering plants, plastid genomes have undergone a more conservative evolution (Knoop, 2004). For many years, only one instance of the acquisition of foreign DNA by a plastid genome was known: the ancient transfer of the Rubisco operon (*rbcL* and *rbcS*) from a proteobacterium into the common ancestor of red algal plastids and their secondary derivatives (Delwiche and Palmer, 1996). In consequence, nucleus- and mitochondrion-to-plastid gene transfers were thought to occur extremely rarely (Leister, 2005; Timmis et al., 2004). However, in addition to the Rubisco operon mentioned above, transfer of a bacterial *rpl36* gene to the ancestor of the cryptophyte and haptophyte—but not heterokont—plastids (Rice and Palmer, 2006) has been reported more recently. Acquisition of a bacterial-derived gene for a subunit of DNA polymerase III (*dnaX*) by lateral gene transfer in an ancestor of Rhodonionas (Khan et al., 2007) has also been noted. Moreover, a 10-kb segment of the exceptionally large inverted repeat of the plastid genome of the green alga *Oedogonium cardiacum* harbors coding sequences not normally found in the chloroplast, notably the *int* and *dpoB* genes (Brouard et al., 2008). The *int* and *dpoB* gene products belong to the family of tyrosine recombinases and the B family of DNA-directed DNA polymerases, respectively. The closest homolog of the *int* gene was identified in the mitochondrial genomes of the green algae *Chaetosphaeridium globosum* and *Prototheca wickerhamii*, whereas the closest homolog of *dpoB* was localized to a linear mitochondrial plasmid of the fungus *Neurospora intermedia*. This strongly suggests that the Oedogonium *int* and *dpoB* genes were acquired through horizontal transfer of mobile elements originating from the mitochondria of an unknown donor (Brouard et al., 2008).

In contrast to the scarcity of gene transfers, horizontal acquisition of group I and group II introns—which are a type of retroelement found in the genomes of bacteria and eukaryotic organelles—might be relatively common in plastids. In the green alga *Pseudendoclonium akinetum*, a group I intron in the *atpA* gene was transferred from the mitochondrion to the plastid (Pombert et al., 2005). Further, evidence exists for several interkingdom horizontal transfers of group II introns, including transfers from a cyanobacterial donor to the chloroplast genome of *Euglena myxocylindracea* (Sheveleva and Hallick, 2004) and to the *psbA* gene of the psychrophilic Chlamydomonas strain CCMP1619 (Odom et al., 2004). Remarkably, these two introns are related to each other and located in the same position (Odom et al., 2004). The group II introns of the cryptophyte alga *Rhodomonas salina* CCMP1319 exhibit an unusual secondary structure that could be the result of fusions between group II introns that may have been laterally transferred multiple times from a euglenid-like species to the cryptophyte plastid (Khan and Archibald, 2008). Thus, lateral gene transfer might have

played an important role in shaping the structure and composition of the cryptophyte plastid (Khan and Archibald, 2008).

3.2.1. Constraints on DNA uptake into the plastid genome

The equivalence of germline and vegetative cells in algae might increase the probability of passing on horizontally acquired DNA. Even so, DNA uptake into the plastome has apparently occurred much less often than into the chondriome. Several explanations for the rarity of DNA uptake into plastids suggest themselves. For instance, the compact nature of the plastid genomes makes it more likely that foreign DNA will disrupt some vital function upon integration (Shinozaki et al., 1986). Alternatively, like mitochondrial genomes, chloroplast genomes might be protected against foreign DNA invasion by their limited potential to undergo nonhomologous recombination (Keeling and Palmer, 2008). However, experimental evidence suggests that double-stranded break (DSB) repair mechanisms which resemble the nuclear, microhomology-mediated non-homologous end-joining (NHEJ) pathways are operative in the *A. thaliana* chloroplast (Kwon et al., 2010; see also below: Section 5.3). This would also explain the *rpl36* gene replacement in the ancestor of the cryptophyte and haptophyte plastids, which somehow occurred by recombination at the very ends of *rpl36*, without the level and length of similarity normally required to support homologous recombination (Rice and Palmer, 2006). Moreover, unlike mitochondria, plastids lack both an efficient uptake system for exogenous DNA and the propensity to fuse with each other (Keeling and Palmer, 2008; Rice and Palmer, 2006).

4. Transfer of Nonfunctional orgDNA Segments to the Nucleus: NUMTs and NUPTs

4.1. Number and frequency of NUMTs and NUPTs in different organisms

In addition to the transfer of functional genes from mitochondria and plastids to the nucleus, nonfunctional mtDNA and cpDNA segments are also found in the nuclear genome and are referred to as NUMTs (Lopez et al., 1994) and NUPTs (Timmis et al., 2004), respectively. Following the pioneering work that detected mtDNA in nuclear DNA by hybridization with mtDNA probes (Dubuy and Riley, 1967), genome sequencing made it possible to identify NUMTs and NUPTs in yeast and plants by bioinformatic methods (Blanchard and Schmidt, 1995, 1996). With the increasing availability of whole genome sequences, NUMTs and NUPTs are being discovered in an ever widening spectrum of eukaryotes, ranging from protists to mammals (Hazkani-Covo et al., 2010; Richly and Leister, 2004a,b). One of the first genomewide surveys encompassed 13 nuclear

genomes (Richly and Leister, 2004a). By 2010, a set of 72 new eukaryotic (nuclear and organelle) genome sequences had become available, allowing the NUMT and NUPT repertoire to be surveyed in 85 fully sequenced genomes, including those of 20 fungi, 11 protists, 7 plant/moss/algae, and 47 animals (Hazkani-Covo et al., 2010). With the advent of advanced sequencing methods, the inventory of known NUMTs and NUPTs is continuously expanding, and recent reports include analyses of norgDNA in the demosponge *Amphimedon queenslandica*, a representative of the oldest phyletic lineage of animals (Erpenbeck et al., 2011), *Equus caballus*, the domestic horse (Nergadze et al., 2010), the jewel wasp *Nasonia vitripennis* (Viljakainen et al., 2010), maize (Roark et al., 2010), and rice (Akbarova et al., 2011). Depending on the search strategy, the level of genome completion, and changes in the curation of the available genome sequence data, the number of orgDNAs detected in a given nuclear genome can vary (Hazkani-Covo et al., 2010). For example, with the inclusion of 4.7 Mb of heterochromatic sequence that was unavailable in the previous versions of the *D. melanogaster* genome, the NUMT content has increased from 0.5 kb (Richly and Leister, 2004a) to the current value of 10.3 kb (Hazkani-Covo et al., 2010). Irrespective of the aforementioned methodologically based variations, the NUMT and NUPT contents are highly variable among species. The abundance of NUMTs in eukaryotic genomes ranges from undetectable (e.g., in *Anopheles gambiae*; Richly and Leister, 2004a) to more than 800 kb in the rice genome and 2.1 Mb in the opossum *Monodelphis domestica* (Hazkani-Covo et al., 2010). Similarly, the abundance of NUPTs in nuclear genomes varies from undetectable (in the green alga *Ostreococcus* sp. RCC809, two apicomplexans and the stramenophile *Aureococcus anophagefferens*) to more than 1 Mb in *O. sativa* subsp. *japonica* (Smith et al., 2011). The fraction of the nuclear genome represented by NUMTs or NUPTs is usually less than 0.1% (Leister, 2005), but it can be higher in flowering plants (Hazkani-Covo et al., 2010; Richly and Leister, 2004a,b) and some fungi (Hazkani-Covo et al., 2010). Because mutation and deletion rapidly make NUMT and NUPT sequences unrecognizable as such, 0.1% represents the steady-state level of recently incorporated orgDNA at any given point in time (Hazkani-Covo et al., 2010). NUMTs and NUPTs vary not only in overall length but also in their size and frequency distributions (Hazkani-Covo et al., 2010; Richly and Leister, 2004a,b; Smith et al., 2011). For example, the largest insertions of norgDNA reported so far are a 620-kb partially duplicated insertion of the 367-kb mtDNA in *A. thaliana* (Stupar et al., 2001) and a 131-kb NUPT in rice (Huang et al., 2005; The Rice Chromosome 10 Sequencing Consortium, 2003). In terms of NUMT frequency, *Apis mellifera*, the Western honeybee, is among the leaders, with more than 1000 orgDNA insertions in its nuclear genome (Behura, 2007; Pamilo et al., 2007), although these are relatively short, with an average length of 96 bp. The highest frequencies of NUPTs are found in

V. vinifera and *Glycine max*, which have more than 3000 nuclear genome insertions each with an average length of around 200 bp (Smith et al., 2011).

4.2. The "limited transfer window" hypothesis

In the early studies that considered relatively few species, no obvious correlation between the abundance of NUMTs and the size of the nuclear or the mitochondrial genomes emerged (Richly and Leister, 2004a), but it was assumed that large genomes with a low gene density should in principle contain more NUPTs (Richly and Leister, 2004b). In fact, as more genomes became available, it was recognized that nuclear genome size and the content of NUMTs and NUPTs are generally correlated (Hazkani-Covo et al., 2010; Smith et al., 2011).

Up until recently, both organellar and nuclear genome sequences were available for only a few plastid-bearing eukaryotes, so only limited NUPT analyses were possible. Nonetheless, the analysis of the available NUPT data resulted in a number of intriguing observations. Thus, the NUPT content in monoplastidic species seems to be much lower than in polyplastidic species (Lister et al., 2003; Martin, 2003; Richly and Leister, 2004b). This finding prompted the formulation of the "limited transfer window" hypothesis (Barbrook et al., 2006), which postulates that DNA transfer to the nucleus is dependent on prior chloroplast rupture. Lysis of the sole chloroplast in a cell would most probably result in death of that cell and consequently interfere with efficient plastid-to-nucleus DNA transfer. Conversely, in flowering plants with many chloroplasts per cell, chloroplast rupture will not jeopardize survival and can facilitate transfer events (Lister et al., 2003; Martin, 2003; Richly and Leister, 2004b). In a recent study, the hypothesis was tested with newly available genomic sequence data (Smith et al., 2011). The number and length of NUPTs were calculated in the nuclear genomes of 11 polyplastidic and 19 monoplastidic—or more specifically, effectively monoplastidic eukaryotes (i.e., organisms in which mitosis and meiosis only occur in cells that contain a single plastid). With the exception of *Volvox carteri* and *A. thaliana*, the polyplastidic species harbored on average 80 times more NUPTs than those that were monoplastidic (Smith et al., 2011). Moreover, analysis of the NUMTs revealed that the NUMT content of monomitochondrial species—with an average of 1.1 kb—was around 300 times lower than that of polymitochondrial taxa (Smith et al., 2011), which is consistent with earlier observations (Hazkani-Covo et al., 2010).

4.3. Ancient and recent instances of NUMT and NUPT integration

The average size, distribution, and number of NUMTs and NUPTs in nuclear genomes can differ markedly even between closely related species (Baldo et al., 2011; Guo et al., 2008; Krampis et al., 2006; Lough et al., 2008;

Nergadze et al., 2010; Roark et al., 2010; Sacerdot et al., 2008) (Table 3.1), implying that NUMT/NUPT insertion is not just the result of an ancient colonization event but is an ongoing and dynamic process. The reasons for the high degree of variation are still elusive but might lie in differences in the relative rates of integration and deletion of orgDNA inserts in the nuclear genome (Richly and Leister, 2004a). Cross-species comparisons and phylogenetic analyses allow one to discriminate between old and recent NUMTs and NUPTs. For example, pairwise genomic alignments of the human and chimpanzee genomes indicate that non-orthologous NUMTs derive mostly from novel NUMTs acquired after the divergence of the two species (Hazkani-Covo and Graur, 2007). Moreover, by sampling the genomes of humans and chimpanzees, 27 (Ricchetti et al., 2004) and 34 (Hazkani-Covo and Graur, 2007) NUMTs have been identified that are specific to humans and must have colonized human chromosomes during the past 6 million years, indicating that, on average, one NUMT integrated in the human germline every 197,000 years. An analysis of five fully sequenced primate genomes led to a similar average rate (1 NUMT each 177,000 years) but showed that insertion rates vary significantly on the different branches (Hazkani-Covo, 2009). In rice, the rate of colonization of nuclear DNA by NUPTs is much higher (47 NUPT integration events in the past 1 million years; Matsuo et al., 2005).

4.4. Evolutionary dynamics of NUMTs and NUPTs

Primary orgDNA insertions are probably large, but they undergo decay over evolutionary time, as they are fragmented (Behura, 2007; Leister, 2005; Pamilo et al., 2007) and shuffled, and it is estimated that 80% of them are eliminated from the nuclear genome within 1 million years (Matsuo et al., 2005). The insertion of transposable elements, and other DNA sequences unrelated to orgDNA, into NUPTs and NUMTs has contributed significantly to this fragmentation process (Noutsos et al., 2005). Moreover, assimilation of mitochondrial genes into the nuclear genome is facilitated by extensive fragmentation of the original inserts (Behura, 2007).

NUMTs and NUPTs are exposed to the evolutionary pressures that act on the nuclear compartment. In plants, where nucleotide substitutions generally occur much less frequently in orgDNA than in the nuclear genome, NUMTs and NUPTs can serve as probes for the types of mutation that govern the evolution of nuclear DNA (Kleine et al., 2009a; Leister, 2005). In two independent studies, a predominance of C → T and G → A transition mutations was observed in large and recent norgDNA inserts in *A. thaliana* and *O. sativa* (Huang et al., 2005; Noutsos et al., 2005). The prevalence of these transitions can be interpreted in the context of the predominantly nonfunctional nature of NUMTs and NUPTs. Their lack

Table 3.1 Amount, number, and average length of NUMTs and NUPTs in selected species

Species	Total NUMT/NUPT amount (kb)	NUMT/NUPT number	NUMT/NUPT average length (bp)	Nuclear genome size (Mb)[a]	NUMT/NUPT percentage of nuclear genome (%)	Reference
Amphimedon queenslandica	15.762/–	71/–	222/–	140	0.01/–	Erpenbeck et al. (2011)
Anopheles gambiae	0/–	0/–	0/–	209.529	0/–	Richly and Leister (2004a)
Apis mellifera	174.480/–, 237.325/–	1380/–, 1619/–	126/–, 147/–	218.1	0.08/–, 1.1/–	Behura (2007), Pamilo et al. (2007)
Arabidopsis thaliana	549/50, 198.105/35.235	1173/332, 572/301	460/150, 346/117	93.655	0.58/0.05, 0.21/0.04	Richly and Leister (2004a,b), Smith et al. (2011)
Chlamydomonas reinhardtii	3.3/1.9	35/35	90/50	105.192	0.003/0.002	Smith et al. (2011)
Drosophila melanogaster	0.777/–, 10.331/–	8/–, 50/–	97/–, 206/–	180	0.0004/–, 0.006/–	Hazkani-Covo et al. (2010), Pamilo et al. (2007)
Equus caballus	77.191/–	82/–	941/–	4808.54	0.0016/–	Nergadze et al. (2010)
Homo sapiens	263.478/–	871/–	303/–	3038	0.0087/–	Hazkani-Covo et al. (2010)
Monodelphis domestica	2094/–	1859/–	1126/–	3472	0.06/–	Hazkani-Covo et al. (2010)
Nasonia vitripennis	42.972/–	76/–	565/–	432.65	0.01/–	Viljakainen et al. (2010)
Oryza sativa, subsp. *indica*	818/782	2544/1541	320/500	466.3[b]	0.18/0.17	Akbarova et al. (2011), Smith et al. (2011)
Oryza sativa, subsp. *japonica*	834/1.073	3072/2036	270/520	433.2[b]	0.19/0.25	Smith et al. (2011)
Ostreococcus sp. RCC809	0/0	0/0	0/0	13.3[c]	0/0	Smith et al. (2011)
Saccharomyces cerevisiae	2.356/–	32/–	73/–	12.1	0.02/–	Sacerdot et al. (2008)

[a] According to the NCBI Genome database (http://www.ncbi.nlm.nih.gov/genomes/leuks.cgi).
[b] Yu et al. (2005).
[c] http://genome.jgi-psf.org/OstRCC809_2/OstRCC809_2.info.html.

of function should favor loss of transcription and concomitantly result in a high rate of methylation of cytosine residues, followed by deamination of 5-methylcytosine, which in turn leads to a G–T mismatch. The mismatch can be restored to the G–C pair, but repair should create an A–T pair with the same probability, resulting in C → T transitions (and G → A on the opposite strand; Noutsos et al., 2005).

4.5. Phylogenetic reconstructions using NUMTs

In contrast to the situation in plants, the mutation rate in the nucleus of animals is much lower than in mitochondria (Brown et al., 1979). Therefore, animal NUMTs represent molecular fossils of mtDNAs. Thus, NUMTs are often viewed as serious hindrances to phylogenetic analyses (Calvignac et al., 2011; Leister, 2005): mistaking NUMTs for mitochondrial sequences can lead to substantial errors in estimates of phylogenetic relationships, population genetic parameters, and measures of biodiversity (Cai et al., 2011; Song et al., 2008). Nevertheless, NUMTs have been exploited to (i) trace ancestral states of mtDNAs and improve mtDNA-based phylogenies by providing suitable outgroups (Bensasson et al., 2001; Perna and Kocher, 1996) and (ii) date NUMT insertions on the basis of mitochondrial trees or patterns of presence and absence in a phylogeny (Hazkani-Covo et al., 2010), or the accumulation of base exchanges (Mishmar et al., 2004; Noutsos et al., 2007). For instance, an analysis of 247 human NUMTs revealed that some of them have accumulated many changes and most probably represent ancient NUMTs, while others are more than 94% similar to the reference human mtDNA, suggesting relatively recent transfer (Mishmar et al., 2004). A sequence analysis of NUMT insertions in primate nuclear genomes showed that NUMTs provide important phylogenetic markers and are suitable for molecular taxonomy (Hazkani-Covo, 2009). Recently, by combining phylogenetic reconstruction with analyses of the pattern of nucleotide substitution on mitochondrial and NUMT branches, the dynamics of NUMT origin and evolution was inferred in *Mesomachilis nearctica* and *M.* cf. *nearctica*—two species of the jumping bristletail (Baldo et al., 2011).

4.6. Genomic distribution and consequences of NUMTs and NUPTs

The most detailed studies of the genomic organization of NUMTs and NUPTs have been performed in *A. thaliana*, *O. sativa*, *S. cerevisiae*, and *H. sapiens*. In the flowering plants *A. thaliana* and *O. sativa*, norgDNA is frequently organized in clusters of insertions that are physically linked to varying degrees ("loose clusters" and "tight clusters") (Richly and Leister, 2004b). Interestingly, many of the tight clusters were shown to contain both

NUMTs and NUPTs (Richly and Leister, 2004b). Based on the state of genome annotations in 2004, about 25% of norgDNAs are located within genes (Richly and Leister, 2004b)—although one must point out that genes make up only 44% and 45% of the genomes of *A. thaliana* and *O. sativa*, respectively. In *O. sativa*, large NUPTs preferentially localize to the pericentromeric regions of the chromosomes; such insertions should be less deleterious than integrations in other chromosomal regions where gene density is higher (Matsuo et al., 2005).

In the yeast *S. cerevisiae*, in *H. sapiens*, *A. thaliana*, and *O. sativa*, a total of 473 NUMTs and NUPTs were identified in, or next to, annotated genes, of which 334 were located in introns and 94 in untranslated regions (Noutsos et al., 2007). A set of 45 insertions contributed sequences to a total of 49 protein-coding exons in 34 genes. Functionality of a subset of those exons was demonstrated on the basis of their mRNA expression and mutational spectrum (Noutsos et al., 2007). Most of the protein sequences do not correspond to preexisting organelle coding sequences or they represent markedly reshaped protein domains, reflecting the recruitment and adaptation of encoded proteins to new functions (Noutsos et al., 2007). In agreement with these results, in a recent study of NUPT insertions in the *O. sativa japonica* nuclear genome, 35 nuclear genes bearing orgDNA insertions in their coding exon(s) and nuclear copies of five known plastid genes with cDNA support were identified (Akbarova et al., 2011). These data are compatible with the idea that transferred orgDNA sequences play a role both in creating novel nuclear genes and in modifying products of existing genes (Akbarova et al., 2011). A comparative analysis of the NUMT content of six fully sequenced yeast species belonging to a monophyletic group (*Candida glabrata*, *Kluyveromyces lactis*, *Kluyveromyces thermotolerans*, *Debaryomyces hansenii*, *Yarrowia lipolytica*, and *S. cerevisiae*) revealed a huge degree of interspecific diversity in NUMT number and organization (Sacerdot et al., 2008). Most NUMTs were found within intergenic regions, including seven NUMTs in pseudogenes. However, five NUMTs overlap with genes in *D. hansenii*, suggesting that NUMTs have a positive impact on protein evolution in yeasts also (Sacerdot et al., 2008), as had been proposed previously (Noutsos et al., 2007). Recently, it was shown that NUMTs in *S. cerevisiae* are rich in key autonomously replicating sequence (ARS) consensus motifs, mutations in which result in reduction or loss of DNA replication activity (Chatre and Ricchetti, 2011). Moreover, NUMTs located close to or within ARS provide key sequence elements for replication. These findings indicate that NUMTs can have an impact on the replication of the nuclear region in which they are inserted (Chatre and Ricchetti, 2011). In *S. pombe*, NUMTs are located exclusively in noncoding regions. But strikingly, chromatin immunoprecipitation experiments revealed that, although NUMTs were located close to DNA replication origins (ORIs), they seldom act as ORIs themselves (Lenglez et al., 2010). In the Western honeybee *A. mellifera*,

NUMTs are scattered all over the 16 nuclear chromosomes (Behura, 2007). Some 84% of the honeybee NUMTs are located in nongenic regions, and the majority (94%) of the NUMTs that are located in predicted nuclear genes have originated from mitochondrial genes coding for cytochrome oxidase and NADH dehydrogenase subunits (Behura, 2007).

The bulk of nuclear insertions of orgDNA is considered to be harmless or even beneficial (in cases where they provide novel exons for nuclear genes). However, the potentially harmful mutagenic effect of orgDNA is supported by examples of association between NUMTs and human diseases, including a severe bleeding condition (Borensztajn et al., 2002), a rare case of Pallister–Hall syndrome which is associated with high-level radioactive contamination following the Chernobyl disaster (Turner et al., 2003), mucolipidosis IV (Goldin et al., 2004), and Usher syndrome type IC (Chen et al., 2005). Further, evidence was recently presented which suggests that norgDNA sequences affect the chronological aging process in *S. cerevisiae* (Cheng and Ivessa, 2010).

5. Mechanism of orgDNA Integration into the Nuclear Genome

The transfer of orgDNA to the nucleus logically requires initial release of DNA from the organelle. The DNA must then traverse the cytoplasm, enter the nucleus, and integrate into the nuclear genome.

5.1. Physical nature of the migrating nucleic acid

Some features of OGE—such as posttranscriptional editing of RNA—are not operative in the nuclear compartment, and *a priori* this would presumably preclude the functional expression of many organellar genes in the nucleus. To overcome this handicap, it has been suggested that mature transcripts which have already been spliced and edited serve as the starting point for transfer (Brennicke et al., 1993). This proposal was made to explain the observation that the nuclear *coxII* sequence in legumes (Covello and Gray, 1992; Nugent and Palmer, 1991) and the nuclear *rps12* sequence in Oenothera (Grohmann et al., 1992) more closely resemble the edited mitochondrial transcripts than the genes encoding these RNAs. However, experimental studies carried out in yeast and tobacco have shown that any segment of an organelle genome can be transferred to the nucleus (Bock and Timmis, 2008; Leister, 2005), and bioinformatics analyses reveal that large orgDNAs spanning several genes or even entire organelle chromosomes exist in the nucleus (Shahmuradov et al., 2003; Stupar et al., 2001). One other hint that migrations of orgDNA sequences

to the nucleus are predominantly DNA-mediated comes from an analysis of the mtDNA insertions in human nuclear DNA (Woischnik and Moraes, 2002). Several of the integrated sequences were composed of fragments that (i) encompassed two or more adjacent mitochondrial genes or (ii) included the control region of mtDNA (the D-loop and the promoter region), and no poly(A) stretches could be detected in the intergenic space between adjacent mitochondrial gene sequences within one fragment, indicating that these insertions must have been derived from unmodified segments of mtDNA (Woischnik and Moraes, 2002).

5.2. Release of DNA from organelles

Pioneering work on DNA release from organelles done in yeast led to the conclusion that DNA escape is facilitated by damage to the structural integrity of the organelle membranes. Thus, increased rates of mtDNA escape have been observed in yeast cells that were frozen and thawed, grown at nonoptimal temperatures, or incubated in glycerol (Fig. 3.3; Thorsness and Fox, 1990). Moreover, all of the cloned *yeast mitochondrial escape* (*yme*) mutants that show elevated rates of mtDNA transfer to the nucleus (Thorsness and Fox, 1993) have defects in proteins that are associated with mitochondria (Hanekamp and Thorsness, 1996; Thorsness et al., 1993a,b). For instance, inactivation of Yme1p, an ATP-dependent metalloprotease localized in mitochondria, causes functional and morphological defects in mitochondria and is associated with a high rate of DNA escape from mitochondria to the nucleus (Campbell and Thorsness, 1998), suggesting that the degradation of abnormal mitochondria facilitates mtDNA escape and migration to the nucleus. This idea is supported by studies of DNA movement across the membranes of isolated chloroplasts from pea (Cerutti and Jagendorf, 1993), and a model has been developed for the incorporation of cpDNA into nuclear chromosomes after chloroplast degradation, either as a result of stress or pollen formation (Cullis et al., 2009). Moreover—as already mentioned in Section 4.2—a screen to detect the transfer of DNA in *C. reinhardtii* from its single chloroplast to the nucleus failed to identify transfer events (Lister et al., 2003). A screen of transplastomic tobacco plants showed that relocation of cpDNA to the nucleus occurs in both somatic and gametophyte tissue, but with a markedly higher frequency of transposition in the male germline (Sheppard et al., 2008). In many eukaryotes, including humans and various flowering plants, orgDNA is maternally inherited. Therefore, programmed degeneration of organelles takes place in flowering plants during pollen development, and in mammals, sperm mtDNA is released when paternal mitochondria degenerate shortly after penetration of the egg by the sperm cell (Leister, 2005).

Direct physical association of the nucleus with mitochondria (Mota, 1963) or chloroplasts (Ehara et al., 1990) and the incorporation of mitochondria into

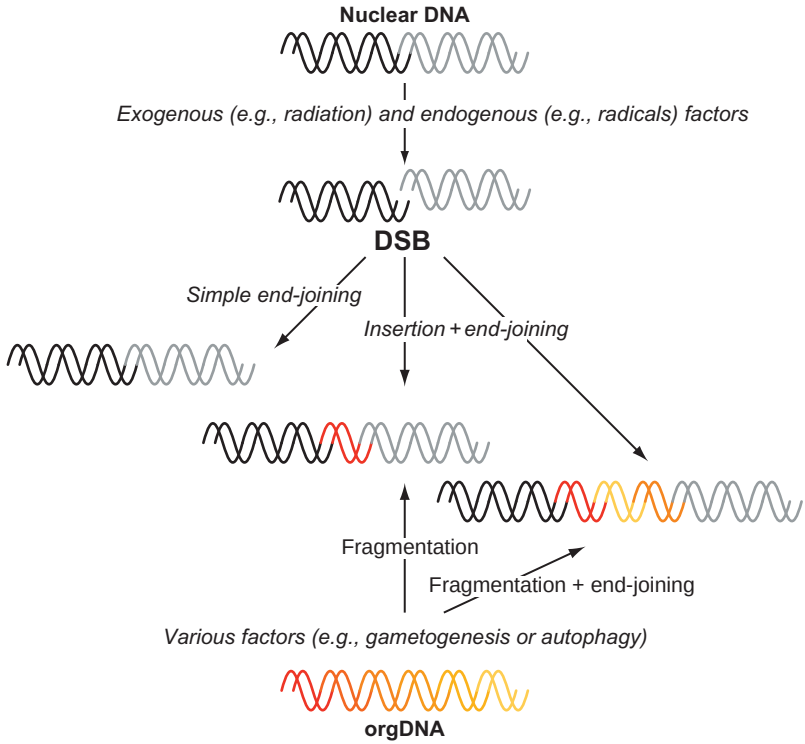

Figure 3.3 Model for the generation of nuclear insertions of orgDNA. Double-stranded breaks (DSBs) are induced by exogenous and endogenous factors. Similarly, the release of orgDNA is associated with various cellular stresses and it is tempting to speculate that the same cellular stresses induce both the induction of DSBs and the release of orgDNAs.

nuclei, as occurs, for instance, in tobacco sperm cells (Yu and Russell, 1994), might also contribute to DNA exchange. But this does not seem to be the major driving force for DNA transfer. In *C. reinhardtii*, DNA molecules extended from the chloroplast nucleoids may even interact with those from nuclear chromosomes during an early phase of the cell cycle (Ehara et al., 1996). In spite of this, no chloroplast-to-nucleus DNA transfer could be detected in this algal species (Lister et al., 2003).

5.3. Possible mechanisms of orgDNA integration into the nuclear chromosome

Based on a survey of NUMT integration sites in yeast and human nuclear DNA, it was proposed that NUMTs are inserted into DSBs by the NHEJ machinery (Fig. 3.3; Blanchard and Schmidt, 1996). That mtDNA is

integrated into the nuclear genome by NHEJ was experimentally shown in yeast under conditions in which homologous recombination was not possible (Ricchetti et al., 1999). Subsequent analyses were consistent with the involvement of NHEJ in NUMT integration in humans (Ricchetti et al., 2004) and NUPT integration in tobacco (Lloyd and Timmis, 2011; Stegemann and Bock, 2006). As in yeast and humans, analyses of the tobacco DNA transfer experiments showed that microhomologies of 2–5 bp often exist adjacent to the integration sites (Lloyd and Timmis, 2011; Stegemann and Bock, 2006), indicating that DSB repair-mediated insertion of orgDNA by NHEJ might be common to all eukaryotes. Further, no putative recombination sites or features typical of bacterial transposons and integrons could be identified in the 10-kb region housing the unusual genes in the *O. cardiacum* inverted repeat (Brouard et al., 2008).

The junctions between chromosomal and orgDNA at each end of a NUMT or NUPT reflect the repair events that have occurred on each side of the original chromosomal break. Repair of DSBs by NHEJ requires only a short stretch of sequence homology (1–7 bp, "microidentities") or no microhomology at all (blunt end repair), enabling the noncomplementary ends of DSBs and orgDNA to be "pasted" to one another (Ricchetti et al., 1999; van Gent et al., 2001). DSBs are regarded as potentially the most deleterious form of DNA damage that can be induced *in vivo* by exogenous and endogenous sources (Puchta, 2005; van Gent et al., 2001). Remarkably, throughout the evolutionary history of human and chimpanzee, more than half of the DSB repair events that involve NUMTs removed or otherwise altered little or none of the adjacent DNA (Hazkani-Covo and Covo, 2008). Thus, orgDNA insertions provide the end-joining machinery with a means of sealing breaks without the need to process the nuclear DNA further using a nuclease (Hazkani-Covo et al., 2010). Providing the repair system with an NUMT or NUPT as a stuffer might be important in cases where the structure of the DSB is chemically complex and processing by nucleases would expose a long stretch of single-stranded DNA, which in turn would increase the risk of generating large deletions, or translocations (Hazkani-Covo et al., 2010). It is thus possible that sealing DSBs with NUMTs might reduce the incidence of harmful deletions associated with normal DSB repair (Hazkani-Covo and Covo, 2008). Interestingly, it has been demonstrated that ionizing radiation increases the frequency of microhomology-mediated DNA integration. Irradiated yeast cells displayed 77% microhomology-mediated integration, compared to 27% in nonirradiated cells (Chan et al., 2007). Moreover, certain stresses may stimulate not only the release of orgDNA caused by organelle damage and decay but also the integration of the released DNA into the nuclear genome (Bock and Timmis, 2008).

6. Concluding Remarks

Transfer of DNA from one compartment to the other, in particular from organelles to the nucleus, is a continuing process and is ubiquitous in eukaryotes. However, whereas organelle-to-nucleus DNA transfer has previously led to the relocation of thousands of genes, this gene flow has now more or less ceased, presumably because the organelles cannot tolerate the removal of any of the relatively few resident genes left, most probably for regulatory reasons. Nevertheless, NUMTs and NUPTs are continuously formed in the nuclear genomes of eukaryotes, and in rare cases, they contribute to reshaping genes by adding novel exons. Even more important and less well studied might be the alteration of gene activity by insertion of NUMTs and NUPTs in DNA regions responsible for gene regulation. In this field of research, full-genome data obtained in the future by novel and cost-effective sequencing methods should provide a more comprehensive view of the impact of intercompartmental DNA transfer on gene and genome evolution.

Intercompartmental DNA transfer appears to be an inevitable process resulting from the incorporation of DNA released from its original compartment during environmental stresses or at certain stages in development. Because of its omnipresence, the process seems to play multiple roles in evolution. Thus, DSBs in nuclear DNA can be healed by the insertion of foreign orgDNA, reducing the harmful effects of ionizing radiation and other mutagenizing agents. The transfer of entire genes to the nucleus was obviously positively selected for, leading to the massive relocation of organellar genes to the nucleus in the past. The reasons for the positive selection for a nuclear location of organellar genes seem straightforward. In the nucleus, the genes of organellar origin can be included in preexisting control networks, contributing to more efficient regulation of organelle function (conversely, genes that must be included in organellar regulatory networks must reside in the organelle). Perhaps equally important, a nuclear location allows for the retargeting of gene products to other cellular compartments by providing opportunities to acquire the necessary targeting sequences—a process which has apparently occurred with high frequency. Taken together, the impact of intercompartmental DNA transfer on life has been substantial, having had significant effects on diverse processes such as DNA repair, gene and genome evolution, and retargeting of proteins between different compartments.

REFERENCES

Abhishek, A., Bavishi, A., Choudhary, M., 2011. Bacterial genome chimaerism and the origin of mitochondria. Can. J. Microbiol. 57, 49–61.

Adams, K.L., Palmer, J.D., 2003. Evolution of mitochondrial gene content: gene loss and transfer to the nucleus. Mol. Phylogenet. Evol. 29, 380–395.

Adams, K.L., Daley, D.O., Qiu, Y.L., Whelan, J., Palmer, J.D., 2000. Repeated, recent and diverse transfers of a mitochondrial gene to the nucleus in flowering plants. Nature 408, 354–357.

Adams, K.L., Qiu, Y.L., Stoutemyer, M., Palmer, J.D., 2002. Punctuated evolution of mitochondrial gene content: high and variable rates of mitochondrial gene loss and transfer to the nucleus during angiosperm evolution. Proc. Natl. Acad. Sci. USA 99, 9905–9912.

Agapakis, C.M., Niederholtmeyer, H., Noche, R.R., Lieberman, T.D., Megason, S.G., Way, J.C., et al., 2011. Towards a synthetic chloroplast. PLoS One 6, e18877.

Akbarova, Y.Y., Solovyev, V.V., Shahmuradov, I.A., 2011. Possible functional and evolutionary role of plastid DNA insertions in rice genome. Appl. Comput. Math. 9, 19–33.

Alcock, F., Clements, A., Webb, C., Lithgow, T., 2010. Tinkering inside the organelle. Science 327, 649–650.

Allen, J.F., 1993. Control of gene-expression by redox potential and the requirement for chloroplast and mitochondrial genomes. J. Theor. Biol. 165, 609–631.

Allen, J.F., Puthiyaveetil, S., Strom, J., Allen, C.A., 2005. Energy transduction anchors genes in organelles. Bioessays 27, 426–435.

Andersson, S.G., Karlberg, O., Canback, B., Kurland, C.G., 2003. On the origin of mitochondria: a genomics perspective. Philos. Trans. R. Soc. Lond. B Biol. Sci. 358, 165–177, discussion 177–169.

Archibald, J.M., 2006. Algal genomics: exploring the imprint of endosymbiosis. Curr. Biol. 16, R1033–R1035.

Arctander, P., 1995. Comparison of a mitochondrial gene and a corresponding nuclear pseudogene. Proc. Biol. Sci. 262, 13–19.

Armbruster, U., Hertle, A., Makarenko, E., Zühlke, J., Pribil, M., Dietzmann, A., et al., 2009. Chloroplast proteins without cleavable transit peptides: rare exceptions or a major constituent of the chloroplast proteome? Mol. Plant 2, 1325–1335.

Atteia, A., Adrait, A., Brugiere, S., Tardif, M., van Lis, R., Deusch, O., et al., 2009. A proteomic survey of *Chlamydomonas reinhardtii* mitochondria sheds new light on the metabolic plasticity of the organelle and on the nature of the alpha-proteobacterial mitochondrial ancestor. Mol. Biol. Evol. 26, 1533–1548.

Baldauf, S.L., Palmer, J.D., 1990. Evolutionary transfer of the chloroplast *tufA* gene to the nucleus. Nature 344, 262–265.

Baldo, L., de Queiroz, A., Hedin, M., Hayashi, C.Y., Gatesy, J., 2011. Nuclear-mitochondrial sequences as witnesses of past interbreeding and population diversity in the jumping bristletail Mesomachilis. Mol. Biol. Evol. 28, 195–210.

Barbrook, A.C., Howe, C.J., Purton, S., 2006. Why are plastid genomes retained in non-photosynthetic organisms? Trends Plant Sci. 11, 101–108.

Barkan, A., Goldschmidt-Clermont, M., 2000. Participation of nuclear genes in chloroplast gene expression. Biochimie 82, 559–572.

Behura, S.K., 2007. Analysis of nuclear copies of mitochondrial sequences in honeybee (*Apis mellifera*) genome. Mol. Biol. Evol. 24, 1492–1505.

Bensasson, D., Zhang, D., Hartl, D.L., Hewitt, G.M., 2001. Mitochondrial pseudogenes: evolution's misplaced witnesses. Trends Ecol. Evol. 16, 314–321.

Benz, J.P., Soll, J., Bölter, B., 2009. Protein transport in organelles: the composition, function and regulation of the Tic complex in chloroplast protein import. FEBS J. 276, 1166–1176.

Berry, S., 2003. Endosymbiosis and the design of eukaryotic electron transport. Biochim. Biophys. Acta 1606, 57–72.

Bhattacharya, D., Archibald, J.M., Weber, A.P.M., Reyes-Prieto, A., 2007. How do endosymbionts become organelles? Understanding early events in plastid evolution. Bioessays 29, 1239–1246.

Blanchard, J.L., Schmidt, G.W., 1995. Pervasive migration of organellar DNA to the nucleus in plants. J. Mol. Evol. 41, 397–406.
Blanchard, J.L., Schmidt, G.W., 1996. Mitochondrial DNA migration events in yeast and humans: integration by a common end-joining mechanism and alternative perspectives on nucleotide substitution patterns. Mol. Biol. Evol. 13, 537–548.
Bock, R., Timmis, J.N., 2008. Reconstructing evolution: gene transfer from plastids to the nucleus. Bioessays 30, 556–566.
Boore, J.L., 1999. Animal mitochondrial genomes. Nucleic Acids Res. 27, 1767–1780.
Borensztajn, K., Chafa, O., Alhenc-Gelas, M., Salha, S., Reghis, A., Fischer, A.M., et al., 2002. Characterization of two novel splice site mutations in human factor VII gene causing severe plasma factor VII deficiency and bleeding diathesis. Br. J. Haematol. 117, 168–171.
Boussau, B., Karlberg, E.O., Frank, A.C., Legault, B.A., Andersson, S.G., 2004. Computational inference of scenarios for alpha-proteobacterial genome evolution. Proc. Natl. Acad. Sci. USA 101, 9722–9727.
Brennicke, A., Grohmann, L., Hiesel, R., Knoop, V., Schuster, W., 1993. The mitochondrial genome on its way to the nucleus—different stages of gene-transfer in higher-plants. FEBS Lett. 325, 140–145.
Brocks, J.J., Logan, G.A., Buick, R., Summons, R.E., 1999. Archean molecular fossils and the early rise of eukaryotes. Science 285, 1033–1036.
Brouard, J.S., Otis, C., Lemieux, C., Turmel, M., 2008. Chloroplast DNA sequence of the green alga *Oedogonium cardiacum* (Chlorophyceae): unique genome architecture, derived characters shared with the Chaetophorales and novel genes acquired through horizontal transfer. BMC Genomics 9, 290.
Brown, W.M., George, M., Wilson, A.C., 1979. Rapid evolution of animal mitochondrial-DNA. Proc. Natl. Acad. Sci. USA 76, 1967–1971.
Cai, Y., Cheng, X.Y., Duan, D., Xu, R., 2011. Mitochondrial COI gene transfers to the nuclear genome of *Dendroctonus valens* and its implications. J. Appl. Entomol. 135, 302–310.
Calvignac, S., Konecny, L., Malard, F., Douady, C.J., 2011. Preventing the pollution of mitochondrial datasets with nuclear mitochondrial paralogs (NUMTs). Mitochondrion 11, 246–254.
Campbell, C.L., Thorsness, P.E., 1998. Escape of mitochondrial DNA to the nucleus in *yme1* yeast is mediated by vacuolar-dependent turnover of abnormal mitochondrial compartments. J. Cell Sci. 111, 2455–2464.
Cavalier-Smith, T., 2006. Origin of mitochondria by intracellular enslavement of a photosynthetic purple bacterium. Proc. Biol. Sci. 273, 1943–1952.
Ceci, L.R., Saiardi, A., Siculella, L., Quagliariello, C., 1993. A tRNA(Val) (GAC) gene of chloroplast origin in sunflower mitochondria is not transcribed. Plant Mol. Biol. 23, 727–736.
Cerutti, H., Jagendorf, A.T., 1993. DNA strand-transfer activity in pea (*Pisum sativum* L.) chloroplasts. Plant Physiol. 102, 145–153.
Chan, C.Y., Kiechle, M., Manivasakam, P., Schiestl, R.H., 2007. Ionizing radiation and restriction enzymes induce microhomology-mediated illegitimate recombination in *Saccharomyces cerevisiae*. Nucleic Acids Res. 35, 5051–5059.
Chatre, L., Ricchetti, M., 2011. Nuclear mitochondrial DNA activates replication in *Saccharomyces cerevisiae*. PLoS One 6, e17235.
Chen, J.M., Chuzhanova, N., Stenson, P.D., Ferec, C., Cooper, D.N., 2005. Meta-analysis of gross insertions causing human genetic disease: novel mutational mechanisms and the role of replication slippage. Hum. Mutat. 25, 207–221.
Cheng, X., Ivessa, A.S., 2010. The migration of mitochondrial DNA fragments to the nucleus affects the chronological aging process of *Saccharomyces cerevisiae*. Aging Cell 9, 919–923.

Cheung, A.Y., Bogorad, L., Vanmontagu, M., Schell, J., 1988. Relocating a gene for herbicide tolerance—a chloroplast gene is converted into a nuclear gene. Proc. Natl. Acad. Sci. USA 85, 391–395.

Chin, J.W., 2006. Modular approaches to expanding the functions of living matter. Nat. Chem. Biol. 2, 304–311.

Choquet, Y., Wollman, F.A., 2002. Translational regulations as specific traits of chloroplast gene expression. FEBS Lett. 529, 39–42.

Claros, M.G., Perea, J., Shu, Y.M., Samatey, F.A., Popot, J.L., Jacq, C., 1995. Limitations to *in vivo* import of hydrophobic proteins into yeast mitochondria—the case of a cytoplasmically synthesized apocytochrome-b. Eur. J. Biochem. 228, 762–771.

Clements, A., Bursac, D., Gatsos, X., Perry, A.J., Civciristov, S., Celik, N., et al., 2009. The reducible complexity of a mitochondrial molecular machine. Proc. Natl. Acad. Sci. USA 106, 15791–15795.

Clifton, S.W., Minx, P., Fauron, C.M., Gibson, M., Allen, J.O., Sun, H., et al., 2004. Sequence and comparative analysis of the maize NB mitochondrial genome. Plant Physiol. 136, 3486–3503.

Cornelissen, M., Vandewiele, M., 1989. Nuclear transcriptional activity of the tobacco plastid *psbA* promoter. Nucleic Acids Res. 17, 19–29.

Covello, P.S., Gray, M.W., 1992. Silent mitochondrial and active nuclear genes for subunit-2 of cytochrome-c-oxidase (cox2) in soybean—evidence for RNA-mediated gene-transfer. EMBO J. 11, 3815–3820.

Cullis, C.A., Vorster, B.J., Van Der Vyver, C., Kunert, K.J., 2009. Transfer of genetic material between the chloroplast and nucleus: how is it related to stress in plants? Ann. Bot. 103, 625–633.

Cummings, M.P., Nugent, J.M., Olmstead, R.G., Palmer, J.D., 2003. Phylogenetic analysis reveals five independent transfers of the chloroplast gene *rbcL* to the mitochondrial genome in angiosperms. Curr. Genet. 43, 131–138.

Daley, D.O., Whelan, J., 2005. Why genes persist in organelle genomes. Genome Biol. 6, 110.

Daley, D.O., Clifton, R., Whelan, J., 2002. Intracellular gene transfer: reduced hydrophobicity facilitates gene transfer for subunit 2 of cytochrome c oxidase. Proc. Natl. Acad. Sci. USA 99, 10510–10515.

de Duve, C., 2007. Essay—the origin of eukaryotes: a reappraisal. Nat. Rev. Genet. 8, 395–403.

Delwiche, C.F., Palmer, J.D., 1996. Rampant horizontal transfer and duplication of Rubisco genes in eubacteria and plastids. Mol. Biol. Evol. 13, 873–882.

Depamphilis, C.W., Palmer, J.D., 1990. Loss of photosynthetic and chlororespiratory genes from the plastid genome of a parasitic flowering plant. Nature 348, 337–339.

Deusch, O., Landan, G., Roettger, M., Gruenheit, N., Kowallik, K.V., Allen, J.F., et al., 2008. Genes of cyanobacterial origin in plant nuclear genomes point to a heterocyst-forming plastid ancestor. Mol. Biol. Evol. 25, 748–761.

Dolezal, P., Likic, V., Tachezy, J., Lithgow, T., 2006. Evolution of the molecular machines for protein import into mitochondria. Science 313, 314–318.

Dubuy, H.G., Riley, F.L., 1967. Hybridization between nuclear and kinetoplast DNAs of *Leishmania enriettii* and between nuclear and mitochondrial DNAs of mouse liver. Proc. Natl. Acad. Sci. USA 57, 790.

Ehara, T., Osafune, T., Hase, E., 1990. Interactions between the nucleus and cytoplasmic organelles during the cell cycle of *Euglena gracilis* in synchronized cultures. IV. An aggregate form of chloroplasts in association with the nucleus appearing prior to chloroplast division. Exp. Cell Res. 190, 104–112.

Ehara, T., Osafune, T., Hase, E., 1996. Association of nuclear and chloroplast DNA molecules in synchronized cells of *Chlamydomonas reinhardtii*. J. Electron Microsc. 45, 159–162.

Elias, M., Archibald, J.M., 2009. Sizing up the genomic footprint of endosymbiosis. Bioessays 31, 1273–1279.
Ellis, J., 1982. Promiscuous DNA—chloroplast genes inside plant mitochondria. Nature 299, 678–679.
Erpenbeck, D., Voigt, O., Adamski, M., Woodcroft, B.J., Hooper, J.N.A., Worheide, G., et al., 2011. NUMTs in the sponge genome reveal conserved transposition mechanisms in metazoans. Mol. Biol. Evol. 28, 1–5.
Esser, C., Ahmadinejad, N., Wiegand, C., Rotte, C., Sebastiani, F., Gelius-Dietrich, G., et al., 2004. A genome phylogeny for mitochondria among alpha-proteobacteria and a predominantly eubacterial ancestry of yeast nuclear genes. Mol. Biol. Evol. 21, 1643–1660.
Esser, C., Martin, W., Dagan, T., 2007. The origin of mitochondria in light of a fluid prokaryotic chromosome model. Biol. Lett. 3, 180–184.
Falcon, L.I., Magallon, S., Castillo, A., 2010. Dating the cyanobacterial ancestor of the chloroplast. ISME J. 4, 777–783.
Figueroa, P., Gomez, I., Holuigue, L., Araya, A., Jordana, X., 1999. Transfer of *rps14* from the mitochondrion to the nucleus in maize implied integration within a gene encoding the iron-sulphur subunit of succinate dehydrogenase and expression by alternative splicing. Plant J. 18, 601–609.
Fitzpatrick, D.A., Creevey, C.J., McInerney, J.O., 2006. Genome phylogenies indicate a meaningful alpha-proteobacterial phylogeny and support a grouping of the mitochondria with the Rickettsiales. Mol. Biol. Evol. 23, 74–85.
Gabaldon, T., Huynen, M.A., 2003. Reconstruction of the proto-mitochondrial metabolism. Science 301, 609.
Gabaldon, T., Huynen, M.A., 2007. From endosymbiont to host-controlled organelle: the hijacking of mitochondrial protein synthesis and metabolism. PLoS Comput. Biol. 3, e219.
Gabaldon, T., Snel, B., van Zimmeren, F., Hemrika, W., Tabak, H., Huynen, M.A., 2006. Origin and evolution of the peroxisomal proteome. Biol. Direct 1, 8.
Gao, L., Su, Y.J., Wang, T., 2010. Plastid genome sequencing, comparative genomics, and phylogenomics: current status and prospects. J. Syst. Evol. 48, 77–93.
Giege, P., Sweetlove, L.J., Cognat, V., Leaver, C.J., 2005. Coordination of nuclear and mitochondrial genome expression during mitochondrial biogenesis in Arabidopsis. Plant Cell 17, 1497–1512.
Goldin, E., Stahl, S., Cooney, A.M., Kaneski, C.R., Gupta, S., Brady, R.O., et al., 2004. Transfer of a mitochondrial DNA fragment to *MCOLN1* causes an inherited case of mucolipidosis IV. Hum. Mutat. 24, 460–465.
Goremykin, V.V., Salamini, F., Velasco, R., Viola, R., 2009. Mitochondrial DNA of *Vitis vinifera* and the issue of rampant horizontal gene transfer. Mol. Biol. Evol. 26, 99–110.
Gould, S.B., Waller, R.F., McFadden, G.I., 2008. Plastid evolution. Annu. Rev. Plant Biol. 59, 491–517.
Gray, M.W., Burger, G., Lang, B.F., 1999. Mitochondrial evolution. Science 283, 1476–1481.
Gray, M.W., Lang, B.F., Burger, G., 2004. Mitochondria of protists. Annu. Rev. Genet. 38, 477–524.
Green, B.R., 2011. Chloroplast genomes of photosynthetic eukaryotes. Plant J. 66, 34–44.
Grohmann, L., Brennicke, A., Schuster, W., 1992. The mitochondrial gene encoding ribosomal-protein S12 has been translocated to the nuclear genome in Oenothera. Nucleic Acids Res. 20, 5641–5646.
Gross, J., Bhattacharya, D., 2009. Revaluating the evolution of the Toc and Tic protein translocons. Trends Plant Sci. 14, 13–20.
Guo, X., Ruan, S., Hu, W., Cai, D., Fan, L., 2008. Chloroplast DNA insertions into the nuclear genome of rice: the genes, sites and ages of insertion involved. Funct. Integr. Genomics 8, 101–108.

Hanekamp, T., Thorsness, P.E., 1996. Inactivation of *YME2/RNA12*, which encodes an integral inner mitochondrial membrane protein, causes increased escape of DNA from mitochondria to the nucleus in *Saccharomyces cerevisiae*. Mol. Cell. Biol. 16, 2764–2771.

Hao, W.L., Palmer, J.D., 2009. Fine-scale mergers of chloroplast and mitochondrial genes create functional, transcompartmentally chimeric mitochondrial genes. Proc. Natl. Acad. Sci. USA 106, 16728–16733.

Hazkani-Covo, E., 2009. Mitochondrial insertions into primate nuclear genomes suggest the use of numts as a tool for phylogeny. Mol. Biol. Evol. 26, 2175–2179.

Hazkani-Covo, E., Covo, S., 2008. NUMT-mediated double-strand break repair mitigates deletions during primate genome evolution. PLoS Genet. 4, e1000237.

Hazkani-Covo, E., Graur, D., 2007. A comparative analysis of NUMT evolution in human and chimpanzee. Mol. Biol. Evol. 24, 13–18.

Hazkani-Covo, E., Zeller, R.M., Martin, W., 2010. Molecular poltergeists: mitochondrial DNA copies (NUMTs) in sequenced nuclear genomes. PLoS Genet. 6, e1000834.

Huang, C.Y., Ayliffe, M.A., Timmis, J.N., 2003. Direct measurement of the transfer rate of chloroplast DNA into the nucleus. Nature 422, 72–76.

Huang, C.Y., Ayliffe, M.A., Timmis, J.N., 2004. Simple and complex nuclear loci created by newly transferred chloroplast DNA in tobacco. Proc. Natl. Acad. Sci. USA 101, 9710–9715.

Huang, C.Y., Grunheit, N., Ahmadinejad, N., Timmis, J.N., Martin, W., 2005. Mutational decay and age of chloroplast and mitochondrial genomes transferred recently to angiosperm nuclear chromosomes. Plant Physiol. 138, 1723–1733.

Jacob, F., 1977. Evolution and tinkering. Science 196, 1161–1166.

Jansen, R.K., Saski, C., Lee, S.B., Hansen, A.K., Daniell, H., 2011. Complete plastid genome sequences of three rosids (Castanea, Prunus, Theobroma): evidence for at least two independent transfers of *rpl22* to the nucleus. Mol. Biol. Evol. 28, 835–847.

Jeon, K.W., Jeon, M.S., 1976. Endosymbiosis in amoebae: recently established endosymbionts have become required cytoplasmic components. J. Cell. Physiol. 89, 337–344.

Jeon, K.W., Lorch, I.J., 1967. Unusual intra-cellular bacterial infection in large, free-living amoebae. Exp. Cell Res. 48, 236–240.

Kanevski, I., Maliga, P., 1994. Relocation of the plastid *rbcL* gene to the nucleus yields functional ribulose-1,5-bisphosphate carboxylase in tobacco chloroplasts. Proc. Natl. Acad. Sci. USA 91, 1969–1973.

Karlberg, O., Canback, B., Kurland, C.G., Andersson, S.G., 2000. The dual origin of the yeast mitochondrial proteome. Yeast 17, 170–187.

Keeling, P.J., 2010. The endosymbiotic origin, diversification and fate of plastids. Philos. Trans. R. Soc. Lond. B Biol. Sci. 365, 729–748.

Keeling, P.J., Palmer, J.D., 2008. Horizontal gene transfer in eukaryotic evolution. Nat. Rev. Genet. 9, 605–618.

Khan, H., Archibald, J.M., 2008. Lateral transfer of introns in the cryptophyte plastid genome. Nucleic Acids Res. 36, 3043–3053.

Khan, H., Parks, N., Kozera, C., Curtis, B.A., Parsons, B.J., Bowman, S., et al., 2007. Plastid genome sequence of the cryptophyte alga *Rhodomonas salina* CCMP1319: lateral transfer of putative DNA replication machinery and a test of chromist plastid Phylogeny. Mol. Biol. Evol. 24, 1832–1842.

Kleine, T., Maier, U.G., Leister, D., 2009a. DNA transfer from organelles to the nucleus: the idiosyncratic genetics of endosymbiosis. Annu. Rev. Plant Biol. 60, 115–138.

Kleine, T., Voigt, C., Leister, D., 2009b. Plastid signalling to the nucleus: messengers still lost in the mists? Trends Genet. 25, 185–192.

Knoop, V., 2004. The mitochondrial DNA of land plants: peculiarities in phylogenetic perspective. Curr. Genet. 46, 123–139.

Krampis, K., Tyler, B.M., Boore, J.L., 2006. Extensive variation in nuclear mitochondrial DNA content between the genomes of *Phytophthora sojae* and *Phytophthora ramorum*. Mol. Plant Microbe Interact. 19, 1329–1336.

Kubo, N., Arimura, S., 2010. Discovery of the *rpl10* gene in diverse plant mitochondrial genomes and its probable replacement by the nuclear gene for chloroplast RPL10 in two lineages of angiosperms. DNA Res. 17, 1–9.

Kubo, T., Mikami, T., 2007. Organization and variation of angiosperm mitochondrial genome. Physiol. Plant. 129, 6–13.

Kubo, T., Newton, K.J., 2008. Angiosperm mitochondrial genomes and mutations. Mitochondrion 8, 5–14.

Kwon, T., Huq, E., Herrin, D.L., 2010. Microhomology-mediated and nonhomologous repair of a double-strand break in the chloroplast genome of Arabidopsis. Proc. Natl. Acad. Sci. USA 107, 13954–13959.

Lang, B.F., Gray, M.W., Burger, G., 1999. Mitochondrial genome evolution and the origin of eukaryotes. Annu. Rev. Genet. 33, 351–397.

Leister, D., 2005. Origin, evolution and genetic effects of nuclear insertions of organelle DNA. Trends Genet. 21, 655–663.

Leister, D., Wang, X., Haberer, G., Mayer, K.F., Kleine, T., 2011. Intra- and intercompartmental transcriptional networks coordinate the expression of genes for organellar functions. Plant Physiol. 157, 386–404. PMID:21775496.

Lenglez, S., Hermand, D., Decottignies, A., 2010. Genome-wide mapping of nuclear mitochondrial DNA sequences links DNA replication origins to chromosomal double-strand break formation in *Schizosaccharomyces pombe*. Genome Res. 20, 1250–1261.

Li, H.M., Chiu, C.C., 2010. Protein transport into chloroplasts. Annu. Rev. Plant Biol. 61, 157–180.

Lister, D.L., Bateman, J.M., Purton, S., Howe, C.J., 2003. DNA transfer from chloroplast to nucleus is much rarer in Chlamydomonas than in tobacco. Gene 316, 33–38.

Liu, Z., Butow, R.A., 2006. Mitochondrial retrograde signaling. Annu. Rev. Genet. 40, 159–185.

Liu, S.L., Zhuang, Y., Zhang, P., Adams, K.L., 2009. Comparative analysis of structural diversity and sequence evolution in plant mitochondrial genes transferred to the nucleus. Mol. Biol. Evol. 26, 875–891.

Lloyd, A.H., Timmis, J.N., 2011. The origin and characterization of new nuclear genes originating from a cytoplasmic organellar genome. Mol. Biol. Evol. 28, 2019–2028.

Lopez, J.V., Yuhki, N., Masuda, R., Modi, W., O'Brien, S.J., 1994. NUMT, a recent transfer and tandem amplification of mitochondrial DNA to the nuclear genome of the domestic cat. J. Mol. Evol. 39, 174–190.

Lough, A.N., Roark, L.M., Kato, A., Ream, T.S., Lamb, J.C., Birchler, J.A., et al., 2008. Mitochondrial DNA transfer to the nucleus generates extensive insertion site variation in maize. Genetics 178, 47–55.

Mans, B.J., Anantharaman, V., Aravind, L., Koonin, E.V., 2004. Comparative genomics, evolution and origins of the nuclear envelope and nuclear pore complex. Cell Cycle 3, 1612–1637.

Marienfeld, J., Unseld, M., Brennicke, A., 1999. The mitochondrial genome of Arabidopsis is composed of both native and immigrant information. Trends Plant Sci. 4, 495–502.

Martin, W., 2003. Gene transfer from organelles to the nucleus: frequent and in big chunks. Proc. Natl. Acad. Sci. USA 100, 8612–8614.

Martin, W., Herrmann, R.G., 1998. Gene transfer from organelles to the nucleus: how much, what happens, and why? Plant Physiol. 118, 9–17.

Martin, W., Schnarrenberger, C., 1997. The evolution of the Calvin cycle from prokaryotic to eukaryotic chromosomes: a case study of functional redundancy in ancient pathways through endosymbiosis. Curr. Genet. 32, 1–18.

Martin, W., Rujan, T., Richly, E., Hansen, A., Cornelsen, S., Lins, T., et al., 2002. Evolutionary analysis of Arabidopsis, cyanobacterial, and chloroplast genomes reveals plastid phylogeny and thousands of cyanobacterial genes in the nucleus. Proc. Natl. Acad. Sci. USA 99, 12246–12251.

Matsuo, M., Ito, Y., Yamauchi, R., Obokata, J., 2005. The rice nuclear genome continuously integrates, shuffles, and eliminates the chloroplast genome to cause chloroplast-nuclear DNA flux. Plant Cell 17, 665–675.

McFadden, G.I., van Dooren, G.G., 2004. Evolution: red algal genome affirms a common origin of all plastids. Curr. Biol. 14, R514–R516.

Millen, R.S., Olmstead, R.G., Adams, K.L., Palmer, J.D., Lao, N.T., Heggie, L., et al., 2001. Many parallel losses of *infA* from chloroplast DNA during angiosperm evolution with multiple independent transfers to the nucleus. Plant Cell 13, 645–658.

Mishmar, D., Ruiz-Pesini, E., Brandon, M., Wallace, D.C., 2004. Mitochondrial DNA-like sequences in the nucleus (NUMTs): insights into our African origins and the mechanism of foreign DNA integration. Hum. Mutat. 23, 125–133.

Mokranjac, D., Neupert, W., 2009. Thirty years of protein translocation into mitochondria: unexpectedly complex and still puzzling. Biochim. Biophys. Acta 1793, 33–41.

Mota, M., 1963. Electron microscope study of relationship between nucleus and mitochondria in *Chlorophytum capense* (L.) Kuntze. Cytologia 28, 409.

Moustafa, A., Bhattacharya, D., 2008. PhyloSort: a user-friendly phylogenetic sorting tool and its application to estimating the cyanobacterial contribution to the nuclear genome of Chlamydomonas. BMC Evol. Biol. 8, 6.

Nada, A., Soll, J., 2004. Inner envelope protein 32 is imported into chloroplasts by a novel pathway. J. Cell Sci. 117, 3975–3982.

Nakazono, M., Nishiwaki, S., Tsutsumi, N., Hirai, A., 1996. A chloroplast-derived sequence is utilized as a source of promotes sequences for the gene for subunit 9 of NADH dehydrogenase (nad9) in rice mitochondria. Mol. Gen. Genet. 252, 371–378.

Nelson, N., Yocum, C.F., 2006. Structure and function of photosystems I and II. Annu. Rev. Plant Biol. 57, 521–565.

Nergadze, S.G., Lupotto, M., Pellanda, P., Santagostino, M., Vitelli, V., Giulotto, E., 2010. Mitochondrial DNA insertions in the nuclear horse genome. Anim. Genet. 41, 176–185.

Neupert, W., Herrmann, J.M., 2007. Translocation of proteins into mitochondria. Annu. Rev. Biochem. 76, 723–749.

Notsu, Y., Masood, S., Nishikawa, T., Kubo, N., Akiduki, G., Nakazono, M., et al., 2002. The complete sequence of the rice (*Oryza sativa* L.) mitochondrial genome: frequent DNA sequence acquisition and loss during the evolution of flowering plants. Mol. Genet. Genomics 268, 434–445.

Noutsos, C., Richly, E., Leister, D., 2005. Generation and evolutionary fate of insertions of organelle DNA in the nuclear genomes of flowering plants. Genome Res. 15, 616–628.

Noutsos, C., Kleine, T., Armbruster, U., DalCorso, G., Leister, D., 2007. Nuclear insertions of organellar DNA can create novel patches of functional exon sequences. Trends Genet. 23, 597–601.

Nugent, J.M., Palmer, J.D., 1991. RNA-mediated transfer of the gene *coxII* from the mitochondrion to the nucleus during flowering plant evolution. Cell 66, 473–481.

Obornik, M., Green, B.R., 2005. Mosaic origin of the heme biosynthesis pathway in photosynthetic eukaryotes. Mol. Biol. Evol. 22, 2343–2353.

Oda, K., Kohchi, T., Ohyama, K., 1992. Mitochondrial-DNA of Marchantia-polymorpha as a single circular form with no incorporation of foreign DNA. Biosci. Biotechnol. Biochem. 56, 132–135.

Odom, O.W., Shenkenberg, D.L., Garcia, J.A., Herrin, D.L., 2004. A horizontally acquired group II intron in the chloroplast *psbA* gene of a psychrophilic Chlamydomonas: *in vitro* self-splicing and genetic evidence for maturase activity. RNA 10, 1097–1107.

Ohyama, K., Takemura, M., Oda, K., Fukuzawa, H., Kohchi, T., Nakayama, S., et al., 2009. Gene content, organization and molecular evolution of plant organellar genomes and sex chromosomes—insights from the case of the liverwort *Marchantia polymorpha*. Proc. Jpn. Acad. Ser. B Phys. Biol. Sci. 85, 108–124.

Ong, H.C., Palmer, J.D., 2006. Pervasive survival of expressed mitochondrial *rps14* pseudogenes in grasses and their relatives for 80 million years following three functional transfers to the nucleus. BMC Evol. Biol. 6, 55.

Pamilo, P., Viljakainen, L., Vihavainen, A., 2007. Exceptionally high density of NUMTs in the honeybee genome. Mol. Biol. Evol. 24, 1340–1346.

Perna, N.T., Kocher, T.D., 1996. Mitochondrial DNA: molecular fossils in the nucleus. Curr. Biol. 6, 128–129.

Pogson, B.J., Woo, N.S., Forster, B., Small, I.D., 2008. Plastid signalling to the nucleus and beyond. Trends Plant Sci. 13, 602–609.

Pombert, J.F., Otis, C., Lemieux, C., Turmel, M., 2005. The chloroplast genome sequence of the green alga *Pseudendoclonium akinetum* (Ulvophyceae) reveals unusual structural features and new insights into the branching order of chlorophyte lineages. Mol. Biol. Evol. 22, 1903–1918.

Pont-Kingdon, G., Okada, N.A., Macfarlane, J.L., Beagley, C.T., Watkins-Sims, C.D., Cavalier-Smith, T., et al., 1998. Mitochondrial DNA of the coral *Sarcophyton glaucum* contains a gene for a homologue of bacterial MutS: a possible case of gene transfer from the nucleus to the mitochondrion. J. Mol. Evol. 46, 419–431.

Puchta, H., 2005. The repair of double-strand breaks in plants: mechanisms and consequences for genome evolution. J. Exp. Bot. 56, 1–14.

Rapoport, T.A., 2007. Protein translocation across the eukaryotic endoplasmic reticulum and bacterial plasma membranes. Nature 450, 663–669.

Rassow, J., Dekker, P.J.T., van Wilpe, S., Meijer, M., Soll, J., 1999. The preprotein translocase of the mitochondrial inner membrane: function and evolution. J. Mol. Biol. 286, 105–120.

Raven, J.A., Allen, J.F., 2003. Genomics and chloroplast evolution: what did cyanobacteria do for plants? Genome Biol. 4, 209.

Reumann, S., Keegstra, K., 1999. The endosymbiotic origin of the protein import machinery of chloroplastic envelope membranes. Trends Plant Sci. 4, 302–307.

Reumann, S., Inoue, K., Keegstra, K., 2005. Evolution of the general protein import pathway of plastids. Mol. Membr. Biol. 22, 73–86.

Reyes-Prieto, A., Bhattacharya, D., 2007. Phylogeny of Calvin cycle enzymes supports Plantae monophyly. Mol. Phylogenet. Evol. 45, 384–391.

Reyes-Prieto, A., Hackett, J.D., Soares, M.B., Bonaldo, M.F., Bhattacharya, D., 2006. Cyanobacterial contribution to algal nuclear genomes is primarily limited to plastid functions. Curr. Biol. 16, 2320–2325.

Rhoads, D.M., Subbaiah, C.C., 2007. Mitochondrial retrograde regulation in plants. Mitochondrion 7, 177–194.

Ricchetti, M., Fairhead, C., Dujon, B., 1999. Mitochondrial DNA repairs double-strand breaks in yeast chromosomes. Nature 402, 96–100.

Ricchetti, M., Tekaia, F., Dujon, B., 2004. Continued colonization of the human genome by mitochondrial DNA. PLoS Biol. 2, E273.

Rice, D.W., Palmer, J.D., 2006. An exceptional horizontal gene transfer in plastids: gene replacement by a distant bacterial paralog and evidence that haptophyte and cryptophyte plastids are sisters. BMC Biol. 4, 31.

Richards, T.A., Dacks, J.B., Campbell, S.A., Blanchard, J.L., Foster, P.G., McLeod, R., et al., 2006. Evolutionary origins of the eukaryotic shikimate pathway: gene fusions, horizontal gene transfer, and endosymbiotic replacements. Eukaryot. Cell 5, 1517–1531.

Richly, E., Leister, D., 2004a. NUMTs in sequenced eukaryotic genomes. Mol. Biol. Evol. 21, 1081–1084.
Richly, E., Leister, D., 2004b. NUPTs in sequenced eukaryotes and their genomic organization in relation to NUMTs. Mol. Biol. Evol. 21, 1972–1980.
Richly, E., Chinnery, P.F., Leister, D., 2003. Evolutionary diversification of mitochondrial proteomes: implications for human disease. Trends Genet. 19 (7), 356–362.
Roark, L.M., Hui, Y., Donnelly, L., Birchler, J.A., Newton, K.J., 2010. Recent and frequent insertions of chloroplast DNA into maize nuclear chromosomes. Cytogenet. Genome Res. 129, 17–23.
Rochaix, J.D., 2001. Posttranscriptional control of chloroplast gene expression. From RNA to photosynthetic complex. Plant Physiol. 125, 142–144.
Roy, S., Ueda, M., Kadowaki, K., Tsutsumi, N., 2010. Different status of the gene for ribosomal protein S16 in the chloroplast genome during evolution of the genus Arabidopsis and closely related species. Genes Genet. Syst. 85, 319–326.
Rumpho, M.E., Summer, E.J., Manhart, J.R., 2000. Solar-powered sea slugs. Mollusc/algal chloroplast symbiosis. Plant Physiol. 123, 29–38.
Sacerdot, C., Casaregola, S., Lafontaine, I., Tekaia, F., Dujon, B., Ozier-Kalogeropoulos, O., 2008. Promiscuous DNA in the nuclear genomes of hemiascomycetous yeasts. FEMS Yeast Res. 8, 846–857.
Sangare, A., Lonsdale, D., Weil, J.H., Grienenberger, J.M., 1989. Sequence analysis of the tRNA(Tyr) and tRNA(Lys) genes and evidence for the transcription of a chloroplast-like tRNA(Met) in maize mitochondria. Curr. Genet. 16, 195–201.
Sato, N., Ishikawa, M., Fujiwara, M., Sonoike, K., 2005. Mass identification of chloroplast proteins of endosymbiont origin by phylogenetic profiling based on organism-optimized homologous protein groups. Genome Inform. 16, 56–68.
Satoh, M., Kubo, T., Nishizawa, S., Estiati, A., Itchoda, N., Mikami, T., 2004. The cytoplasmic male-sterile type and normal type mitochondrial genomes of sugar beet share the same complement of genes of known function but differ in the content of expressed ORFs. Mol. Genet. Genomics 272, 247–256.
Scheller, H.V., Jensen, P.E., Haldrup, A., Lunde, C., Knoetzel, J., 2001. Role of subunits in eukaryotic Photosystem I. Biochim. Biophys. Acta 1507, 41–60.
Schuster, W., Brennicke, A., 1987. Plastid, nuclear and reverse-transcriptase sequences in the mitochondrial genome of Oenothera—is genetic information transferred between organelles via RNA. EMBO J. 6, 2857–2863.
Shahmuradov, I.A., Akbarova, Y.Y., Solovyev, V.V., Aliyev, J.A., 2003. Abundance of plastid DNA insertions in nuclear genomes of rice and Arabidopsis. Plant Mol. Biol. 52, 923–934.
Shao, Z.Y., Graf, S., Chaga, O.Y., Lavrov, D.V., 2006. Mitochondrial genome of the moon jelly *Aurelia aurita* (Cnidaria, Scyphozoa): a linear DNA molecule encoding a putative DNA-dependent DNA polymerase. Gene 381, 92–101.
Sheppard, A.E., Timmis, J.N., 2009. Instability of plastid DNA in the nuclear genome. PLoS Genet. 5, e1000323.
Sheppard, A.E., Ayliffe, M.A., Blatch, L., Day, A., Delaney, S.K., Khairul-Fahmy, N., et al., 2008. Transfer of plastid DNA to the nucleus is elevated during male gametogenesis in tobacco. Plant Physiol. 148, 328–336.
Sheveleva, E.V., Hallick, R.B., 2004. Recent horizontal intron transfer to a chloroplast genome. Nucleic Acids Res. 32, 803–810.
Shinozaki, K., Ohme, M., Tanaka, M., Wakasugi, T., Hayashida, N., Matsubayashi, T., et al., 1986. The complete nucleotide sequence of the tobacco chloroplast genome: its gene organization and expression. EMBO J. 5, 2043–2049.

Smith, D.R., Crosby, K., Lee, R.W., 2011. Correlation between nuclear plastid DNA abundance and plastid number supports the limited transfer window hypothesis. Genome Biol. Evol. 3, 365–371.

Somanchi, A., Mayfield, S.P., 1999. Nuclear-chloroplast signalling. Curr. Opin. Plant Biol. 2, 404–409.

Song, H., Buhay, J.E., Whiting, M.F., Crandall, K.A., 2008. Many species in one: DNA barcoding overestimates the number of species when nuclear mitochondrial pseudogenes are coamplified. Proc. Natl. Acad. Sci. USA 105, 13486–13491.

Stegemann, S., Bock, R., 2006. Experimental reconstruction of functional gene transfer from the tobacco plastid genome to the nucleus. Plant Cell 18, 2869–2878.

Stegemann, S., Hartmann, S., Ruf, S., Bock, R., 2003. High-frequency gene transfer from the chloroplast genome to the nucleus. Proc. Natl. Acad. Sci. USA 100, 8828–8833.

Stern, D.B., Lonsdale, D.M., 1982. Mitochondrial and chloroplast genomes of maize have a 12-kilobase DNA sequence in common. Nature 299, 698–702.

Stern, D.B., Goldschmidt-Clermont, M., Hanson, M.R., 2010. Chloroplast RNA metabolism. Annu. Rev. Plant Biol. 61, 125–155.

Stupar, R.M., Lilly, J.W., Town, C.D., Cheng, Z., Kaul, S., Buell, C.R., et al., 2001. Complex mtDNA constitutes an approximate 620-kb insertion on *Arabidopsis thaliana* chromosome 2: implication of potential sequencing errors caused by large-unit repeats. Proc. Natl. Acad. Sci. USA 98, 5099–5103.

Suzuki, K., Miyagishima, S., 2010. Eukaryotic and eubacterial contributions to the establishment of plastid proteome estimated by large-scale phylogenetic analyses. Mol. Biol. Evol. 27, 581–590.

Szklarczyk, R., Huynen, M.A., 2010. Mosaic origin of the mitochondrial proteome. Proteomics 10, 4012–4024.

The Rice Chromosome 10 Sequencing Consortium, 2003. In-depth view of structure, activity, and evolution of rice chromosome 10. Science 300, 1566–1569.

Thorsness, P.E., Fox, T.D., 1990. Escape of DNA from mitochondria to the nucleus in *Saccharomyces cerevisiae*. Nature 346, 376–379.

Thorsness, P.E., Fox, T.D., 1993. Nuclear mutations in *Saccharomyces cerevisiae* that affect the escape of DNA from mitochondria to the nucleus. Genetics 134, 21–28.

Thorsness, P.E., White, K.H., Fox, T.D., 1993a. Inactivation of *YME1*, a member of the FTSH-SEC18-PAS1-CDC48 family of putative ATPase-encoding genes, causes increased escape of DNA from mitochondria in *Saccharomyces cerevisiae*. Mol. Cell. Biol. 13, 5418–5426.

Thorsness, P.E., White, K.H., Ong, W.C., 1993b. *AFG2*, an essential gene in yeast, encodes a new member of the SEC18P, PAS1P, CDC48P, TBP-1 family of putative ATPases. Yeast 9, 1267–1271.

Timmis, J.N., Ayliffe, M.A., Huang, C.Y., Martin, W., 2004. Endosymbiotic gene transfer: organelle genomes forge eukaryotic chromosomes. Nat. Rev. Genet. 5, 123–135.

Tong, J., Dolezal, P., Selkrig, J., Crawford, S., Simpson, A.G., Noinaj, N., et al., 2011. Ancestral and derived protein import pathways in the mitochondrion of *Reclinomonas americana*. Mol. Biol. Evol. 28, 1581–1591.

Tsuzuki, T., Nomiyama, H., Setoyama, C., Maeda, S., Shimada, K., 1983. Presence of mitochondrial-DNA-like sequences in the human nuclear-DNA. Gene 25, 223–229.

Turner, C., Killoran, C., Thomas, N.S., Rosenberg, M., Chuzhanova, N.A., Johnston, J., et al., 2003. Human genetic disease caused by *de novo* mitochondrial-nuclear DNA transfer. Hum. Genet. 112, 303–309.

Tzin, V., Galili, G., 2010. New insights into the shikimate and aromatic amino acids biosynthesis pathways in plants. Mol. Plant 3, 956–972.

Ueda, M., Fujimoto, M., Arimura, S., Tsutsumi, N., Kadowaki, K., 2008a. Presence of a latent mitochondrial targeting signal in gene on mitochondrial genome. Mol. Biol. Evol. 25, 1791–1793.

Ueda, M., Nishikawa, T., Fujimoto, M., Takanashi, H., Arimura, S., Tsutsumi, N., et al., 2008b. Substitution of the gene for chloroplast RPS16 was assisted by generation of a dual targeting signal. Mol. Biol. Evol. 25, 1566–1575.

van Gent, D.C., Hoeijmakers, J.H., Kanaar, R., 2001. Chromosomal stability and the DNA double-stranded break connection. Nat. Rev. Genet. 2, 196–206.

Veronico, P., Gallerani, R., Ceci, L.R., 1996. Compilation and classification of higher plant mitochondrial tRNA genes. Nucleic Acids Res. 24, 2199–2203.

Viljakainen, L., Oliveira, D., Werren, J.H., Behura, S.K., 2010. Transfers of mitochondrial DNA to the nuclear genome in the wasp *Nasonia vitripennis*. Insect Mol. Biol. 19, 27–35.

Vonheijne, G., 1986. Why mitochondria need a genome. FEBS Lett. 198, 1–4.

Wang, D., Wu, Y.W., Shih, A.C.C., Wu, C.S., Wang, Y.N., Chaw, S.M., 2007. Transfer of chloroplast genomic DNA to mitochondrial genome occurred at least 300 MYA. Mol. Biol. Evol. 24, 2040–2048.

Woischnik, M., Moraes, C.T., 2002. Pattern of organization of human mitochondrial pseudogenes in the nuclear genome. Genome Res. 12, 885–893.

Woodson, J.D., Chory, J., 2008. Coordination of gene expression between organellar and nuclear genomes. Nat. Rev. Genet. 9, 383–395.

Yoon, H.S., Hackett, J.D., Ciniglia, C., Pinto, G., Bhattacharya, D., 2004. A molecular timeline for the origin of photosynthetic eukaryotes. Mol. Biol. Evol. 21, 809–818.

Yu, H.S., Russell, S.D., 1994. Occurrence of mitochondria in the nuclei of tobacco sperm cells. Plant Cell 6, 1477–1484.

Yu, J., Wang, J., Lin, W., Li, S.G., Li, H., Zhou, J., et al., 2005. The genomes of *Oryza sativa*: a history of duplications. PLoS Biol. 3, 266–281.

CHAPTER FOUR

Structure, Regulation, and Evolution of the Plastid Division Machinery

Shin-ya Miyagishima,* Hiromitsu Nakanishi,† *and* Yukihiro Kabeya*

Contents

* Center for Frontier Research, National Institute of Genetics, Yata, Mishima, Shizuoka, Japan
† Satellite Venture Business Laboratory, Shinshu University, Tokida, Ueda, Nagano, Japan

International Review of Cell and Molecular Biology, Volume 291
ISSN 1937-6448, DOI: 10.1016/B978-0-12-386035-4.00004-5

Abstract

Plastids have evolved from a cyanobacterial endosymbiont, and their continuity is maintained by the plastid division and segregation which is regulated by the eukaryotic host cell. Plastids divide by constriction of the inner- and outer-envelope membranes. Recent studies revealed that this constriction is performed by a large protein and glucan complex at the division site that spans the two envelope membranes. The division complex has retained certain components of the cyanobacterial division complex along with components developed by the host cell. Based on the information on the division complex at the molecular level, we are beginning to understand how the division complex has evolved and how it is assembled, constricted, and regulated in the host cell. This chapter reviews the current understanding of the plastid division machinery and some of the questions that will be addressed in the near future.

Key Words: Dynamin, Endosymbiosis, Evolution, FtsZ, Mitochondrial division, Plastid division.

1. Introduction

Mitochondria and plastids, double-membrane energy-converting organelles in eukaryotic cells, arose by serial endosymbiotic events more than 1 billion years ago. Mitochondria first arose from an alpha-proteobacterial ancestor that was integrated into a primitive eukaryotic host cell. Plastids later arose from a cyanobacterial ancestor acquired by a eukaryote in which mitochondria had been established (Archibald, 2009; Gould et al., 2008). Reminiscent of their free-living bacterial ancestors, both organelles possess their own genomes and machinery sufficient for expressing the genomic information (e.g., nucleoids and ribosomes). In addition, mitochondria and plastids proliferate as the result of the division of these preexisting organelles. However, while retaining various bacterial features, the functionality and multiplication of these organelles rely on and are regulated by host-nucleus-encoded proteins that are targeted to these organelles. This is largely because mitochondria and chloroplasts have lost most of their genes, and some of these genes have relocated into the nuclear genome. For example, the genomes of cyanobacteria *Synechocystis* sp. PCC6803 and *Microleus chthonoplastes* contain 3200 and 8300 genes, respectively. In contrast, the plastid genome contains ~240 genes at most. Most of the genes that are encoded in plastid genomes are related to photosystems or the maintenance and expression of the genomic information, and the plastid genome lacks the information required for proliferation (Race et al., 1999). Thus, plastids cannot divide by themselves, so the division is carried out under the control of nucleus-encoded proteins. This control has ensured the

robust inheritance of plastids, both during the course of cell division and from generation to generation (Rodriguez-Ezpeleta and Philippe, 2006).

The proliferation of plastids through division was first reported in the late nineteenth century, which became the major evidence for the first endosymbiotic theory proposed by Mereschkowsky in 1905 (Martin and Kowallik, 1999). After various controversies and debates, it came to be accepted by the 1980s that plastids are never synthesized *de novo*, but rather, multiply by a process of division along with the duplication and separation of their nucleoids (DNA-protein complex; Kuroiwa, 1991; Leech et al., 1981; Possingham and Lawrence, 1983). The first information about the mechanism of plastid division was supplied by electron microscopic observation of dividing plastids. These studies identified ring structures encircling the zone of constriction at the division site, raising the possibility that plastid division is performed by a constriction of these ring structures, as in the case of the contractile ring in cytokinesis (Kuroiwa et al., 1998). Many subsequent microscopic studies reported plastid division in various lineages of algae and plants, and characterized relationship between environmental stimuli and plastid division (Possingham and Lawrence, 1983). However, it was only during the past decade that molecular genetic and biochemical studies have begun to elucidate the mechanism of plastid division.

Recent studies have established that chloroplast division is performed by a macromolecular protein complex at the division site, encompassing both the inside and the outside of the two envelope membranes. This division complex has retained certain components of the cyanobacterial division complex and several additional components that have been subsequently developed by the host cell (Maple and Moller, 2010; Miyagishima and Kabeya, 2010; Yang et al., 2008). Based on the information at the molecular level, we are beginning to understand how plastids divide by utilizing the division complex, how the host cell regulates the proliferation of plastids, and how this system has evolved. In addition, studies at the molecular level have found a certain similarity between the plastid and the mitochondrial division machinery. Thus, characterization of the plastid division machinery will lead to the understanding of these double-membraned, endosymbiotic organelles. In addition, a better understanding would also give significant insights into how the host cell has controlled the replication of the endosymbiotic bacteria so as to turn them into subcellular organelles.

This review summarizes the current understanding of the mechanism, regulation, and evolution of the plastid division machinery. Because most of the current understanding is based on studies of chloroplasts and there are certain differences in the mode and mechanism of the division between chloroplasts and other types of plastids, here we use the term "chloroplasts" for photosynthetic plastids and "nongreen plastids" for all other types of plastids, as appropriate.

2. Timing and Mode of Plastid Division

The term "plastid" originated from the organelle's plasticity. In vascular plants (ferns and seed plants), proplastids in the meristematic tissues differentiate into several different types of plastid, such as amyloplasts, chromoplasts, etioplasts, and chloroplasts, depending upon which function they need to play in the cell (Lopez-Juez and Pyke, 2005). Proplastids are also responsible for the continuity of plastids from generation to generation in vascular plants. However, in algae and mosses, chloroplasts are usually the only type of plastid present. This is consistent with the fact that plastids are derived from a photosynthetic cyanobacterium. Thus, from an evolutionary standpoint, the chloroplast is the origin of the plastids and the plastid differentiation system based on the proplastids evolved later in vascular plants.

Plastids generally divide by binary fission, but multiple fission events also occur in certain cases. Multiple constrictions in a single plastid have been observed in the chloroplasts of ferns (Duckett and Ligrone, 1993) and embryonic cap cells in the angiosperm *Pelargonium zonale* (Kuroiwa et al., 2001). In addition, multiple fission events are often evident in nongreen plastids in seed plants (Momoyama et al., 2003; Yun and Kawagoe, 2009). Both the earlier electron microscopy studies and more recent studies at the molecular level have shown that all types of plastids are capable of constriction division.

The majority of algae (both unicellular and multicellular) have either just one or only a few chloroplasts per cell. Therefore, chloroplasts divide once per cell cycle, before the host cell completes cytokinesis. This connection between the host cell cycle and chloroplast division maintains the number of chloroplasts per cell constant from generation to generation (Fig. 4.1). In contrast, land plant (Embryophyta) cells generally contain numerous plastids, and the plastids divide nonsynchronously, even in individual cells, independently of the cell cycle (Fig. 4.1). In addition, the rate of plastid division changes, and therefore, the size and number of plastids vary considerably depending on the cell type, developmental stage, and environmental conditions. For example, in *Arabidopsis thaliana*, the shoot meristematic cells contain 10–20 proplastids. During leaf development, proplastids differentiate into chloroplasts, which divide in accord with cell expansion but without cell division (yet with replication of nuclear DNA that gives rise to multiploid cells), and the number of chloroplasts per mesophyll cell reaches more than 100 in fully expanding leaves (Lopez-Juez and Pyke, 2005). During leaf development, the rate of chloroplast division decreases, and as a result, the size of the chloroplasts increases (Fig. 4.1). In the moss *Physcomitrella patens*, the protonemal cell contains

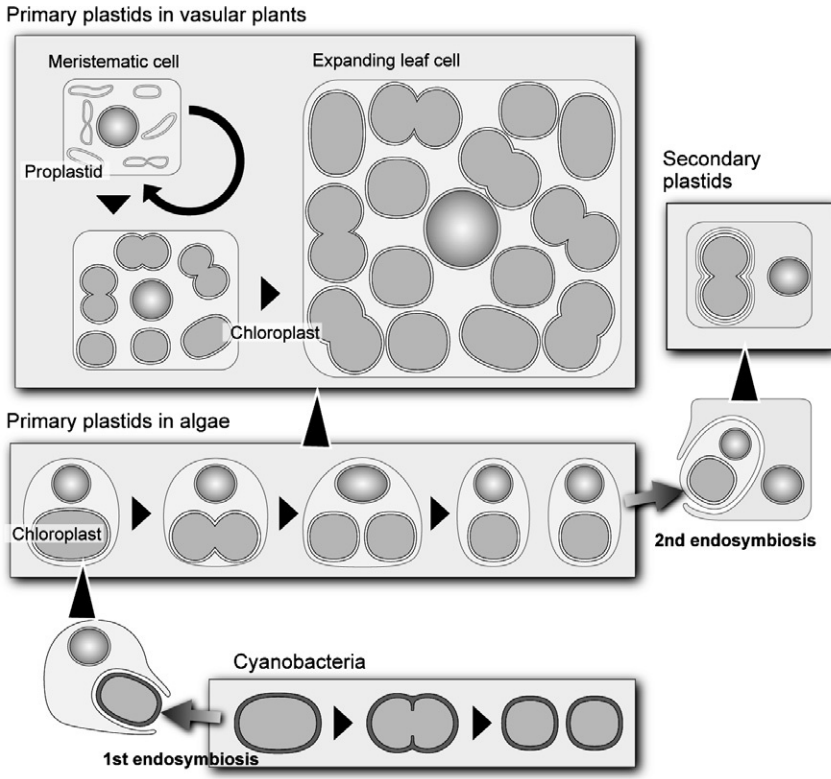

Figure 4.1 Evolution of plastids and plastid division in algae, land plants, and algae that possess plastids of secondary endosymbiotic origin. In unicellular algal cells, which have one or just a few chloroplasts of primary or secondary endosymbiotic origin, plastid (usually chloroplast) division occurs once per cell cycle prior to cytokinesis. In meristematic cells in vascular plants, the rate of proplastid and cell multiplication is almost the same, thereby allowing daughter cells to receive nearly the same number of proplastids as the mother cell. After leaf cells start to differentiate, proplastids differentiate into chloroplasts. During the early proliferative stage in which mitosis takes place, chloroplast replication keeps pace with cell division, even though chloroplasts divide nonsynchronously. During the late expanding stage, cell division ceases, but chloroplast division continues for two or three more cycles and nuclear DNA replication also continues, resulting in an enlarged cell with a high degree of ploidy.

40–50 chloroplasts and chloroplast division occurs nonsynchronously in the same cell. When the formation of buds, from which gametophytes arise, is induced by cytokinin, the rate of chloroplast division increases. As a result, the apical cell of the bud contains more numerous and smaller chloroplasts than in protonemal cells (Okazaki et al., 2009). Thus, land plant cells have evolved mechanisms to control the rate of chloroplast division upon cell differentiation, independently of the cell cycle.

3. Structural and Molecular Mechanisms of Plastid Division

Earlier studies using electron microscopy showed that plastids divide by simultaneous constriction of the inner and outer envelopes (Leech et al., 1981; Possingham and Lawrence, 1983), except for the chloroplasts in glaucophyte algae (described later). Those studies also identified an electron-dense structure, called the "plastid-dividing" (PD) ring, encircling the plastid division site (Kuroiwa et al., 1998). Subsequent studies at the molecular level over the past decade have identified several proteins that form a macromolecular complex at the division site, encompassing both the inside and the outside of the two envelopes (Maple and Moller, 2010; Miyagishima and Kabeya, 2010; Yang et al., 2008). Here, we summarize the observations achieved by electron microscopy (Fig. 4.2), the understanding of plastid division at the molecular level, and the relationship between the two (Fig. 4.3).

3.1. The plastid-dividing ring

The PD ring has been detected by electron microscopy at the plastid division site (both in chloroplasts and in nongreen plastids) in numerous photosynthetic eukaryotes, usually as two distinct structures: the outer PD ring composed of filaments which are 5–7 nm in diameter on the cytosolic side of the outer envelope (Mita et al., 1986; Miyagishima et al., 2001a), and the inner PD ring observed as belt of 5 nm thick on the stromal side of the inner envelope (Hashimoto, 1986; Miyagishima et al., 2001b). A middle PD ring has been observed in the intermembrane space in the unicellular red alga *Cyanidioschyzon merolae* (Miyagishima et al., 2001b) and the unicellular green alga *Nannochloris bacillaris* (Sumiya et al., 2008) (Fig. 4.2).

The morphology and behavior of the two (or three) PD rings differ and the dynamics of assembly, constriction, and disassembly have been analyzed in a series of ultrastructural studies utilizing *C. merolae* cells, the cell cycle and organelle division of which are synchronized by a light and dark cycle (Miyagishima et al., 2001b; Suzuki et al., 1994) (Fig. 4.2). In *C. merolae*, the inner PD ring assembles first, followed by near simultaneous assembly of the middle and outer PD rings. Once all three rings are in place, chloroplast constriction commences. Quantitative analyses have shown that the inner and middle PD rings maintain a constant thickness and appear to lose volume during constriction, indicating that the progressive decrease in ring diameter is probably accompanied by the loss of ring components. In contrast, the outer PD ring widens and thickens during constriction while maintaining a constant volume. The middle and the inner PD rings disassemble late in constriction, but before the daughter plastids are separated,

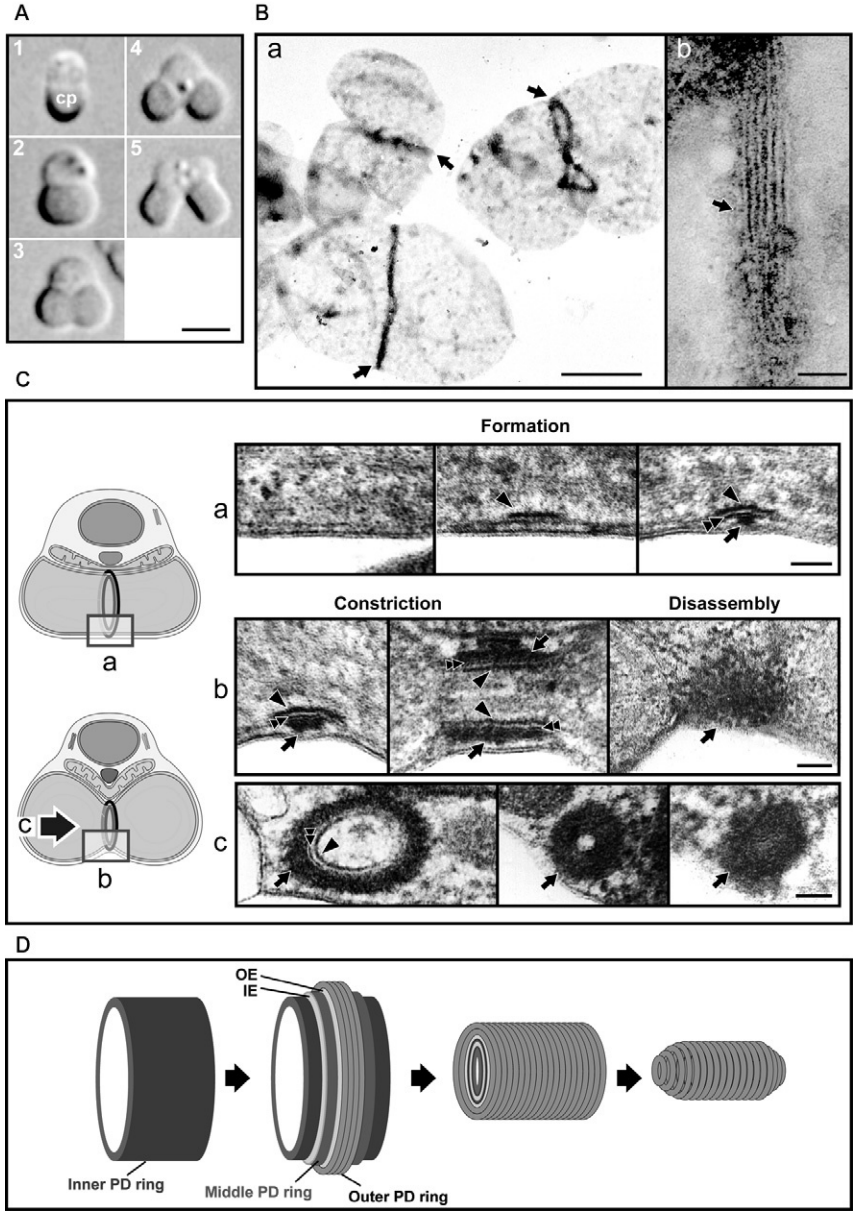

Figure 4.2 Structure and behavior of the PD ring during plastid division. (A) Cell and chloroplast division of the unicellular red alga *C. merolae*. The cell contains a single chloroplast (cp). The chloroplast divides once a cell cycle (2–4) before cytokinesis (5). (B) A negative stain electron microscopic image of the outer PD ring. An image of the three rings (Ba) and a magnified view of a part of a ring (Bb) are shown. (C) Transmission electron microscopic images of the PD ring during formation, constriction, and

whereas the outer PD ring remains attached to both daughter plastids, forming a tube-like bridge that remains positioned between and attached to the daughter plastids until after they have fully separated (Miyagishima et al., 2001b) (Fig. 4.2).

Although less well characterized in other organisms, similar dynamics and structural characteristics have been observed in green algae (Chida and Ueda, 1991; Ogawa et al., 1995) and land plants (Duckett and Ligrone, 1993; Kuroiwa et al., 2002), suggesting that the rings are composed of orthologous components throughout the photosynthetic eukaryotes. A very recent study showed that the outer PD ring is a bundle of glucan filaments (see below) (Yoshida et al., 2010), but the components of the inner and the middle PD ring are still unknown at present.

3.2. Stromal components of the division complex descended from cyanobacteria

3.2.1. FtsZ1 and FtsZ2

The first protein that was shown to play a role in plastid division was a nucleus-encoded plant and algal homolog of the key bacterial division protein FtsZ (Osteryoung and Vierling, 1995; Osteryoung et al., 1998; Strepp et al., 1998). Bacterial FtsZ was identified by analyses of filamenting temperature-sensitive (*fts*) *Escherichia coli* mutants collected in the late 1960s (Hirota et al., 1968). The *fts* mutants have a defect in cytokinesis and, as a result, elongate to form filamentous cells. FtsZ is a GTPase that is structurally similar to eukaryotic tubulin (Lowe and Amos, 1998) and self-assembles into a ring structure beneath the cytoplasmic membrane at the bacterial division site (Bi and Lutkenhaus, 1991). FtsZ is conserved in most bacteria and certain lineages of archaea. The formation of the FtsZ ring is the first event at the division site and initiates the recruitment of the other proteins that constitute the bacterial division complex. Therefore, of the several proteins involved in bacterial cell division, FtsZ is thought to play the pivotal role (Harry et al., 2006). A recent study showed that bacterial FtsZ self-assembles into a ring that constricts liposomes *in vitro*, suggesting that the FtsZ ring generates constrictive force as well as functioning as a scaffold for assembly of the division complex (Osawa et al., 2008).

Plastid-targeted FtsZ was first found in the nuclear genome of *Arabidopsis thaliana* in 1995 (Osteryoung and Vierling, 1995) and FtsZ homologs have since been reported in several photosynthetic eukaryotes. These eukaryotic

disassembly. Sections which cut the cell perpendicular to the division plane (Ca, Cb) and cut along the division plane (Cc) are shown. (D) Schematic representation of the behavior of the inner, the middle, and the outer PD rings during *C. merolae* chloroplast division. The arrows, arrowheads, and double arrowheads indicate the outer, the inner, and the middle PD ring, respectively. Scale bar: 2 μm (A), 500 nm (Ba), and 50 nm (Bb, C).

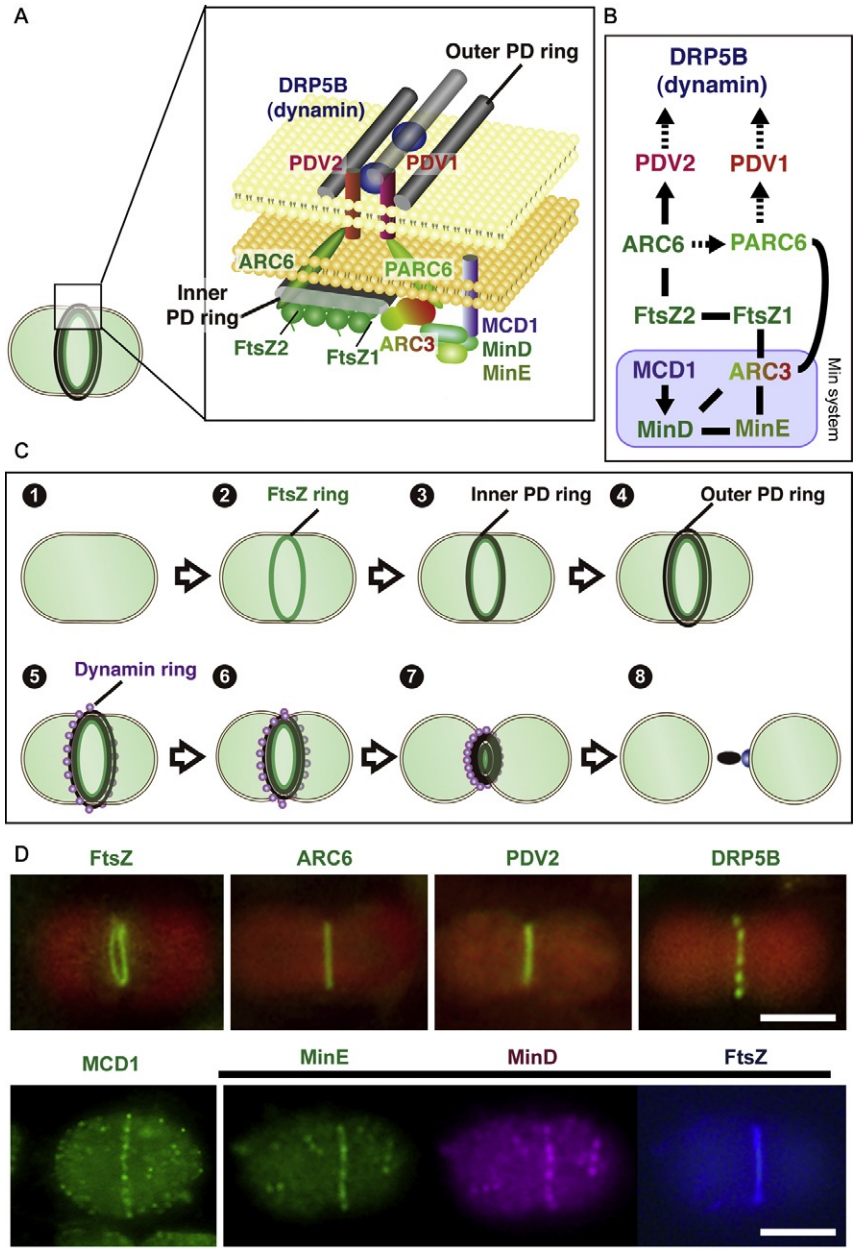

Figure 4.3 Components of the plastid division complex and their dynamics during plastid division. (A) Components of the plastid division complex in *A. thaliana*. (B) Diagram showing the pathway of chloroplast division complex assembly. Only the known division-site-localized components and proteins that determine the division site are shown. The order of recruitment is indicated by the arrows (recruitment by direct

FtsZ proteins are most closely related to their cyanobacterial counterparts, which indicates their descent from the endosymbiotic progenitor of plastids (Kiefel et al., 2004; Miyagishima et al., 2004; Stokes and Osteryoung, 2003) (Fig. 4.4). Plant and algal FtsZ proteins were shown to be involved in plastid division by the effect of depletion of FtsZ, which resulted in the emergence of drastically reduced numbers of enlarged plastids (Osteryoung et al., 1998; Strepp et al., 1998). In addition, immunocytochemical studies showed that FtsZ forms a ring structure on the stromal side of the plastid division site, corresponding to the localization of FtsZ in bacteria (Kuroiwa et al., 2002; McAndrew et al., 2001; Mori et al., 2001; Vitha et al., 2001). In plastids, the FtsZ ring locates on the stromal side of the inner PD ring (Kuroiwa et al., 2002; Miyagishima et al., 2001c) (Fig. 4.3).

Most bacteria, including cyanobacteria, have a single FtsZ gene (Vaughan et al., 2004). In contrast, two types of phylogenetically and functionally distinct FtsZ proteins have evolved in algae and plants by gene duplication and differentiation (Kiefel et al., 2004; Miyagishima et al., 2004; Osteryoung et al., 1998; Stokes and Osteryoung, 2003) (Fig. 4.4). These two proteins (FtsZ1 and FtsZ2) colocalize, even when the expression level and assembly pattern of each were altered experimentally in *A. thaliana* (McAndrew et al., 2001). Both FtsZ1 and FtsZ2 have GTPase activity and coassemble into bundled filaments *in vitro* (El-Kafafi el et al., 2005; Olson et al., 2010; Smith et al., 2010). However, unlike alpha- and beta-tubulin, which coassemble in a strict 1:1 stoichiometry, FtsZ1 and FtsZ2 can coassemble in other ratios, and each protein alone assembles into a filament (Olson et al., 2010; Smith et al., 2010). One remarkable difference between FtsZ1 and FtsZ2 is the conservation in FtsZ2, but not in FtsZ1, of a short C-terminal motif (termed the C-terminal core domain) that exists in most bacterial FtsZs, which is known to interact with the FtsZ assembly regulators FtsA and ZipA in *E. coli* (Osteryoung and McAndrew, 2001). Although neither FtsA nor ZipA is found in cyanobacteria or photosynthetic eukaryotes, FtsZ2 interacts with the plastid division protein ARC6, through the C-terminal core domain (Maple et al., 2005) (Fig. 4.3). In contrast, FtsZ1, but not FtsZ2, interacts with the FtsZ ring positioning protein ARC3 (Maple et al., 2007) (Fig. 4.3).

interaction) or broken arrows (indicating it is not known whether two components directly interact or not). The bar indicates that a direct interaction between the two proteins has been shown experimentally. The positional relationship between the PD ring and the other components are deduced from that in the red alga *C. merolae*. (C) Diagram showing sequential transition of the plastid division complex in the red alga *C. merolae*. (D) Immunofluorescence images showing the localization of the plastid division proteins. The fluorescence signal of the respective proteins is green, and the autofluorescence of chlorophyll is red in the upper panel. In the lower panel, MinE (green), MinD (red), and FtsZ (blue) were immunostained simultaneously by using Zenon labeling (Invitrogen). Scale bar: 5 μm (D).

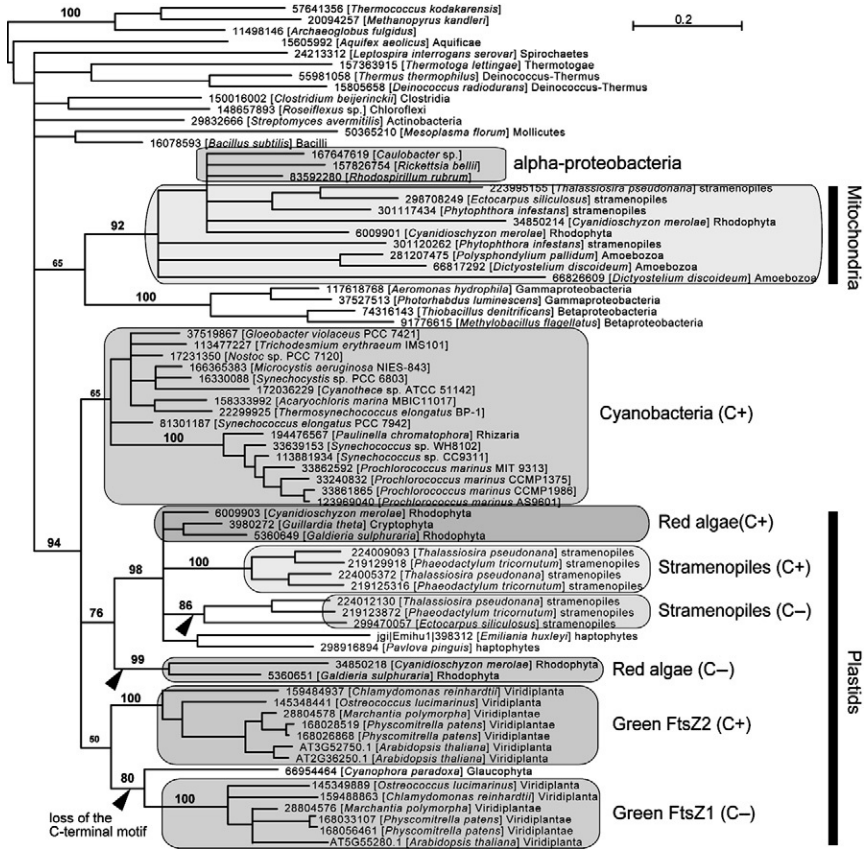

Figure 4.4 Phylogenetic relationships in the FtsZ proteins showing the origins of the proteins that are involved in plastid and mitochondrial division. The tree shown was constructed by the Bayesian method (MrBayes 3.1.2; Ronquist and Huelsenbeck, 2003). Bootstrap values >50% by a maximum likelihood analysis (RaxML 7.0.4; Stamatakis, 2006) are shown above the selected branches that are supported by the posterior probabilities >0.95 obtained by the Bayesian analysis. GI numbers or locus IDs of the proteins are shown along with the names of the species. C+ and C− indicate the proteins with and without the C-terminal core domain, respectively. Branch lengths are proportional to the number of amino acid substitutions, which are indicated by the scale bar above the tree.

3.2.2. ARC6 and PARC6

ARC6 was identified by forward genetic studies using *A. thaliana* chloroplast division mutants. The *arc* (accumulation and replication of chloroplasts) mutants, which were isolated in 1990s, exhibit an altered number and size of the chloroplasts per leaf mesophyll cell (Marrison et al., 1999; Pyke, 1999; Pyke and Leech, 1992, 1994; Pyke et al., 1994). Of these mutants, *arc6* has

only one or two giant plastids per cell, which is similar to *ftsZ* mutants (Pyke et al., 1994). The *arc6* mutation was mapped to an *A. thaliana* nuclear gene that is orthologous to the cyanobacterial cell division gene *ftn2/zipN* (Vitha et al., 2003).

ARC6 spans the inner envelope at the plastid division site, and its homologs are only evident in photosynthetic eukaryotes and cyanobacteria (Vitha et al., 2003). The stromal portion of ARC6 binds with FtsZ2 through the C-terminal core domain of FtsZ2 (Maple et al., 2005) (Fig. 4.2). This is similar to Ftn2/ZipN, which spans the cell membrane at the division site and interacts with FtsZ in cyanobacteria (Mazouni et al., 2004). Unlike Ftn2/ZipN, the N-terminal portion of ARC6 recruits the land-plant-specific protein PDV2 to the division site through direct interaction in the intermembrane space (Glynn et al., 2008) (Fig. 4.2). ARC6 and Ftn2 each contains the "J-domain" on the stromal side, a domain known to interact with the molecular chaperone HSP70 (Koksharova and Wolk, 2002; Vitha et al., 2003), but interaction between ARC6 (or Ftn2) and HSP70 has not been reported. Short and disordered FtsZ filaments are observed in *arc6* mutants, whereas excessively long FtsZ filaments are formed in ARC6 overexpressers, suggesting that ARC6 promotes FtsZ filament assembly and/or stabilizes FtsZ filaments (Vitha et al., 2003).

The vascular plant genome encodes an additional ARC6-like inner-envelope-spanning protein, termed PARC6, which acts downstream of ARC6 at the plastid division site. In contrast to ARC6, which binds to FtsZ2 and promotes FtsZ polymerization, PARC6 interacts with ARC3 and inhibits FtsZ assembly. In addition, PARC6 does not bind to PDV2 and is not required for PDV2 recruitment, unlike ARC6, but PARC6 is essential for the recruitment of PDV1 at the division site (Glynn et al., 2009) (Fig. 4.2).

3.3. Components of the division complex developed in the eukaryotic host cell

3.3.1. DRP5B

The characterization of a dynamin-related protein that is unique to photosynthetic eukaryotes in *C. merolae* (Miyagishima et al., 2003) (Fig. 4.5) and the cloning of the *arc5* locus in *A. thaliana* (Gao et al., 2003) resulted in the identification of the dynamin-related protein DRP5B, which is involved in plastid division. This was the first identification of a plastid division protein that had been developed by the eukaryotic host cell.

The dynamin family of GTPases self-assemble into spirals on the surface of membranes, where they tubulate the membrane (Heymann and Hinshaw, 2009). The most well-characterized member of this family is dynamin, which assembles into a ring or spiral at the neck of clathrin-coated pits (Hinshaw and Schmid, 1995; Takei et al., 1995), where it pinches

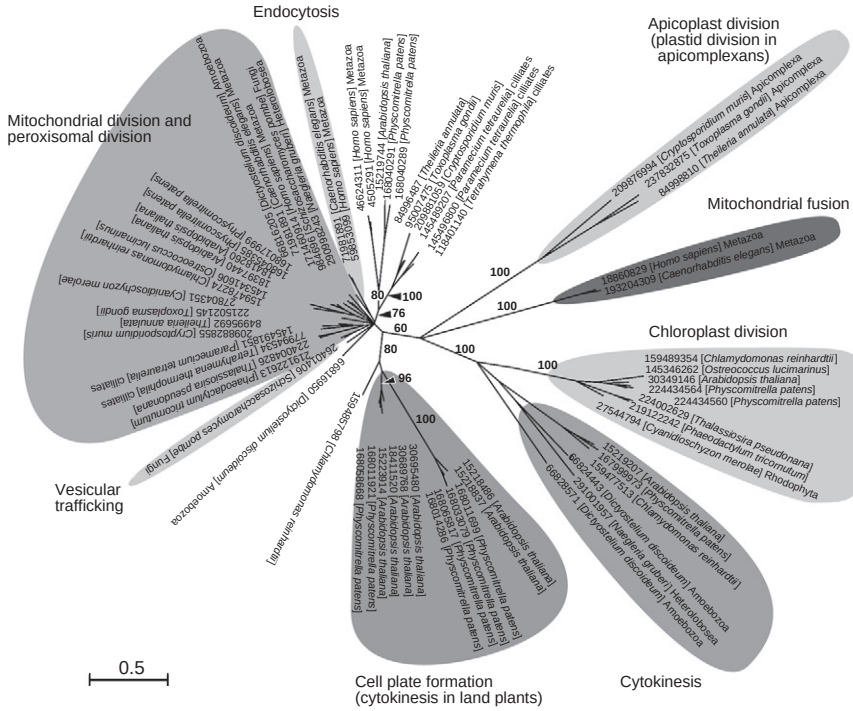

Figure 4.5 Phylogenetic relationships in the dynamin family of proteins. The tree shown was constructed by the Bayesian method (MrBayes 3.1.2) (Ronquist and Huelsenbeck, 2003). Bootstrap values >75% by a maximum likelihood analysis (RaxML 7.0.4) (Stamatakis, 2006) are shown above the selected branches that are supported by the posterior probabilities >0.95 obtained by the Bayesian analysis. GI numbers or locus IDs of the proteins are shown along with the names of the species. Branch lengths are proportional to the number of amino acid substitutions, which are indicated by the scale bar below the tree.

vesicles off from the plasma membrane (Bashkirov et al., 2008; Pucadyil and Schmid, 2008). The dynamin family is unique to eukaryotes, but proteins that are distantly related to dynamin do exist in bacteria (Low et al., 2009). Thus, the common ancestor of the dynamin family may be of bacterial origin. There are divergencies in the dynamin family, and the function of each member has been assigned to a distinct eukaryotic membrane remodeling, such as transport vesicle budding, organelle division, cytokinesis, and pathogen resistance (Heymann and Hinshaw, 2009) (Fig. 4.5). In some cases, two or more functions have been assigned to the same protein. This is the case for the plastid division protein DRP5B, which was recently shown to also be involved in peroxisomal division in *A. thaliana* (Zhang and Hu, 2010).

The *arc5* (*drp5B*) mutants exhibit defects in chloroplast constriction and have enlarged, dumbbell-shaped chloroplasts in the leaf mesophyll cells. DRP5B is recruited on the cytosolic side of the plastid division complex prior to the onset of division-site constriction (Gao et al., 2003; Miyagishima et al., 2003) (Fig. 4.3). In *A. thaliana*, DRP5B recruitment depends on the PDV1 and PDV2 proteins (Miyagishima et al., 2006) (Fig. 4.3). Phylogenetically, the proteins most closely related to DRP5B are involved in cytokinesis in *A. thaliana* and the slime mold *Dictyostelium discoideum* (Miyagishima et al., 2008) (Fig. 4.5). These results suggest that the dynamin in plastid division evolved from the cytokinetic activity of the eukaryotic host cell.

3.3.2. PDV1 and PDV2

PDV1 and PDV2 were identified by forward genetic analyses of *A. thaliana* mutants which exhibit *drp5B*-like phenotype (Miyagishima et al., 2006). PDV1 and PDV2 span the outer envelope at the division site. PDV2 is only evident in land plants (Embryophyta), and its paralog, PDV1, is unique to vascular plants. Both proteins expose their N-terminal region, containing a coiled-coil domain, to the cytosolic side (Miyagishima et al., 2006). The C-terminal region of PDV2 interacts with ARC6 in the intermembrane space (Glynn et al., 2008), whereas PDV1 localization is dependent on PARC6 (Glynn et al., 2009) (Fig. 4.2). Whether PDV1 binds PARC6 is uncertain at present. PDV1 and PDV2 appear to have overlapping functions in the recruitment of the cytosolic protein DRP5B because DRP5B is not recruited to the division site in the *pdv1pdv2* double mutant (Miyagishima et al., 2006). However, it is not known whether the PDV proteins and DRP5B directly interact. The PDV proteins apparently connect the stromal division machinery descended from cyanobacteria and the cytosolic machinery derived from the host cell (Fig. 4.2). However, these proteins are specific to land plants, suggesting that there are as-yet-unknown linker proteins in algal plastids, and most likely in land plants as well.

3.3.3. PDR1 and polyglucan filaments in the outer PD ring

A very recent study which was performed by dissecting the plastid division complex in the red alga *C. merolae* (Yoshida et al., 2006) showed that the outer PD ring is a bundle of polyglucan filaments (Yoshida et al., 2010). These filaments are associated with the PDR1 protein, which is most closely related to the eukaryotic glycogenin proteins. Because the glycogenin proteins are known to polymerize glucose to initiate glycogen synthesis, PDR1 is likely to be involved in synthesis of the polyglucan filaments of the PD ring. The filaments of the outer PD ring have been observed in several different algae and plants, and potential orthologs of PDR1 are encoded in land-plant genomes (Yoshida et al., 2010). However, the genomes of other plastid-carrying eukaryotes, such as green algae and stramenopiles (which

possess chloroplasts of red algal secondary endosymbiotic origin), apparently lack the gene encoding PDR1. Thus, how the filament is synthesized in such cases is uncertain at present.

3.4. Division-site placement

Chloroplasts, in general, and nongreen plastids in certain tissues divide at the midpoint, yielding two daughter plastids of equal size, which effect is achieved by the medial FtsZ ring placement. After the original identification of a nucleus-encoded FtsZ, searches of the *A. thaliana* nuclear genome database led to the identification of homologs of the bacterial division-site-determining proteins MinD (Colletti et al., 2000) and MinE (Itoh et al., 2001). In bacteria, MinC forms a complex with MinD and suppresses FtsZ ring formation at sites other than the midcell position. In *E. coli*, MinE sweeps away MinCD from the midcell position by pole-to-pole oscillation. On the other hand, in *B. subtilis*, which lacks MinE, MinCD does not oscillate, but is tethered to the cell poles by DivIVA. Thus, the mechanisms for restricting FtsZ ring assembly to the midcell vary among bacteria (Harry et al., 2006).

Cyanobacterial genomes encode all three Min proteins as well as DivIVA-like protein Cdv3, which has been shown to be involved in the cell division, suggesting additional complexity in the mechanisms of division-site placement in cyanobacteria (Mazouni et al., 2004; Miyagishima et al., 2005). Reverse genetic studies using *A. thaliana* confirmed that cyanobacteria-derived MinD (Colletti et al., 2000) and MinE (Itoh et al., 2001) regulate the positioning of the plastid FtsZ ring (Fig. 4.6). Both plant MinD (Nakanishi et al., 2009) and MinE colocalize at the chloroplast division site (Fig. 4.3) as does MinD in *B. subtilis* (Marston et al., 1998). In plastids, MinD and MinE localize also in punctate structures which are dispersed on the inner-envelope membrane (Nakanishi et al., 2009) (Fig. 4.3).

Unlike the case in cyanobacteria, MinC and Cdv3 are missing in vascular plants, although certain algal lineages and the moss *P. patens* still possess a MinC-like protein of cyanobacterial origin (Miyagishima and Kabeya, 2010; Yang et al., 2008). Recent studies have shown that ARC3 (Maple et al., 2007; Shimada et al., 2004), which is found in green algae and land plants, and MCD1 (Nakanishi et al., 2009), which is unique to land plants, regulate plastid FtsZ ring formation in collaboration with cyanobacteria-descended MinD and MinE in *A. thaliana* (Fig. 4.3). ARC3 is a stromal protein which is composed of an incomplete FtsZ-like domain and the MORN (membrane occupation and recognition nexus) motif (Shimada et al., 2004). Overexpression of ARC3 inhibits chloroplast division, most likely through an inhibition of the FtsZ assembly (Fig. 4.6), as in the case of bacterial MinC (Maple et al., 2007). In addition, ARC3 interacts with

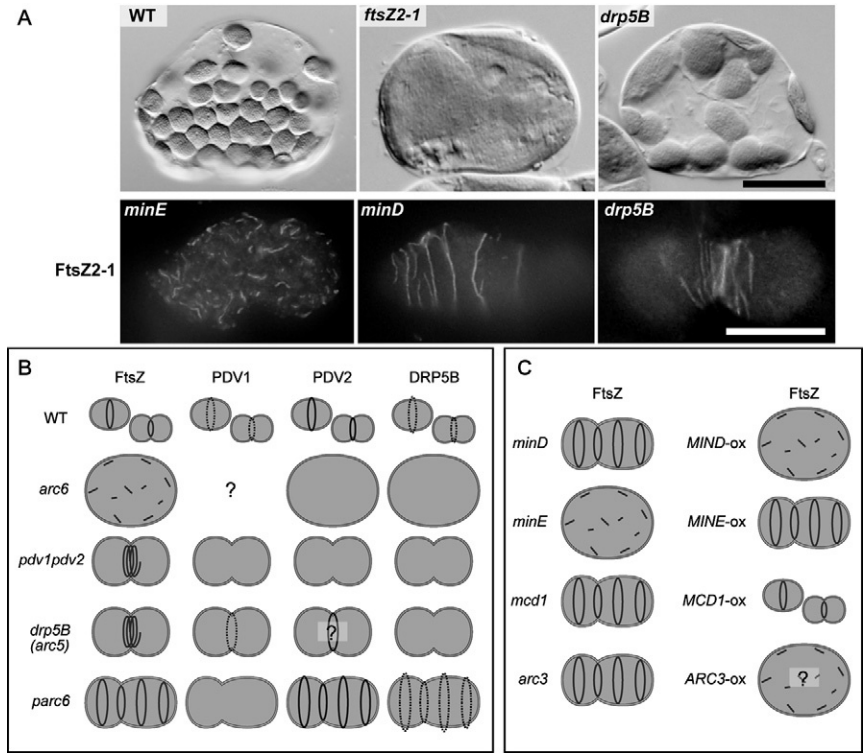

Figure 4.6 Phenotypes of plastid division mutants suggesting the role of the respective proteins and stepwise assembly of the division complex. (A, upper panels) Chloroplasts in single leaf mesophyll cells in *A. thaliana* wild type, *ftsZ2-1*, and *drp5B*. Single leaf mesophyll cells observed by Nomarski optics are shown. (A, lower panels) Localization of FtsZ2-1 in single chloroplasts in *minE*, *minD*, and *drp5B* mutants. (B) Schematic representation of the localization of the plastid division proteins in plastid division mutants. For example, FtsZ ring formation is impaired in the *arc6* mutant (FtsZ forms numerous short filaments), whereas FtsZ coils around the division site many times in the *pdv1pdv2* double mutant and in the *drp5B* mutant. In the *parc6* mutant, multiple FtsZ rings form at certain intervals. (C) Schematic representation of FtsZ localization in mutants or overexpressers of the min system components. Scale bar: 20 μm (A).

FtsZ1, MinD, MinE (Maple et al., 2007), and PARC6 (Glynn et al., 2009) and localizes at the division site and poles (Maple et al., 2007; Shimada et al., 2004) (Fig. 4.3). The *arc3* mutant exhibits multiple FtsZ rings within a single enlarged chloroplast (Glynn et al., 2007), similar to the *A. thaliana minD* mutant and the bacterial *minC* and *minD* mutants (Fig. 4.6). Thus, it appears that ARC3 took over the function of MinC in plastid division (Maple et al., 2007). MCD1 spans the inner envelope and bears a coiled-coil motif on the

stromal side. MCD1 recruits MinD to the chloroplast division site and punctate structures on the inner envelope (Fig. 4.3). The *mcd1* mutant also exhibits multiple FtsZ rings in a single chloroplast (Nakanishi et al., 2009) (Fig. 4.6). Although the composition varies, the Min system is widely conserved in algae and land plants, but the genome of the red alga *C. merolae* does not encode any of the proteins described above. Currently, it is unknown how the FtsZ ring is positioned at the midpoint in this organism.

3.5. Stepwise assembly and constriction of the plastid division complex

Studies in *A. thaliana* (Glynn et al., 2009; Yang et al., 2008) and *C. merolae* (Miyagishima et al., 2003; Yoshida et al., 2010) suggest that the plastid division complex is assembled from the inside to the outside of the plastid before the onset of division-site constriction, in the successive order of the FtsZ ring, inner PD ring, outer PD ring, and DRP5B ring (Fig. 4.3). The stromal division complex assembles independently of the cytosolic complex, whereas the assembly of the cytosolic complex depends on the stromal complex as described below. Thus, topological information is conveyed from the stromal complex that is descended from the cyanobacterial endosymbiont to the cytosolic complex of host eukaryotic origin (Fig. 4.3).

Studies on protein–protein interactions and the localization of division complex components in plastid division mutants in *A. thaliana* have revealed the following scheme (Figs. 4.3 and 4.6): (1) FtsZ ring formation is promoted by ARC6 (Vitha et al., 2003), (2) PDV2 localization is dependent on ARC6 through direct interaction (Glynn et al., 2008), (3) PARC6 localizes at the division site in a manner dependent on ARC6 and recruits PDV1 (Glynn et al., 2009), and (4) PDV1 and PDV2 directly or indirectly recruit DRP5B (Miyagishima et al., 2006) and then the division complex starts to constrict. Although the relationship between the above-mentioned proteins and the PD ring has not been characterized in *A. thaliana*, formation of the PD ring is preceded by that of FtsZ ring before the onset of constriction in other land plants (Kuroiwa et al., 2002; Momoyama et al., 2003). Immunocytochemical studies using a synchronous culture of *C. merolae* have shown that FtsZ, the inner PD, the middle/outer PD, and the DRP5B rings form in this order (Miyagishima et al., 2003) (Fig. 4.3). In addition, when *pdr1* was knocked down in *C. merolae*, the FtsZ ring formed but DRP5B was not recruited to the division site, indicating that FtsZ ring formation is not dependent on the subsequent formation of PD and DRP5B rings and that DRP5B localization is dependent on the outer PD ring formation (Yoshida et al., 2010). This is consistent with the presence of

the PD ring at the constricted region of giant chloroplasts in the *A. thaliana drp5B* (*arc5*) mutant (Robertson et al., 1996).

Currently, how the division complex mechanistically constricts the two envelopes is essentially a matter of speculation. Bacterial FtsZ self-assembles into rings inside of liposomes and induces constrictions of these liposomes *in vitro* (Osawa et al., 2008). The helical self-assembly of dynamin (Bashkirov et al., 2008; Pucadyil and Schmid, 2008) and Dnm1 (a dynamin-related protein involved in mitochondria) (Mears et al., 2011) tabulates the liposomes, and disassembly of the helix results in membrane fission *in vitro*. Thus, FtsZ and DRP5B probably participate in the generation of constrictive force required in plastid division. However, there is a certain time lag between FtsZ ring formation and the onset of plastid division-site constriction (Miyagishima et al., 2001c; Momoyama et al., 2003). Constriction starts after the other components of the division complex have been assembled in the division complex (Miyagishima et al., 2003). A similar time lag has been observed in bacterial cell division (Aarsman et al., 2005; Gamba et al., 2009). It is proposed that the sliding of the PD ring filaments mediated by DRP5B likely produces the constrictive force (Yoshida et al., 2006, 2010), but such sliding of the filaments has not been demonstrated. Dynamin, which is involved in vesicle budding during endocytosis, self-assembles into a helical tube with an inner diameter of ~20 nm, which constricts upon the binding of GTP *in vitro* (Sweitzer and Hinshaw, 1998). Dnm1, which is involved in mitochondrial division, forms a helical tube with an inner diameter of ~90 nm, which constricts down to ~20 nm (Mears et al., 2011). Although divergent depending on species, the diameter of chloroplast division site is 1–10 μm, which is much larger than the diameter of dynamin or the Dnm1 helix. DRP5B forms a punctate ring at the chloroplast division site, unlike other components of the division complex, which have been observed by fluorescence microscopy to form continuous rings (Gao et al., 2003; Miyagishima et al., 2003) (Fig. 4.3). At present, it is not known how DRP5B constricts the outer-envelope membrane. In *A. thaliana*, the enlarged chloroplasts in *drp5B* (*arc5*) (Robertson et al., 1996) and *pdv1pdv2* (Miyagishima et al., 2006) mutants can still divide by constriction (Fig. 4.6). Also, in the moss *Physcomitrella patens*, even when all of the DRP5B has been depleted, each cell still contains four to five chloroplasts (Sakaguchi et al., 2011), indicating that chloroplasts divide in proliferating mutant cells. The chloroplast division which takes place in the absence of DRP5B is probably not due to a functional redundancy of dynamin proteins because DRP5A, which is most closely related to DRP5B, is not involved in plastid division, as described above. Future functional studies *in vivo* and *in vitro* at a higher resolution will ultimately shed light on how the division complex constricts double-membraned plastids.

4. Evolution and Diversity of the Plastid Division Machinery

4.1. Evolution of the plastid division machinery

4.1.1. Loss, retention, and translocation of the cyanobacterial division genes

The plastid division machinery is a fusion of the cyanobacterial cytokinetic machinery and proteins developed by the eukaryotic host cell, as described above (Fig. 4.7). In order to understand the evolution of the division machinery, more detailed information on cyanobacterial division is required. The current understanding of the mechanism of bacterial cytokinesis is mainly based on analyses of *E. coli* (Gram-negative, a proteobacterium) and *B. subtilis* (Gram-positive, a firmicute). The cell division in both types of bacteria is based on FtsZ ring formation and they share several components in their division complex, but there are also notable differences in the composition of the division complex and the mechanism of FtsZ ring positioning (Harry et al., 2006). Although cyanobacteria have the outer membrane characteristic of Gram-negative bacteria, they also have a Gram-positive-like peptidoglycan layer and are phylogenetically distinct from proteobacteria and firmicutes (Hoiczyk and Hansel, 2000). By identifying homologs of *E. coli* and *B. subtilis* division proteins and identifying division proteins unique to cyanobacteria, the architecture of the cyanobacterial division complex has started to emerge (Marbouty et al., 2009b) (Fig. 4.8).

In cyanobacteria, FtsZ, Ftn2 (ZipN; a cyanobacterial ortholog of ARC6), Ftn6 (ZipS), and SepF localize at the division site, where Ftn2, Ftn6, and SepF regulate FtsZ polymerization (Marbouty et al., 2009a,b,c). In addition, cyanobacterial genomes encode FtsQ, FtsW, FtsI, FtsK, and FtsE proteins (Miyagishima et al., 2005), which are components of the cell division complex in other bacteria. Although the localization of these proteins has not been determined in cyanobacteria, a study did show that FtsQ, FtsW, and FtsI are required for cyanobacterial cell division (Marbouty et al., 2009c). The positioning of the FtsZ ring in cyanobacteria is regulated by MinC, MinD, MinE (Mazouni et al., 2004), and probably the DivIVA-like protein Cdv3 (Miyagishima et al., 2005). Of these, *ftsQ, ftsK, ftsE, ftn6*, and *cdv3* are not present in the algal and plant genomes thus far sequenced, suggesting that these genes were lost relatively soon after the initial endosymbiotic event (Fig. 4.7).

FtsZ and ARC6 are encoded in the nuclear genome in algae and plants, suggesting that these genes are relocated into the host nuclear genome relatively soon after the endosymbiotic event. However, retention of other cyanobacterial division genes and their location (i.e., the plastid genome or nuclear genome) are different, depending on the lineage

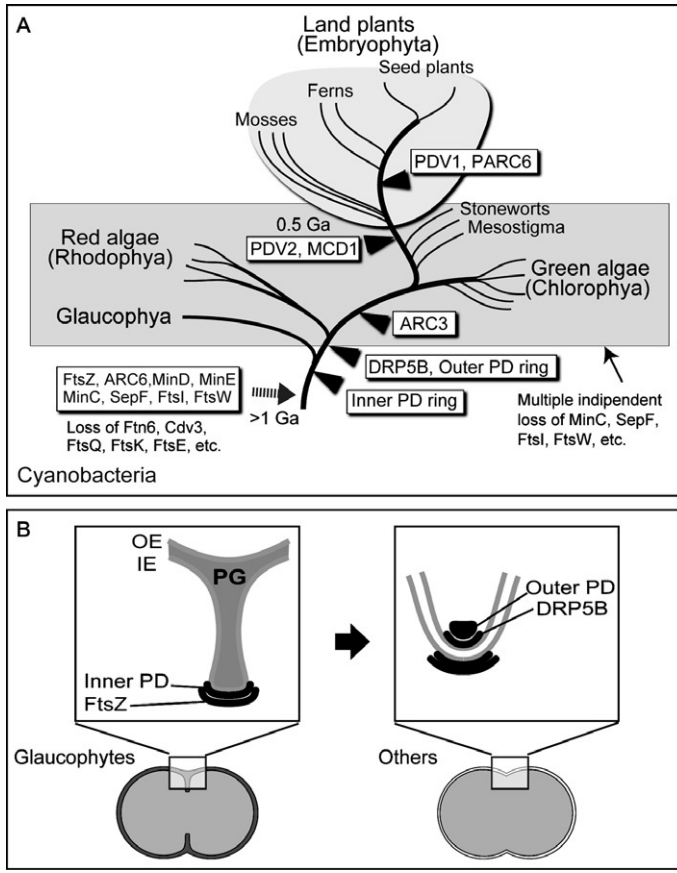

Figure 4.7 Evolution of the plastid division machinery. (A) Phylogenetic relationship of organisms that possess the primary plastid (Plantae) and the deduced timings of the loss and acquisition of the components are shown. The details are available in Yang et al. (2008) and Miyagishima and Kabeya (2010). (B) Schematic comparison between the plastid of glaucophytes and that in other lineages. Glaucophyte plastids have a peptidoglycan layer (PG) between the inner- and the outer-envelope membrane, as do cyanobacteria.

(Miyagishima and Kabeya, 2010). For example, the plastid genome of the glaucophyte *Cyanophora paradoxa* encodes FtsW and SepF, whereas the plastid genome of the green alga (prasinophyte) *Nephroselmis olivacea* encodes FtsI, FtsW, and MinD. In contrast, the plastid genomes of the majority of algae and land plants sequenced to date do not exhibit any homologs of the cyanobacterial division genes. *sepF*, *ftsI*, and *ftsW* are not present in the nuclear genomes of green algae and land plants, but *minD* is usually found in the nuclear genome. These observations suggest that several cyanobacterial

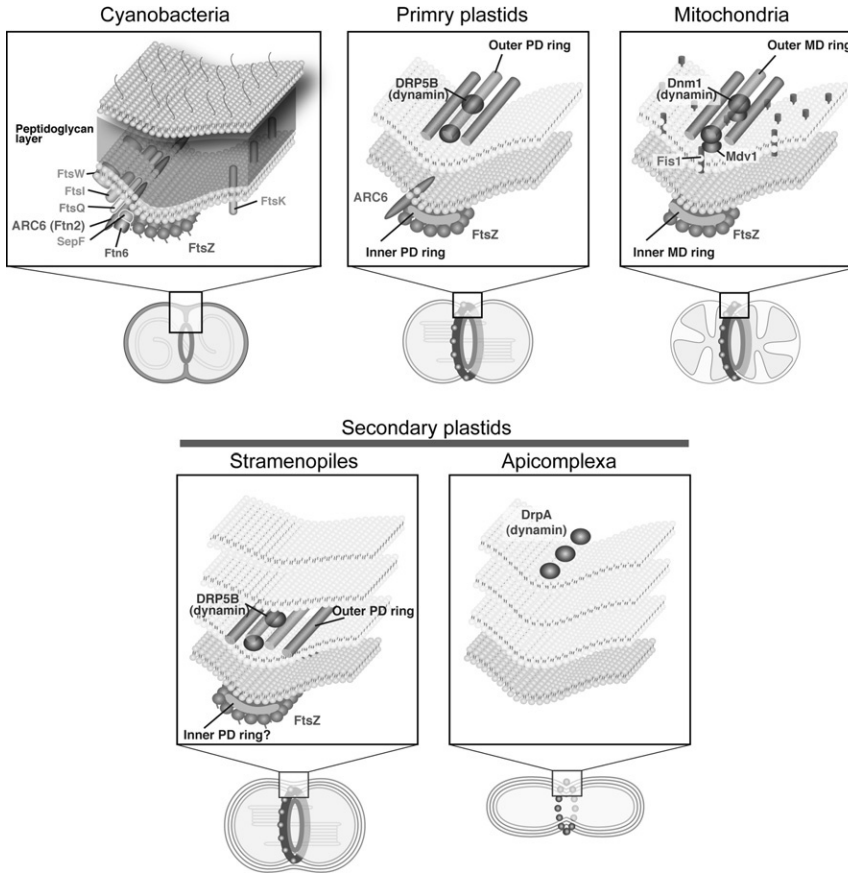

Figure 4.8 Comparison of the cyanobacterial, primary plastid, secondary plastid, and mitochondrial division machinery. Components unique to land plants and components of the min system are not shown. For the mitochondrial division machinery, components in the red alga *C. merolae* are shown.

division genes were lost or relocated to the host nuclear genome independently in distinct lineages (Miyagishima and Kabeya, 2010) (Fig. 4.7), as observed in other plastid genes (Martin et al., 1998), thus giving rise to the diversity in both the composition of the plastid division complex and the machinery responsible for the FtsZ ring positioning.

4.1.2. Development of new components and paralogous proteins

The eukaryotic host-derived components of the plastid division machinery thus far identified are the outer PD ring (glucan filaments and PDR1), the dynamin-related protein DRP5B, PDV1/PDV2, ARC3, and MCD1.

The inner PD ring also appears to have been added by the host cell because this structure has never been reportedly observed at a cyanobacterial division site. The PD ring has been detected in several lineages of algae and land plants, although glaucophyte algae possess the inner, but not the outer PD ring (see the next section for the detail). Thus it is suggested that the inner PD ring emerged first in a common ancestor of Plantae, while the outer PD ring developed later in a common ancestor of the red and green lineages (Fig. 4.7). The distribution patterns of the other proteins in algal and plant genomes suggest that DRP5B was integrated in a common ancestor of the red and green lineages, while ARC3 was developed in a common ancestor of green algae and land plants (Fig. 4.7). PDV and MCD1 are unique to land plants. Thus, these proteins are probably derived from a common ancestor of land plants (Miyagishima and Kabeya, 2010; Yang et al., 2008) (Fig. 4.7).

Besides the integration of purely novel proteins, both duplication and differentiation of the division-related genes have played significant roles in the evolution of the plastid division machinery. As mentioned above, one example is the green algal and land-plant FtsZ1, which emerged by duplication of the *FtsZ2* gene, and the subsequent loss of its C-terminal core domain. In addition, phylogenetic analyses suggest that the same event occurred in red algae and during the course of a secondary endosymbiotic event, independently from the one in green plants (i.e., on at least three different occasions; Fig. 4.4) (Kiefel et al., 2004; Miyagishima et al., 2004), suggesting that this event was critical to the development of the machinery for the control of plastid division. The N-terminal half of ARC3 originated from FtsZ and acquired a function related to FtsZ ring positioning, probably by acting as a negative regulator of FtsZ ring formation. PARC6 and PDV1 emerged in a common ancestor of vascular plants by gene duplication and the divergence of ARC6 and PDV2 (Fig. 4.7), and ultimately acquired functions different from those of ARC6 and PDV2, as described above.

4.2. Plastids with a peptidoglycan layer in glaucophytes

Unlike plastids in other organisms, the chloroplasts of glaucophyte algae (called cyanelles) have retained a peptidoglycan layer between the two envelope membranes that is descended from the cyanobacterial endosymbiont. Evolutionary studies suggest that glaucophyte algae were the earliest to branch off from the common ancestor of Plantae, prior to the divergence of the red algae and green lineages (green algae and land plants) (Reyes-Prieto and Bhattacharya, 2007). Thus, glaucophyte chloroplasts might have retained division machinery that is intermediate between cyanobacteria and plastids in the red and green lineages.

In plastids of both the red and green lineages, the inner and the outer envelopes constrict simultaneously during plastid division. Thus, the interval between the inner and the outer envelopes at the division site is almost

the same as that in other parts of the plastid. In contrast, the inner envelope in glaucophyte chloroplasts starts to constrict earlier than the outer-envelope membrane, and this is accompanied by an ingrowth of the peptidoglycan layer, reminiscent of the relationship between the cytoplasmic membrane and outer membrane in cyanobacterial cell division. Therefore, the interval between the two envelopes at the division site becomes much larger than that in other parts of the chloroplast in glaucophytes (Iino and Hashimoto, 2003; Sato et al., 2009) (Fig. 4.7).

Chloroplast division in the glaucophyte *C. paradoxa* involves FtsZ ring formation on the stromal side of the division site (Sato et al., 2009). FtsW and SepF are encoded in the chloroplast genome. Analyses of EST indicate that the nuclear genome of *C. paradoxa* encodes MinD and MinE of cyanobacterial origin (Reyes-Prieto et al., 2006). In addition, a structure similar to the inner PD ring has been detected by electron microscopy (Iino and Hashimoto, 2003; Sato et al., 2009). However, the outer PD ring is not evident (Iino and Hashimoto, 2003; Sato et al., 2009) and the plastid division genes of eukaryotic host origin, including *drp5B*, are not found in the EST database. Thus, it appears that the outer-envelope division in glaucophytes does not involve mechanisms that are developed in plastids in other lineages but still utilizes a mechanism similar to that in cyanobacteria (Fig. 4.7). However, studies on the division of the peptidoglycan layer and the outer membrane in bacteria are just beginning (de Boer, 2010). Information from the whole glaucophyte genome, and further studies of the bacterial cell wall and outer-membrane division, will ultimately clarify the relationship between the loss of the peptidoglycan layer and evolution of the plastid division machinery.

Peptidoglycans have never been detected in plastids other than in glaucophytes, but it should be noted that some algal and plant genomes still encode cyanobacteria-descended proteins that are involved in or related to peptidoglycan synthesis in bacteria. Disruption of the nucleus-encoded *mur* or *mra* genes impairs chloroplast division in the moss *P. patens* (Homi et al., 2009; Machida et al., 2006). The chloroplast genome of certain green algal lineages encodes FtsI, which cross-links the glycan strands, and FtsW, which transports lipid-linked peptidoglycan precursors during peptidoglycan synthesis at the bacterial division site (Mohammadi et al., 2011). However, the functions of these gene products in plastids are currently unknown.

4.3. Plastid differentiation and nongreen plastid division in vascular plants

The current understanding of plastid division is almost entirely based on chloroplasts, despite the fact that vascular plants contain several different types of plastids. Thus, a question remains as to whether nongreen plastid division shares the same mechanism with chloroplasts, but there has been

only limited information available (Miyagishima, 2011; Pyke, 2010). This is largely because nongreen plastids are smaller than chloroplasts and observation thus requires fluorescent staining or electron microscopy. In addition, some plastids exhibit irregular shapes with numerous tubular connections between them called stromules (Hanson and Sattarzadeh, 2008). Thus it is difficult to define the division site based on the plastid shape, even by electron microscopy. In some cases, multiple FtsZ rings form in a single nongreen plastid, and multiple fission events have been reportedly observed (Momoyama et al., 2003; Yun and Kawagoe, 2009).

Observational studies of nongreen plastids in chloroplast division mutants and analyses of the localization of the chloroplast division proteins in nongreen plastids have shown that nongreen plastid division in vascular plants utilizes division machinery similar to that in chloroplasts. That is, FtsZ, ARC6, and PDV proteins localize at the nongreen plastid division site, and these proteins are involved in division (McAndrew et al., 2008; Miyagishima et al., 2006; Okazaki et al., 2009). In addition, the inner and the outer PD rings have been detected in nongreen plastids (Kuroiwa et al., 1998). However, these investigations have also revealed certain differences between chloroplasts and the nongreen plastids. For example, there is no detectable defect in proplastid division in the *drp5B* (*arc5*) mutant (Robertson et al., 1996) and the DRP5B protein is not detected in the shoot apical meristem (Okazaki et al., 2009). Thus, land plants apparently have evolved a plastid division mechanism that does not require the DRP5B protein. There might be a paralog of DRP5B that is involved in proplastid division, but this is probably not the case because DRP5A, which is most closely related to DRP5B, is not involved in plastid division, as described above.

In addition, there might be a plastid division mechanism that does not utilize the known plastid division complex. Whereas the *arc6* mutation impairs FtsZ assembly (Vitha et al., 2003) and results in severe defects in both chloroplast and proplastid division (Robertson et al., 1995), the photosynthetic cells in *arc6* contain irregularly shaped nongreen plastids along with chloroplasts. These abnormal plastids somehow proliferate in the *arc6* mutant (Chen et al., 2009). A similar type of plastid proliferation also occurs in a tomato chloroplast division mutant, where budding and fragmentation of the plastids are observed (Forth and Pyke, 2006). A recent study showed that *A. thaliana* mutants, in which the FtsZ proteins are completely depleted, are viable, and the mesophyll cells still contained one or two enlarged chloroplasts. This result suggests that the plastids, at least in the meristematic tissues, somehow proliferate without FtsZ (Schmitz et al., 2009), although the FtsZ rings are always evident in the proplastid division which occurs in the wild type (McAndrew et al., 2001; Okazaki et al., 2009). Because these abnormal types of plastid proliferation have been reported to occur only in mutants, further studies are required to examine the possibility of as-yet-unknown mechanisms of plastid proliferation in wild-type plants.

4.4. Plastid division in organisms possessing secondary plastids

A diverse array of eukaryotic lineages possess plastids (most are chloroplasts) that were acquired through secondary endosymbiotic events in which a eukaryotic alga was integrated into another eukaryotic cell and most of the algal contents other than the chloroplasts had been degraded (Fig. 4.1). The secondary endosymbiosis of a red algal ancestor gave rise to plastids in stramenopiles (diatom, brown algae, etc.), haptophytes, cryptophytes, most of the photosynthetic dinoflagellates, and apicomplexan parasites (these are grouped as Chromalveolata). Euglenids and chlorarachniophytes possess chloroplasts of a green algal origin (Archibald, 2009; Gould et al., 2008). The question of exactly how many endosymbiotic events have given rise to this evident diversity remains elusive. However, several reports have indicated a preference for the hypothesis that the red algal endosymbiosis and subsequent reduction into chloroplasts occurred only once in the common ancestor of chromalveolates. This scenario also suggests that several chromalveolate lineages, such as ciliates, oomycetes, and the plastid-lacking dinoflagellate lineages, have subsequently lost the plastids (Archibald, 2009; Gould et al., 2008). Little is known about how secondary plastids in the diverse eukaryotic lineages divide, but a few studies of stramenopile chloroplast division and recent genome investigations of stramenopiles, haptophytes, and cryptophytes suggest that a part of the chloroplast division machinery in these lineages is descended from a red algal endosymbiont.

The chloroplasts in stramenopiles, haptophytes, and cryptophytes are surrounded by four membranes. The inner two membranes are descended from the inner and the outer envelopes of the primary chloroplast. The two additional membranes are thought to correspond to the plasma membrane of the engulfed alga and the phagosomal membrane of the host cell, respectively (Archibald, 2009; Gould et al., 2008). The outermost membrane is connected with the outer nuclear envelope either directly or indirectly through a rough ER. Studies of stramenopile chloroplast division by electron microscopy have shown that a filamentous outer PD ring encircles the chloroplast division site. The ring is located on the outer side of the second innermost membrane, which corresponds to the position of the outer PD ring in primary chloroplasts (Hashimoto, 1998, 2005; Weatherill et al., 2007) (Fig. 4.8). The nucleomorph (a remnant of the engulfed red algal nucleus) genome of cryptophytes (Fraunholz et al., 1998) encodes a FtsZ protein. Nuclear genomes of stramenopiles and a haptophyte encode FtsZ proteins of a red algal origin (Fig. 4.4). Genome investigations of stramenopiles and haptophytes identified the *minC*, *minD*, *minE*, and *drp5B* genes, in addition to *ftsZ* (Miyagishima and Kabeya, 2010). DRP5B is of a red algal origin and localizes at the

chloroplast division site in the stramenopile *Thalassiosira pseudonana* (Miyagishima, 2011). Thus, the division of the inner pair of membranes in secondary chloroplasts involves at least a portion of the primary chloroplast division machinery that is descended from the engulfed red alga (Fig. 4.8).

Currently, it is not known how the outer pair of membranes divides. Thus far, no clearly evident structures such as the PD ring have been observed at the division site of the outer two membranes by electron microscopy. However, observations in stramenopile species suggest that the division is carried out by a mechanism that is distinct from the division of the inner pair of membranes. In many stramenopile species, the outer pair of membranes divides in the same plane as the inner pair, but the constriction of the outer pair takes place behind that of the inner pair (Hashimoto, 1998, 2005). In addition, spherical vesicles have been observed in the space between the two pairs of membranes (called the periplastid compartment) at the division site (Hashimoto, 1998, 2005). In rare cases, such as in *Synchroma*, a number of chloroplasts with two inner membranes share a single outer pair of membranes, indicating that the division of the inner and the outer pair is not coupled (Horn et al., 2007). In *Aurearena cruciata*, the third and the outermost membrane division is not coupled, suggesting that these two membrane division events utilize different mechanisms (Kai et al., 2008).

Apicomplexans, such as malaria parasites (*Plasmodium*), also possess four-membrane-bound nonphotosynthetic plastids (called apicoplasts) of a red algal origin. In this group, the plastid division is performed by simultaneous constriction of the four membranes. In contrast to stramenopiles, haptophytes, and cryptophytes, apicomplexan genomes do not encode any of the known primary plastid division proteins. A recent study in the apicomplexan *Toxoplasma gondii* showed that the dynamin-like protein TgDRPA localizes on the cytosolic side of the apicoplast division site (i.e., on the outermost membrane), where it is required for apicoplast division (van Dooren et al., 2009) (Fig. 4.8). DRPA is well conserved and unique to the apicomplexans (i.e., DRPA is not a descendant of the DRP5B in the primary chloroplast division; Fig. 4.5) (van Dooren et al., 2009). Thus, apicomplexans have probably lost the primary chloroplast division machinery and developed a new mechanism for performing apicoplast division.

4.5. Similarity between the plastid and mitochondrial division machinery

Another DNA-containing organelle in eukaryotic cells, the mitochondrion, was established by endosymbiotic event of an alpha-proteobacterium earlier than the acquisition of plastids. Like plastid division, mitochondrial division is performed by simultaneous constriction of the inner and the outer

membrane at the division site. Although there is a variety in the molecular mechanism of mitochondrial division in eukaryotes, a dynamin-related protein is universally involved in mitochondrial division (Kiefel et al., 2006). In the yeast *Saccharomyces cerevisiae*, the dynamin-related protein Dnm1p is recruited to the division site by Mdv1p, which is anchored to the outer membrane by the outer-membrane-spanning protein Fis1p (Kageyama et al., 2011). Fis1p is also well conserved in eukaryotes. Mdv1p has been found in fungi and the red alga *C. merolae* (Nishida et al., 2007), and a possible ortholog is encoded in the amoeba *Naegleria gruberi* (GI number: 290987632). In contrast, there are no obvious paralogs of Fis1p or Mdv1p which are involved in plastid division. Thus mechanism for dynamin recruitment is probably different between plastids and mitochondria. However, other lines of evidence presented below suggest that there is a considerable similarity in the evolution of the plastid and mitochondrial division machinery (Fig. 4.8).

The nuclear genome of certain eukaryotic lineages (other than fungi, animals, green algae, land plants, etc.) encodes FtsZ proteins of alphaproteobacterial origin (Beech et al., 2000; Kiefel et al., 2004; Takahara et al., 2000). These proteins localize on the matrix side of the mitochondrial division site and are involved in the division process (Beech et al., 2000; Gilson et al., 2003; Nishida et al., 2003). As in the case of plastids, the *C. merolae* and slime mold *D. discoideum* genomes encode two types of mitochondrial FtsZ proteins, one of which lacks the C-terminal sequence (Gilson et al., 2003; Kiefel et al., 2004; Miyagishima et al., 2004). In addition, a structure similar to the PD ring, termed the MD ring, has been observed by electron microscopy at the mitochondrial division site in red algae (Kuroiwa et al., 1993), an amoeba (Kuroiwa et al., 2006), and a stramenopile (Hashimoto, 2004). The behavior of the MD ring is similar to that of the PD ring in *C. merolae* (Miyagishima et al., 2001b). In *C. merolae*, the FtsZ, MD, and dynamin rings form in this order during mitochondrial division (Nishida et al., 2003). This is similar to plastid division, in which the FtsZ, PD, and dynamin rings form in this order (Miyagishima et al., 2003) (Fig. 4.8). Thus, when it was established in primitive eukaryotes, mitochondrial division involved FtsZ, MD, and dynamin rings and later the FtsZ and MD rings were lost in certain eukaryotic lineages.

5. Regulation of Plastid Division

5.1. Regulation through the division complex

The continuity of plastids in eukaryotic cells is believed to have been originally established by the synchronization of endosymbiotic cell division with the host cell cycle, as seen in existent algae (Rodriguez-Ezpeleta and

Philippe, 2006) (Figs. 4.1 and 4.2). In contrast, land-plant cells, each of which contains numerous plastids, apparently have lost the tight linkage between the cell cycle and the timing of plastid division (Fig. 4.1). Even though plastids divide nonsynchronously in the same cell, the rate of plastid division in the meristematic cell keeps pace with cell division so that newly formed cells inherit almost exactly the same number of plastids. During cell differentiation and development, the plastid division rate changes, thereby changing the size and number of plastids. Thus, there must be mechanisms that coordinate the proliferation of plastids with cell proliferation in meristematic tissues, and with cell differentiation in other tissues in land plants (Fig. 4.1). Currently, it is largely unknown how plastid division is regulated by eukaryotic host cells. However, on the basis of the information on the plastid division machinery, recent studies have started to provide information on how plastid division in algae and land plants are regulated by the host cell through the division complex.

The observation of the synchronization of the algal cell cycle by the light–dark cycle led to the finding that chloroplast division gene expression is regulated by the host cell division cycle. For example, in the unicellular red alga *C. merolae*, the nucleus-encoded *ftsZ*, *drp5B*, *pdr1* genes are expressed in the S phase, and the respective proteins are degraded in the late M phase (Fujiwara et al., 2009; Miyagishima et al., 2003; Takahara et al., 2000; Yoshida et al., 2010). In the green alga *Chlamydomonas reinhardtii*, the nucleus-encoded *ftsZ*, *minD*, and *minE* transcripts accumulate during cell division, when the chloroplast divides (Adams et al., 2008). In addition, in the diatom (a stramenopile) *Seminavis robusta*, a single cell of which contains two chloroplasts of a red algal secondary endosymbiotic origin, the nucleus-encoded *ftsZ* transcript accumulates during the S/G2 phase, when the chloroplasts divide (Gillard et al., 2008). Overall, these reports suggest that the cell cycle-based expression of the chloroplast division genes contributes to the regulation by which the chloroplast divides in a specific phase of the host cell division cycle.

On the other hand, the expression of the plastid division genes in *A. thaliana* is apparently constant during the cell cycle, based on the experimental results of cell cycle synchronization in a cultured cell line (Menges et al., 2003). This is consistent with the fact that plastids divide nonsynchronously, even in the same cell. At present, there is little information on how the number of proplastids is maintained by meristematic cells during proliferation in land plants. Regarding the development in land plants, a recent study revealed that the land-plant-specific plastid division proteins PDV1 and PDV2 regulate plastid division rate in accord with cell differentiation. *A. thaliana pdv1* and *pdv2* mutants contain larger and fewer plastids than the wild type, as do certain other plastid division mutants (Miyagishima et al., 2006). When PDV proteins are overexpressed in *A. thaliana*, the number of chloroplasts in leaf cells increases and the size is

reduced compared to the wild type. This effect contrasts with the other genes related to plastid division, in which overexpression either has no effect or impairs plastid division.

The PDV level is highest in the apical meristem and young emerging leaves but decreases during leaf development, during which time the chloroplast division rate also decreases. In contrast, the DRP5B level increases, but the FtsZ and ARC6 levels remain constant during leaf development (Okazaki et al., 2009). It was shown that cytokinin treatment or overexpression of cytokinin-responsive transcription factor CRF2 increases the PDV levels, but not those of the other division components, in parallel with an increase in the chloroplast division rate (Okazaki et al., 2009). Similarly, overexpression of the *PDV* gene accelerates chloroplast division in the moss *P. patens*. When bud formation is induced by cytokinin, where chloroplast division is accelerated, transcription of *PDV*, but not those of other plastid division genes, is upregulated (Okazaki et al., 2009). Since mosses branched earliest in land-plant evolution (Kenrick and Crane, 1997), the results suggest that the integration of PDV proteins into the division machinery enabled land-plant cells to change the chloroplast size and number in accord with the fate of cell differentiation. Mosses contain chloroplasts throughout the life cycle, as do algae. Therefore, PDV proteins were probably acquired to modulate photosynthetic chloroplast division prior to the evolutionary emergence of the differentiation system based on the proplastids. However, mosses have PDV2 and ARC6, but not PDV1 and PARC6, which are conserved in vascular plants (Glynn et al., 2009; Okazaki et al., 2009). Therefore, modulation of the chloroplast division rate by PDV proteins and the paralogous evolution of the PDV and ARC6 interactions by gene duplication and functional differentiation appear to have been critical for the evolution of the plastid differentiation system in vascular plants.

5.2. Other proteins related to plastid division

Other proteins in addition to the ones described above have also been implicated in plastid division in *A. thaliana*. When the *GC1* (also called *AtSulA*) (Maple et al., 2004; Raynaud et al., 2004), *CRL* (Asano et al., 2004), *MSL* (*MSL2* and *MSL3*) (Haswell and Meyerowitz, 2006), *AtCDT1* (Raynaud et al., 2005), or *CPN60* gene (Suzuki et al., 2009) are inactivated, plastid division is impaired and giant plastids are generated in *A. thaliana*, as in other *bona fide* plastid division genes. At present, it is not known whether these proteins are directly involved in plastid division machinery, or how these proteins are related to plastid division.

CRL and GC1 are descended from a cyanobacterial endosymbiont. Some of the bacterial orthologs of GC1 are annotated as SulA-like proteins. SulA functions as an inhibitor of FtsZ assembly in *E. coli* (Harry et al., 2006).

However, there is no evident similarity between GC1 and *E. coli* SulA at the level of primary structure and no experimental evidence that GC1 is a functional counterpart of SulA. MSL proteins are homologs of bacterial mechanosensitive ion channels and likely control plastid size and shape (Haswell and Meyerowitz, 2006). AtCDT1 (Cdc10-dependent transcript 1) is targeted to both the nucleus and plastids and likely coordinates the cell cycle as well as plastid division (Raynaud et al., 2005).

5.3. Plastid genome replication and segregation

Plastids have retained their own genome of cyanobacterial origin and plastid division involves segregation of duplicated DNA, as does bacterial cell division. Although plastid envelope fission has been characterized and the information is summarized in this review, little information is available about the replication and segregation mechanism of plastid DNA or their relationship with envelope division. The size of the plastid genome has been reduced to less than one-tenth of the original bacterial genome (Race et al., 1999). As in bacteria, chloroplast DNA is held together with proteins in a compact structure called a nucleoid (Kuroiwa, 1991).

The relationship between the replication and segregation of the genome and bacterial cell division has been characterized in *E. coli* and *B. subtilis*. Because these bacteria and many other bacteria have a single chromosome, there is a tight linkage between replication and segregation of the nucleoids and the initiation of cytokinesis. That is, the two duplicated nucleoids move apart and the cell division complex forms at the midcell position, which corresponds to a gap between the two nucleoids (Harry et al., 2006). In contrast, cyanobacteria (Binder and Chisholm, 1990) and plastids (Kuroiwa, 1991) contain multiple copies of identical genomes, and in land plants, the copy number of DNA in each plastid nucleoid and the number of nucleoids and the copy number of the genome in each plastid change during the course of development and differentiation (Kuroiwa, 1991). Nearly equal copies of the genome are inherited by daughter plastids, suggesting that there are mechanisms for segregating the nucleoids during plastid division. Nevertheless, the segregation of genome copies is apparently not strict in plastids and cyanobacteria. In addition, genome replication is not linked with plastid division in many cases, as described below.

In seed plants, many earlier studies showed that chloroplast division in expanding leaves occurs without significant replication of plastid DNA, resulting in a reduction of the copy number of genome per plastid (Possingham and Lawrence, 1983). In some algae, which undergo two or three round of successive S and M phase after a long G1 phase (i.e., the second and third division occurs without growth), the second and third chloroplast division occurs without plastid DNA replication (Kuroiwa et al.,

1989). In the red alga *C. merolae*, the chloroplast divides even when plastid genome replication and segregation are inhibited (Itoh et al., 1997).

In bacteria, which have a single chromosome, the mechanism called "nucleoid occlusion" suppresses Z ring assembly at sites occupied by the nucleoid, thereby allowing the FtsZ ring to form at the midcell position from which two duplicate nucleoids have separated (Harry et al., 2006). This mechanism, which has been well studied in *E. coli* and *B. subtilis*, couples cytokinesis to chromosome replication, as nucleoid partitioning and Z ring formation cannot occur until after the chromosome has replicated (Harry et al., 2006). However, in cyanobacteria, nucleoids are segregated just before the completion of cytokinesis (Miyagishima et al., 2005; Schneider et al., 2007) and the chromosome copy number varies between the two daughter cells (Binder and Chisholm, 1990; Schneider et al., 2007). Similarly, plastid division starts without any moving away of the nucleoids from the division site (e.g., Momoyama et al., 2003; Suzuki et al., 1994).

6. Concluding Remarks

Based on the identification of the proteins that are involved in plastid division, recent studies have yielded significant progress in the understanding of the mechanism of plastid division and regulation and evolution of the division machinery, but many questions still remain to be answered, and new questions are emerging.

The most noteworthy issues concerning the mechanism of plastid division are how the division complex constricts and splits plastids, and how the constrictive force is generated. Although dynamin proteins and FtsZ can constrict liposomes *in vitro*, it should be determined how these molecules constrict plastids *in vivo*, in concert with the glucan filament of the PD ring. Another question is how the stromal division complex descended from a cyanobacterial endosymbiont relays the topological information to the cytosolic complex developed by the host cell. Although the PDV proteins play at least a part of this role in land plants, PDV is absent in the algal chloroplast, suggesting that an as-yet-unknown mechanism has linked the two complexes since the establishment of plastids. As mentioned briefly in this review, the mechanisms of replication and segregation of the plastid genome and their relationship with plastid division have not been elucidated yet.

In terms of evolution, it is not known how the chloroplast division machinery was structured in early Plantae. The ancient chloroplast should have had a peptidoglycan layer as in the glaucophyte chloroplasts. The division genes of endosymbiont/chloroplast would have been encoded in the endosymbiont/chloroplast genome in the initial step of the

endosymbiotic event. Thus, the questions are, first, how did the genes transfer from the cyanobacterial endosymbiont to the host genome, and second, how did certain host-derived mechanisms enable the host cell to regulate plastid division. Further studies should provide important insights into an understanding of not only organelle division but also the mechanisms of membrane fission and endosymbiosis.

ACKNOWLEDGMENTS

Our work was supported by Grant-in-Aid for Scientific Research from the Ministry of Education, Culture, Sports, Science and Technology (no. 22687020 to S. M. and no. 22770061 to Y. K.).

REFERENCES

Aarsman, M.E., Piette, A., Fraipont, C., Vinkenvleugel, T.M., Nguyen-Disteche, M., den Blaauwen, T., 2005. Maturation of the *Escherichia coli* divisome occurs in two steps. Mol. Microbiol. 55, 1631–1645.

Adams, S., Maple, J., Moller, S.G., 2008. Functional conservation of the MIN plastid division homologues of *Chlamydomonas reinhardtii*. Planta 227, 1199–1211.

Archibald, J.M., 2009. The puzzle of plastid evolution. Curr. Biol. 19, R81–R88.

Asano, T., Yoshioka, Y., Kurei, S., Sakamoto, W., Machida, Y., 2004. A mutation of the *CRUMPLED LEAF* gene that encodes a protein localized in the outer envelope membrane of plastids affects the pattern of cell division, cell differentiation, and plastid division in Arabidopsis. Plant J. 38, 448–459.

Bashkirov, P.V., Akimov, S.A., Evseev, A.I., Schmid, S.L., Zimmerberg, J., Frolov, V.A., 2008. GTPase cycle of dynamin is coupled to membrane squeeze and release, leading to spontaneous fission. Cell 135, 1276–1286.

Beech, P.L., Nheu, T., Schultz, T., Herbert, S., Lithgow, T., Gilson, P.R., et al., 2000. Mitochondrial FtsZ in a chromophyte alga. Science 287, 1276–1279.

Bi, E.F., Lutkenhaus, J., 1991. FtsZ ring structure associated with division in Escherichia coli. Nature 354, 161–164.

Binder, B.J., Chisholm, S.W., 1990. Relationship between DNA cycle and growth rate in *Synechococcus* sp. strain PCC 6301. J. Bacteriol. 172, 2313–2319.

Chen, Y., Asano, T., Fujiwara, M.T., Yoshida, S., Machida, Y., Yoshioka, Y., 2009. Plant cells without detectable plastids are generated in the crumpled leaf mutant of *Arabidopsis thaliana*. Plant Cell Physiol. 50, 956–969.

Chida, Y., Ueda, K., 1991. Division of chloroplasts in a green alga, *Trebouxia potteri*. Ann. Bot. 67, 435–442.

Colletti, K.S., Tattersall, E.A., Pyke, K.A., Froelich, J.E., Stokes, K.D., Osteryoung, K.W., 2000. A homologue of the bacterial cell division site-determining factor MinD mediates placement of the chloroplast division apparatus. Curr. Biol. 10, 507–516.

de Boer, P.A., 2010. Advances in understanding *E. coli* cell fission. Curr. Opin. Microbiol. 13, 730–737.

Duckett, J., Ligrone, R., 1993. Plastid-dividing rings in fern. Ann. Bot. 72, 619–627.

El-Kafafi el, S., Mukherjee, S., El-Shami, M., Putaux, J.L., Block, M.A., Pignot-Paintrand, I., et al., 2005. The plastid division proteins, FtsZ1 and FtsZ2, differ in their biochemical properties and sub-plastidial localization. Biochem. J. 387, 669–676.

Forth, D., Pyke, K.A., 2006. The suffulta mutation in tomato reveals a novel method of plastid replication during fruit ripening. J. Exp. Bot. 57, 1971–1979.
Fraunholz, M.J., Moerschel, E., Maier, U.G., 1998. The chloroplast division protein FtsZ is encoded by a nucleomorph gene in cryptomonads. Mol. Gen. Genet. 260, 207–211.
Fujiwara, T., Misumi, O., Tashiro, K., Yoshida, Y., Nishida, K., Yagisawa, F., et al., 2009. Periodic gene expression patterns during the highly synchronized cell nucleus and organelle division cycles in the unicellular red alga *Cyanidioschyzon merolae*. DNA Res. 16, 59–72.
Gamba, P., Veening, J.W., Saunders, N.J., Hamoen, L.W., Daniel, R.A., 2009. Two-step assembly dynamics of the *Bacillus subtilis* divisome. J. Bacteriol. 191, 4186–4194.
Gao, H., Kadirjan-Kalbach, D., Froehlich, J.E., Osteryoung, K.W., 2003. ARC5, a cytosolic dynamin-like protein from plants, is part of the chloroplast division machinery. Proc. Natl. Acad. Sci. USA 100, 4328–4333.
Gillard, J., Devos, V., Huysman, M.J., De Veylder, L., D'Hondt, S., Martens, C., et al., 2008. Physiological and transcriptomic evidence for a close coupling between chloroplast ontogeny and cell cycle progression in the pennate diatom *Seminavis robusta*. Plant Physiol. 148, 1394–1411.
Gilson, P.R., Yu, X.C., Hereld, D., Barth, C., Savage, A., Kiefel, B.R., et al., 2003. Two Dictyostelium orthologs of the prokaryotic cell division protein FtsZ localize to mitochondria and are required for the maintenance of normal mitochondrial morphology. Eukaryot. Cell 2, 1315–1326.
Glynn, J.M., Miyagishima, S.Y., Yoder, D.W., Osteryoung, K.W., Vitha, S., 2007. Chloroplast division. Traffic 8, 451–461.
Glynn, J.M., Froehlich, J.E., Osteryoung, K.W., 2008. Arabidopsis ARC6 coordinates the division machineries of the inner and outer chloroplast membranes through interaction with PDV2 in the intermembrane space. Plant Cell 20, 2460–2470.
Glynn, J.M., Yang, Y., Vitha, S., Schmitz, A.J., Hemmes, M., Miyagishima, S.Y., et al., 2009. PARC6, a novel chloroplast division factor, influences FtsZ assembly and is required for recruitment of PDV1 during chloroplast division in Arabidopsis. Plant J. 59, 700–711.
Gould, S.B., Waller, R.F., McFadden, G.I., 2008. Plastid evolution. Annu. Rev. Plant Biol. 59, 491–517.
Hanson, M.R., Sattarzadeh, A., 2008. Dynamic morphology of plastids and stromules in angiosperm plants. Plant Cell Environ. 31, 646–657.
Harry, E., Monahan, L., Thompson, L., 2006. Bacterial cell division: the mechanism and its precision. Int. Rev. Cytol. 253, 27–94.
Hashimoto, H., 1986. Double-ring structure around the constricting neck of dividing plastids of *Avena sativa*. Protoplasma 135, 166–172.
Hashimoto, H., 1998. Electron-opaque annular structure girdling the constricting isthmus of the dividing chloroplasts of *Heterosigma akashiwo* (Raphidophyceae, Chromophyta). Protoplasma 197, 210–216.
Hashimoto, H., 2004. Mitochondrion-dividing ring in an alga *Nannochloropsis oculata* (Eustigmatophyceae, Heterokonta). Cytologia 69, 323–326.
Hashimoto, H., 2005. The ultrastructural features and division of secondary plastids. J. Plant Res. 118, 163–172.
Haswell, E.S., Meyerowitz, E.M., 2006. MscS-like proteins control plastid size and shape in *Arabidopsis thaliana*. Curr. Biol. 16, 1–11.
Heymann, J.A., Hinshaw, J.E., 2009. Dynamins at a glance. J. Cell Sci. 122, 3427–3431.
Hinshaw, J.E., Schmid, S.L., 1995. Dynamin self-assembles into rings suggesting a mechanism for coated vesicle budding. Nature 374, 190–192.

Hirota, Y., Ryter, A., Jacob, F., 1968. Thermosensitive mutants of *E. coli* affected in the processes of DNA synthesis and cellular division. Cold Spring Harb. Symp. Quant. Biol. 33, 677–693.

Hoiczyk, E., Hansel, A., 2000. Cyanobacterial cell walls: news from an unusual prokaryotic envelope. J. Bacteriol. 182, 1191–1199.

Homi, S., Takechi, K., Tanidokoro, K., Sato, H., Takio, S., Takano, H., 2009. The peptidoglycan biosynthesis genes *MurA* and *MraY* are related to chloroplast division in the moss *Physcomitrella patens*. Plant Cell Physiol. 50, 2047–2056.

Horn, S., Ehlers, K., Fritzsch, G., Gil-Rodriguez, M.C., Wilhelm, C., Schnetter, R., 2007. *Synchroma grande* spec. nov. (Synchromophyceae class. nov., Heterokontophyta): an amoeboid marine alga with unique plastid complexes. Protist 158, 277–293.

Iino, M., Hashimoto, H., 2003. Intermediate features of cyanelle division of *Cyanophora paradoxa* (Glaucocystophyta) between cyanobacterial and plastid division. J. Phycol. 39, 561–569.

Itoh, R., Takahashi, H., Toda, K., Kuroiwa, H., Kuroiwa, T., 1997. DNA gyrase involvement in chloroplast-nucleoid division in *Cyanidioschyzon merolae*. Eur. J. Cell Biol. 73, 252–258.

Itoh, R., Fujiwara, M., Nagata, N., Yoshida, S., 2001. A chloroplast protein homologous to the eubacterial topological specificity factor minE plays a role in chloroplast division. Plant Physiol. 127, 1644–1655.

Kageyama, Y., Zhang, Z., Sesaki, H., 2011. Mitochondrial division: molecular machinery and physiological functions. Curr. Opin. Cell Biol. 23, 427–434.

Kai, A., Yoshii, Y.T.N., Inouye, I., 2008. Aurearenophyceae classis nova, a new class of Heterokontophyta based on a new marine unicellular alga *Aurearena cruciata* gen. et sp. nov. inhabiting sandy beaches. Protist 159, 435–457.

Kenrick, P., Crane, P.R., 1997. The origin and early evolution of plants on land. Nature 389, 33–39.

Kiefel, B.R., Gilson, P.R., Beech, P.L., 2004. Diverse eukaryotes have retained mitochondrial homologues of the bacterial division protein FtsZ. Protist 155, 105–115.

Kiefel, B.R., Gilson, P.R., Beech, P.L., 2006. Cell biology of mitochondrial dynamics. Int. Rev. Cytol. 254, 151–213.

Koksharova, O.A., Wolk, C.P., 2002. A novel gene that bears a DnaJ motif influences cyanobacterial cell division. J. Bacteriol. 184, 5524–5528.

Kuroiwa, T., 1991. The replication, differentiation, and inheritance of plastids with emphasis on the concept of organelle nuclei. Int. Rev. Cytol. 128, 1–62.

Kuroiwa, T., Nagashima, H., Fukuda, I., 1989. Chloroplast division without DNA synthesis during the life cycle of the unicellular alga *Cyanidium caldarium* M-8 as revealed by quantitative fluorescence microscopy. Protoplasma 149, 120–129.

Kuroiwa, T., Suzuki, K., Kuroiwa, H., 1993. Mitochondrial division by an electron-dense ring in *Cyanidioschyzon merolae*. Protoplasma 175, 173–177.

Kuroiwa, T., Kuroiwa, H., Sakai, A., Takahashi, H., Toda, K., Itoh, R., 1998. The division apparatus of plastids and mitochondria. Int. Rev. Cytol. 181, 1–41.

Kuroiwa, H., Mori, T., Takahara, M., Miyagishima, S.Y., Kuroiwa, T., 2001. Multiple FtsZ rings in a pleomorphic chloroplasts in embryonic cap cells of *Pelargonium zonale*. Cytologia 66, 227–233.

Kuroiwa, H., Mori, T., Takahara, M., Miyagishima, S.Y., Kuroiwa, T., 2002. Chloroplast division machinery as revealed by immunofluorescence and electron microscopy. Planta 215, 185–190.

Kuroiwa, T., Nishida, K., Yoshida, Y., Fujiwara, T., Mori, T., Kuroiwa, H., et al., 2006. Structure, function and evolution of the mitochondrial division apparatus. Biochim. Biophys. Acta 1763, 510–521.

Leech, R.M., Thomson, W.W., Platt-Aloika, K.A., 1981. Observations on the mechanism of chloroplast division in higher plants. New Phytol. 87, 1–9.
Lopez-Juez, E., Pyke, K.A., 2005. Plastids unleashed: their development and their integration in plant development. Int. J. Dev. Biol. 49, 557–577.
Low, H.H., Sachse, C., Amos, L.A., Lowe, J., 2009. Structure of a bacterial dynamin-like protein lipid tube provides a mechanism for assembly and membrane curving. Cell 139, 1342–1352.
Lowe, J., Amos, L.A., 1998. Crystal structure of the bacterial cell-division protein FtsZ. Nature 391, 203–206.
Machida, M., Takechi, K., Sato, H., Chung, S.J., Kuroiwa, H., Takio, S., et al., 2006. Genes for the peptidoglycan synthesis pathway are essential for chloroplast division in moss. Proc. Natl. Acad. Sci. USA 103, 6753–6758.
Maple, J., Moller, S.G., 2010. The complexity and evolution of the plastid-division machinery. Biochem. Soc. Trans. 38, 783–788.
Maple, J., Fujiwara, M.T., Kitahata, N., Lawson, T., Baker, N.R., Yoshida, S., et al., 2004. GIANT CHLOROPLAST 1 is essential for correct plastid division in Arabidopsis. Curr. Biol. 14, 776–781.
Maple, J., Aldridge, C., Moller, S.G., 2005. Plastid division is mediated by combinatorial assembly of plastid division proteins. Plant J. 43, 811–823.
Maple, J., Vojta, L., Soll, J., Moller, S.G., 2007. ARC3 is a stromal Z-ring accessory protein essential for plastid division. EMBO Rep. 8, 293–299.
Marbouty, M., Saguez, C., Cassier-Chauvat, C., Chauvat, F., 2009a. Characterization of the FtsZ-interacting septal proteins SepF and Ftn6 in the spherical-celled cyanobacterium *Synechocystis* strain PCC 6803. J. Bacteriol. 191, 6178–6185.
Marbouty, M., Saguez, C., Cassier-Chauvat, C., Chauvat, F., 2009b. ZipN, an FtsA-like orchestrator of divisome assembly in the model cyanobacterium *Synechocystis* PCC6803. Mol. Microbiol. 74, 409–420.
Marbouty, M., Mazouni, K., Saguez, C., Cassier-Chauvat, C., Chauvat, F., 2009c. Characterization of the *Synechocystis* strain PCC 6803 penicillin-binding proteins and cytokinetic proteins FtsQ and FtsW and their network of interactions with ZipN. J. Bacteriol. 191, 5123–5133.
Marrison, J.L., Rutherford, S.M., Robertson, E.J., Lister, C., Dean, C., Leech, R.M., 1999. The distinctive roles of five different ARC genes in the chloroplast division process in Arabidopsis. Plant J. 18, 651–662.
Marston, A.L., Thomaides, H.B., Edwards, D.H., Sharpe, M.E., Errington, J., 1998. Polar localization of the MinD protein of *Bacillus subtilis* and its role in selection of the mid-cell division site. Genes Dev. 12, 3419–3430.
Martin, W., Kowallik, K., 1999. Annotated English translation of Mereschkowsky's 1905 paper "Uber Natur und Ursprung der Chromatophoren im Pflanzenreiche" Eur. J. Phycol. 34, 287–295.
Martin, W., Stoebe, B., Goremykin, V., Hapsmann, S., Hasegawa, M., Kowallik, K.V., 1998. Gene transfer to the nucleus and the evolution of chloroplasts. Nature 393, 162–165.
Mazouni, K., Domain, F., Cassier-Chauvat, C., Chauvat, F., 2004. Molecular analysis of the key cytokinetic components of cyanobacteria: FtsZ, ZipN and MinCDE. Mol. Microbiol. 52, 1145–1158.
McAndrew, R.S., Froehlich, J.E., Vitha, S., Stokes, K.D., Osteryoung, K.W., 2001. Colocalization of plastid division proteins in the chloroplast stromal compartment establishes a new functional relationship between FtsZ1 and FtsZ2 in higher plants. Plant Physiol. 127, 1656–1666.
McAndrew, R.S., Olson, B.J., Kadirjan-Kalbach, D.K., Chi-Ham, C.L., Vitha, S., Froehlich, J.E., et al., 2008. In vivo quantitative relationship between plastid division

proteins FtsZ1 and FtsZ2 and identification of ARC6 and ARC3 in a native FtsZ complex. Biochem. J. 412, 367–378.
Mears, J.A., Lackner, L.L., Fang, S., Ingerman, E., Nunnari, J., Hinshaw, J.E., 2011. Conformational changes in Dnm1 support a contractile mechanism for mitochondrial fission. Nat. Struct. Mol. Biol. 18, 20–26.
Menges, M., Hennig, L., Gruissem, W., Murray, J.A., 2003. Genome-wide gene expression in an Arabidopsis cell suspension. Plant Mol. Biol. 53, 423–442.
Mita, T., Kanbe, T., Tanaka, K., Kuroiwa, T., 1986. A ring structure around the dividing plane of the Cyanidium caldarium chloroplast. Protoplasma 130, 211–213.
Miyagishima, S.Y., 2011. Mechanism of plastid division: from a bacterium to an organelle. Plant Physiol. 155, 1533–1544.
Miyagishima, S.Y., Kabeya, Y., 2010. Chloroplast division: squeezing the photosynthetic captive. Curr. Opin. Microbiol. 13, 738–746.
Miyagishima, S., Takahara, M., Kuroiwa, T., 2001a. Novel filaments 5 nm in diameter constitute the cytosolic ring of the plastid division apparatus. Plant Cell 13, 707–721.
Miyagishima, S., Kuroiwa, H., Kuroiwa, T., 2001b. The timing and manner of disassembly of the apparatuses for chloroplast and mitochondrial division in the red alga *Cyanidioschyzon merolae*. Planta 212, 517–528.
Miyagishima, S., Takahara, M., Mori, T., Kuroiwa, H., Higashiyama, T., Kuroiwa, T., 2001c. Plastid division is driven by a complex mechanism that involves differential transition of the bacterial and eukaryotic division rings. Plant Cell 13, 2257–2268.
Miyagishima, S.Y., Nishida, K., Mori, T., Matsuzaki, M., Higashiyama, T., Kuroiwa, H., et al., 2003. A plant-specific dynamin-related protein forms a ring at the chloroplast division site. Plant Cell 15, 655–665.
Miyagishima, S.Y., Nozaki, H., Nishida, K., Matsuzaki, M., Kuroiwa, T., 2004. Two types of FtsZ proteins in mitochondria and red-lineage chloroplasts: the duplication of FtsZ is implicated in endosymbiosis. J. Mol. Evol. 58, 291–303.
Miyagishima, S.Y., Wolk, C.P., Osteryoung, K.W., 2005. Identification of cyanobacterial cell division genes by comparative and mutational analyses. Mol. Microbiol. 56, 126–143.
Miyagishima, S.Y., Froehlich, J.E., Osteryoung, K.W., 2006. PDV1 and PDV2 mediate recruitment of the dynamin-related protein ARC5 to the plastid division site. Plant Cell 18, 2517–2530.
Miyagishima, S.Y., Kuwayama, H., Urushihara, H., Nakanishi, H., 2008. Evolutionary linkage between eukaryotic cytokinesis and chloroplast division by dynamin proteins. Proc. Natl. Acad. Sci. USA 105, 15202–15207.
Mohammadi, T., van Dam, V., Sijbrandi, R., Vernet, T., Zapun, A., Bouhss, A., et al., 2011. Identification of FtsW as a transporter of lipid-linked cell wall precursors across the membrane. EMBO J. 30, 1425–1432.
Momoyama, Y., Miyazawa, Y., Miyagishima, S.Y., Mori, T., Misumi, O., Kuroiwa, H., et al., 2003. The division of pleomorphic plastids with multiple FtsZ rings in tobacco BY-2 cells. Eur. J. Cell Biol. 82, 323–332.
Mori, T., Kuroiwa, H., Takahara, M., Miyagishima, S.Y., Kuroiwa, T., 2001. Visualization of an FtsZ ring in chloroplasts of *Lilium longiflorum* leaves. Plant Cell Physiol. 42, 555–559.
Nakanishi, H., Suzuki, K., Kabeya, Y., Miyagishima, S.Y., 2009. Plant-specific protein MCD1 determines the site of chloroplast division in concert with bacteria-derived MinD. Curr. Biol. 19, 151–156.
Nishida, K., Takahara, M., Miyagishima, S.Y., Kuroiwa, H., Matsuzaki, M., Kuroiwa, T., 2003. Dynamic recruitment of dynamin for final mitochondrial severance in a primitive red alga. Proc. Natl. Acad. Sci. USA 100, 2146–2151.

Nishida, K., Yagisawa, F., Kuroiwa, H., Yoshida, Y., Kuroiwa, T., 2007. WD40 protein Mda1 is purified with Dnm1 and forms a dividing ring for mitochondria before Dnm1 in *Cyanidioschyzon merolae*. Proc. Natl. Acad. Sci. USA 104, 4736–4741.

Ogawa, S., Ueda, K., Noguchi, T., 1995. Division apparatus of chloroplast in *Nannochloris bacillaris* (Chlorophyta). J. Phycol. 31, 132–137.

Okazaki, K., Kabeya, Y., Suzuki, K., Mori, T., Ichikawa, T., Matsui, M., et al., 2009. The PLASTID DIVISION1 and 2 components of the chloroplast division machinery determine the rate of chloroplast division in land plant cell differentiation. Plant Cell 21, 1769–1780.

Olson, B.J., Wang, Q., Osteryoung, K.W., 2010. GTP-dependent heteropolymer formation and bundling of chloroplast FtsZ1 and FtsZ2. J. Biol. Chem. 285, 20634–20643.

Osawa, M., Anderson, D.E., Erickson, H.P., 2008. Reconstitution of contractile FtsZ rings in liposomes. Science 320, 792–794.

Osteryoung, K.W., McAndrew, R.S., 2001. The plastid division machine. Annu. Rev. Plant Physiol. Plant Mol. Biol. 52, 315–333.

Osteryoung, K.W., Vierling, E., 1995. Conserved cell and organelle division. Nature 376, 473–474.

Osteryoung, K.W., Stokes, K.D., Rutherford, S.M., Percival, A.L., Lee, W.Y., 1998. Chloroplast division in higher plants requires members of two functionally divergent gene families with homology to bacterial *ftsZ*. Plant Cell 10, 1991–2004.

Possingham, J.V., Lawrence, M.E., 1983. Controls to plastid division. Int. Rev. Cytol. 84, 1–56.

Pucadyil, T.J., Schmid, S.L., 2008. Real-time visualization of dynamin-catalyzed membrane fission and vesicle release. Cell 135, 1263–1275.

Pyke, K.A., 1999. Plastid division and development. Plant Cell 11, 549–556.

Pyke, K.A., 2010. Plastid division and development. AoB Plants 2010, plq16. doi:10.1093/aobpla/plq1016.

Pyke, K.A., Leech, R.M., 1992. Chloroplast division and expansion is radically altered by nuclear mutations in *Arabidopsis thaliana*. Plant Physiol. 99, 1005–1008.

Pyke, K.A., Leech, R.M., 1994. A genetic analysis of chloroplast division and expansion in *Arabidopsis thaliana*. Plant Physiol. 104, 201–207.

Pyke, K.A., Rutherford, S.M., Robertson, E.J., Leech, R.M., 1994. *arc6*, a fertile Arabidopsis mutant with only two mesophyll cell chloroplasts. Plant Physiol. 106, 1169–1177.

Race, H.L., Herrmann, R.G., Martin, W., 1999. Why have organelles retained genomes? Trends Genet. 15, 364–370.

Raynaud, C., Cassier-Chauvat, C., Perennes, C., Bergounioux, C., 2004. An Arabidopsis homolog of the bacterial cell division inhibitor SulA is involved in plastid division. Plant Cell 16, 1801–1811.

Raynaud, C., Perennes, C., Reuzeau, C., Catrice, O., Brown, S., Bergounioux, C., 2005. Cell and plastid division are coordinated through the prereplication factor AtCDT1. Proc. Natl. Acad. Sci. USA 102, 8216–8221.

Reyes-Prieto, A., Bhattacharya, D., 2007. Phylogeny of nuclear-encoded plastid-targeted proteins supports an early divergence of glaucophytes within Plantae. Mol. Biol. Evol. 24, 2358–2361.

Reyes-Prieto, A., Hackett, J.D., Soares, M.B., Bonaldo, M.F., Bhattacharya, D., 2006. Cyanobacterial contribution to algal nuclear genomes is primarily limited to plastid functions. Curr. Biol. 16, 2320–2325.

Robertson, E.J., Pyke, K.A., Leech, R.M., 1995. *arc6*, an extreme chloroplast division mutant of Arabidopsis also alters proplastid proliferation and morphology in shoot and root apices. J. Cell Sci. 108 (Pt 9), 2937–2944.

Robertson, E.J., Rutherford, S.M., Leech, R.M., 1996. Characterization of chloroplast division using the Arabidopsis mutant *arc5*. Plant Physiol. 112, 149–159.

Rodriguez-Ezpeleta, N., Philippe, H., 2006. Plastid origin: replaying the tape. Curr. Biol. 16, R53–R56.

Ronquist, F., Huelsenbeck, J.P., 2003. MrBayes 3: Bayesian phylogenetic inference under mixed models. Bioinformatics 19, 1572–1574.

Sakaguchi, E., Takechi, K., Sato, H., Yamada, T., Takio, S., Takano, H., 2011. Three *dynamin-related protein 5B* genes are related to plastid division in *Physcomitrella patens*. Plant Sci. 180, 789–795.

Sato, M., Mogi, Y., Nishikawa, T., Miyamura, S., Nagumo, T., Kawano, S., 2009. The dynamic surface of dividing cyanelles and ultrastructure of the region directly below the surface in *Cyanophora paradoxa*. Planta 229, 781–791.

Schmitz, A.J., Glynn, J.M., Olson, B.J., Stokes, K.D., Osteryoung, K.W., 2009. Arabidopsis FtsZ2-1 and FtsZ2-2 are functionally redundant, but FtsZ-based plastid division is not essential for chloroplast partitioning or plant growth and development. Mol. Plant 2, 1211–1222.

Schneider, D., Fuhrmann, E., Scholz, I., Hess, W.R., Graumann, P.L., 2007. Fluorescence staining of live cyanobacterial cells suggest non-stringent chromosome segregation and absence of a connection between cytoplasmic and thylakoid membranes. BMC Cell Biol. 8, 39.

Shimada, H., Koizumi, M., Kuroki, K., Mochizuki, M., Fujimoto, H., Ohta, H., et al., 2004. ARC3, a chloroplast division factor, is a chimera of prokaryotic FtsZ and part of eukaryotic phosphatidylinositol-4-phosphate 5-kinase. Plant Cell Physiol. 45, 960–967.

Smith, A.G., Johnson, C.B., Vitha, S., Holzenburg, A., 2010. Plant FtsZ1 and FtsZ2 expressed in a eukaryotic host: GTPase activity and self-assembly. FEBS Lett. 584, 166–172.

Stamatakis, A., 2006. RAxML-VI-HPC: maximum likelihood-based phylogenetic analyses with thousands of taxa and mixed models. Bioinformatics 22, 2688–2690.

Stokes, K.D., Osteryoung, K.W., 2003. Early divergence of the *FtsZ1* and *FtsZ2* plastid division gene families in photosynthetic eukaryotes. Gene 320, 97–108.

Strepp, R., Scholz, S., Kruse, S., Speth, V., Reski, R., 1998. Plant nuclear gene knockout reveals a role in plastid division for the homolog of the bacterial cell division protein FtsZ, an ancestral tubulin. Proc. Natl. Acad. Sci. USA 95, 4368–4373.

Sumiya, N., Hirata, A., Kawano, S., 2008. Multiple FtsZ ring formation and reduplicated chloroplast DNA in *Nannochloris bacillaris* (Chlorophyta, Trebouxiophyceae) under phosphate-enriched culture. J. Phycol. 44, 1476–1489.

Suzuki, K., Ehara, T., Osafune, T., Kuroiwa, H., Kawano, S., Kuroiwa, T., 1994. Behavior of mitochondria, chloroplasts and their nuclei during the mitotic cycle in the ultramicroalga *Cyanidioschyzon merolae*. Eur. J. Cell Biol. 63, 280–288.

Suzuki, K., Nakanishi, H., Bower, J., Yoder, D.W., Osteryoung, K.W., Miyagishima, S.Y., 2009. Plastid chaperonin proteins Cpn60 alpha and Cpn60 beta are required for plastid division in *Arabidopsis thaliana*. BMC Plant Biol. 9, 38.

Sweitzer, S.M., Hinshaw, J.E., 1998. Dynamin undergoes a GTP-dependent conformational change causing vesiculation. Cell 93, 1021–1029.

Takahara, M., Takahashi, H., Matsunaga, S., Miyagishima, S., Takano, H., Sakai, A., et al., 2000. A putative mitochondrial ftsZ gene is present in the unicellular primitive red alga *Cyanidioschyzon merolae*. Mol. Gen. Genet. 264, 452–460.

Takei, K., McPherson, P.S., Schmid, S.L., De Camilli, P., 1995. Tubular membrane invaginations coated by dynamin rings are induced by GTP-gamma S in nerve terminals. Nature 374, 186–190.

van Dooren, G.G., Reiff, S.B., Tomova, C., Meissner, M., Humbel, B.M., Striepen, B., 2009. A novel dynamin-related protein has been recruited for apicoplast fission in *Toxoplasma gondii*. Curr. Biol. 19, 267–276.

Vaughan, S., Wickstead, B., Gull, K., Addinall, S.G., 2004. Molecular evolution of FtsZ protein sequences encoded within the genomes of archaea, bacteria, and eukaryota. J. Mol. Evol. 58, 19–29.

Vitha, S., McAndrew, R.S., Osteryoung, K.W., 2001. FtsZ ring formation at the chloroplast division site in plants. J. Cell Biol. 153, 111–120.

Vitha, S., Froehlich, J.E., Koksharova, O., Pyke, K.A., van Erp, H., Osteryoung, K.W., 2003. ARC6 is a J-domain plastid division protein and an evolutionary descendant of the cyanobacterial cell division protein Ftn2. Plant Cell 15, 1918–1933.

Weatherill, K., Lambiris, I., Pickett-Heaps, J.D., Deane, J.A., Beech, P.L., 2007. Plastid division in Mallomonas (Synurophyceae, Heterokonta). J. Phycol. 43, 535–541.

Yang, Y., Glynn, J.M., Olson, B.J., Schmitz, A.J., Osteryoung, K.W., 2008. Plastid division: across time and space. Curr. Opin. Plant Biol. 11, 577–584.

Yoshida, Y., Kuroiwa, H., Misumi, O., Nishida, K., Yagisawa, F., Fujiwara, T., et al., 2006. Isolated chloroplast division machinery can actively constrict after stretching. Science 313, 1435–1438.

Yoshida, Y., Kuroiwa, H., Misumi, O., Yoshida, M., Ohnuma, M., Fujiwara, T., et al., 2010. Chloroplasts divide by contraction of a bundle of nanofilaments consisting of polyglucan. Science 329, 949–953.

Yun, M.S., Kawagoe, Y., 2009. Amyloplast division progresses simultaneously at multiple sites in the endosperm of rice. Plant Cell Physiol. 50, 1617–1626.

Zhang, X., Hu, J., 2010. The Arabidopsis chloroplast division protein DYNAMIN-RELATED PROTEIN5B also mediates peroxisome division. Plant Cell 22, 431–442.

CHAPTER FIVE

Reprogramming Mediated by Cell Fusion Technology

Oleg L. Serov, Natalia M. Matveeva, *and* Anna A. Khabarova

Contents

Institute of Cytology and Genetics, Academy of Sciences of Russia, Siberian Branch, Novosibirsk, Russia

International Review of Cell and Molecular Biology, Volume 291
ISSN 1937-6448, DOI: 10.1016/B978-0-12-386035-4.00005-7

Abstract

This review is focused on recent advances in fusion-based reprogramming of cells of different pluripotent statuses or lineage origins. Recent findings are discussed from standpoints of both the developmental potency of hybrid cells generated by fusion of pluripotent embryonic stem (ES) cells, embryonal carcinoma (EC) cells, and somatic cells and epigenetic mechanisms and other aspects involved in the reprogramming process. Complete reprogramming occurs at least 5–7 days after fusion and includes at least two steps. (i) initiation at the heterokaryon stage and choice of the direction of reprogramming using an "all-or-none principle" to establish the dominance of one parental genome and (ii) "fixation" of the newly acquired expression profile by epigenetic mechanisms. The first step is realized without cell division, whereas the second requires cell proliferation. Reprogramming in hybrid cells is rapid and complete. Thus, cell fusion is a powerful tool for reprogramming.

Key Words: Hybrid cells, Cell fusion, Reprogramming, Heterokaryons, Epigenome, Gene expression, Cell differentiation

1. Introduction

Development is an orderly process leading to the appearance of 200–220 distinct types of somatic cells in adults (Surani, 2001; Wolpert et al., 2006). Cell specification and loss of developmental potential are key processes in development. The specific characteristics of various somatic cells arise due to the orderly selection of the genes that are expressed while the rest are silenced. Moreover, a crucial characteristic of cell differentiation is the ability to transmit gene expression patterns from one cell to daughter cells through division. This phenomenon is defined as "cell memory" (Lyko and Paro, 1999), "molecular memory" (Surani, 2001), or "epigenetic memory" (Goldberg et al., 2007), that is, heritable effects on gene expression that are not due to changes in the DNA sequence. Thus, development occurs through the close coordination of genetic and epigenetic programs (Surani et al., 2007). Under normal circumstances, the pattern of gene expression of specialized somatic cells is stable and heritable; however, it is not fixed and irreversible. In fact, experiments involving somatic cell nuclei transfer (SCNT) into oocytes have demonstrated that the epigenome of specialized somatic cells can be reset to a totipotent state (Gurdon, 1962; Wakayama et al., 1998; Wilmut et al., 1997). In other words, the reprogramming by which a somatic cell acquires totipotency is based on epigenetic mechanisms and not on alterations of any DNA sequences.

At present, there are three approaches to reprogram the genome of differentiated cells: SCNT into oocytes, fusion of embryonic stem (ES)

cells and somatic cells or fusion of cells of different lineages, and exogenous expression of defined transcription factors in somatic cells to generate induced pluripotent stem (iPS) cells. Although these approaches are considered effective, each of them has advantages and limitations (Hanna et al., 2010; Papp and Plath, 2011; Yamanaka and Blau, 2010). Progress in understanding of reprogramming using SCNT and iPS cell technologies has been thoroughly reviewed (Hanna et al., 2010; Hochedlinger and Jaenisch, 2003, 2006; Papp and Plath, 2011; Yamanaka and Blau, 2010; Yang et al., 2007); however, few reviews have been devoted to the cell fusion approach (Ambrosi and Rasmussen, 2005; Do et al., 2006; Pralong et al., 2006; Serov et al., 2001). Meanwhile, recent studies of hybrid cells generated by the fusion of ES cells and somatic cells have provided new data regarding both the timing of the silencing of tissue-specific genes and the activation of pluripotent genes within the parental genomes as well as the epigenetic mechanisms involved in the bidirectional reprogramming that is common to all types of hybrid cells. This review focuses on cell fusion as a powerful tool for the study of reprogramming and provides a comparison of this technique with the SCNT and iPS cell approaches. Two types of hybrid cells will be considered here: those obtained by fusion of ES or embryonal carcinoma (EC) cells with somatic cells and those obtained by fusion of somatic cells from different lineages.

2. Historical Review of EC Cell Fusion-Mediated Reprogramming

Hybrid cells obtained by fusion of EC cells with somatic cells were the first tools available for the study of the interaction between genomes with different developmental potentials within a common hybrid nucleus. EC cells originating from embryo-derived tumors (teratocarcinomas) resemble cells of early embryos in morphological, biochemical, and cell surface properties and in developmental potential. Like ES cells, EC cells are pluripotent, as manifested by their capacity to differentiate *in vitro* and *in vivo* into derivatives of three germ layers. Further, some EC cell lines have been shown to participate in the formation of chimeric mice after injection into blastocysts (Dewey et al., 1977; Mintz and Illmensee, 1975; Papaioannou et al., 1978; Rossant and McBurney, 1982). Though the degree of chimerism in animals generated from these blastocysts was generally very low (Papaioannou et al., 1978), in rare cases, the tested EC cells were identified in many tissues of chimeric animals (Dewey et al., 1977), including even the germ line (Bradly et al., 1984; Stewart and Mintz, 1981). Interestingly, significant phenotypic variability has been observed in hybrid cells generated by fusion of EC cells and somatic cells, as some hybrid cell clones resembled the parental somatic cells, whereas others demonstrated EC cell-like

morphology and other features of pluripotent cells. The phenotypic variability of hybrid cells often depends on the nature of the somatic partner.

2.1. EC cell–somatic cell hybrids with phenotypes similar to the somatic partner

Dominance of the somatic partner genome was reported in hybrid cells obtained by fusion of EC cells with Friend erythroleukemia cells (McBurney et al., 1978). These hybrid cells had a phenotype similar to erythroleukemia cells and expressed hemoglobin genes derived from the EC genome. McBurney et al. (1978) concluded that the EC cell genome was reprogrammed to express erythroid genes following cell fusion and interaction with the Friend cell genome. Similar observations were reported in a study of hybrid cells generated by fusion of F9 murine EC cells and PFHR9 cells, a parietal endodermal cell line with a near-diploid karyotype (Howe and Oshima, 1982). The authors did not detect hybrid clones with EC phenotypes; all hybrid cells had endoderm-like phenotypes and expressed typical endodermal markers including plasminogen activators, basement membrane proteins, and endoderm cytoskeletal proteins. Moreover, EC cell characteristics such as tumorigenicity, expression of stage-specific embryonic antigen (SSEA), and alkaline phosphatase activity were suppressed in the hybrid cells (Howe and Oshima, 1982). Importantly, fusion of EC cells with endoderm cytoplasts (enucleated endoderm cells) or with neuroblastoma cytoplasts resulted in cybrid colonies that resembled the EC parent (Schaap et al., 1982). These data suggest that endoderm and neuroblastoma cytoplasm contain no factors capable of inducing the EC cell differentiation. McBurney and Strutt (1979) made a similar observation in their study of hybrids generated by fusion of EC cells with cytoplasts and karyoplasts prepared from fibroblasts. The cybrids generated in this study retained the developmental potential of the EC cell, whereas hybrids generated from whole cells and karyobrids (karyoplast–EC cell hybrids) resembled the fibroblast parent cells.

The phenotypic resemblance of EC cell–fibroblast hybrid cells to somatic parental cells was also observed by Rousset et al. (1979). Reactivation of *H-2* (*MHC* gene) alleles that were inactive in EC cells was detected in the fibroblast-like hybrid cells generated in this study. Moreover, the use of tetraploid EC cells as the pluripotent partner in this study did not result in a pluripotent phenotype in the hybrid cells; instead, all hybrid cells displayed the somatic phenotype and properties (Rousset et al., 1979). A similar phenotypic phenomenon was noted in experiments involving the fusion of mouse EC cells and primary human fibroblasts. The resulting hybrid cells resembled the differentiated fibroblasts rather than the undifferentiated EC cells and expressed human but not mouse collagen (Schaap et al., 1984). Ben-Shushan et al. (1993) later demonstrated the suppression of *Oct4*, a gene that is characteristic of pluripotent cells, in the fibroblast-like hybrids generated by fusion of mouse EC cells

and fibroblasts. The suppression of *Oct4* expression was accompanied by changes in the methylation status and chromatin structure of the 5′-regulatory region of this gene (Ben-Shushan et al., 1993).

Thus, the phenotypes of the cell hybrids described above suggest the dominance of the somatic genome over the pluripotent genome. This dominance may be a result of the induced differentiation of the hybrid genome due to effects of the somatic genome or instead may be evidence of bidirectional reprogramming of parental genomes (see below).

2.2. EC cell–somatic cell hybrids with phenotypes similar to the pluripotent partner

In contrast to the hybrid cells discussed above, hybrids generated by fusion of EC cells with thymocytes or splenocytes had characteristics similar to those of EC cells and retained pluripotent potential. These hybrid cells were able to give rise to true teratomas containing derivatives of all three embryonic germ layers (Andrews and Goodfellow, 1980; Atsumi et al., 1982; Rousset et al., 1983; Takagi, 1983) or to differentiate *in vitro* and form complex embryoid bodies (EBs) in suspension culture (Takagi, 1993). Moreover, interspecific EC cell–somatic cell hybrids derived by fusion of mouse EC cells and rat hepatoma cells were able to form chimeras and to contribute to multiple tissues (Duboule et al., 1982). After injection of these hybrid cells into mouse blastocysts, several rat chromosomes were identified in cells derived from the chimeric fetuses, demonstrating the presence of xenogenic chromosomes in functional mouse organs (Duboule et al., 1982). An EC-like phenotype and the presence of SSEA1 on the cell surface have been observed in intra- and interspecific hybrids obtained by fusion of EC cells and thymocytes, peripheral blood lymphocytes, or myeloma cells (Correani and Croce, 1980; Forejt et al., 1984; Serov et al., 1990). For instance, EC cell–thymocyte hybrid cells displayed EC cell-like morphology, high levels of alkaline phosphatase, and the capacity to produce subcutaneous teratomas containing different tissues, including derivatives of all three embryonic germ layers. Importantly, these hybrid cells lost some properties of the differentiated parent cells; they failed to express the *Thy1* alloantigen, which is a thymocyte cell marker, but expressed *H2* antigens characteristic of the thymocyte cell surface (Miller and Ruddle, 1976, 1977). Interestingly, hybrids generated by fusion of the nullipotent F9 EC cell line and thymocytes produced multidifferentiated tumors in mice, whereas the F9 parental cells gave rise to tumors formed exclusively of EC cells (Rousset et al., 1983). The similarity of hybrid cells such as EC cell–thymocyte and EC cell–splenocyte to EC cells suggests that the EC cell genome is dominant over the somatic genome. However, a study using an identical fusion system showed that hybrid cells obtained by fusion of EC cells and normal mouse splenocytes resembled parental EC cells but that EC cell–mouse thymoma hybrids resembled neither parental cell and instead

phenotypically resembled fibroblasts (Gmür et al., 1981). Moreover, the authors of this study suggested that there was no consistent dominant or recessive pattern in the EC cell–splenocyte hybrids because they observed a transition from clones with EC-like morphology to clones with differentiated phenotypes and vice versa. Regardless, hybrid cells with different patterns of parental genome dominance have provided a new technology for the study of reprogramming of parental genomes.

2.3. Reprogramming in EC cell–somatic cell hybrids

Notably, EC cell–somatic cell hybrids showed evidence of reprogramming of both parental genomes. For instance, in EC-like hybrid cells generated by fusion of EC cells and thymocytes, the t^{12} embryonic antigen, which is normally expressed only in early embryonic cells, was reactivated in the thymocyte genome (Artzt et al., 1980). The reactivation of this particular gene and the suppression of thymocyte-specific *Thy1* alloantigen expression in hybrid cells of this type (Miller and Ruddle, 1977) are indicative of reprogramming of the somatic cell genome in these hybrid cells. An alteration in the gene expression program of the somatic genome has also been demonstrated in pluripotent hybrids generated by fusion of lymphocytes with PCC4 EC cells (Forejt et al., 1984). All lymphocyte-specific proteins disappeared in the hybrid cells.

Another evidence of somatic genome reprogramming in EC cell–thymocyte and EC cell–splenocyte hybrids was provided by the reactivation of the inactive X chromosome derived from the somatic partner. An active status of both X chromosomes is a property of pluripotent cells with a female genotype (XX) and of some EC cell lines (McBurney and Strutt, 1980). A series of studies implemented by Takagi's group demonstrated reactivation of inactive X chromosome derived from somatic cells after fusion of EC cells with female thymocytes or splenocytes (Mise et al., 1996; Okuyama et al., 1986; Takagi, 1993; Takagi et al., 1983). The reactivation of X chromosome occurred soon after fusion and was accompanied by changes in the methylation status of both X chromosomes (Mise et al., 1996). Thus, reprogramming of the somatic partner genome was observed at the level of either the particular genes or the whole X chromosome.

As for the hybrid cells resembling somatic partner, there were evidences of the EC cell genome reprogramming: activation of hemoglobin genes of EC genome in hybrids between EC cells and erythroleukemia cells (McBurney et al., 1978); extinction of EC cell characteristics at fusion of EC cells with parietal endodermal cells (Howe and Oshima, 1982); reactivation of inactive in EC cells H-2 alleles of MHC gene (Rousset et al., 1979) or suppression of gene *Oct4* characteristic for the pluripotent cells (Ben-Shushan et al., 1993) in fibroblast-like hybrids, generated with participation of fibroblasts.

Thus, these studies have highlighted important features of EC cell–somatic cell hybrids. These hybrid cells exhibit evidence of reprogramming of either the somatic cell genome or the genome of the pluripotent partner;

however, the explanation for the phenotypic variability of EC cell–somatic cell hybrids has been complicated by uncertainty in the ratio of the parental chromosomes in the hybrid karyotypes due to insufficient numbers of markers capable of distinguishing the parental chromosomes and the impossibility of identifying chromosomes by direct cytogenetic analysis upon intraspecific cell hybridization. In addition, abnormal karyotypes are common in these hybrids due to loss of the Y chromosome, trisomy, deletions, or translocations in EC cells (Modinski et al., 1990; Rousset et al., 1983; Takagi et al., 1983).

Despite these complications, hybrid cells formed by fusion of EC cells and somatic cells continue to be used in studies of reprogramming. For instance, Flasza et al. (2003) demonstrated that some of the interspecific hybrid cells constructed by fusion of murine EC cells (P19) and the cells of a human T-lymphoma cell line expressed human transcription factors characteristic of undifferentiated pluripotent stem cells, *Oct4* and *Sox-2*. Activation of these endogenous human markers of pluripotency has been shown by real-time PCR using species-specific primers. Simultaneously, *CD45*, a marker present in lymphocytes, was downregulated in some hybrids. Moreover, expression of human *lamininb1*, *collagenIVa1*, and *nestin*, markers of nonlymphoid differentiated cells, was observed in differentiated derivatives of hybrid cell clones. All these changes in gene expression indicated that cell fusion resulted in reprogramming of the human cells to the pluripotent state (Flasza et al., 2003).

Similar results were obtained in a study of hybrid cells constructed by fusion of F9 EC cells with neurosphere cells (NSCs; Do et al., 2007). F9–NSC hybrids expressed the pluripotency markers *Oct4* and *Nanog* and showed signs of somatic genome reprogramming, such as reactivation of the inactive X chromosome and inactivation of the tissue-specific genes *Nestin* and *Glutamate receptor 6* (*Glur6*). The authors found not only that F9 EC cells can reprogram NSCs but also that the epigenetic memory of the NSCs was indeed lost, as determined by the differentiation potential, the change in gene expression and the methylation status of the F9–NSC hybrids during induced differentiation. A later study of the same F9–NSC hybrids described the timing of the reprogramming of the somatic genome to the pluripotent state (Han et al., 2008).

Nevertheless, because EC cells have more restricted developmental potential than ES cells, hybrid cells generated by fusion of ES cells with somatic cells provide a more efficient system for restoring pluripotency and reprogramming differentiated cells than EC cell–somatic cell hybrids.

3. Key Characteristics of ES Cell–Somatic Cell Hybrids

As mentioned above, hybrid cells obtained by fusion of EC cells and somatic cells often show phenotypes similar to either the pluripotent partner or the somatic one. It should be noted that most of the studies cited above

did not report a detailed cytogenetic analysis of hybrid cells and that the parental chromosomes were not reliably marked, making it difficult to analyze the data, as the actual ratio of the parental chromosomes in the hybrid cells cannot be accurately estimated.

3.1. Phenotype of ES cell–somatic cell hybrids

In contrast to EC cells, ES cells have normal diploid karyotypes and high degrees of pluripotency. Numerous reports indicate that ES cells derived from preimplantation embryos retain their pluripotency under *in vitro* culture conditions (Donovan, 1994; Joyner, 1993; Robertson, 1987). Upon injected into blastocysts, the ES cells give rise to chimeras in which they contribute to many different tissues and organs, including the germ line (Allan, 1987; Hogan et al., 1994; Joyner, 1993; Robertson and Bradley, 1986). Further, upon transfer into enucleated oocytes, nuclei from ES cells are able to provide more complete development than nuclei from somatic cells (Campbell et al., 1995, 1996; Keefer et al., 1994; Sims and First, 1993; Stice et al., 1996).

These findings prompted us to take advantage of the developmental potential of ES cells to reprogram the splenocyte genome in hybrid cells generated by fusion of ES cells and splenocytes (Matveeva et al., 1996, 1998). ES cell–splenocyte hybrid cells had morphologic and growth characteristics similar to those of ES cells (Matveeva et al., 1996). A later study showed that these ES cell–splenocyte hybrid cells had a high degree of pluripotency, as indicated by their ability to form chimeras (Matveeva et al., 1998). Some later, hybrid cells with similar characteristics were obtained by a group of Japanese researchers in experiments involving the fusion of ES cells and thymocytes (Tada et al., 2001, 2003).

At present, at least eight types of hybrid cells have been generated by fusion of human and mouse ES cells and different types of somatic cells (Table 5.1). All the hybrid cells generated from ES cells have a phenotype similar to that of ES cells: these hybrids have morphologic and growth characteristics similar to those of ES cells, and all are positive for the typical pluripotent markers (*Oct4*, *Nanog*, and others) and surface antigens characteristic of ES cells (ECMA-7, SSEA4, TRA1-61, and TRA1-80). Further, high levels of telomerase activity and increased telomere lengths similar to those of ES cells were reported in ES cell–fibroblast hybrid cells (Sumer et al., 2010).

Taken together, these data indicate the dominance of the genome derived from the ES cell partner over the somatic genome in hybrid cells. Notably, this dominance is not dependent on the type of somatic cell partner used for cell fusion. Theoretically, the dominance of a parental genome may occur due to partial or complete loss of chromosomes from the other cell partner; thus, there is a reason to consider the behavior of parental chromosomes in hybrid cells.

Table 5.1 A list of hybrid cells obtained by fusion of human or mouse ES cells with different somatic cells

Year	Somatic partner	References
1996	Mouse splenocytes	Matveeva et al. (1996)
2001	Mouse T and B thymocytes	Tada et al. (2001)
2002	Mouse brain progenitor cells (NSCs)	Ying et al. (2002)
2002	Mouse immature bone marrow cells	Terada et al. (2002)
2005	Mouse cumulus cells	Do and Schöler (2005)
2006	Mouse primary embryonic fibroblasts	Sullivan et al. (2006)
2008	Mouse mesenchymal cells	Sumer et al. (2009)
2005	Human fibroblasts	Cowan et al. (2005)
2005	Human osteoblasts	Cowan et al. (2005)
2006	Human myeloid precursor cells	Yu et al. (2006)
2010	Human hepatocytes	Guo et al. (2010)
2010	Mouse tetraploid embryonic fibroblasts	Kruglova et al. (2010)

3.2. The fate of parental chromosomes in ES cell–somatic cell hybrids

After fusion of two mouse diploid cells, the expected number of chromosomes in hybrid cells is 80; however, direct counting of chromosomes in hybrid cells of different types, including ES cell–splenocyte (Matveeva et al., 1998, 2005), ES cell–thymocyte (Tada et al., 2001, 2003), ES cell–NSC (Pells et al., 2002; Ying et al., 2002), and ES cell–fibroblast (Ambrosi et al., 2007; Cowan et al., 2005; Kruglova et al., 2008), demonstrated that, as a rule, the hybrid cells contained lower chromosome numbers than the tetraploid complement. The chromosome loss in hybrid cells depends on the cell type of the somatic partner. For instance, the most extensive chromosome loss observed in a somatic partner was reported in ES cell–splenocyte hybrid cells, which contained as few as that some hybrid clones contained, four splenocyte chromosomes in the presence of a complete set of ES cell chromosomes (Matveeva et al., 1998, 2005). In contrast, ES cell–fibroblast hybrid cells often contained a near-tetraploid chromosome complement (Ambrosi et al., 2007; Cowan et al., 2005; Kruglova et al., 2008; Matveeva et al., 2005; Sumer et al., 2010), and ES cell–thymocyte and ES cell–NSC hybrids had a tetraploid karyotype (Tada et al., 2001; Ying et al., 2002). Variability in chromosome numbers is observed even among hybrid cells of one type; among 10 tested diploid ES cell–diploid fibroblast hybrid clones, in four, more than 80% of cells had 76–80 chromosomes (near-tetraploid), whereas, in six others, only 40–60% of cells were near-tetraploid (Kruglova et al., 2008). A similar variability in chromosome numbers was reported in mouse ES cell–fibroblast hybrid cells (Sumer et al., 2010) and human ES cell–human fibroblast hybrid cells (Hasegawa et al., 2010).

Hybrid cells obtained by spontaneous cell fusion (Terada et al., 2002; Ying et al., 2002) have a more stable tetraploid karyotype than hybrid cells generated by fusion induced by polyethylene glycol (Cowan et al., 2005; Kruglova et al., 2008; Matveeva et al., 1998, 2005; Pells et al., 2002) or electrofusion (Tada et al., 2003). Notably, Wang et al. (2003) have also identified cells with a near-diploid karyotype among *in vivo*-generated hybrid cells in the liver. This finding implies that the appearance of cells with a near-diploid karyotype was due to chromosome segregation by an unknown mechanism in initially tetraploid or hexaploid hybrid cells (Medvinsky and Smith, 2003).

The phenotype of ES cell–somatic cell hybrids could be dependent on the ratio of the parental chromosomes. As mentioned above, segregation of chromosomes in hybrid cells raises a problem in identifying the parental chromosomes. There are at least two approaches to distinguish parental chromosomes in hybrid cells. First, microsatellite analysis allows the marking of parental chromosomes in intraspecific hybrid cells (Kruglova et al., 2008; Matveeva et al., 2005; Pells et al., 2002; Terada et al., 2002; Vasilkova et al., 2007). The second approach is highly effective for interspecific hybrid cells (e.g., *Mus musculus* ES cell–*Mus caroli* splenocyte hybrid cells) and is based on two-color fluorescent *in situ* hybridization (FISH) with a species-specific probe for one species and chromosome-specific painting probes for individual chromosomes originating from both species (Fig. 5.1; Battulin et al., 2009;

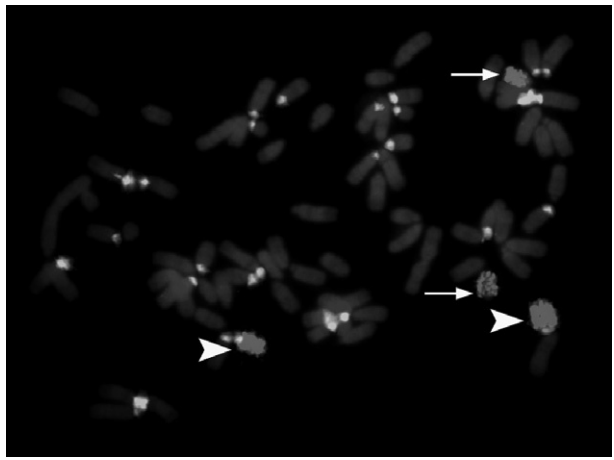

Figure 5.1 Identification of parental chromosome 17 in *M. musculus* ES cell–*M. caroli* splenocyte hybrid cells by two-color fluorescent *in situ* hybridization with a species-specific probe for *M. musculus* (green signal over centromere) and a chromosome-specific painting probe for chromosome 17 originating from both species (red). Metaphase chromosomes of an HMC4 hybrid cell with two labeled *M. musculus* (arrowheads) and two *M. caroli* chromosomes 17 (arrows).

Matveeva et al., 2005; Pristyazhnyuk et al., 2010). Microsatellite and direct two-color FISH cytogenetic analyses of ES cell–somatic cell hybrids demonstrated that in most examined hybrid clones, chromosomes of the somatic partner were preferentially lost (Kruglova et al., 2008; Matveeva et al., 2005; Pristyazhnyuk et al., 2010; Serov et al., 2001; Vasilkova et al., 2007). This finding holds true for hybrid cells at early passages. Nonrandom segregation at early passages implies that initial epigenetic differences in the homologous parental chromosomes were not immediately equalized, suggesting at least transient persistence of the differentiated epigenotype (Matveeva et al., 2005); however, bilateral loss of parental chromosomes was reported at late passages, probably after epigenetic equalization of parental chromosomes occurs and the segregation process becomes stochastic (Pristyazhnyuk et al., 2010). In fact, the ratio of individual chromosomes from one parental cell to those from the other parental cell can vary from 1-to-3 to 3-to-1 within a population of the same hybrid clone (Battulin et al., 2009; Pristyazhnyuk et al., 2010). It is important to note that two-color FISH analysis has demonstrated that the karyotypes of ES cell–somatic cell hybrids contain few chromosomal rearrangements (Pristyazhnyuk et al., 2010).

3.3. Assessment of pluripotency in ES cell–somatic cell hybrids

As mentioned above, a key feature of ES cells is pluripotency. Despite the variability in chromosomal composition, all examined ES cell–somatic cell hybrids had many characteristics of ES cells, including a high degree of pluripotency. As a rule, pluripotency is estimated using a set of tests: *in vitro* formation of EBs, generation of teratomas upon subcutaneous injection of the tested cells into immunodeficient mice, and generation of chimeras upon injection of the tested cells into blastocysts.

The capacity to form *in vitro* EBs in suspension culture conditions is a common characteristic of different types of ES cell–somatic cell hybrids, including mouse ES cell–mouse fibroblast (Ambrosi et al., 2007; Hasegawa et al., 2010; Sumer et al., 2010), ES cell–NSC (Do and Schöler, 2005; Pells et al., 2002), ES cell–splenocyte (Matveeva et al., 1998; Vasilkova et al., 2007), ES cell–immature bone marrow cell (Terada et al., 2002), and human ES cell–human myeloid cell hybrids (Yu et al., 2006). Histological and immunohistochemical analyses of EBs formed by these hybrids have demonstrated the presence of derivatives of all embryonic layers. Amazingly, presumptive germ cells expressing meiotic- and postmeiotic-specific genes, such as *Haprin*, *Acrosin*, *Scyp1*, *Scyp3*, and *Stra-8*, were identified in EBs generated by ES cell–splenocyte hybrids (Lavagnolli et al., 2009). Together, the results of EB tests reveal that the potential of various ES cell–somatic cell hybrids is similar to that of normal diploid ES cells.

Derivatives of ectoderm, mesoderm, and endoderm were regularly identified in teratomas formed after subcutaneous injection of different types of ES cell–somatic cell hybrids, including human ES cell–human fibroblast (Cowan et al., 2005), ES cell–thymocyte (Tada et al., 2003), and ES cell–splenocyte hybrids (Matveeva et al., 1998; Vasilkova et al., 2007). After injection, however, the tested hybrid cells were grown in nonselective conditions, and it is thus possible that an additional loss of chromosomes of the somatic partner occurred. In fact, microsatellite marker analysis demonstrated that loss of the somatic chromosomes occurred in some teratomas (Vasilkova et al., 2007). In general, the teratoma test is useful for estimation of the developmental potential of ES cell–somatic cell hybrids.

The most accurate method for estimation of pluripotency is the chimerism test; however, the application of this test is complicated by differences in ploidy between diploid cells of recipient embryos and the tested hybrid cells, which are often tetraploid or near-tetraploid (Pells et al., 2002; Ying et al., 2002). Moreover, the combination of tetraploid and diploid embryonic cells is known to lead to the development of the entire fetus from either diploid cells of the inner cell mass or diploid culture-derived ES cells (Eakin and Behringer, 2003; Nagy and Rossant, 1993; Nagy et al., 1990). Upon injection into tetraploid blastocysts, the diploid ES cells give rise to the epiblast, whereas the tetraploid host cells give rise only to the placenta (Eggan et al., 2001; Nagy et al., 1990). Unsurprisingly, tetraploid ES cell–thymocyte hybrid cells marked by the lacZ reporter and injected into diploid blastocysts have been shown to contribute as single cells in 8 out of 20 embryos at embryonic day 7.5 (E7.5; Tada et al., 2001). The poor contribution of the hybrid cells has been explained by "a severe loss of tetraploid cells in the chimeras of diploid and tetraploid embryos" (Tada et al., 2001). In light of these data, reports of the birth of two chimeras generated by the injection of ES cell–NSC hybrids with a tetraploid karyotype into diploid blastocysts appear remarkable (Pells et al., 2002; Ying et al., 2002). Notably, in both of these reports, the fate of the initial tetraploid karyotype of the tested hybrid cells during development of the chimeras was not studied. Whether the chimeras were derived from hybrid cells with an initial tetraploid karyotype or from their derivatives with an altered karyotype (e.g., because of a loss of some parental chromosomes) remains unclear.

Recent studies have reported two series of experiments involving the detailed study of karyotypes during the development of chimeras generated by the injection of ES cell -splenocyte and ES cell -fibroblast hybrid cells into the blastocysts (Kruglova et al., 2008; Vasilkova et al., 2007). In the first series of experiments, chimeras were generated using two interspecific *M. musculus* ES cell–*M. caroli* splenocyte hybrid clones, HMC15 and HMC29 (Vasilkova et al., 2007). Clone HMC15 contained three chromosomes from *M. caroli* (15, 18, and X), and the subclone HMC15-4 contained

a single *M. caroli* X chromosome in the presence of a near-triploid *M. musculus* chromosome background. HMC29 and the subclone HMC29-3 were unique; their karyotypes were near-diploid and essentially "heterozygous" for 12–13 parental chromosomes. Parental chromosomes in the hybrid cells were identified by FISH analysis with a species-specific probe for *M. musculus* chromosomes and microsatellite markers. Analysis of adult chimeras demonstrated that *Gla* and Catsper1, gene markers specific for *M. caroli* chromosomes X and 19, were present in various tissues (Vasilkova et al., 2007). These data clearly indicate that the tested hybrid cells retained *M. caroli* chromosomes X and 19 during the development of the chimeras. In the second series of experiments, 21 adult chimeras were generated by the injection of near-tetraploid ES cell–fibroblast hybrid cells into diploid C57BL blastocysts (Kruglova et al., 2008). The contribution of the green fluorescent protein (GFP)-labeled hybrid cells to adult chimeras was significant and comparable to that of parental GFP-labeled ES cells (Fig. 5.2). Further, after injection of these hybrid cells, 20 chimeric embryos were identified at 11–13 days postconception, and many of these embryos contained a large number of GFP-positive descendants of the tested hybrid cells (Fig. 5.2; Kruglova et al., 2008). Moreover, the extraembryonic membranes (amnion and yolk sac) in these chimeras were mosaic. Importantly, cytogenetic and microsatellite analyses of cell cultures derived from chimeric embryos or adults indicated that the initial near-tetraploid karyotype of the tested hybrid cells remained stable during the development of the chimeras, that is, the hybrid cells were mainly responsible for the generation of the chimeras (Kruglova et al., 2008). These reports show unambiguously that the degree of pluripotency of ES cell–fibroblast hybrids

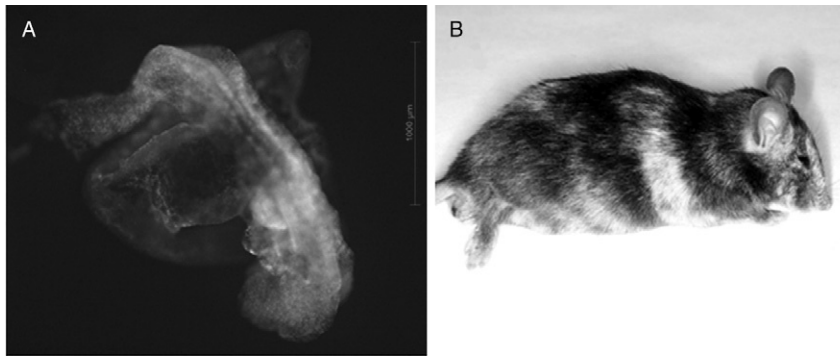

Figure 5.2 Chimeras generated by injection of tef4 hybrid cells with a near-tetraploid chromosome complement into C57BL blastocysts. (A) A 11-day chimeric embryo with a high content of GFP-positive cells (green). (B) Anesthetized adult male tef4 #7-48 chimera with overt coat-color chimerism.

is similar or identical to that of the parental ES cells; these findings may be interpreted as demonstrating the dominance of the pluripotent genome over the somatic genome.

3.4. Direct signs of reprogramming in ES cell–somatic cell hybrids

As mentioned above, the hybrid cells generated by fusion of pluripotent ES cells and somatic cells had phenotypes and properties characteristic of ES cells. Thus, the nuclei of differentiated cells were exposed to the pluripotent partner, resulting in the genomic loss of properties of differentiated cells but the acquisition of ES cell properties that occurs during reprogramming. Reprogramming is manifested in changes in the gene expression profile, global and local DNA methylation, and chromatin modification. In ES cell–somatic cell hybrids, two processes are involved in these changes: activation of previously inactive genes typical of ES cells in the somatic genome and suppression of genes whose activity is typical for differentiated cells.

3.4.1. Reactivation and silencing of genes of the somatic genome

Few studies have addressed the activation or silencing of distinct parental genes in ES cell–somatic cell hybrids. The reactivation of the somatic alleles of the "pluripotent genes," such as *Oct4* and *Nanog*, has been observed in these hybrid cells. For instance, the reactivation of thymocyte-derived *Oct4* has been described in *M. musculus* ES cell–*M. molossinus* thymocyte hybrids (Kimura et al., 2004), active expression of the fibroblast *Oct4* allele in human ES cell–human fibroblast hybrid cells (Cowan et al., 2005), and reactivation of splenocyte alleles at the *Oct4* and *Nanog* loci has been observed in *M. musculus* ES cell–*M. caroli* splenocyte hybrid cells (Battulin et al., 2009). Considering the key role of the *Oct4* and *Nanog* genes in the maintenance of pluripotency, reactivation of their somatic alleles in hybrid cells could potentially facilitate the acquisition of pluripotency by the somatic genome (Battulin et al., 2009), as increased levels of Nanog protein in hybrid cells are sufficient for the somatic genome to be reset to a state of pluripotency (Silva et al., 2006).

Further, activation of other genes initially silenced in the somatic partner was observed in ES cell–somatic cell hybrids. For instance, reactivation of the fibroblast-derived *CRIPTO/TDGF1* allele has been established in human ES cell–human fibroblast hybrid cells (Cowan et al., 2005), reactivation of fibroblast alleles of *Piwil2* (piwi-like homolog 2) and *Chd1l* (chromodomain helicase DNA binding protein 1-like) genes has been observed in murine ES cell–fibroblast cell hybrids (Ambrosi et al., 2007), and reactivation of the *M. caroli Gla* (α-galactosidase) allele has been observed in *M. musculus* ES cell–*M. caroli* splenocyte hybrid cells (Puzakov et al., 2007).

Examples of silencing of the genes whose activities are typical for differentiated cells in ES cell–somatic hybrid cells include the silencing of the thymocyte *Thy-1* gene in *M. musculus* ES cell–*M. molossinus* thymocyte hybrid cells (Kimura et al., 2004), silencing of the *Lmna* gene of splenocyte origin in *M. musculus* ES cell–*M. caroli* splenocyte hybrid cells (Battulin et al., 2009), silencing of the *Nestin* and *Glur6* genes in ES cell–NSC hybrids (Do and Schöler, 2004), and silencing of the *Lh-R* (a receptor of luteinizing hormone) and *Tsg-6* (TNF-α-stimulating factor 6) genes in ES cell–cumulus cell hybrids (Do and Schöler, 2004). Thus, both activation and silencing of distinct genes in ES cell–somatic cell hybrids provide unambiguous evidence of reprogramming. Interestingly, the mono-allelic expression of the imprinted *H19* and *Igf3r* loci remained unchanged in hybrid cells obtained by fusion of mouse ES cells and mouse thymocytes, demonstrating that reprogramming did not disrupt imprinting of these somatic genes (Tada et al., 2001).

3.4.2. Reactivation of the inactive X chromosome derived from the somatic genome

Reactivation of the inactive X chromosome in ES cell–somatic cell hybrids is one reliable indicator of reprogramming. The first study of replication patterns of X chromosomes in six hybrid clones obtained by fusion of XY male ES cells and XX female thymocytes demonstrated that all X chromosomes were replicated synchronously, whereas asynchronous replication of X chromosomes is characteristic of XX female somatic cells (Tada et al., 2001). Moreover, Xist (inactive X-specific transcript) RNA was unstably accumulated (spotted) on all X chromosomes in two ES hybrid cell lines examined by RNA FISH, whereas Xist RNA accumulation was stable on the inactive X chromosome in XX thymocytes (Tada et al., 2001). These data demonstrate the reactivation of the initially inactive X chromosome derived from thymocytes (Tada et al., 2001).

3.4.3. Genome-wide analysis of gene expression profiles in ES cell–somatic cell hybrids

The most complete picture of reprogramming can be obtained through microarray analysis of gene expression profiles. In fact, comparison of gene expression profiles of human ES cells, human fibroblasts, and ES cell–fibroblast hybrid cells showed that the expression profiles of ES cells and ES cell–fibroblast hybrid cells differed minimally; only 12 of 3855 genes active in fibroblasts were expressed at levels higher than those observed in ES cells (Cowan et al., 2005), and 20 of 2521 ES cell-specific transcripts were expressed at levels two times lower than those observed in ES cells in the hybrid cells (Cowan et al., 2005). Importantly, markers of pluripotency such as *OCT4*, *NANOG*, *TDGF1*, and *REX1* were expressed at levels equivalent to those in ES cells (Cowan et al., 2005). Thus, active expression

of genes typical of the pluripotent cell partner and suppression of genes typical of fibroblasts were observed in the hybrid cells. Cowan et al. (2005) concluded that reprogramming affects more than 99% of genes of the somatic genome in human ES cell–human fibroblast hybrid cells.

Ambrosi's group has conducted a detailed analysis of the gene expression profile in hybrid cells obtained by fusion of mouse ES cells and mouse embryonic fibroblasts (Ambrosi et al., 2007). According to Ambrosi et al. (2007), 21,266 genes are active in ES cells, 20,810 genes are active in fibroblasts, and 20,598 genes are active in ES cell–fibroblast hybrid cells. The authors demonstrated that 1694 genes were differentially expressed in parental ES cells and fibroblasts. The correlation coefficients of the gene expression profiles were 0.778 for ES cells and hybrid cells, −0.949 for ES cells and fibroblasts, and −0.936 for fibroblasts and hybrid cells. Thus, statistical analysis indicated significant similarity (positive correlation) but not complete identity between the gene expression profiles of ES cells and hybrid cells and a negative correlation between the gene expression profiles of fibroblasts and hybrid cells. The studies of Ambrosi et al. (2007) and Cowan et al. (2005) both reflect large-scale reprogramming of the somatic genome in hybrid cells.

4. Epigenetic Events Accompanying Reprogramming in ES Cell–Somatic Cell Hybrids

The data presented above regarding the large-scale somatic genome reprogramming in embryonic hybrid cells suggest that this process is accompanied by extensive epigenetic changes. DNA methylation represents a major epigenetic modification of the genome that is involved in the transcriptional suppression of specific genes (Caiafa and Zampieri, 2005; Jaenisch and Bird, 2003). It is not surprising that the reactivation of initially silenced genes derived from the somatic genome in ES cell–somatic cell hybrids is also accompanied by changes in the methylation patterns of their promoters. Some groups have reported demethylation of CpG sites within the somatic promoters of key genes that maintain pluripotency, such as *Oct4* and *Nanog*, in hybrid cells; specifically, these studies have reported demethylation of the fibroblast *OCT4* allele in human ES cell–human fibroblast hybrid cells (Cowan et al., 2005; Hasegawa et al., 2010), the *M. musculus molossinus* thymocyte *Oct4* allele in *M. musculus musculus* ES cell–*M. musculus molossinus* thymocyte hybrid cells (Kimura et al., 2004), and the *M. caroli* splenocyte *Oct4* and *Nanog* alleles in *M. musculus* ES cell–*M. caroli* splenocyte hybrids (Battulin et al., 2009). Interestingly, induction of the *de novo* differentiation of two *M. musculus* ES cell–*M. caroli* splenocyte hybrid clones

as demonstrated by the teratoma test was accompanied by heavy *de novo* methylation of the *Oct4* promoter. Importantly, we have found no differences in *de novo* DNA methylation between the reactivated *M. caroli* splenocyte *Oct4* allele and its counterpart of ES cell origin in differentiated hybrid cells (Battulin et al., 2009). This finding provides indirect evidence that upon fusion of *M. musculus* ES cells and *M. caroli* splenocytes, the reprogrammed splenocyte *Oct4* allele acquired epigenetic characteristics similar or identical to those of its ES cell counterpart and, as a result, similar behavior during *de novo* differentiation.

Here is a reason to consider tight close relationship between DNA methylation of the imprinted *Dlk1-Dio3* locus and pluripotency. Several groups have shown that iPS cells differ from ES cells, which are considered to be the "gold standard" of pluripotency (Chan et al., 2009; Hanna et al., 2010; Kim et al., 2010). It has been suggested that several errors in reprogramming can occur during the generation of iPS cells. One such "reprogramming error" is dysregulation of the imprinted *Dlk1-Dio3* locus located on mouse chromosome 12 (Liu et al., 2010; Stadtfeld et al., 2010). This dysregulation includes hypermethylation and decreased expression of the imprinted genes at the *Dlk1-Dio3* locus. In turn, the dysregulation of this locus leads to altered gene expression that drastically limits the developmental capacity of iPS cells. This phenomenon was observed in 95% of mouse iPS cell lines (Stadtfeld et al., 2010).

These data prompted us to study the imprinted *Dlk1-Dio3* locus in four ES cell–fibroblast hybrid clones with near-tetraploid karyotypes that were able to efficiently generate chimeric embryos and adult chimeras (Kruglova et al., 2008). We studied the methylation status and expression of *Gtl2*, *Rian1*, and *Mirg* genes within the imprinted *Dlk1-Dio3* locus. Our findings clearly demonstrated that *Gtl2*, *Rian1*, and *Mirg* were active in all examined ES cell–fibroblast hybrid clones. Despite interclonal variability, the expression of these genes is comparable to that of ES cells. Quantitative analysis of the DNA methylation status of the intergenic differentially methylated region (IG DMR) within the *Dlk1-Dio3* locus by pyrosequencing and bisulfite sequencing clearly showed that the DNA methylation status of this region in the tested hybrid clones was comparable to that of ES cells. In contrast to iPS cells, our data suggest that the reprogramming process in a hybrid cell system is realized without marked alteration of the imprinted *Dlk1-Dio3* locus, its methylation status, or the expression of the *Gtl2*, *Rian1*, and *Mirg* genes (Battulin et al., 2011). Interestingly, according to a report from Tada's group (Tada et al., 2001), the differential methylation patterns at the imprinted *H19* and *Igf3r* loci observed in parental cells were maintained in mouse ES cell–mouse thymocyte hybrid cells (Tada et al., 2001).

Another type of epigenetic modification of the genome is the acetylation of histones, which also affects the functional activity of genes. Kimura et al.

(2004) demonstrated that the reprogrammed somatic genome of *M. musculus musculus* ES cell–*M. musculus molossinus* thymocyte hybrid cells became hyperacetylated at histones H3 and H4, while lysine 4 (K4) of H3 became globally hyper-di- and -trimethylated. In the *Oct4* promoter region, histones H3 and H4 were acetylated, and H3–K4 was highly trimethylated in both the ES and the reprogrammed somatic genomes, which correlated with gene activation and DNA demethylation; however, H3–K4 was also di- and trimethylated in the promoter regions of *Neurofilament-M* (*Nfm*), *Nfl*, and *Thy-1*, which are all silent in both parental ES cells and hybrid cells. Kimura et al., 2004 suggested that H3–K4 di- and trimethylation of the somatic genome represents one of the major events that occur during its reprogramming.

There is reason to compare the efficiency of reprogramming by ES cell–somatic cell fusion with that achieved by generation of iPS cells. This comparison was recently made by Pera's group (Hasegawa et al., 2010). According to their findings, fusing human ES cells with human fibroblasts provides much faster and more efficient reprogramming of somatic cells than generating iPS cells. Generation of iPS cells required at least 4 weeks and was less than 0.001% efficient, whereas reprogramming by generation of hybrid cells required approximately 10 days and was more than 0.005% efficient (Hasegawa et al., 2010). It is also important to note that complete reprogramming occurred in almost all hybrid clones, whereas partial reprogramming was common in iPS cells.

5. Reprogramming Is Initiated in Heterokaryons

The formation of heterokaryons after cell fusion is the first stage in the generation of hybrid cells (Fig. 5.3). The main feature of heterokaryons is the presence of both parental nuclei in a common cytoplasm. The heterokaryon stage can continue from one to several days before the first division of parental nuclei. This is a marked advantage of heterokaryons, as it allows for the detection of the time at which the first signs of reprogramming appear and the dissection of the effects of *trans*-acting factors.

5.1. Reprogramming in heterokaryons generated by fusion of cells from different lineages

The first studies of heterokaryons obtained by fusion of proliferating cells of permanent lines such as human HeLa cells, mouse L and A cells, and nonproliferating cells including chicken erythrocytes, rabbit macrophages, and rat lymphocytes demonstrated the activation of DNA and RNA

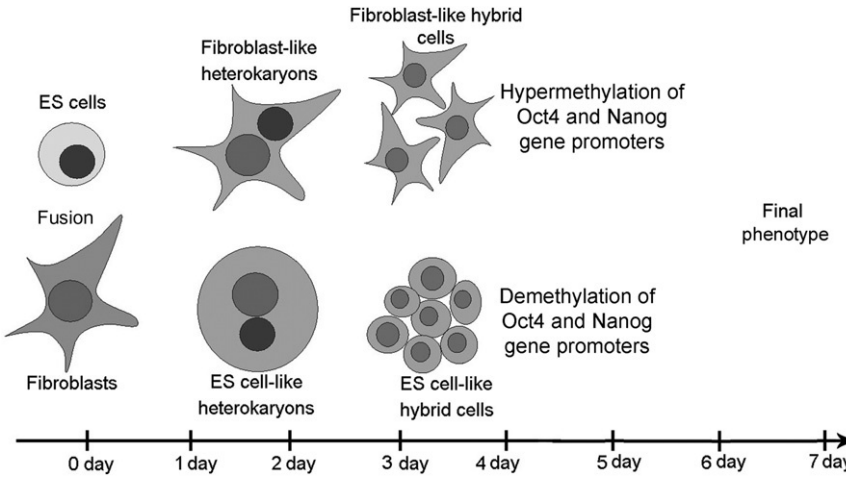

Figure 5.3 Time scale of the formation of heterokaryons and hybrid cells after fusion of mouse diploid ES cells and mouse diploid fibroblasts and time course of bidirectional reprogramming, including the final step involving demethylation/hypermethylation of the "pluripotent gene" promoters.

synthesis in nuclei derived from nonproliferating partners (Harris, 1965; Harris et al., 1966, 1969). Activation of the chicken hypoxanthine phosphoribosyltransferase and adenine phosphoribosyltransferase genes was observed in heterokaryons generated by fusion of chicken erythrocytes and human HeLa cells or mouse L cells (Harris and Cook, 1969; Ringertz and Savage, 1976). A low level of synthesis of chicken myosin was observed in chicken erythrocyte–rat myoblast heterokaryons (Carlsson et al., 1970), and synthesis of rat myosin light chains was observed in chicken myoblast–rat glial cell heterokaryons (Wright, 1984).

The suppression of the synthesis of tissue-specific products under the influence of *trans*-acting factors, such as the suppression of chicken hemoglobin synthesis in chicken erythroblast–mouse A cell heterokaryons, has often been observed (Ringertz and Savage, 1976). The suppression of immunoglobulin production in single heterokaryons formed from human myeloma cells and various other cell types that do not produce immunoglobulin was reported by Zeuthen et al. (1976). Importantly, the loss of immunoglobulin λ-light chain synthesis was observed in these heterokaryons shortly after fusion (4–6 h; Zeuthen et al., 1976). Further, suppression of the synthesis of tyrosine aminotransferase in rat hepatoma cell–mouse epithelial cell heterokaryons was demonstrated by Thompson and Gelehrter (1971). Both the activation of silent genes and the repression of tissue-specific genes are signs of reprogramming in heterokaryons; however, it

should be noted that the first studies of the generation of heterokaryons involved the use of highly aneuploid transformed cells that inevitably led to limitations in the interpretation of the data regarding the expression of parental genes.

Early pioneering studies performed by Blau's group (Blau et al., 1983, 1985; Chiu and Blau, 1984, 1985) have clearly demonstrated that in heterokaryons obtained by fusion of diploid adult cells from different lineages, reprogramming was initiated before cell division. Blau et al. (1983) described the presence of human myosin chains 1 and 2 as well as human MB- and MM-creatine kinase in 24-h heterokaryons generated by fusion of human diploid amniocytes and mouse muscle cells. Moreover, human MM-creatine kinase and the surface antigen 5.1H11 were detected in the heterokaryons regardless of whether DNA synthesis occurred (Chiu and Blau, 1984). This group later significantly extended the list of heterokaryons generated by fusion of diploid muscle cells with various human somatic cells derived from different embryonic layers, including mesoderm (fetal and adult skin fibroblasts, lung fibroblasts, chondrocytes, and amniotic fibroblasts), ectoderm (keratinocytes), and endoderm (hepatocytes; Blau et al., 1985). Although markers of human muscle cells, including MM- and MB-creatine kinase, myosin light chains (fetal, 1s, 2s, 2f, and actin mRNA α-cardiac), and cell surface antigens (24.1D5 and 5.1H11), were detected in all types of heterokaryons, the percentage of heterokaryons positive for muscle markers varied; for instance, human 5.1H11 antigen was detected in 95% of fibroblast–muscle cell heterokaryons, in 60% of keratinocyte–muscle cell heterokaryons, and only in 25% of hepatocyte–muscle cell heterokaryons. Thus, the activation of human muscle-specific genes in the tested heterokaryons was dependent on the nature of the somatic cell partner (Blau et al., 1985). Interestingly, the presence of trace quantities of human albumin was detected in hepatocyte–muscle cell heterokaryons until day 15 (Blau et al., 1985). These findings demonstrate the coexpression of the parental tissue-specific markers albumin and 5.1H11 in the heterokaryons and incomplete suppression of tissue-specific gene expression. A study by Miller et al. (1988) reported similar findings; in this study, simultaneous expression of human albumin and human muscle 5.1H11 antigen was detected in 1% of 2687 heterokaryons produced by fusion of mouse muscle cells and hepatoma cells synthesizing albumin.

Summarizing the findings obtained in studies of heterokaryons generated by fusion of diploid adult cells from different lineages demonstrates the reversibility of the differentiation status of specialized cells despite the stable and heritable nature of gene expression patterns in differentiated cells under normal circumstances (Blau et al., 1985).

Interestingly, the direction of reprogramming in hybrid cells often depends on the gene dose. This phenomenon was also observed in

heterokaryons. For instance, the expression of parental alleles in heterokaryons obtained by fusion of mouse muscle cells and human keratinocytes depended on the ratio of the parental nuclei; the human muscle antigen 5.1H11 (skeletal muscle neural cell adhesion molecule; NCAM) and human MyoD (the myogenic basic helix–loop–helix transcription factor MyoD) appeared significantly faster in heterokaryons with equal or near-equal numbers of mouse muscle and human keratinocyte or fibroblast nuclei than in heterokaryons with excess numbers of nonmuscle cell nuclei (Pavlath and Blau, 1986; Zhang et al., 2007). Moreover, alternative dominance of parental genomes was observed in mouse skeletal muscle cell–human keratinocyte heterokaryons; an excess of keratinocyte nuclei led to the activation of the keratinocyte program in muscle nuclei, and the muscle program was activated in keratinocyte nuclei when muscle cell nuclei were in excess (Palermo et al., 2009). A similar observation has been reported in other types of heterokaryons, such as mouse fibroblast–rat hepatoma heterokaryons (Mèvel-Ninio and Weiss, 1981).

5.2. Reprogramming in heterokaryons formed by fusion of cells with different developmental potential

5.2.1. Reprogramming in EC cell–somatic cell heterokaryons

There are few publications concerning heterokaryons generated by fusion of pluripotent EC cells and nonpluripotent cells. In addition, early studies often involved the use of heteroploid cells as somatic partners. Moreover, fusion of EC cells and somatic cells of established cell lines resulted in the formation of heterokaryons but not of viable hybrids (Featherstone and McBurney, 1981). For instance, mouse EC cells formed heterokaryons after fusion with 3T3 mouse fibroblasts, IMR90 human fibroblasts, HeLa cells, and Chinese hamster ovary (CHO) cells; however, only EC cell–3T3 heterokaryons developed into viable hybrids at a high frequency, whereas EC cell–HeLa, EC cell–IMR90, and EC cell-CHO heterokaryons were unable to give rise to hybrid cells. Featherstone and McBurney (1981) suggested that both developmental and phylogenetic differences between parental cells may contribute to the ability of heterokaryons to proliferate and to form hybrid cells.

An interesting observation has been made in a study in which *Oct4-GFP* transgenes were used to visualize the temporal onset of somatic cell genome reprogramming to the pluripotent state in F9–NSC hybrids (Han et al., 2008). These *Oct4-GFP* transgenes marked NSCs, and the reprogramming status of somatic cells could be determined by monitoring the expression of the *Oct4-GFP* transgene after cell fusion. The *Oct4-GFP* transgene was activated within 22 h of fusion, and within 24 h of fusion, the *Oct4-GFP* transgene and the endogenous *Oct4* and *Nanog* genes were demethylated. As the doubling time of F9 EC cells and hybrid cells was approximately 20 h, the

authors postulated that reprogramming of the somatic cell genome began during or immediately after the first cell cycle in the fused hybrid cells.

5.2.2. Time course of reprogramming in ES cell–somatic cell heterokaryons

The first study of interspecific heterokaryons involving ES cells focused on the timing of reprogramming (Pereira et al., 2008). The authors of this study produced heterokaryons by fusion of human B lymphocytes and mouse ES cells and enriched these heterokaryons up to 98–99% by FACS. It should be noted that the high proportion of heterokaryons in this study was maintained for 2 days before the number of heterokaryons dramatically decreased due to the increasing number of hybrid cells (Pereira et al., 2008). Unfortunately, cytogenetic analysis of these hybrid cells was not performed, and the composition of their chromosome complement thus remains unknown. Meanwhile, it is well known that extensive chromosomal segregation occurs in interspecific ES or EC cell–somatic cell hybrids obtained by the fusion of cells derived from remote species (Featherstone and McBurney, 1981; Serov et al., 1990).

Analysis of viable heterokaryons demonstrated that the first signs of reprogramming are manifested within 1–2 days of fusion. Expression of the human B lymphocyte-specific genes *CD19*, *CD37*, and *CD45* was not detected on the second day after fusion, and expression of *CD20* and *Pax5* was not detected on the third day, whereas reactivation of the human ES cell-specific genes *OCT4*, *NANOG*, *CRIPTO*, *DNMT3b*, *TIE1*, and *REX1* was observed within this time period (Pereira et al., 2008). Activation of these ES cell-specific genes occurred within 1–2 days; however, these genes were expressed at a very low level (< 1% of that detected in human ES cells). It is important to note that although the demethylation of the human *OCT4* promoter was detected prior to nuclear fusion and cell division, the methylation level remained high (56% vs. 9% in ES cells; Pereira et al., 2008).The authors of this study observed an interesting phenomenon: "irregularity of reprogramming" within the heterokaryon population. For instance, 13–16% of the examined cells were positive for the human ES cell-specific SSEA4 antigen. Moreover, the sorted SSEA4-positive cells were positive for human *OCT4*, *NANOG*, and *CRIPTO*, whereas SSEA4-negative cells were negative for *OCT4*, *NANOG*, and *CRIPTO*. The researchers concluded that "... only a proportion of heterokaryons are successfully reprogrammed..." (Pereira et al., 2008); however, these results can also be interpreted as evidence for bidirectional reprogramming (see below).

A more recent study by Bhutani et al. (2010) reported extensive demethylation of the human *OCT4* and *NANOG* promoters in heterokaryons 2–3 days after fusion of mouse ES cells and human fibroblasts. Further, it has been suggested that activation-induced cytidine deaminase

(AID) was responsible for the active demethylation in these cells because short interfering RNA (siRNA)-mediated knockdown of AID resulted in dramatic decreases in the transcriptional activity of the human *AID*, *OCT4*, and *NANOG* genes, and the *OCT4* and *NANOG* promoters remained hypermethylated in the treated heterokaryons (Bhutani et al., 2010). These data contradict the results of Pereira et al. (2008), who, as mentioned above, demonstrated partial demethylation of the *OCT4* promoter and observed low expression of pluripotency genes. It should be noted that AID activity is much higher in human B lymphocytes than in human fibroblasts (only 5% of that in lymphocytes), and the demethylase activity of AID would thus be expected to be higher in mouse ES cell–human B lymphocyte heterokaryons than in mouse ES cell–human fibroblast heterokaryons. DNA demethylation of the *OCT4* promoter should therefore be more effective in the former than the latter. To increase reprogramming activity, Bhutani et al. (2010) used a gene dosage effect with an excess of ES cells for cell fusion experiments. The resulting heterokaryons (polykaryons) thus contained an excess of nuclei derived from ES cells, whereas the heterokaryons described by Pereira et al. (2008) contained parental nuclei at a ratio close to 1:1. This difference in nuclear ratios is a potential explanation for the contradictory results obtained in these studies. In general, although a new role of AID as an active DNA demethylase was convincingly demonstrated (Bhutani et al., 2010), its role in the reprogramming process is not clear (Hanna et al., 2010). Low transcriptional activity of pluripotency genes in heterokaryons is a characteristic peculiar to "partially reprogrammed cells that express low levels of the endogenous *Oct4* gene without being demethylated" (Mikkelsen et al., 2008). Together, these findings suggest the view of Hanna et al. (2010) that ". . . AID may not be enough to induce complete pluripotential reprogramming" is valid.

More recently, we have performed immunofluorescent analysis of markers specific for parental genomes in heterokaryons and hybrid cells soon after the fusion of diploid ES cells marked with GFP and diploid embryonic fibroblasts labeled with blue fluorescent beads (Gridina and Serov, 2010). In addition, an analysis of parental mitochondrial DNA was used for reliable identification of the heterokaryons. Within 20 h of fusion, most heterokaryons (up to 80%) had a fibroblast-like phenotype, being positive for typical fibroblast markers (collagen type I, fibronectin, lamin A/C) and for the me3H3K27 chromatin modification marking the inactive X chromosome but negative for Oct4 and Nanog. Approximately, 20% of heterokaryons had an alternative ES cell-like phenotype, being positive for Oct4 and Nanog with signs of reactivation of the previously inactive X chromosome but negative for fibroblast markers. Hybrid cells with alternative phenotypes were easily identified 24–48 h after fusion. The level of DNA methylation of the promoter of the fibroblast *Oct4* allele in the ES cell-like hybrid cells on day 4 was similar to that of ES cells, but at the same time, both parental *Oct4* alleles were heavily methylated in fibroblast-like hybrid

cells. We concluded that bidirectional reprogramming initiated at the heterokaryon stage leads to the formation of two types of hybrid cells with alternative dominance of the parental genomes. The fates of these two types of hybrid cells are different: ES-like hybrid cells form colonies 4–6 days after fusion, but no colonies are derived from the fibroblast-like hybrid cells. Similar to mouse embryonic fibroblasts, the fibroblast-like hybrid cells grow as disconnected single cells and are unable to form colonies. Notably, the unilateral dominance of the ES genome over the somatic genome that has been reported in many publications can be partially explained by the nature of the somatic cell partners used in fusion experiments, such as splenocytes, thymocytes, lymphocytes, NSCs, or bone marrow cells (Matveeva et al., 1998; Pells et al., 2002; Tada et al., 2001; Terada et al., 2002; Ying et al., 2002), which are unable to grow as a monolayer and thus unable to give rise to hybrid colonies.

Taken together, the studies described above demonstrated unambiguously that reprogramming is initiated at the heterokaryon stage before the first mitosis. These findings are similar to those observed in EC cell–somatic cell hybrids (Han et al., 2008); however, it remains unclear when reprogramming is completed. Demethylation or hypermethylation of promoters of "pluripotency genes," such as *Oct4*, *Nanog*, and others, to levels characteristic of ES cells or the somatic partner can serve as an indicator of the completion of reprogramming. Although demethylation of the promoter of the lymphocyte *Oct4* allele is initiated in mouse ES cell–human lymphocyte heterokaryons in the first 2 days after fusion, its methylation level remains much higher than that observed in ES cells (Pereira et al., 2008). Further, we have observed nearly complete demethylation of the promoter of the fibroblast *Oct4* allele in ES cell–fibroblast cell hybrids with an ES cell-like phenotype at 4 days after fusion, and conversely, the level of hypermethylation of the ES cell *Oct4* allele in ES cell–fibroblast hybrids with a fibroblast-like phenotype was similar to that observed in fibroblasts (Gridina and Serov, 2010). In other words, these data have clearly demonstrated that the epigenetic equalization of the parental *Oct4* alleles is completed by 4 days after fusion. These data indicate that reprogramming in ES cell–somatic cell hybrids is realized through at least two steps: (i) silencing of genes specific for the somatic cell partner and simultaneous activation of genes specific for ES cells are initiated at the heterokaryon stage and (ii) the "fixation" of the new gene expression profile is continued through epigenetic mechanisms, in particular, through DNA methylation (Fig. 5.3). The total time required to complete reprogramming is at least 4–5 days; thus, reprogramming is complete upon the appearance of colonies of hybrid cells containing many hundreds of cells. The formation of these colonies undoubtedly requires cell division. Similarly, Hasegawa et al. (2010) estimated that reprogramming required 7–10 days in human ES cell–human fibroblast hybrid cells.

Based on this concept, reprogramming should be considered incomplete at the heterokaryon stage. Direct evidence supporting this statement was obtained by Sumer et al. (2009). The authors of this report studied heterokaryons obtained by fusion of tetraploid ES cells and diploid mesenchymal cells. As was expected, the heterokaryons acquired many characteristics typical of ES cells within 48 h of fusion. Removal of nuclei derived from tetraploid ES cells from heterokaryons by centrifugation (Pralong et al., 2005) allowed the authors to study the effect of the transient presence of tetraploid ES cell nuclei on the gene expression profile of the retained mesenchymal genome. After enucleation, "the ex-heterokaryons" had a tendency "to be reverted to an intermediate state that mostly resembles the donor somatic cell" (Sumer et al., 2009). Thus, the presence of both parental nuclei within the common cytoplasm is sufficient for the initiation of reprogramming but not for its completion.

6. Factors Determining the Direction of Reprogramming

6.1. Role of the nucleus and cytoplasm in reprogramming

Cell fusion technology allows the joining of two parental cells so that two nuclei are present within "a cytoplasm mixture" derived from both parental cells. Reprogramming is initiated at the heterokaryon stage, raising the question of the roles of the nucleus and the cytoplasm in this process. For a long time, most researchers thought that the cytoplasm played the lead role in reprogramming. This view was based on successful SCNT into the enucleated oocytes of mammals and amphibians (Di Berardino, 1997; Gurdon, 2006; Hochedlinger and Jaenisch, 2003, 2006). The exchange of nuclear factors between the donor cell nucleus and the enucleated egg cytoplasm was considered to be important for this process (Collas and Robl, 1991; Stice and Robl, 1988). The development of reconstructed cell technology allowed the assessment of the role of the nucleus and cytoplasm in cell fusion-mediated reprogramming.

Do and Schöler (2004) have prepared nucleus-free cell fragments (cytoplasts; cyESCs) and karyoplasts (kaESCs) containing minimal cytoplasm from mouse ES cells. Mouse NSCs carrying a GFP transgene under the control of the Oct4 promoter were then fused with either cyESCs or kaESCs derived from mouse ES cells. The authors observed the appearance of GFP-positive kaESC–NSC hybrid cells 2 days after fusion. Because the Oct4-GFP transgene is inactive in NSCs, its activation in the kaESC–NSC hybrid cells suggests that karyoplast-derived ES cells are able to reprogram the NSC genome. Moreover, these cells formed ES cell-like colonies and expressed pluripotency markers including Oct4, Rex-1, and Nanog.

In contrast, in experiments involving the fusion of cyESCs with NSCs or kaNSCs, no formation of hybrid cells was observed 3 or more days after fusion. In addition, cyESCs were unable to reactivate *Oct4-GFP* in NSCs (Do and Schöler, 2004). These data demonstrate that cyESCs lack factors crucial for reactivation of pluripotency genes.

However, results obtained by Strelchenko et al. (2006) indicate an important role for cytoplasm in reprogramming. Reconstructed cells generated by fusion of cytoplasts derived from human ES cells and karyoplasts derived from human fibroblasts acquired morphological characteristics similar to ES cells and were positive for Oct4. Thus, these data suggest that the cytoplasm of ES cells is able to reprogram the nucleus of fibroblasts and that reconstructed cells acquire the properties of ES cells. Strelchenko et al. (2006) proposed that these contradictory results could be explained by the much greater cytoplasmic volume in human ES cells when compared to mouse ES cells. Thus, the roles of the nucleus and cytoplasm in the process of reprogramming remain unclear.

6.2. Ploidy of parental cells determines the direction of reprogramming

It is known from previous research that the phenotype of hybrid cells depends on the relative number of chromosomes in each of the parental cells. A doubling of the chromosome number (2s) of one parental cell can yield hybrid cells in which previously unexpressed genes of the other cell partner can be activated. This phenomenon is known as the gene dosage effect. For example, the expression of glycerol-3-phosphate dehydrogenase in 1s glial cells is completely inhibited when these cells are fused with fibroblasts, but glycerol-3-phosphate dehydrogenase expression is only partially inhibited in hybrids generated by fusion of 2s glial cells with the same fibroblasts (Davidson and Benda, 1970). Similarly, melanin synthesis is inhibited in hybrid cells generated by fusion of 1s melanoma cells with fibroblasts but not in hybrid cells generated by fusion of 2s melanoma cells with the same fibroblasts (Davidson, 1972; Fougère et al., 1972). A gene dosage effect was also observed in many studies focused on parental tissue-specific gene expression. For example, some hybrid cells generated by fusion of subtetraploid mouse fibroblasts and rat hepatoma cells with a near-tetraploid chromosome complement were able to synthesize mouse serum albumin, whereas the hybrid cells generated by fusion of the same fibroblasts with rat hepatoma cells with a near-diploid karyotype were not able to produce mouse serum albumin (Peterson and Weiss, 1972). The activation of mouse liver genes for tyrosine aminotransferase, alanine aminotransferase, aldolase B, and alcohol dehydrogenase occurs in hybrid cells created by fusion of 2s rat hepatoma cells and mouse lymphoid cells but not in hybrids created by fusion of 1s rat hepatoma cells and lymphoid cells (Brown and Weiss, 1975). Complete

inhibition of hemoglobin synthesis occurs in hybrid cells generated by fusion of 1s mouse erythroleukemia (MEL) cells and nonerythroid cells (Axelrod et al., 1978; Disseroth et al., 1976; Orkin et al., 1975), whereas hemoglobin synthesis is not blocked in hybrids generated by fusion of 2s MEL cells with human or mouse fibroblasts (Axelrod et al., 1978).

These data prompted us to study gene dosage effects in hybrid cells generated by fusion of ES cells with somatic cells. Recently, we have produced a set of hybrid clones by fusion of mouse diploid ES cells carrying the GFP transgene with mouse tetraploid fibroblasts (Kruglova et al., 2010). Cytogenetic analysis demonstrated that most cells from these hybrid clones contained near-hexaploid chromosome complements. The presence of chromosomes derived from both parental cells was confirmed by analyzing of polymorphic microsatellites. All hybrid cells were positive for GFP and exclusively demonstrated fibroblast-like growth characteristics and morphology. Moreover, most hybrid cells were positive for typical fibroblast markers, such as collagen type I, fibronectin, and lamin A/C but were negative for Oct4 and Nanog. The methylation status of the *Oct4* and *Nanog* gene promoters was analyzed using bisulfite genomic sequencing analysis. The CpG sites of the *Oct4* and *Nanog* gene promoters were highly methylated in hybrid cells, whereas the same CpG sites were unmethylated in the parental ES cells. Thus, the fibroblast genome dominated the ES genome in the diploid ES cell–tetraploid fibroblast hybrid cells (Kruglova et al., 2010). Immunofluorescent analysis of the pluripotent and fibroblast markers demonstrated that the fibroblast phenotype was established in all heterokaryons shortly (4–8 h) after fusion. As mentioned above, among the population of heterokaryons obtained by fusion of diploid ES cells and diploid fibroblasts, 20% of the cells had ES-like phenotypes and 80% had fibroblast-like phenotypes (Gridina and Serov, 2010). These data demonstrate that increasing the ploidy of the somatic partner results in a shift from bidirectional reprogramming to unidirectional reprogramming.

Further, we performed experiments involving the fusion of karyoplasts and cytoplasts derived from tetraploid fibroblasts with whole diploid ES cells and found that karyoplasts were able to establish the fibroblast phenotype in the reconstructed cells but that fibroblast-derived cytoplasts were not (Kruglova et al., 2010). Taken together, these data suggest that the dominance of parental genomes in ES cell–somatic cell hybrids depends on the ploidy of the somatic partner.

6.3. Effect of cell cycle stages of fused partners on nuclear reprogramming

It is obvious that at the time of fusion, the parental cells may be at different stages of the cell cycle. How the cell cycle of fused cells can affect nuclear reprogramming has been studied by Sullivan et al. (2006). In one series of

fusion experiments, the authors investigated whether nuclear reprogramming activity in ES cells is sensitive to the state of organization of the incoming chromatin by fusing ES cells with quiescent fibroblasts. In these experiments, ES cells were fused with either cycling fibroblasts or quiescent nonproliferating fibroblasts after 6 days of serum starvation, and a 38.6-fold increase in the number of hybrid cell colonies was observed when ES cells were fused with quiescent fibroblasts. All hybrids displayed an ES cell phenotype. Moreover, the authors demonstrated that the difference in colony numbers was not due to a difference in death rates or an increased fusion rate between ES cells and cycling or quiescent fibroblast populations. It should be noted that heterokaryon formation was slightly decreased when ES cells were fused with quiescent fibroblasts.

In another series of experiments, thymocytes were fused with ES cells at different degrees of confluence to investigate the effect of the cell cycle stage of ES cells on reprogramming. Fusions between thymocytes and ES cells showed that the number of hybrid colonies was greatest when the ES cells were 90–100% confluent. At this level of confluence, the ES cell population contained the highest proportion (88.1%) of S + G2/M cells. Considering that serum starvation caused the majority of fibroblasts to remain in G0, the researchers concluded that hybrid cell colonies most effectively arise by fusion of ES cells in the S or G2/M phases with G0 somatic cells. They also suggested that successful nuclear reprogramming requires an initial round of replication of quiescent somatic nuclei in the presence of factors that are active in the ES cytoplasm at the S and G2/M phases (Sullivan et al., 2006).

7. Concluding Remarks

Somatic nuclei can be reprogrammed via fusion of the targeted cells with ES cells, EC cells, or somatic cells derived from other lineages. The phenotype of the resulting hybrid cells is determined by the dominance of the genome of one of the parental cells only, that is, an "all-or-none principle." The establishment of the dominance of one genome is initiated at the heterokaryon stage, when parental nuclei are present as distinct units in a common cytoplasm. At the same stage, a choice occurs to determine which parental genome will be dominant. Several factors influence this choice, including the ploidy of the parental cells or the nuclear ratio in polykaryons (muscle cell–nonmuscle cell heterokaryons), the cell cycle status of the parental cells, the balance between the transcription factors derived from the parental cells, and the receptivity of the recessive genome to transcription factors derived from the dominant genome. Despite these findings, the nature of bilateral reprogramming remains obscure.

The main peculiarity of ES cell-mediated reprogramming is the restoration of developmental potential in hybrid cells to a degree similar to that of

diploid ES cells. This restoration of developmental potential can be observed in the capacity of hybrid cells to generate chimeric embryos and adult chimeras and in their capacity to give rise to derivatives of the three germ layers and presumptive germ cells during *in vitro* and *in vivo* differentiation. The reprogramming process is realized via wide-scale silencing of genes specific for the somatic partner and activation of genes specific for the pluripotent partner in the somatic partner genome. It has been suggested that although gene activation and silencing are coordinated events in reprogramming, they are mechanistically distinct (Hasegawa et al., 2010; Terranova et al., 2006). Complete reprogramming requires a period of at least 5–7 days after cell fusion; reprogramming is complete at the time point when the first colonies of hybrid cells appear and give rise to hybrid clones. The initial events of reprogramming at the heterokaryon stage and in early hybrid cells must then be "fixed" by epigenetic remodeling of the somatic genome to yield a new state of chromatin organization and gene expression profiles similar to those of ES cells. These epigenetic events require cell division. Cell division is especially important for changes in global and local DNA methylation states. In conclusion, cell fusion technology is an effective tool for providing rapid and complete reprogramming.

REFERENCES

Allan, B., 1987. Production and analysis of chimeric mice. In: Robertson, E.J. (Ed.), Teratocarcinoma and Embryonic Stem Cells: A Practical Approach. IRL Press, Oxford, England, pp. 125–139.

Ambrosi, D.J., Rasmussen, T.P., 2005. Reprogramming mediated by stem cell fusion. Cell. Mol. Med. 9, 320–330.

Ambrosi, D.J., Tanasijevic, B., Kaur, A., Obergfell, C., O'Neill, R.J., Krueger, W., et al., 2007. Genome-wide reprogramming in hybrids of somatic cells and embryonic stem cells. Stem Cells 25, 1104–1113.

Andrews, P.W., Goodfellow, P.N., 1980. Antigen expression by somatic cell hybrids of a murine embryonal carcinoma cell with thymocytes and L cells. Somatic Cell Genet. 6, 271–284.

Artzt, K., Jacob-Cohen, R.J., Dimeo, A., Alton, A.K., Darling, G., 1980. Reexpression of a T/t-complex antigen (t^{12}) in thymocyte x embryonal carcinoma cell hybrids. Somatic Cell Genet. 7, 423–434.

Atsumi, T., Shirayoshi, Y., Takeichi, M., Ocada, T.S., 1982. Nullipotent teratocarcinoma cells acquire the pluripotency for differentiation by fusion with somatic cells. Differentiation 23, 83–86.

Axelrod, D.E., Gopalakrishnan, T.V., Willing, M., Anderson, W.F., 1978. Maintenance of hemoglobin inducibility in somatic cell hybrids of tetraploid (2S) mouse erythroleukemia cells with mouse or human fibroblasts. Somatic Cell Genet. 4, 157–168.

Battulin, N.R., Pristyazhnyuk, I.E., Matveeva, N.M., Fishman, V.S., Vasilkova, A.A., Serov, O.L., 2009. Allelic expression and DNA methylation profiles of promoters at the parental Oct4 and Nanog genes in *Mus musculus* ES cell/*Mus caroli* splenocyte hybrid cells. Cell Tissue Res. 337, 439–448.

Battulin, N.R., Kruglova, A.A., Boyarskih, U.A., Menzorov, A.G., Filipenko, M.L., Serov, O.L., 2011. Reprogramming somatic cells by fusion with embryonic stem cells does cause not silencing of Dlk1-Dio3 region in mice. World J. Stem Cells (submitted).

Ben-Shushan, E., Pikarsky, E., Klar, A., Berhgman, Y., 1993. Extinction of *Oct-3/4* gene expression in embryonal carcinoma x fibroblast somatic cell hybrids is accompanied by changes in the methylation status, chromatin structure, and transcriptional activity of the Oct-3/4 upstream region. Mol. Cell. Biol. 13, 891–901.

Bhutani, N., Brady, J.J., Damian, M., Sacco, A., Corbel, S.Y., Blau, H.M., 2010. Reprogramming towards pluripotency requires AID-dependent DNA demethylation. Nature 463, 1042–1047.

Blau, H.M., Chiu, C.-P., Webster, C., 1983. Cytoplasmic activation of nuclear genes in stable heterocaryons. Cell 32, 1171–1180.

Blau, H.M., Pavlath, G.K., Hardeman, E.C., Chiu, C.-K., Silberstein, L., Webster, S.G., et al., 1985. Plasticity of the differentiated state. Science 230, 738–766.

Bradly, A., Evans, M., Kaufman, M.H., Robertson, E., 1984. Formation of germ-line chimaeras from embryo-derived teratocarcinoma cell lines. Nature 309, 255–256.

Brown, J.E., Weiss, M.C., 1975. Activation of production of mouse liver enzymes in rat hepatoma-mouse lymphoid cell hybrids. Cell 6, 481–494.

Caiafa, P., Zampieri, M., 2005. DNA methylation and chromatin structure: the puzzling CpG islands. J. Cell. Biochem. 94, 257–265.

Campbell, K.H.S., McWhir, J., Ritchie, W.A., Wilmut, I., 1995. Production of live lambs following nuclear transfer of cultured embryonic disc cells. Theriogenology 43, 181–188.

Campbell, K.H.S., McWhir, J., Ritchie, W.A., Wilmut, I., 1996. Sheep cloned by nuclear transfer from a cultured cell line. Nature 380, 64–66.

Carlsson, S.-A., Savage, R.E., Ringertz, N.R., 1970. Behaviour of differentiated hen nuclei in cytoplasm of rat myoblasts and myotubes. Nature 228, 869–871.

Chan, E.M., Ratanasirintrawoot, S., Park, I.H., Manos, P.D., Loh, Y.H., Huo, H., et al., 2009. Live cell imaging distinguishes bona fide human iPS cells from partially reprogrammed cells. Nat. Biotechnol. 27, 1033–1037.

Chiu, C.-P., Blau, H.M., 1984. Reprogramming cell differentiation in the absence of DNA synthesis. Cell 37, 879–887.

Chiu, C.-P., Blau, H.M., 1985. 5-Azacytidine permits gene activation in a previously noninducible cell type. Cell 40, 417–424.

Collas, P., Robl, J.M., 1991. Relationship between nuclear remodeling and development in nuclear transplant rabbit embryos. Biol. Reprod. 45, 455–465.

Correani, A., Croce, C.M., 1980. Expression of the teratocarcinoma phenotype in hybrids between totipotent mouse teratocarcinoma and myeloma cells. J. Cell. Physiol. 105, 73–79.

Cowan, C.A., Atienza, J., Melton, D.A., Eggan, K., 2005. Nuclear reprogramming of somatic cells after fusion with human embryonic stem cells. Science 309, 1369–1373.

Davidson, R.L., 1972. Regulation of melanin synthesis in mammalian cells: effect of gene dosage on the expression differentiation. Proc. Natl. Acad. Sci. USA 69, 951–955.

Davidson, R.L., Benda, P., 1970. Regulation of specific functions of glial cells in somatic hybrids. II. Control of inducibility of glycerol-3-phosphate dehydrogenase. Proc. Natl. Acad. Sci. USA 67, 1870–1877.

Dewey, M.J., Martin, D.W., Martin, G.R., Mintz, B., 1977. Mosaic mice with teratocarcinoma-derived mutant cells deficient in hypoxanthine phosphoribosyltransferase. Proc. Natl. Acad. Sci. USA 74, 5564–5568.

Di Berardino, M.A., 1997. Genomic Potential of Differentiated Cells. Columbia University Press, New York.

Disseroth, A., Velez, R., Burk, R.D., Minna, J., Anderson, W.F., Nienhuis, A., 1976. Extinction of globin gene expression in human fibroblast x mouse erythroleukemia cell hybrids. Somatic Cell Genet. 2, 373–384.

Do, J.T., Schöler, H.R., 2004. Nuclei of embryonic stem cells reprogram somatic cells. Stem Cells 22, 941–949.

Do, J.T., Schöler, H.R., 2005. Comparison of neurosphere cells with cumulus cells after fusion with embryonic stem cells: reprogramming potential. Reprod. Fertil. Dev. 17, 143–149.

Do, J.T., Han, D.W., Schöler, H.R., 2006. Reprogramming somatic gene activity by fusion with pluripotent cells. Stem Cell Rev. 2, 257–264.

Do, J.T., Han, D.W., Gentile, L., Sobek-Klocke, I., Stehling, M., Lee, H.T., et al., 2007. Erasure of cellular memory by fusion with pluripotent cells. Stem Cells 25, 1013–1020.

Donovan, P., 1994. Growth factor regulation of mouse primordial germ cell development. Curr. Top. Dev. Biol. 229, 189–225.

Duboule, D., Croce, C.M., Illmensee, K., 1982. Tissue preference and differentiation of malignant rat x mouse hybrid cells in chimaeric mouse fetuses. EMBO J. 1, 1595–1603.

Eakin, G.S., Behringer, R.R., 2003. Tetraploid development in the mouse. Dev. Dyn. 228, 751–766.

Eggan, K., Akutsu, H., Loring, J., Jackson-Grusby, L., Klemm, M., Rideout III, W.M., et al., 2001. Hybrid vigor, fetal overgrowth, and viability of mice derived by nuclear cloning and tetraploid embryo complementation. Proc. Natl. Acad. Sci. USA 98, 6209–6214.

Featherstone, M.S., McBurney, M.W., 1981. Formation and fate of heterokaryons involving embryonal carcinoma cells. Somatic Cell Genet. 7, 205–217.

Flasza, M., Shering, A.F., Smith, K., Andrews, P.W., Talley, P., Johnson, P.A., 2003. Reprogramming in inter-species embryonal carcinoma–somatic cell hybrids induces expression of pluripotency and differentiation markers. Cloning Stem Cells 5, 339–354.

Forejt, J., Gregorova, S., Dohnal, K., Nosek, J., 1984. Gene expression of differentiated parent in teratocarcinoma cell hybrids. Repression or reprogramming? Cell Differ. 15, 229–234.

Fougère, C., Ring, E., Ephrussi, B., 1972. Gene dosage dependence of pigment synthesis in melanoma x fibroblast hybrids. Proc. Natl. Acad. Sci. USA 69, 330–334.

Gmür, R., Knowles, B.B., Solter, D., 1981. Regulation of phenotype in somatic cell hybrids derived by fusion of teratocarcinoma cell lines with normal or tumor-derived mouse cells. Dev. Biol. 81, 245–254.

Goldberg, A.D., Allis, C.D., Bernstein, E., 2007. Epigenetics: a landscape takes shape. Cell 128, 635–638.

Gridina, M.M., Serov, O.L., 2010. Bidirectional reprogramming of mouse embryonic stem cell/fibroblast hybrid cells is initiated at the heterokaryon stage. Cell Tissue Res. 342, 377–389.

Guo, J., Tacirlioglu, R.T., Ngnyen, L., Koh, K., Jenkin, G., Trounson, A., 2010. Reprogramming factors involved in hybrids and cybrids of human embryonic stem cells with hepatocytes. Cell. Reprogram. 12, 529–541.

Gurdon, J.B., 1962. Adult frogs derived from the nuclei of single somatic cells. Dev. Biol. 4, 256–273.

Gurdon, J.B., 2006. The reversal of cell differentiation. Annu. Rev. Cell Dev. Biol. 22, 1–22.

Han, D.W., Do, J.T., Gentile, L., Stehling, M., Lee, H.T., Schöler, H.R., 2008. Pluripotential reprogramming of the somatic genome in hybrid cells occurs with the first cell cycle. Stem Cells 26, 445–454.

Hanna, J.H., Saha, K., Jaenisch, R., 2010. Pluripotency and cellular reprogramming: facts, hypotheses, unresolved issues. Cell 143, 508–525.

Harris, H., 1965. Behavior of differentiated nuclei in heterokaryons of animal cells from different species. Nature 206, 583–588.
Harris, H., Cook, P.R., 1969. Synthesis of an enzyme determined by an erythrocyte nucleus in a hybrid cell. J. Cell Sci. 5, 121–133.
Harris, H., Watkins, J.F., Ford, C.E., Schoefl, G.I., 1966. Artificial heterokaryons of animal cells from different species. J. Cell Sci. 1, 1–30.
Harris, H., Sidebottom, E., Grace, D.M., Bramwell, M.E., 1969. The expression of genetic information: a study with hybrid animal cells. J. Cell Sci. 4, 499–525.
Hasegawa, K., Zhang, P., Wei, Z., Pomeroy, J.E., Lu, W., Pera, M.F., 2010. Comparison of reprogramming efficiency between transduction of reprogramming factors, cell–cell fusion, and cytoplast fusion. Stem Cells 28, 1338–1348.
Hochedlinger, K., Jaenisch, R., 2003. Nuclear transplantation, embryonic stem cells, and the potential for cell therapy. N. Engl. J. Med. 349, 275–286.
Hochedlinger, K., Jaenisch, R., 2006. Nuclear reprogramming and pluripotency. Nature 441, 1061–1067.
Hogan, B., Beddington, R., Constantini, F., Lacy, E., 1994. Manipulating the Mouse Embryo, second ed. Cold Spring Harbor Laboratory Press, Cold Spring Harbor.
Howe, W.E., Oshima, R.G., 1982. Coordinate expression of parietal endodermal functions in hybrids of embryonal carcinoma and endodermal cells. Mol. Cell. Biol. 2, 331–337.
Jaenisch, R., Bird, A., 2003. Epigenetic regulation of gene expression: how the genome integrates intrinsic and environmental signals. Nat. Genet. 33, 245–254.
Joyner, A.L., 1993. Gene Targeting: A Practical Approach. Oxford University Press, Oxford, England.
Keefer, C.L., Stice, S.L., Mathews, D.L., 1994. Bovine inner cell mass cells as donor nuclei in the production of nuclear transfer embryos and calves. Biol. Reprod. 50, 935–939.
Kim, K., Doi, A., Wen, B., Ng, K., Zhao, R., Cahan, P., et al., 2010. Epigenetic memory in induced pluripotent stem cells. Nature 467, 285–290.
Kimura, H., Tada, M., Nakatsuji, N., Tada, T., 2004. Histone code modifications on pluripotential nuclei of reprogrammed somatic cells. Mol. Cell. Biol. 24, 5710–5720.
Kruglova, A.A., Kizilova, E.A., Zhelezova, A.I., Gridina, M.M., Golubitsa, A.N., Serov, O.L., 2008. Embryonic stem cell/fibroblast hybrid cells with near-tetraploid karyotype provide high yield of chimeras. Cell Tissue Res. 334, 371–380.
Kruglova, A.A., Matveeva, N.M., Gridina, M.M., Battulin, N.R., Karpov, A., Kiseleva, E.V., et al., 2010. Dominance of parental genomes in embryonic stem cell/fibroblast hybrid cells depends on the ploidy of the somatic partner. Cell Tissue Res. 340, 437–450.
Lavagnolli, T.M.C., Fonseca, S.A.S., Serafima, R.C., Pereira, V.S., Santos, E.J., Abdelmassih, S., et al., 2009. Presumptive germ cells derived from mouse pluripotent somatic cell hybrids. Differentiation 78, 124–130.
Liu, L., Luo, G.Z., Yang, W., Zhao, X., Zheng, Q., Lv, Z., et al., 2010. Activation of the imprinted Dlk1-Dio3 region correlates with pluripotency levels of mouse stem cells. J. Biol. Chem. 285, 19483–19490.
Lyko, F., Paro, R., 1999. Chromosomal elements conferring epigenetic inheritance. Bioessays 21, 824–832.
Matveeva, N.M., Shilov, A.G., Bayborodin, S.I., Philimonenko, V.V., Rolinskaya, I.V., Serov, O.L., 1996. Hybrids between murine embryonal stem and somatic cells maintain their pluripotency. Dokl. Akad. Nauk. (Russian) 349, 129–132.
Matveeva, N.M., Shilov, A.G., Kaftanovskaya, E.M., Maximovsky, L.P., Zhelezova, A.I., Golubitsa, A.N., et al., 1998. *In vitro* and *in vivo* study of pluripotency in intraspecific hybrid cells obtained by fusion of murine embryonic stem cells with splenocytes. Mol. Reprod. Dev. 50, 128–138.

Matveeva, N.M., Pristyazhnyuk, I.E., Temirova, S.A., Menzorov, A.G., Vasilkova, A., Shilov, A.G., et al., 2005. Unequal segregation of parental chromosomes in embryonic stem cell hybrids. Mol. Reprod. Dev. 71, 305–314.

McBurney, M.W., Strutt, B.J., 1979. Fusion of embryonal carcinoma cells to fibroblast cells, cytoplasts, and karyoplasts: Developmental properties of viable fusion products. Exp. Cell Res. 124, 171–180.

McBurney, M.W., Strutt, B.J., 1980. Genetic activity of X chromosomes in pluripotent female teratocarcinoma cells and their differentiated progeny. Cell 21, 357–364.

McBurney, M.V., Featherstone, M.S., Kaplan, H., 1978. Activation of teratocarcinoma-derived hemoglobin genes in teratocarcinoma-Friend cell hybrids. Cell 15, 1323–1330.

Medvinsky, A., Smith, A., 2003. Stem cells: fusion brings down barriers. Nature 422, 823–825.

Mèvel-Ninio, M., Weiss, M.C., 1981. Immunofluorescence analysis of the time-course of extinction, reexpression, and activation of albumin production in rat hepatoma-mouse fibroblast heterokaryons and hybrids. J. Cell Biol. 90, 339–350.

Mikkelsen, T.S., Hanna, J., Zhang, X., Ku, M., Wernig, M., Schorderet, P., et al., 2008. Dissecting direct reprogramming through integrative genomic analysis. Nature 454, 49–55.

Miller, R.A., Ruddle, F.H., 1976. Pluripotent teratocarcinoma–thymus somatic cell hybrids. Cell 9, 45–55.

Miller, R.A., Ruddle, F.H., 1977. Properties of teratocarcinoma-thymus somatic cell hybrids. Somatic Cell Genet. 3, 247–261.

Miller, S.C., Pavlath, G.K., Blakely, B.T., Blau, H.M., 1988. Muscle cell components dictate hepatocyte gene expression and the distribution of the Golgi apparatus in heterokaryons. Genes Dev. 2, 330–340.

Mintz, B., Illmensee, K., 1975. Normal genetically mosaic mice produced from malignant teratocarcinoma cells. Proc. Natl. Acad. Sci. USA 72, 3585–3589.

Mise, N., Sado, T., Tada, S., Takagi, N., 1996. Activation of the inactive X chromosome induced by cell fusion between a murine EC and female somatic cell accompanies reproducible changes in the methylation pattern of the *Xist* gene. Exp. Cell Res. 223, 193–202.

Modinski, J.A., Gerhauser, D., Lioli, B., Winking, H., Illmensee, K., 1990. Nuclear transfer from teratocarcinoma cells into mouse oocytes and eggs. Development 108, 337–348.

Nagy, A., Rossant, J., 1993. Production of completely ES-derived fetuses. In: Joyner, A. (Ed.), Gene Targeting: A Practical Approach. IRL Press, Oxford, England, pp. 147–179.

Nagy, A., Gocza, E., Diaz, E.M., Prideaux, V.R., Ivany, M., Markkula, M., et al., 1990. Embryonic stem cells alone are able to support fetal development in the mouse. Development 110, 815–821.

Okuyama, K., Takagi, N., Sasaki, M., 1986. Sequential X-chromosome reactivation and inactivation in cell hybrids between murine embryonal carcinoma cells and female rat thymocytes. Exp. Cell Res. 1164, 323–334.

Orkin, S.H., Harosi, F.I., Leder, P., 1975. Differentiation in erythroleukemic cells and their somatic hybrids. Proc. Natl. Acad. Sci. USA 72, 98–102.

Palermo, A., Doyonnas, R., Bhutani, N., Pomerantz, J., Alkan, O., Blau, H.M., 2009. Nuclear reprogramming in heterokaryons is rapid, extensive, and bidirectional. FASEB J. 23, 1431–1440.

Papaioannou, V.E., Gardner, R.L., McBurney, M.W., Babinet, C., Evans, M.J., 1978. Participation of cultured teratocarcinoma cells in mouse embryogenesis. J. Embryol. Exp. Morphol. 44, 93–104.

Papp, B., Plath, K., 2011. Reprogramming to pluripotency: stepwise resetting of the epigenetic landscape. Cell Res. 3, 486–501.

Pavlath, G.K., Blau, H.M., 1986. Expression of muscle genes in heterokaryons depends on gene dosage. J. Cell Biol. 102, 124–130.

Pells, S., Di Domenico, A.I., Gallagher, E.J., McWhir, J., 2002. Multipotentiality of neuronal cells after spontaneous fusion with embryonic stem cells and nuclear reprogramming *in vitro*. Cloning Stem Cells 4, 331–338.

Pereira, C.F., Terranova, R., Ryan, N.K., Santos, J., Morris, K.J., Cui, W., et al., 2008. Heterokaryon-based reprogramming of human B lymphocytes for pluripotency requires Oct4 but not Sox2. PLoS Genet. 4, e1000170.

Peterson, J., Weiss, M.C., 1972. Expression of differentiated functions in rat hepatoma-mouse fibroblast hybrids. Proc. Natl. Acad. Sci. USA 69, 571–575.

Pralong, D., Mrozik, K., Occhiodoro, F., Wijesundara, N., Sumer, H., van Boxtel, A.L., et al., 2005. A novel method for somatic cell nuclear transfer to mouse embryonic stem cells. Cloning Stem Cells 7, 265–271.

Pralong, D., Trounson, A.O., Verma, P.J., 2006. Cell fusion for reprogramming pluripotency. Toward elimination of the pluripotent genome. Stem Cell Rev. 2, 331–340.

Pristyazhnyuk, I.E., Matveeva, N.M., Graphodatskii, A.S., Serdyukova, N.A., Serov, O.L., 2010. Chromosome composition of interspecies hybrid embryonic stem cells in mice. Cell Tissue Biol. 4, 128–135.

Puzakov, M.V., Battulin, N.R., Temirova, S.A., Matveeva, N.M., Serdiukova, N.A., Graphodatsky, A.S., et al., 2007. Analysis expression of parental alleles Xist and Gla in interspecific embryonic hybrid cells during induced in vitro inactivation of the X-chromosomes. Russ. J. Dev. Biol. 38, 164–170.

Ringertz, N.R., Savage, R.E., 1976. Cell Hybrids. Academic Press, New York, London, San Francisco.

Robertson, E.J., 1987. Embryo-derived stem cell lines. In: Robertson, E.J. (Ed.), Teratocarcinomas and Embryonic Stem Cells: A Practical Approach. IRL Press, Oxford, England, pp. 71–112.

Robertson, E., Bradley, A., 1986. Production of permanent cell lines from early embryos and their use in studying developmental problems. In: Rossant, J., Pedersen, R.A. (Eds.), Experimental Approaches to Mammalian Embryonic Development. Cambridge University Press, Cambridge, England, pp. 475–508.

Rossant, J., McBurney, M.W., 1982. The developmental potential of a euploid male teratocarcinoma cell line after blastocyst injection. J. Embryol. Exp. Morphol. 70, 99–112.

Rousset, J.-P., Dubois, P., Lasserre, C., Aviles, D., Fellous, M., Jami, J., 1979. Phenotype and surface antigens of mouse teratocarcinoma x fibroblast cell hybrids. Somatic Cell Genet. 5, 739–752.

Rousset, J.-P., Bucchini, D., Jami, J., 1983. Hybrids between F9 nullipotent teratocarcinoma and thymus cells produce multidifferentiated tumors in mice. Dev. Biol. 96, 331–336.

Schaap, G.H., Verkerk, A., Van Der Kamp, A.V.M., Jongking, J.F., 1982. Selection of proliferating cybrid cells by dual laser flow sorting. Exp. Cell Res. 140, 299–305.

Schaap, G.H., Devilee, P., van Klaveren, P., Jongkind, F., 1984. Gene expression in flow sorted mouse teratocarcinoma x human fibroblast heterokaryons. Differentiation 26, 127–133.

Serov, O.L., Zhdanova, N.S., Pack, S.D., Lavrentieva, M.V., Shilov, A.G., Rivkin, M.I., et al., 1990. The mink X-chromosome: organization and inactivation. In: Izozymes: Structure, Function, and Use in Biology and Medicine. Progress in Clinical and Biological Research, vol. 344. Wiley-Liss, New York, pp. 589–619.

Serov, O., Matveeva, N., Kuznetsov, S., Kaftanovskaya, E., Mittmann, J., 2001. Embryonic hybrid cells: a powerful tool for studying pluripotency and reprogramming of the differentiated cell chromosomes. An. Acad. Bras. Cienc. 73, 561–568.

Silva, J., Chambers, I., Pollard, S., Smith, A., 2006. Nanog promotes transfer of pluripotency after cell fusion. Nature 44, 997–1001.
Sims, M., First, N.L., 1993. Production of calves by nuclear transfer of nuclei from cultured inner cell mass cells. Proc. Natl. Acad. Sci. USA 91, 6143–6147.
Stadtfeld, M., Apostolou, E., Akutsu, H., Fukuda, A., Follett, P., Natesan, S., et al., 2010. Aberrant silencing of imprinted genes on chromosome 12qF1 in mouse induced pluripotent stem cells. Nature 465, 175–181.
Stewart, T.A., Mintz, B., 1981. Successive generation of mice produced from an established culture line of euploid teratocarcinoma cells. Proc. Natl. Acad. Sci. USA 78, 6314–6318.
Stice, S.L., Robl, J.M., 1988. Nuclear reprogramming in nuclear transplant rabbit embryos. Biol. Reprod. 39, 657–664.
Stice, S.L., Strelchenko, N.S., Keefer, C., Mathews, L., 1996. Pluripotent bovine embryonic cell lines direct embryonic development following nuclear transfer. Biol. Reprod. 54, 100–110.
Strelchenko, N., Kukharenko, V., Shkumatov, A., Verlinsky, J., Kuliev, A., Verlinsky, Y., 2006. Reprogramming of human somatic cells by embryonic stem cell cytoplast. Reprod. Biomed. Online 12, 107–111.
Sullivan, S., Pells, S., Hooper, M., Gallagher, E.D., McWhir, J., 2006. Nuclear reprogramming of somatic cells by embryonic stem cells is affected by cell cycle stage. Cloning Stem Cells 8, 174–188.
Sumer, H., Jones, K.L., Liu, J., Rollo, B.N., van Boxtel, A.L., Pralong, D., et al., 2009. Transcriptional changes in somatic cells recovered from ES-somatic heterokaryons. Stem Cells Dev. 18, 1361–1368.
Sumer, H., Nicholls, G., Pinto, A.R., Indraharan, D., Liu, J., Lim, M.L., et al., 2010. Chromosomal and telomeric reprogramming following ES–somatic cell fusion. Chromosoma 119, 167–176.
Surani, M.A., 2001. Reprogramming of genome function through epigenetic inheritance. Nature 414, 122–128.
Surani, M.A., Hayashi, K., Hajkova, P., 2007. Genetic and epigenetic regulators of pluripotency. Cell 128, 747–762.
Tada, M., Takahama, Y., Abe, K., Nakatsuji, N., Tada, T., 2001. Nuclear reprogramming of somatic cells by *in vitro* hybridization with ES cells. Curr. Biol. 11, 1553–1558.
Tada, M., Morizane, A., Kimura, H., Kawasaki, H., Ainscough, J.F.X., Sasai, Y., et al., 2003. Pluripotency of reprogrammed somatic genomes in embryonic stem hybrid cells. Dev. Dyn. 227, 504–510.
Takagi, N., 1983. De novo X-chromosome inactivation in somatic hybrid cells between the XO mouse embryonic carcinoma cell and XY rat lymphocyte. Exp. Cell Res. 145, 397–404.
Takagi, N., 1993. Variable X chromosome inactivation patterns in near-tetraploid murine EC x somatic cell hybrid cells differentiated *in vitro*. Genetica 88, 107–117.
Takagi, N., Yoshida, M.A., Sugawara, O., Sasaki, M., 1983. Reversal of X-inactivation in female mouse somatic cells hybridized with murine teratocarcinoma stem cells *in vitro*. Cell 43, 1053–1062.
Terada, N., Hamazaki, T., Oka, M., Hoki, M., Mastalerz, D.M., Nakano, Y., et al., 2002. Bone marrow cells adopt the phenotype of other cells by spontaneous fusion. Nature 416, 542–545.
Terranova, R., Pereira, C.F., Du Roure, C., Merkenschlager, M., Fisher, A.G., 2006. Acquisition and extinction of gene expression programs are separable events in heterokaryon reprogramming. J. Cell Sci. 119, 2065–2072.
Thompson, E.B., Gelehrter, T.D., 1971. Expression of tyrosine aminotransferase activity in somatic cell heterokaryons: evidence for negative control of enzyme expression. Proc. Natl. Acad. Sci. USA 68, 2589–2593.

Vasilkova, A.A., Kizilova, H.A., Puzakov, M.V., Shilov, A.G., Zhelezova, A.I., Golubitsa, A.N., et al., 2007. Dominant manifestation of pluripotency in embryonic stem cell hybrids with various numbers of somatic chromosomes. Mol. Reprod. Dev. 74, 941–951.

Wakayama, T., Perry, A.C.F., Zuccotti, M., Johnson, K.R., Yanagimachi, R., 1998. Full-term development of mice from enucleated oocytes injected with cumulus cell nuclei. Nature 394, 369–394.

Wang, X., Willenbring, H., Akkari, Y., Torimaru, Y., Foster, M., Al-Dhalimy, M., et al., 2003. Cell fusion is the principal source of bone-marrow-derived hepatocytes. Nature 422, 897–901.

Wilmut, I., Schniek, A.E., McWhir, J., Kind, A.J., Campbell, K.H.S., 1997. Viable offspring derived from fetal and adult mammalian cells. Nature 385, 810–813.

Wolpert, L., Smith, J., Jessel, T., Lawrence, P., Robertson, E., Meyerowitx, E., 2006. Principles of Development, third ed. Oxford University Press, Oxford, England.

Wright, W.E., 1984. Induction of muscle genes in neural cells. J. Cell Biol. 98, 27–35.

Yamanaka, S., Blau, H.M., 2010. Nuclear reprogramming to a pluripotent state by three approaches. Nature 465, 704–712.

Yang, X., Smith, S.L., Tian, X.C., Lewin, H.A., Renard, J.-P., Wakayama, T., 2007. Nuclear reprogramming of cloned embryos and its implications for therapeutic cloning. Nat. Genet. 39, 295–302.

Ying, Q.-L., Nichols, J., Evans, E.P., Smith, A.G., 2002. Changing potency by spontaneous fusion. Nature 416, 545–548.

Yu, J., Vodyanik, M.A., He, P., Slukvin, I.I., Thomson, J.A., 2006. Human embryonic stem cells reprogram myeloid precursors following cell–cell fusion. Stem Cells 24, 168–176.

Zeuthen, J., Stenman, S., Fabricius, H.-A., Nilsson, K., 1976. Expression of immunoglobulin synthesis in human myeloma x non-lymphoid cell heterokaryons: evidence for negative control. Cell Differ. 4, 369–383.

Zhang, F., Pomerantz, J.H., Sen, G., Palermo, G.A., Blau, H.M., 2007. Active tissue-specific DNA demethylation conferred by somatic cell nuclei in stable heterokaryons. Proc. Natl. Acad. Sci. USA 104, 4395–4400.

CHAPTER SIX

New Insights into the Characteristics of Sweet and Bitter Taste Receptors

Piero A. Temussi

Contents

Abstract

Understanding the molecular bases of taste is of primary importance for the field of human senses as well as for translational medical science. This chapter describes the complexity of the mechanism of action of sweet, bitter, and umami receptors. Most molecular weight sweeteners interact with orthosteric sites of the sweet receptor. The mechanism of action of sweet proteins is more difficult to interpret. In the only general mechanism proposed for the action of sweet proteins, the "wedge model," it is hypothesized that proteins bind to an external active site of the active conformation of the sweet receptor. This model can be updated by building topologically correct complexes of proteins with the receptor. Among the recent advances that will be described here are the

Department of Chemistry, Universita di Napoli Federico II, via Cinthia, Napoli, Italy
National Institute for Medical Research, The Ridgeway, London, United Kingdom

International Review of Cell and Molecular Biology, Volume 291
ISSN 1937-6448, DOI: 10.1016/B978-0-12-386035-4.00006-9

discovery of taste modulators and the possibility that certain bitter compounds are recognized by the umami receptor.

Key Words: Sweeteners, Taste receptors, Wedge model, Sweet proteins

1. Introduction

Until a decade ago, the molecular biology of taste was less known than those of other senses, to the extent that Lindemann (1996) defined taste as *the Cinderella of senses*. The cloning of several taste receptors rekindled the interest in this sense (Firestein, 2000) and opened entirely new perspectives for the design of artificial sweeteners. The sweet receptor was identified almost simultaneously by several different groups (Bachmanov et al., 2001; Kitagawa et al., 2001; Li et al., 2001; Max et al., 2001; Montmayeur et al., 2001; Nelson et al., 2001; Sainz et al., 2001). Knowing the nature of the receptor provided a better understanding of the molecular bases of sweet taste but many questions are left unanswered. Among these is the puzzling phenomenon of sweet proteins. Disclosing the mechanism of action of sweet proteins covers a key role in understanding the structure–activity relationship of sweet molecules and helps to frame the role of taste qualities linked to food acceptance.

Although a sharp classification of tastes is not universally accepted (Delwiche, 1996), the existence of five basic tastes, that is, sweet, bitter, salty, sour, and umami, is acknowledged by most scientists (Lindemann, 2001). Among these taste qualities, sweet and bitter are the most important for food acceptance or rejection. The central role of sweet taste is shown by the widespread response of most people to the sensation of sweetness, with a propensity for sweet foods that for many goes back to early life.

Since glucose is the body's main source of energy, recognition of sweet molecules may have evolved to accept sugars. The ability to recognize bitter molecules may have protected many animals from the ingestion of toxic compounds, mainly those produced by plants. Many people associate sweet taste only with sugars. However, this is not at all true: among sweet molecules, there are hundreds of synthetic and natural sweeteners, found in early times mainly by serendipity and, in more recent times, by conscious search of new sweeteners. Till the half of the past century, organic chemists used to taste the compounds they synthesized because organoleptic features were part of the standard characterization procedure and many substances turned out to be sweet (Moncrieff, 1967). Sweet molecules belong to many families of different chemical constitution: sugars, amino acids, olefinic alcohols, nitroanilines, peptides, proteins, and many other organic

compounds. More than the diversity in chemical constitution, it was striking to acknowledge that sweet molecules can have hugely different volumes, from very small glycine to large proteins (Morris, 1976), a puzzling feature in the hypothesis that they interact with the same receptor. For instance, the molecular volumes of brazzein and saccharin can be estimated as 7863 and 133 A^3, respectively. The demonstration, by *in silico* calculations, that proteins stabilize the active form of the T1R2–T1R3 receptor clarified the multiple site characteristic of the receptor (Temussi, 2002).

An additional role in food acceptance is played by the umami taste. Umami taste may have been useful in evolution to recognize sources of proteins because umami receptors respond to several amino acids deriving from the breakdown of proteins. It will be shown that the main umami receptor may play a pivotal role between bitter and sweet receptors.

2. Taste Receptors

As mentioned in Section 1, molecular–biological studies on taste were scanty before 1990s, but then, in a short time, many combined efforts yielded a large number of proteins related to sensory transduction mechanisms (Kinnamon, 2000). The first proteins identified in the signaling cascade of taste cells were components of the G proteins oligomers, in particular, α-gustducin (McLaughlin et al., 1992) and α-transducin (McLaughlin et al., 1994), but it was not clear whether they were functionally significant (Lindemann, 1999). The first taste-specific G-protein-coupled receptor (GPCR) cloned and characterized was one of the umami taste receptors (Chaudhari et al., 2000). Almost at the same time, Chandrashekar et al. (2000) reported the characterization of a large family of putative mammalian bitter taste receptors, T2Rs, and another group identified a family of candidate taste receptors, the TRBs (Matsunami et al., 2000).The main features of taste receptors are beautifully summarized in a review by Chandrashekar et al. (2006). After the mentioned attempts to find the first taste receptors, it was soon found that the receptors for sweet and umami, the taste modalities related to acceptance of food, belong to a family of (GPCRs), T1Rs, related to other class C GPCRs (Bachmanov et al., 2001; Kitagawa et al., 2001; Li et al., 2001; Max et al., 2001; Montmayeur et al., 2001; Nelson et al., 2001; Sainz et al., 2001).

The members of the family involved in the recognition of sweet molecules are T1R2 and T1R3. Functional expression studies showed convincingly that the T1R2–T1R3 heterodimer recognizes all known sweet molecules, including sugars, synthetic sweeteners, R-amino acids, and even a few sweet proteins (Li et al., 2002). Umami taste, the unique savory

sensation originally proposed by Japanese scientists, is exemplified by the taste of two acidic amino acids, glutamate and aspartate. These molecules are recognized, in taste cells, by yet another heterodimeric receptor of the T1R family: T1R1–T1R3. However, contrary to the sweet taste receptor, this is not unique. A few different receptors have been proposed for umami: in addition to the mentioned first taste-specific GPCR characterized by Chaudhari et al. (2000), a second umami receptor different from T1R1–T1R3 is a truncated mGluR1 (San Gabriel et al., 2005).

In contrast to the sweet taste, for which a single receptor can recognize many widely different ligands, the many different bitter compounds found in nature are recognized by a family of more than 30 GPCRs, called collectively T2Rs. These GPCRs are different from those of the T1R family because they have no prominent extracellular domain, but essentially only the seven-transmembrane (7TM) domain.

Salt and sour tastes are characterized less than sweet, bitter, and umami. Several studies seem to suggest that salty and sour ligands, such as cations and protons, enter directly in taste cells using membrane channels. The identification of specific salt receptors is still a matter of debate (Lyall et al., 2004), but there is recent evidence that PKD2L1 functions as the acid receptors in the taste system (Huang et al., 2006).

2.1. 7TM GPCRs

GPCRs constitute a family of transmembrane receptors that can recognize a large variety of molecules present outside the cell, activate signal transduction pathways, and in turn cause cellular responses. The human genome encodes thousands of GPCRs, which detect hormones, growth factors, and other endogenous ligands. Classically, the GPCR family was divided into three main classes (A, B, and C) with no clear sequence homology between them. Class A accounts for ca. 85% of the GPCR genes, notably olfactory receptors and several receptors that recognize endogenous ligands. Later on, a more articulate classification has been proposed (Attwood and Findlay, 1994). According to this proposal, GPCRs can be grouped into six classes: class A (rhodopsin-like), class B (secretin receptor-like), class C (metabotropic), class D (mating pheromone receptors), class E (cyclic AMP receptors), and class F (frizzled). Figure 6.1 shows cartoons illustrating the main features of generic 7TM GPCRs (A) and class C GPCRs (B). Figure 6.1B shows also the two main domains of a dimer of class C GPCRs, the VFT domain and the 7TM domain common to all GPCRs.

The molecules that can be recognized and consequently can activate these receptors include not only tastants but also a variety of other compounds: light-sensitive molecules, neurotransmitters, hormones, pheromones, etc. A ligand bound to the receptor induces a conformational change in the GPCR, which, transmitted to the cytoplasmic end of the GPCR, allows it

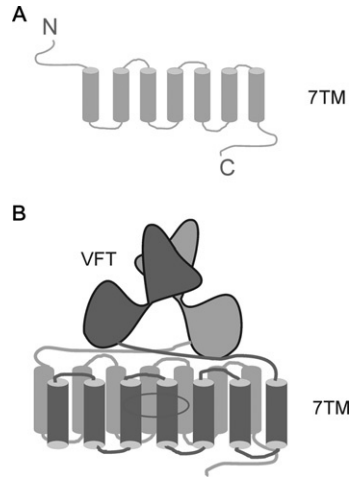

Figure 6.1 Schematic models of GPCRs. (A) A simple 7TM GPCRs (classes A–F). (B) A heterodimer of a class C GPCRs. The two protomers are represented with different shades of gray.

to act as a guanine nucleotide exchange factor. In turn, the GPCR can then activate a coupled G-protein by exchanging its bound GDP for a GTP. The G-protein's α subunit, together with the bound GTP, can then dissociate from the β and γ subunits affecting intracellular signaling proteins.

In mammals, bitter molecules are recognized by a number of GPCRs, termed T2Rs (Adler et al., 2000; Matsunami et al., 2000). Each T2R can detect a wide variety of bitter molecules, consistently with the need, for humans and most mammals, to recognize many bitter compounds with a relatively small number of receptors. Many of these receptors are still orphaned but recent progress has begun to identify their substrates (Behrens and Meyerhof, 2006). T2Rs are class F GCPR receptors (frizzled). The T2Rs, although expressed in dedicated taste receptor cells, share common signal transduction components with cells detecting sweet and umami taste qualities. As they lack the extensive N-terminal domain characteristic of class C GPCRs, the active sites are shaped only by the juxtaposition of their 7TM helices. The flexibility of the transmembrane domains makes them ideally suited to accept a large number of chemically different molecules, but this also makes the modeling of their active sites rather difficult (Floriano et al., 2006; Miguet et al., 2006).

2.2. Metabotropic GPCRs

As previously mentioned, the first sweet receptor, T1R3, a member of the T1R family was identified in 2001 as the result of combined efforts from several laboratories (Bachmanov et al., 2001; Kitagawa et al., 2001;

Li et al., 2001; Max et al., 2001; Montmayeur et al., 2001; Nelson et al., 2001; Sainz et al., 2001). To understand the rationale of the approaches followed by these groups, it is convenient to follow the description found in Montmayeur et al. (2001). On the basis of numerous biochemical and electrophysiological studies, it seemed highly probable that at least some of the taste receptors were GPCRs (Gilbertson et al., 2000). The Sac locus is one of the genetic loci that control sensitivity, in mouse or humans, to bitter or sweet compounds (Bachmanov et al., 1997; Blizard et al., 1999; Capeless and Whitney, 1995; Fuller, 1974; Lush, 1989; Lush et al., 1995). To identify genes controlling sweet taste, Montmayeur et al. (2001) followed an approach similar to the one that had located some T2R genes at or near genetic loci that control sensitivity to bitter taste (Adler et al., 2000; Matsunami et al., 2000). Montmayeur et al. (2001), looking for genes that encode GPCRs, identified T1R3, a gene encoding a protein that is expressed in part of the taste cells in mouse, and found allelic differences between Sac taster and nontaster strains that could result in differences in Sac phenotype. In addition, they found that T1R2, a related receptor, is expressed in the same taste cells expressing T1R3, hinting at the possibility that the two receptors might function as heterodimers or that these cells recognize more than one ligand. Looking at the behavior of most metabotropic, or class C, GPCR, most researchers believed that the sweet taste receptor was a (T1R3) homodimer. However, shortly afterward, Li et al. (2002) demonstrated that although T1R3 is able to recognize some sugars, only heterodimer T1R2–T1R3 can function as a sweet receptor.

The similarity with the binding of Glu in mGluR1 suggest that the sweet taste of small molecular weight sweeteners can certainly be accounted for by binding at orthosteric sites, even if the details will remain in part obscure, at least till a receptor structure with better resolution than homology models will be available. Can the taste of sweet proteins be also explained by the knowledge of the structure of the receptor? There is no obvious answer. Let us postpone an answer after we examine models and mechanisms of sweet receptors.

2.3. Models of the sweet receptor

The first structure of the N-terminal domain of a class C GPCR, the mGluR1 glutamate receptor (Kunishima et al., 2000), was reported only a few months before the discovery of T1R3. Combining this knowledge with the significant homology of the sequence of T1R3 to those of several other metabotropic receptors, in particular, to that of mGluR1, with which it shares ca. 20% identity, it was possible to build reliable models. The first homology model of the sweet receptor that used the structure of mGluR1 as template and the murine sequence of T1R3 was built as a homodimer of

two T1R3 chains (Max et al., 2001). These authors aligned the N-terminal domain of T1R3 and mGluR1 using the Clustal W program (Thompson et al., 1994) and then used the coordinates of one of the crystal structures of the N-terminal domain determined by Kunishima et al. (2000) to model the T1R3 homodimer. Modeling was performed with MODELLER (Sali and Blundell, 1993). The choice of a homodimer was a natural one because it was common knowledge that most class C GPCRs function as homodimers. Max et al. (2001), on the basis of their model, postulated that the main difference between tasters and nontasters resides in substitutions that affect N-linked glycosylation at N58, precluding correct dimerization. Another homodimeric model was used to show that the active site of T1R3 can consistently host very sweet small molecular weight molecules (Walters, 2002). This author used the human T1R3 sequence and the crystal structure of mGluR1 extracellular domain (Kunishima et al., 2000) in the active form binding glutamate (Protein Data Bank code: 1ewk) as template. In this case, homology modeling was performed using the Protein Design module of Quanta 98 (Accelrys, Inc., San Diego, CA).

After Li et al. (2002) demonstrated that only the heterodimer T1R2–T1R3 can function as a sweet receptor for all classes of sweet molecules, it was necessary to revise homology models also. The only possible template was still the structure of mGluR1, but it was necessary to build more than a single homology model since Kunishima et al. (2000) have published three different forms: one complexed with two molecules of glutamate and two ligand-free forms. Both the complexed form (1ewk.pdb) and the uncomplexed free form II (1ewv.pdb) are open–closed conformations and correspond to the active state of the receptor, whereas the other ligand-free form (1ewt.pdb) is in an open–open conformation and corresponds to a resting state of the receptor. The first heterodimeric T1R2–T1R3 homology model was built using the mouse sequences of the two protomers and the complexed form of mGluR1 as the template, arbitrarily choosing only one of the two possible active models, that is, the one with T1R2 closed and T1R3 open (Temussi, 2002).

The combination of two sequences (T1R2 and T1R3) and two conformations (open or closed) can generate four possible heterodimers: two inactive (open–open) and two active (open–closed). Morini et al. (2005) built all these models from the human sequences and used them to identify all possible sites of interaction. If we model T1R2 on chain A and T1R3 on chain B of the 1ewt template, we get the inactive form Roo_AB, whereas when we model T1R3 on chain A and T1R2 on chain B of the 1ewt template, we get inactive form Roo_BA. If we model T1R2 on chain A and T1R3 on chain B of 1ewk, we get Aoc_AB, whereas when we model T1R3 on chain A and T1R2 on chain B of 1ewk, we get Aoc_BA, the two possible active dimers. Figure 6.2 shows the molecular models of the four possible forms of the sweet receptor.

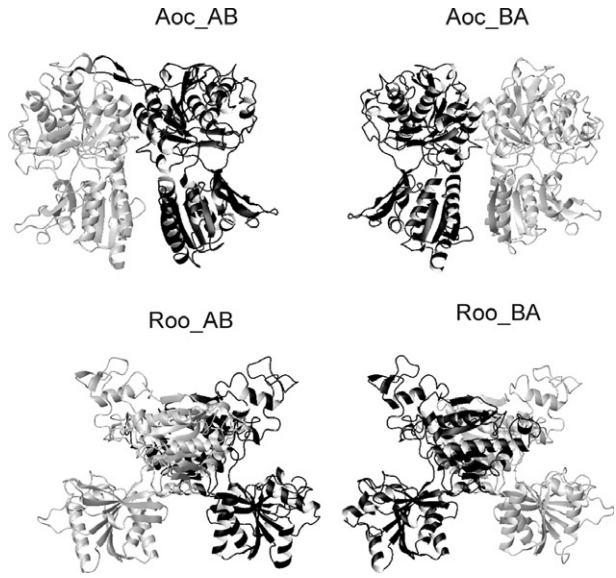

Figure 6.2 Molecular models of the four possible forms of the sweet receptor. Aoc_AB (T1R2 closed/T1R3 open), Aoc_BA (T1R3 closed /T1R2 open), Roo_AB (T1R2 open/T1R3 open), and Roo_BA (T1R3 open/T1R2 open). T1R2 protomers are represented as gray ribbons; T1R3 as black ribbons. Molecular models were generated with MOLMOL (Koradi et al., 1996).

2.4. Receptor modulators

The biggest new discovery during the past few years, in the field of taste receptors, is probably the identification of positive allosteric modulators (PAMs) of the sweet receptor. It had been known for a few years that GPCRs can be influenced by ligands that do not behave as agonists, yet are capable of exerting a profound influence on the mechanism of action of the receptors (May and Christopoulos, 2003). These atypical ligands are called PAMs. According to May and Christopoulos (2003), the simplest manifestation of an allosteric effect, that is, an alteration of orthosteric ligand affinity, can be described, in general, on the basis of the ternary complex model. However, some allosteric modulators of GPCRs do not fit within the ternary complex model. Some PAMs affect orthosteric ligand efficacy independently of, or in addition to, effects on orthosteric ligand binding, whereas others modify receptor function even in the absence of orthosteric ligand.

In the field of taste, it is common knowledge that umami taste can be greatly enhanced by the concomitant effect of ribonucleotides. It is interesting to note that this phenomenon represents a rare example of PAM for GPCRs occurring in nature. Inosine-5′-monophosphate (IMP) and

guanosine-5′-monophosphate (GMP) have been known for many years to potentiate the umami taste intensity of glutamate. Zhang et al. (2008) have recently elucidated the molecular mechanism of the IMP/GMP as PAM in the umami receptor. They showed that when glutamate is bound in the cavity of the VFT domain inducing the closure of the two lobes, IMP and GMP can further stabilize the closed conformation by binding near the opening of the domain.

Recently, Servant et al. (2010) developed PAMs of the human sweet taste receptor and, using mutagenesis and molecular modeling, found that the sweet enhancers follow mechanism similar to that of natural molecules responsible for the synergism of the umami taste. The chemical skeleton of SE-1 is somewhat akin to those of hypoxanthine and guanine, the aromatic moieties of the natural umami enhancers. Other compounds with analogous chemical skeletons proved good selective enhancers for sucralose (SE-2) or of both sucralose and sucrose (SE-3). These enhancers are not at all sweet on their own. In fact, they do not bind to the orthosteric site inducing the closure of the Venus flytrap domain; instead, like was the case for the umami enhancers, they bind close to the opening and further stabilize the closed and active conformation of the receptor.

3. Mechanisms of Interaction of Sweet Molecules

3.1. Small molecular weight compounds

When speaking of sweet taste, most people generally associate it with sugars. In addition to sucrose, there are many other molecules commonly referred to as *sugars*, that is, not only other water-soluble carbohydrates but also sugar alcohols with a characteristic sweet taste. The most obvious feature of all these compounds is that they are characterized by the presence on their skeleton of several hydroxyl groups, but it is not easy to find a unique distribution of these substituents attributable only to sweet sugars. Even considering the two monosaccharides contained in sucrose, that is, fructose and glucose, it is easy to see that they have the same number of hydroxyl groups but have a somewhat different sweetening power: 25% and 75% as sweet as sucrose, respectively. A class of polyol compounds distinct from sugar is that of sugar alcohols. The most important of these sugar substitutes are erythritol, glycerol, mannitol, and sorbitol.

The majority of amino acids of the L configuration, that is, the building blocks of proteins, are tasteless or bitter, but glycine, alanine, and some hydrophobic amino acids of R configuration are sweet (Solms et al., 1965). Actually, the very name of glycine comes from the Greek word for sweet. In addition to amino acids, there are several very sweet peptides. However,

although composed of natural amino acidic residues, they are not found in nature and are related to aspartame, L-aspartyl-phenylalanine methyl ester, the first sweet dipeptide, discovered by serendipity by Mazur et al., (1969) now widely used as an artificial sweetener.

Some extracts from plants are intensely sweet and, in turn, have led to the discovery of several sweet natural glycosides. The best known of them is stevioside, a component of *Eupatorium rebaudianum* (Bridel and Lavieille, 1931), 150–300 times sweeter than sucrose. Other natural sweeteners of small molecular weight are classified as semisynthetic when the original natural substance, although not sweet, becomes sweet after minor chemical modification (Morris, 1976). For instance, naringin dihydrochalcone, that is bitter, becomes very sweet when transformed into its dihydrochalcone (DuBois et al., 1981). The aglicone of neohesperidine dihydrochalcone represents a class of compounds that can be called isovanillyl sweet compounds (Bassoli et al., 2002a). The most representative natural isovanillyl molecules are phyllodulcin, dihydroquercetin 3-acetate, and hematoxylin, but the sweetest isovanillyl compounds are synthetic modifications discovered in the laboratory of Merlini (Bassoli et al., 2002a).

A very large number of organic molecules that were found to be sweet in the course of many decades of research in synthetic organic chemistry, either aimed at finding new sweeteners or serendipitous. In the past, it was a common practice among organic chemists to taste the new compounds they synthesized and many substances turned out to be sweet. In general, they are considerably more hydrophobic than most natural sweeteners.

In the first attempts to understand structure–taste relationships of molecules, researchers tried to identify specific atoms or groups of atoms (*sapophores*) that could impart a given taste to molecules. However, it was soon clear that these groups belonged to sweet and tasteless molecules with similar frequency, whereas other features, for example, the steric disposition of groups probably played an important role (Moncrieff, 1967). The first successful generalization was made by Shallenberger and Acree (1967) who hypothesized that the main signature for sweet molecules could reside in the presence on their skeleton of a hydrogen bond donor (AH) and a hydrogen bond acceptor (B) spaced 0.3–0.4 nm, because these two groups, by interacting with a complementary pair of hydrogen bond donor and acceptor on the receptor, would anchor the sweetener to the receptor. A few years later, more general indirect models of the active site were developed using the shape of conformationally rigid sweet molecules as molecular molds. For instance, Temussi and coworkers (Kamphuis et al., 1992; Temussi et al., 1978, 1984), combining several observations on rigid molds and using also flexible compounds, notably aspartame (Lelj et al., 1976), proposed a detailed quasi-planar outline of the active site. This is often referred to as the *Temussi model* (Walters, 1995; Walters et al., 1986). Another topological model was developed by Goodman et al. (1997). This model, while

incorporating most of the features of the Temussi model, differed in some sterical aspects related to the conformation of aspartame. A way to discriminate between the models of Temussi and Goodman would have been to know the conformation of aspartame in the actual receptor. Experimental structural studies on isolated aspartame were not sufficient to give an unequivocal answer: the conformer found in the crystal structure of aspartame (Hatada et al., 1985) is consistent with Goodman's model, whereas that of the more rigid and sweeter [(L-α-Me)Phe] aspartame (Polinelli et al., 1992) is consistent with Temussi's model.

The most popular model was that of Tinti and Nofre (1991). On the basis of their discovery of very potent guanidinium sweeteners (Nofre et al., 1988; Tinti and Nofre, 1991), they proposed a 3D model for an ideal sweetener that besides the AH-B entity has six additional interaction points connected by a complex network of distances. Just before the discovery of the sweet taste receptor, Bassoli et al. (2002b) proposed a unifying model able to explain and predict semiquantitatively the sweet taste of compounds belonging to different families. This model was based on the possibility of building artificial active sites using amino acid side chains unrelated to the (unknown) residues lining the actual receptor active site by means of PrGen (Vedani et al., 1995), a program that allows also the comparison of calculated binding affinity for ligands with the experimental sweetness. After the discovery of the sweet receptor, Morini et al. (2005) improved this hypothetical model using the actual residues lining the cavity of the T1R2–T1R3 receptor. The very possibility of modeling the VFT cavities had been questioned because the resolution of homology models is necessarily limited. For instance, Gokulan et al. (2005) had warned that the considerable conformational changes implied by the binding mechanism of VFT domains might represent an obstacle for accurately modeling the active sites of the receptor. However, Morini et al. (2005) exploited the conservation of key residues and the amino acidic nature of some sweetener to show that both active sites of active protomers can be used and account quantitatively for the relative sweetness of most sweet molecules. As mentioned earlier, the sweet receptor can be activated by simple hydrophobic amino acids and dipeptides. Residues lining the wall of the part of the cavity that binds amino acidic moieties should be highly conserved in going from mGluR1 to T1R2–T1R3. Indeed, residues that bind the α-amino acid moiety in mGluR1 are well conserved, not only in T1R2–T1R3 but also in the sequences of other families of metabotropic GPCRs (Pin et al., 2003). On the other hand, residues of the other part of the cavity are expected to be more variable, as in the sweet taste receptor, this part of the active site ought to accommodate molecular fragments of different size and chemical constitution. Consistently, the alignments corresponding to the four models show that residues binding the glutamate side chain in mGluR1 are changed to less polar or uncharged residues (Morini and Temussi, 2005).

In mGluR1, both closed (MOL1) and open (MOL2) protomers bind glutamate (Kunishima et al., 2000; Tsuchiya et al., 2002). Similarly, it was shown that sweeteners of different dimensions can bind also open VFT cavities (Morini et al., 2005). To probe semiquantitatively the fit of sweeteners in the active sites of the models, Morini et al. (2005) chose a large number of sweet molecules belonging to different families including sugars, peptides, and super sweeteners. Their fit was evaluated by means of PrGen (Vedani et al., 1995), using the actual residues of the sites in Aoc_AB and Aoc_BA, as previously done with hypothetical residues. It was possible to fit a large number of representative sweet compounds also in the binding sites of the open protomers. Although PrGen allows changes in the relative positions of the residues defining the site, the final active sites showed only minor changes with respect to those of the original homology models (Morini et al., 2005). The agreement between experimental and calculated relative sweetness for a large number of powerful sweeteners was remarkable.

The models of active sites belonging to the VFT domains of the sweet receptor can explain the taste of nearly all small molecular weight sweet molecules but none of them can explain the enormous increase in activity in going from small molecular weight compounds to proteins: monellin, for example, one of the best characterized sweet proteins, is 100,000 times sweeter than sucrose on a molar basis (Hung et al., 1999).

3.2. Pivotal role of sweet proteins

When mentioning sweet proteins, it is not unusual to hear the question: "Sweet proteins? In what sense?" It must be admitted that sweetness is not one of the qualities one normally associates with proteins. Yet, in the field of taste, it is now well known that there are in nature a few proteins that taste sweet and some of them are among the sweetest known molecules, on a molecular basis. Let us briefly examine all known sweet proteins.

Monellin and thaumatin were the first two sweet proteins clearly identified and characterized. Even the discoverers (Inglett and May, 1969) initially believed it was a carbohydrate because the very concept of a sweet protein was utterly unacceptable at the time. Morris and Cagan (1972), after they established that the sweet principle was a protein, named it monellin, after the Monell Chemical Senses Center where they worked. The sweetness of monellin, relative to sucrose, as measured by these authors was 3000:1 on a weight basis, corresponding to a ratio of 90,000:1 on a molar basis. Unlike most globular proteins, monellin is made up of two noncovalently linked subunits held together only by secondary forces (Bohak and Li, 1976). The sequence of monellin, like all sweet proteins, bears no significant similarity to that of any of the other sweet proteins (Temussi, 2006). Only whole monellin is sweet, whereas the

individual subunits, easily separated by heating, are not sweet (Bohak and Li, 1976). When the two chains are covalently linked, single-chain monellins retain the same sweetness as native monellin but have greatly increased thermal stability (Kim et al., 1989; Tancredi et al., 1992). The structures of both two-chain and single-chain forms of monellin have been thoroughly characterized by X-Ray and NMR (nuclear magnetic resonance) studies (Hung et al., 1999; Lee et al., 1999; Somoza et al., 1995; Spadaccini et al., 2001). The solution structure of MNEI, a single-chain monellin obtained by inserting a Gly-Phe dipeptide between the B and A chains (Tancredi et al., 1992), can be described as an α-helix cradled into the concave side of a five-strand antiparallel β-sheet (Spadaccini et al., 2001). To reconcile small and large sweeteners, some researchers postulated the existence, on the surface of monellin, of some kind of "sweet finger," that is, a protruding structural element hosting one or more glucophores similar to those of small sweeteners, in particular, the sequence TyrA13-AspA16 of native monellin (Kim et al., 1991). However, even drastic point mutations on residues A13 and A16 of synthetic monellin (Ariyoshi and Kohmura, 1994) did not lead to a significant decrease of sweetness. Extensive mutagenesis studies both on single-chain and wild-type monellin (Kohmura et al., 1992; Somoza et al., 1995) hinted at a large area of interaction with the receptor. The residues whose mutation causes a decrease of sweetness of two or more orders of magnitude are Ile6, Asp7, Gly9 (Kohmura et al., 1992), and Arg39 (Sung et al., 2001) whereas mutations of Gln13, Lys36, Lys43, Arg72, Arg88, or deletion of Pro92-Pro96 cause a decrease of one order of magnitude (Kohmura et al., 1992; Somoza et al., 1995). The distribution of key residues on a large area was confirmed, without recurring to any hypothesis on the mechanism of interaction, that is, in a completely objective way, by a surface survey based on novel NMR techniques (Niccolai et al., 2001).

Inglett and May (1968) reported that a West African plant, *Thaumatococcus danielli*, contains a sweet substance that is not a sugar but failed to identify it as a protein. The mysterious sweet substance was characterized by van der Wel and Loeve (1972) as a mixture of two proteins called thaumatin I and II. Their sweetening power was estimated as 100,000 times higher than that of sucrose on a molar basis. Thaumatin is a single polypeptide chain of 207 residues (Iyengar et al., 1979) belonging to the osmotin, thaumatin-like superfamily. The 3D structure of thaumatin, solved in the solid state by X-Ray studies (de Vos et al., 1985; Ogata et al., 1992), contains three domains, mainly composed of β-sheets.

The structure–activity relationship of thaumatin has been studied less than that of monellin. If one runs a comparison of the sequence of thaumatin with those of other sweet-tasting proteins by Clustal X (Thompson et al., 1997), the similarities are negligible (Tancredi et al., 2004). Suspecting the critical role of positive charges, Kaneko and Kitabatake (2001) found

that phosphopyridoxylation of Lys78, Lys97, Lys106, Lys137, or Lys187 reduced sweetness significantly. Combination of these results with those ensuing from modifications of other charged residues led them to suggest that there is a charged side of the protein that is important for sweetness. Recently, Ohta et al. (2008) performed a more systematic search for critical residues. They prepared mutant thaumatin proteins in which lysine or arginine residues were substituted by alanine residues. Four lysine residues (K49, K67, K106, and K163) and three arginine residues (R76, R79, and R82) were found to play significant roles in thaumatin sweetness, particularly K67 and R82. These studies are not conclusive but seem to point to a large surface of interaction also for thaumatin.

Brazzein was isolated fairly recently from *Pentadiplandra brazzeana B* (Ming and Hellekant, 1994). This protein is approximately 17,000 times sweeter than sucrose on a molar basis (Assadi-Porter et al., 2010). The structure of brazzein, determined by ^{1}H NMR spectroscopy in solution at pH 5.2 (Caldwell et al., 1998), contains one α-helix and three strands of antiparallel β-sheet. The structure is stabilized by four disulfide bonds, three connecting the helix to the β-sheet and the fourth one (C24–C52) linking N- and C-terminal peptides. The key residues for sweetness have been clustered by Assadi-Porter et al. (2010) in three sites. Site 1 is made up of residues 39–43, site 2 contains residues 2, 50, and 54, whereas site 3 is essentially defined by two disulfide bridges: 16–47 and 22–37. The same authors reported a spectacular double mutation that greatly increases the sweetening power: E41K/K42E.

Two new sweet proteins were isolated by Hu and Min (1983) from the seed of *Capparis masaikai* Levl., a plant of the subtropical region of China, and named mabinlin I and II. Mabinlin II has a sweetness with respect to sucrose of approximately 375:1 on a molar basis (Liu et al., 1993). It is in order to emphasize that mabinlin, although much sweeter than sucrose, is considerably less sweet than monellin, thaumatin, and brazzein. Mabinlin II contains two peptide chains (A and B) joined by four disulfide bridges (Liu et al., 1993). All sweetness can be attributed to chain B alone. The recently solved crystal structure revealed structural features typical of an "all α" fold, with an amphiphilic surface: a cationic side and a neutral side. In addition, mabinlin II is characterized by a unique structural motif consisting of a special sequence, NL-P-NI-C-NI-P-NI, which may play a role in receptor binding (Li et al., 2008).

Hen egg white (HEW) lysozyme is a small enzyme that breaks the cell walls of bacteria by hydrolysis of their polysaccharides. This protein has been included among sweet proteins only recently: according to Masuda et al. (2005), the sweetening power of HEW lysozyme corresponds to a threshold value of around 7 μM, a value that is at least three orders of magnitude lower than those of typical sweet proteins (monellin and thaumatin) but still higher than that of sucrose.

The fruits of *Synepalum dulcificum* have the very unusual property to cause sour substances to taste sweet. That's why the berries gained the name of miracle fruit (Morris, 1976) and the protein responsible for the phenomenon was named miraculin (Theerasilp and Kurihara, 1988). Miraculin is a polypeptide chain with 191 amino acid residues with a high homology to the amino acid sequence of the soybean trypsin inhibitor (Theerasilp et al., 1989). Gibbs et al. (1996) have claimed that miraculin can have a maximum value of sweetness 400,000 times that of sucrose, but it is difficult to compare this figure to those of the sweet-tasting proteins since the mechanism of action of miraculin apparently requires preventive (nonactive) occupancy of the receptor and it becomes sweet only after acidification (Kurihara and Beidler, 1969). Recently, Paladino et al. (2010) have tried to interpret the mechanism of action of miraculin on the basis of MD calculations. In particular, they conducted molecular dynamics simulations on wild-type miraculin and on three mutated dimers (H29A, H59A, and H29A/H59A) both at neutral and acidic pH. Their results suggest that at acidic pH, the presence of two charged His at the interface of the dimer induces a structural rearrangement of the two monomers, thus leading to their relative opening and the following adaptation of their conformation to the receptor surface.

No protein with both sweet-tasting and taste-modifying activities had previously been found. Curculin, a new taste-modifying protein discovered in 1990 (Yamashita et al., 1990), elicits a sweet taste, albeit very weak (equivalent to the sweetness of 0.35 M sucrose). After curculin, water elicits sweet taste and sour substances induce a stronger sense of sweetness. Shirasuka et al. (2004) and Suzuki et al. (2004) isolated a gene that encodes a novel protein highly homologous to curculin. Using cDNAs of the previously known curculin (dubbed curculin1) and the novel curculin isoform (curculin2), Suzuki et al. (2004) produced a panel of homodimeric and heterodimeric recombinant curculins by *Escherichia coli* expression systems. They found that sweet-tasting and taste-modifying activities were exhibited solely by the heterodimer of curculin1 and curculin2. Shirasuka et al. (2004) named this heterodimer neoculin and, on the basis of the isoelectric points, neoculin basic subunit (NBS), the polypeptide corresponding to curculin1 and neoculin acid subunit (NAS) curculin2.

3.3. The wedge model and its topological refinement

3.3.1. The wedge model

The discovery of the first sweet proteins (Morris, 1976) was a great shock for researchers studying sweet–activity relationship, even before the nature of taste receptors was elucidated. As mentioned in Section 1, the volume of a sweet protein is so different from those of all other sweet molecules that it was difficult to hypothesize an interaction with the same active sites

proposed for small molecular weight sweeteners. Another difficulty comes from the lack of similarity among sweet proteins. When studying a protein family, the first approach in the search for a common function is the comparison of their sequences, in search for corresponding parts. An alignment of these sequences performed by Clustal X (Thompson et al., 1997) shows that no sequence homology can be detected among monellin, thaumatin, brazzein, mabinlin, miraculin, and curculin (Tancredi et al., 2004). In principle, one could hypothesize that the interaction of proteins with the receptor might be due to some kind of sweet finger. Were it possible to identify, on the surface of the proteins, protruding features hosting moieties chemically similar to small sweeteners, it would be possible to unify the interaction of molecules of widely different dimensions under a common mechanism. As mentioned earlier, early ELISA tests hinted at the sequence TyrA13–AspA16 of native monellin and that comprising residues Tyr57–Asp59 of thaumatin as potential sweet fingers (Kim et al., 1991). Tancredi et al. (2004) undertook a systematic investigation to identify possible sweet fingers on the surface of brazzein, monellin, and thaumatin. The similarity among the tertiary folds of these three proteins is as low as that among their sequences. A 3D search of structures of each of the three proteins against the whole database by means of DALI (Holm and Sander, 1995) did not even retrieve the other two proteins. However, there are structural elements on each of the three surfaces that could be potential candidates for sweet fingers. Likely protruding elements should also have a sufficiently stable secondary structure: thus, we restricted our search to β-hairpins present in all three proteins. The case of brazzein is the simplest because its structure contains only one such hairpin, loop L23 (Tancredi et al., 2004). Its length and the presence of residues containing suitable glucophores are consistent with the requirements outlined above. In the case of MNEI (Tancredi et al., 2004), a single-chain monellin, the best choice is loop L34 that, although not completely free, is structurally similar to the loop of brazzein and, in addition, corresponds to the original sweet finger proposed by Kim et al. (1991). In the case of thaumatin, there are numerous loops with sufficient length to probe the receptor cavity, but nearly all are tightly bound to adjacent β-sheets. The only loop that is free enough to interact with the receptor is loop L56 (Tancredi et al., 2004). All three loops contain, among the side chains, an aromatic ring in relative spatial orientation, with respect to a pair of hydrogen bond donors or acceptors, similar to that found in aspartame. Starting from the sequences of these loops, Tancredi et al. (2004) synthesized the corresponding cyclic peptides: c[C56YFDDSGSGIC66], c[C61LYVYASDKLFRAC73], and c[C37FYDEKRNLQC47], with cyclization assured by disulfide bridges. The cyclic peptides do assume conformations consistent with the conformation of the same sequences in the parent proteins. However, none of them was sweet (Tancredi et al., 2004). Therefore, the sweet fingers hypothesis was abandoned.

The similarity between the sequences of T1Rs and that of mGluR1 suggested that the sweet receptor might have the same general features as mGluR1, particularly with respect to the mechanism of activation. Like mGluR1, the sweet receptor should also exist as a mixture of three forms: a complexed form, activated by low molecular weight sweeteners, and a resting ligand-free form I and ligand-free form II, with a structure nearly identical to that of the active complexed form. The equilibrium between form I and form II is generally shifted by acceptance by the receptor of a small sweetener but can also be shifted in another way. The top panel of Fig. 6.3A illustrates how stabilization can be achieved by external binding of a macromolecule on a secondary binding site on the surface of the active form of the receptor.

The main difference between the inactive open–open form (Roo, Fig. 6.3A) and the active open–closed form (Aoc, Fig. 6.3B) in equilibrium with it is the onset, in the active form, of a deep cavity. This cavity can host the tip of large proteins, as illustrated by docking calculations (Temussi, 2002). The use of a specific *in silico* docking procedure was not, however,

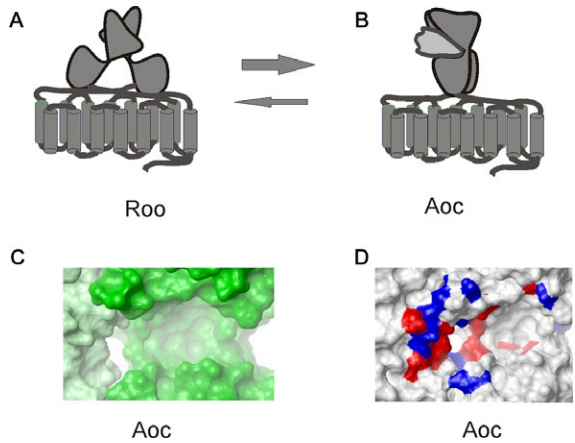

Figure 6.3 Wedge model. (A) Cartoon representation of the resting conformation of the sweet receptor (Roo, open–open). (B) Cartoon representation of the active conformation of the sweet receptor (Aoc, closed–open). This conformation here is stabilized by a sweet protein (represented as a gray wedge) binding to an external cavity involving both protomers (T1R2 and T1R3). (C) Molecular model of Aoc highlighting the shape of the cavity. The T1R2 protomer is colored in pale green; the T1R3 protomer is colored in dark green. (D) Molecular model of Aoc highlighting the distribution of charged residues in the cavity. Both protomers are colored white. Acidic residues inside the cavity are colored in red, whereas basic residues are colored in blue. Molecular models were generated with MOLMOL (Koradi et al., 1996).

an integral part of the wedge model and its limitations should be well understood. The use of GRAMM (Vakser, 1995; Vakser et al., 1999) or of any other docking program is only instrumental to show convincingly that sweet proteins with a wedge-shaped tip could actually dock the receptor using the same region (Morini et al., 2005; Temussi, 2002): we considered highly significant that our calculations hinted at the same active site for three proteins with completely different sequences and structures.

The resulting 3D models can only be a *fuzzy* representation of the complexes, not only because the sequence homology between template and target with either chains of the sweet receptor (T1R2 and/or T1R3) is low but also because the docking program could only be used meaningfully in its low-resolution mode. It is clear that, in the ensemble of a given sweet protein, individual models bind with different orientations of the same surface or even with different parts of their surface (Temussi, 2011). It is important to bear in mind that the essence of the wedge model rests on the acknowledgment of the homology between the sweet receptor and the glutamate receptor. The two proteins share 20% identity and 40% homology. This degree of homology is well above the twilight zone (Blake and Cohen, 2001), particularly when one is interested in the conservation of active sites. It has been shown that the active sites of distantly related proteins can have very similar geometries because of the coupling of the structural changes that has occurred during evolution (Lesk and Chothia, 1980). With such a degree of homology, we therefore expect that comparative modeling is reliable (Pastore and Lesk, 1990).

The shape of the external active site of Aoc that can host the tips of proteic wedges is a wide, narrow, and deep cavity, as shown by the model of Fig. 6.3C. It is necessary that the shape of the tip of a sweet protein should also be wide and narrow and obviously convex. In addition, the surface of the tip should host charged residues complementary to those of the receptor. The surface of the Aoc form of the receptor is prevalently negative (Esposito et al., 2006; Morini et al., 2005; Temussi, 2002), but the charged residues are not uniformly distributed inside the active site. Figure 6.3D shows a contact surface representation of Aoc in which the acidic residues inside the active site are colored in red and the basic residues in blue, respectively: the tip of a potential partner in the complex must have a complementary polarity.

Is it possible to select a single meaningful complex from this fuzzy ensemble? The best ways to improve the accuracy of the complexes are either to solve a high-resolution structure or to identify, by mutagenesis studies, key residues on sweet proteins and/or on the receptor, which may hint at a surface of interaction. However, the derivation of the detailed structure of a complex between two proteins on the basis of mutagenesis data is far from trivial. If the structures of two proteins are known at high resolution, it is possible to use powerful docking programs, but if the

structure of one of the partners is known at lower resolution, it is necessary to look for a different approach. In the numerous papers validating the monellin complex (De Simone et al., 2006; Esposito et al., 2006; Niccolai et al., 2001; Spadaccini et al., 2003), the procedure to extract a unique complex was implicit but was never explicitly illustrated. Recently, it has been shown that it only requires some topological considerations (Temussi, 2011). The case of sweet proteins is paradigmatic because only the structure of the sweet proteins is known at high resolution, whereas that of the receptor is at very low resolution. On the other hand, the shape and electronic features of the active site of the receptor offer unique topological constraints that can guide the choice of a meaningful complex. The shape of the external active site of Aoc, illustrated in Fig. 6.3C, is a wide, narrow, and deep cavity spanning both protomers. The shape of the tip of a sweet protein ought to have complementary properties, that is, it should also be wide and narrow and obviously convex. In addition, the surface of the sweet protein should host charged residues complementary to those of the receptor. It has been shown that the surface of the Aoc form of the receptor is prevalently negative (Esposito et al., 2006; Morini et al., 2005; Temussi, 2002), but the charged residues are not uniformly distributed inside the active site. Figure 6.3D shows a contact surface representation of Aoc in which the acidic residues inside the active site are colored in red and the basic residues in blue, respectively. Accordingly, the tip of a potential partner in the complex must have the same polarity, that is, with an uneven distribution of key charged residues.

Bearing in mind the two conditions illustrated by Fig. 6.3C and D, one can adjust low-resolution complexes to accurate locations on the sweet protein surface. The two proteins best suited to illustrate this validation procedure are monellin and brazzein, because of the great number of known mutants affecting sweetness, whereas fewer mutants have been reported for thaumatin (Ohta et al., 2008). The simultaneous use of accurate coordinates from key residues of the sweet protein imposes strong topological constraints: it is very unlikely that several residues of two sweet proteins have a one-to-one correspondence to receptor residues only by chance. Such a procedure, although not comparable to structure determination by experimental methods, should be sufficient to validate the model of interaction and to test its heuristic value with mutants not explicitly used in the validation procedure. Consistent with our previous findings, only the most likely active form of the receptor, according to Morini et al. (2005), was chosen, the T1R2 (closed)–T1R3 (open) model, dubbed Aoc_AB.

3.3.2. Refined complex of monellin

The wedge model for the complex of monellin with the sweet receptor has been validated indirectly, as documented in several papers (De Simone et al., 2006; Esposito et al., 2006; Niccolai et al., 2001; Spadaccini et al.,

2003), but the model did not yield precise coordinates of the complex because the low resolution of the receptor hindered such an approach. Recently, we have tried to yoke the complex to mutagenesis data to obtain a more detailed structure (Temussi, 2011). The architecture of monellin, like that of all cystatins, can be described as a wedge-shaped structure consisting of a five-strand β-sheet partially "wrapped" around an α-helix (Murzin, 1993).

Figure 6.4A(i) shows the surface of MNEI in contact with the receptor, suggested by previous studies. Figure 6.4A(ii) shows the same surface after a rotation of 180° around an axis perpendicular to the illustration. In order to perform some kind of tethered docking, we chose only charged residues (D7, K36, R39, K43, R72, and R88) among those whose mutation causes a decrease in sweetness from one (Q13, K36, K43, R72, R88, P92–P96) to two or more (I6, D7, G9, R39) orders of magnitude (Somoza et al., 1995; Spadaccini et al., 2003). This apparently arbitrary choice is motivated by the fact that it is simpler to find a one-to-one correspondence to charged residues of the receptor with respect to interactions of neutral residues that can interact with several residues at comparable distance. Figure 6.4(iii), (iv) shows the same MNEI models of Fig. 6.4(i), (ii) as would be seen from the solution when complexed to the receptor. The side chains of charged residues inside the cavity are color coded, as customarily, in blue for basic and red for acidic, respectively. Charged MNEI side chains are colored in cyan and magenta for basic and acidic residues, respectively. It is clear that locating most charged residues of MNEI on the left side of the cavity (Fig. 6.4A(iii)) is consistent with a satisfactory match of positive and negative charges located on the receptor, whereas the other possible orientation of the wedge would lead the charged residues of MNEI to a side of the cavity that does not contain a sufficient number of complementary charged residues (Temussi, 2011). If, by a tethered docking procedure, one is able to bring all charged residues within salt bridge distance from residues of complementary charge on the internal cavity of the receptor, the solution can be deemed topologically correct. This kind of docking was performed by feeding the information gathered from the low-resolution docking and from the key mutants on MNEI into the Web version of GRAMM. This version of the program allows the inclusion of a limited number of key receptors, that is, (T1R2)_D169, E170, R172, D173, K174, R176, D213, R217, D218, D456, R457 and (T1R3)_R177, D190, R191, D216, and ligand residues (D7, R39, K36, K43, R72, and R88).

The best result of this procedure, judged on the basis of the collective topological arrangement of *all* charged residues, is a complex of MNEI with the sweet receptor in which distances between atoms of opposite charges range from 3 to 7 Å, that is, close enough to reach optimal salt bridge distance, provided respective side chains conformations are optimized.

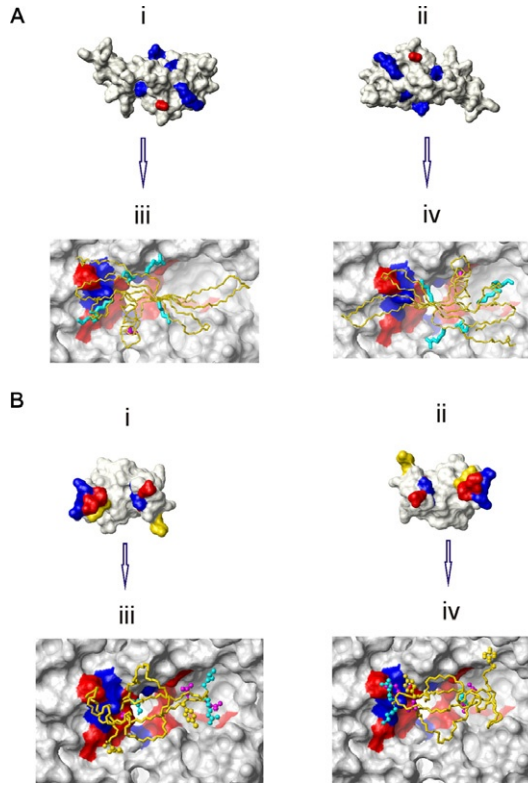

Figure 6.4 Topological models of MNEI and brazzein as wedges. (A) (i) Potential interacting side of MNEI, represented as a contact surface (viewed from the receptor). Key charged residues whose mutation causes a decrease in sweetness are colored according to the nature of their side chains. D7 is colored in red; K36, R39, K43, R72, and R88 are colored in blue. (ii) Same as A (i), rotated by 180° along an axis orthogonal to the plane of the figure. (iii) Superposition of the neon representation of MNEI, oriented as in A (i), but viewed from the solution side to the cavity of the receptor. To avoid confusion with the colors of the cavity, acidic residues of MNEI are colored in magenta and basic residues are colored in cyan. (iv) Superposition of the neon representation of MNEI, oriented as in A (ii), but viewed from the solution side to the cavity of the receptor. (B) (i) Potential interacting side of brazzein, represented as a contact surface. Key residues whose mutation affects sweetness are colored according to the nature of their side chains. D2, D40, E41, and D50 are colored in red; K5, K42, and R43 are colored in blue; Y39 and Y54 are colored in gold. (ii) Same as A, rotated by 180° along an axis orthogonal to the plane of the figure. (iii) Superposition of the neon representation of brazzein, oriented as in (i), but viewed from the solution side, to the cavity of the receptor. To avoid confusion with the colors of the cavity, acidic residues of brazzein are colored in magenta and basic residues are colored in cyan. (iv) Superposition of the neon representation of brazzein, oriented as in (ii), but viewed from the solution side. Models were built with MOLMOL (Koradi et al., 1996).

However, no optimization was attempted for the same reason that prevented a conventional docking procedure, that is, the low resolution of the receptor (Temussi, 2011).

Table 6.1 summarizes the one-to-one contacts between receptor residues, found by the tethered docking, and MNEI residues corresponding to key mutations. The bulk of MNEI occupies mainly the moiety of the cavity lined by residues of T1R3, but crucial one-to-one contacts between pairs of residues of opposite charge involve the same number of T1R2 and T1R3 residues (Temussi, 2011).

3.3.3. Refined complex of brazzein

Although no general model, other than the wedge model, has been proposed to explain collectively the taste of all sweet proteins, a specific mode of interaction has been hypothesized for brazzein by Jiang et al. (2004). These authors have suggested that brazzein binds to the Cys-rich domain (CRD) of the T1R3 protomer (Jiang et al., 2004). Using human/mouse chimeras of T1R3 coupled to human T1R2, they found that human T1R3 residues 536–545 within the cysteine-rich region are required for responsiveness to brazzein (Jiang et al., 2004). This potential active site is problematic, mainly because it is difficult to match residues of the CRD to corresponding mutations on brazzein. That is, the numerous point mutations on surface residues of brazzein that either decrease or increase its sweetness do not have clearly identifiable complementary residues on the CRD. Even more intriguing, the surface of the brazzein on which the main

Table 6.1 One-to-one contacts between receptor residues and sweet protein residues in refined complexes of monellin (MNEI) and brazzein

Receptor (T1R2)	Receptor (T1R3)	MNEI	Brazzein
	R247	D7	
D456		K36	
D188		R39	
	D215	K43	
D173		R72	
	E48	R88	
Q221			D2
	E47		K5
R457			D40
K174			D40
S458			E41
D456			K42
Q441			R43
	S59		D50

point mutations can be mapped (Assadi-Porter et al., 2010) is much wider than the surface of the CRD that should host it (Cui et al., 2006). One possible explanation is that tampering with the CRD can impair proper transmission of the signal from the VFT domains to the TM domains (Muto et al., 2007). If one could show that it is possible to find a complex between brazzein and the sweet receptor that satisfies all requirements of the wedge model, it would be sufficient evidence that it is not necessary to look for an *ad hoc* site for each protein. Low-resolution docking suggested that brazzein, like monellin and thaumatin, can bind to the external cavity, but also in this case, we had never identified the coordinates of a well-defined complex (Morini et al., 2005; Temussi, 2002). The only detailed complex of brazzein with the sweet receptor derived in the framework of the wedge model has been reported by Walters and Hellekant (2006), using two homology models corresponding to the models originally calculated by Morini et al. (2005): Aoc_AB, with T1R2 (closed)–T1R3 (open), and Aoc_BA, with T1R3 (closed)–T1R2 (open). These authors performed the docking procedure of brazzein on the two models of the sweet receptor using an approach similar to that used by Temussi (2002). Their docking calculations led to one preferred orientation of brazzein, complexed with the Aoc_BA-like receptor model, consistent with mutations known at the time (Walters and Hellekant, 2006). Recently, Assadi-Porter et al. (2010) found both models built by Walters and Hellekant (2006) inconsistent with a series of new mutants. However, Temussi (2011), by applying to brazzein the same topological approach illustrated for monellin, found it is possible to reconcile the findings of Walters and Hellekant (2006) with those of Assadi-Porter et al. (2010).

The new key mutants described by Assadi-Porter et al. (2010) are clustered in three sites. Mutants of sites 1 and 2 involve mainly charged residues, whereas changes of site 3 affect mainly disulfide bridges. Since it is well known that the stability of small proteins can be greatly affected by disruption of their disulfide bridges, Assadi-Porter et al. (2010) were very careful in checking that site 3 mutants are still folded. They simply checked that their NMR spectra had the correct dispersion of amide signals typical of properly folded proteins. However, the persistence of a regular fold cannot, by itself, prove that the topology of the surface of interaction is retained. We had previously observed, in the case of MNEI, that even the small distortion of the surface of interaction induced by the G16A mutation is sufficient to decrease sweetness by an order of magnitude (Spadaccini et al., 2003). It cannot be excluded that mutants affecting site 3 of brazzein, albeit properly folded, host severe distortions of their surface. Therefore, before considering them as relevant as the mutants of sites 1 and 2, it ought to be necessary to determine their structure. Accordingly, we decided not to use site 3 mutants in the search for the best wedge complex of brazzein. It was immediately clear that residues of sites 1 and 2 (Fig. 6.4B(i), (ii)) define a

unique surface of the protein, at the tip of an almost idealized wedge. As done for monellin, to find the correct topology of this wedge inside the cavity of the external active site of T1R2–T1R3, we chose complementarity of charges as the main initial criterion (Temussi, 2011). Figure 6.4B(iii), (iv) shows that brazzein can fit only with site 1 on the left side of the cavity (Fig. 6.4B(iv)) to be consistent with a good match of positive and negative charges because the right-hand side of the cavity does not contain a sufficient number of complementary charged residues (Temussi, 2011).

By combining the information gathered from the low-resolution docking with that coming from the key mutants on brazzein (Assadi-Porter et al., 2010), it is again possible to exploit the web version of GRAMM. For the cavity, the residues used were the same previously employed for MNEI: (T1R2)_D169, E170, R172, D173, K174, R176, D213, R217, D218, D456, R457 and (T1R3)_R177, D190, R191, D216. For the ligand protein, we used those reported by Assadi-Porter et al. (2010), that is, D2, K5, D40, E41, K42, R43, and D50. In the refined complex, each of the key charged residues of brazzein is close to a receptor residue of opposite charge or to a residue with which it can form a hydrogen bond. However, although the main part of the cavity of the receptor interacting with brazzein is similar to that interacting with monellin, there are significant differences.

Whereas in MNEI all key charged residues but one are basic, in brazzein most key charged residues are not and some of the brazzein residues (D2, E41, R43, and D50) do not have a one-to-one correspondence with a receptor residue of opposite charge but rather with neutral hydrophilic residues with which they can form hydrogen bonds (Q221, S458, Q441, and S59).

Table 6.1 offers a comparison of brazzein and MNEI interactions with receptor's residues.

An interesting pair involving a neutral hydrophilic residue is that formed by D2 and (T1R2)_Q221. While most residues classified as site 2 interact with receptor residues belonging to T1R3, D2 interacts with a T1R2 residue, thus "chelating" the two protomers and effectively freezing the active conformation of the receptor.

The most spectacular among the brazzein mutations described by Assadi-Porter et al. (2010) are those involving residues D40, E41, and K42. In the final model, D40 is found midway between (T1R2)_R457 and (T1R2)_K174, with distances between acidic and basic moieties that are not ideal. This finding reflects the complexity of this part of the surface. It is necessary to accommodate several residues with identical and opposite charge: D40, E41, and K42. Another reason why both interactions (with (T1R2)_R457 and (T1R2)_K174) may need some side chain adjustment is the vicinity of (T1R2)_D456. This and other aspects can be discussed in the framework of the heuristic power of the refined models.

Since brazzein and monellin have different sequences and structures (Temussi, 2006), it is legitimate to ask whether their topologically refined

complexes with the receptor have something in common. We can grasp an overview by looking at Table 6.1; although in general the receptor's residues are different for the two proteins, D456 is present in both interacting surfaces. In addition, there are several neighboring residues that take part to the two surfaces, notably R457 and S458, D173/K174, and E47/E48. The similarity of the two areas can be best evaluated from Fig. 6.5.

In this representation of the Aoc form of the sweet receptor, residues interacting with MNEI are colored in gold, whereas those interacting with brazzein are colored in violet, and D456 that is common to both surfaces is colored in red. The good superposition of the two areas speaks highly in favor of the validity of the wedge model and of the accuracy of the refined models of MNEI and brazzein reported (Temussi, 2011). A key point is that the number of residues of T1R2 is nearly the same as that of T1R3, confirming the basic assumption of the wedge model: sweet proteins can *freeze* the active form of the receptor. Last but not least, the models of the two complexes are consistent with observations not used in the tethered docking (Temussi, 2011). For instance, the result for MNEI is consistent with the Y65R mutant. We had shown that, by changing selected noncharged residues of its interacting surface into basic residues (Esposito et al., 2006), it is possible to find mutants even sweeter than monellin: Y65R–MNEI is nearly twice as sweet as MNEI itself.

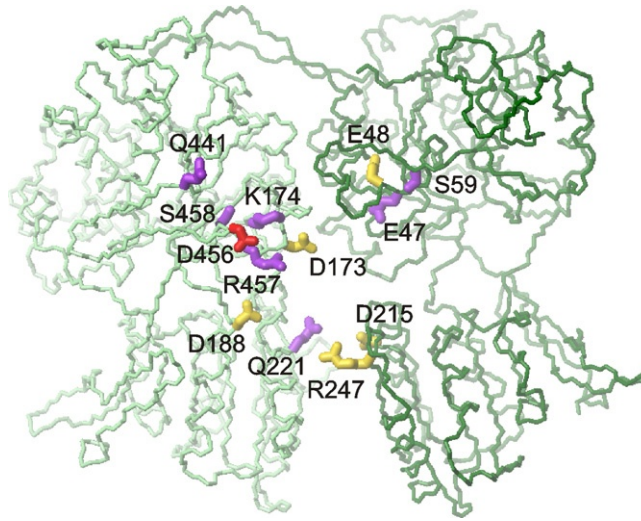

Figure 6.5 Comparison of the two complexes: interacting residues on the receptor interface. The two protomers of the receptor are colored in green: pale green for T1R2 and dark green for T1R3. The side chains of residues interacting with key residues of MNEI are colored in gold, those interacting with brazzein are colored in violet, D456 that is common to both surfaces is colored in red. The receptor model was built with MOLMOL (Koradi et al., 1996).

In the topological complex, changing Y65 into R65 brings the charged moiety of arginine 65 very close to (T1R2)_D456, an ideal situation to reinforce the existing charge–charge interaction with K36.

In the case of brazzein, the most important and unpredictable prediction concerns residues E41 and K42. E41 can be considered together with the adjacent K42 because the double mutation E41K, K42E that leads to a maximal increase in sweetness (Assadi-Porter et al., 2010). Figure 6.6 shows the environment of residues 41 and 42 after the double mutation E41K, K42E. In the double mutant, it is possible to form two salt bridges, a clear improvement with respect to the "wild" environment (Temussi, 2011).

4. Relationships Among Receptors

Sweet, bitter, and umami are probably the most important taste qualities for food acceptance among the five recognized taste sensations (Ikeda, 2002). Sweet and umami taste are normally linked to acceptance in food recognition, whereas bitter is clearly related to the rejection of food, not only in mammals but also in many other animals. It is reasonable to think that recognition of sweet molecules evolved to accept sugars, the body's main source of energy. It is likely that umami taste was helpful in recognizing protein sources, because the umami receptors can sense several amino acids, which may derive from the hydrolysis of proteins. Bitter

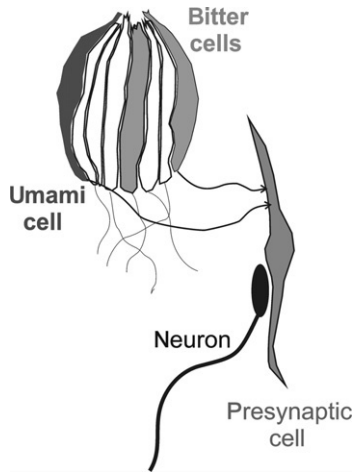

Figure 6.6 Cartoon illustrating the relationship among taste cells that explains a possible cross-talk between umami and bitter receptor cells. Signals from two (type II) receptor cells labeled for umami (dark gray) and bitter (light gray) tastes in the same taste bud converge onto presynaptic (type III) cells (light gray) via purinergic cell–cell communication.

molecules are very often toxic compounds, mainly of plant origin. Are sweet, bitter, and umami taste related?

Umami taste in humans is mainly linked to a uniform type of ligand, in fact essentially two compounds: glutamate and aspartate (Kurihara and Kashiwayanagi, 2000). On the contrary, sweet and bitter molecules, both natural and synthetic, belong to very diverse chemical families (Moncrieff, 1967; Temussi, 2007). Additionally, in many cases, tiny changes in chemical constitution can change a sweet molecule into a bitter one, and several sweet compounds have a distinct bitter aftertaste. Thus, it is not surprising that in the past nearly everybody believed that bitter and sweet molecules were recognized by similar receptors (Moncrieff, 1967; Verkade, 1967). Well-described pairs of bitter/sweet compounds not only come from isomers of aromatic compounds but also from congeners, conformational analogs, and optical isomers (Verkade, 1967). For instance, among the benzoylbenzoic acids, taste can vary from bitter with a sweet aftertaste in the parent compound to intensely bitter (and then very sweet) by substituting hydrogens with methyls (Verkade, 1967). Saccharin has a lingering bitter aftertaste, which limits its use as artificial sweetener (Schiffman et al., 1979), and substitutions at the 6-position can again yield a full spectrum of taste from sweet to bitter. When the 6-hydrogen atom is successively replaced with F, Cl, and Br, the substituted saccharins are still sweet, but with an increasingly bitter aftertaste. 6-Iodosaccharin is tasteless (Moncrieff, 1967), suggesting a precise steric relationship between the active sites of sweet and bitter receptors (Tancredi et al., 1979; Temussi et al., 1978). The best example of pairs for which the change from sweet to bitter is due to a change in conformational freedom is provided by flavonoid glycosides and their dihydrochalcones, which represent their open-chain counterparts (Shin et al., 1995; Williams, 1964). Naringin and neohesperidine, two glycosides found in several citrus fruits, are very bitter, but their dihydrochalcones are so sweet that they have been used as artificial sweeteners. Last but not least, there are several cases in which the relationship between the sweet and the bitter partners is optical isomerism.

Considering the wide variety of chemical classes and molecular dimensions covered by sweet and bitter compounds, it was inevitable to think that there would be several sweet taste receptors and that one or more of these sweet receptors had a bitter counterpart (Beidler and Gross, 1971; Birch and Mylvaganam, 1976; Hall et al., 1975). It is clear that such a view was untenable after the discovery that mammals have essentially only one sweet taste receptor, the T1R2–T1R3 heterodimer (Li et al., 2002), and several bitter taste receptors (Chandrashekar et al., 2006). I have recently put forward a simple hypothesis to try to explain the puzzling relationship between many sweet compounds and their bitter isomers (Temussi, 2009). This hypothesis starts from the paradox of optical isomers with different taste. The current explanation of the existence of bitter–sweet pairs of positional isomers, congeners, conformational analogs, etc., is more

or less consciously attributed to chance. It cannot be excluded that after slight constitutional variations, some molecules are no longer recognized by the sweet receptor but are recognized by one of the ~30 T2R receptors. However, it is not possible to attribute only to a chance the taste relationship between bitter/sweet enantiomeric pairs and other chiral isomers. Chirality plays a central role in controlling many kinds of molecular recognition and interactions in biology (Cline, 1996). The changes involving inversion of chiral centers speak for very strict stereochemical requirements in recognition, suggesting the existence of two very similar active sites that detect the change in chirality. It has been reported that an inversion of the configuration of the α-carbon of apolar amino acids is sufficient to change their taste from bitter to sweet (Shallenberger et al., 1969; Solms, 1969). Aromatic aminoacids are bitter (L-Trp > L-Phe > L-Tyr), whereas D-Trp, D-Phe, and D-Tyr are all sweet, in order of decreasing sweetness. A similar chiral relationship was also found for dipeptides related to aspartame of the general formula Asp-X (Mazur et al., 1969). The best known dipeptide sweetener, α-L-Asp-L-PheOMe, is very sweet, with a sweetness relative to sucrose on a molar basis of 172 (Mazur et al., 1969), whereas α-D-Asp-D-PheOMe is bitter (Castiglione-Morelli et al., 1990; Mazur et al., 1969). Even more surprisingly, the two diastereomers α-D-Asp-L-PheOMe and α-L-Asp-D-PheOMe are also bitter (Mazur et al., 1969). These examples involving chiral relationships imply that the receptor that recognizes bitter molecules is structurally related to the receptor recognizing sweet molecules. Also, a corollary is that the active sites of the two receptors are structurally similar.

Ideally, an unknown receptor that is able to recognize the bitter partners of chiral pairs should be structurally similar to the T1R2–T1R3 (sweet) receptor and should in general be able to recognize only molecules with opposite chirality with respect to well-known (chiral) sweet molecules. These features are typical of heterodimeric T1R receptors and could, in principle, apply to a yet undiscovered T1R dimer. However, there is no need to search for new members of the T1R family because a receptor with all features previously described is already well known: it is the T1R1–T1R3 umami receptor (Li et al., 2002). The structural similarity of T1R1–T1R3 with the T1R2–T1R3 sweet receptor is guaranteed by their sequence similarity (identity between the VFT domains of T1R1 and T1R2 of 39%) and by the comparison of the T1R1–T1R3 (Zhang et al., 2008) and T1R2–T1R3 homology models (Morini et al., 2005). T1R1–T1R3 can recognize L-aminoacids, but it does not recognize D-aminoacids, for example, very sweet D-Trp (Chandrashekar et al., 2006; Li et al., 2002).

Is bitter stimulation, not mediated by T2Rs, possible? A hypothesis to this end has been recently formulated (Temussi, 2009). The two simplest explanations for responses to multiple taste qualities coming from individual taste cells are that either (i) some receptor cells might host multiple taste receptors or (ii) cross-talk exists between receptor cells (Tomchik et al., 2007). Both

possibilities violate the currently accepted "dogma" of specialized taste cells (Chandrashekar et al., 2006). However, it has been shown that the two opposing views on taste coding can be reconciled (Tomchik et al., 2007). Gustatory signaling in taste bud cells is mediated by two classes of cells, that is, "receptor" cells that detect the five canonical taste qualities and "presynaptic" cells. According to Tomchik et al. (2007), most receptor cells (more than 80%) in taste buds are indeed labeled and respond to only one taste stimulus. However, the majority (more than 80%) of presynaptic cells, that is, cells accepting signals from specialized receptor cells, can respond to two or more different taste qualities. Possibility (ii) seems better suited to the problem described here. As shown in the cartoon of Fig. 6.6, the signals originating from umami and bitter taste cells may converge on the same presynaptic cell (Temussi, 2009). If such an umami cell is stimulated by the "bitter partner" of a bitter–sweet pair, for example, L-Trp, the signal will be interpreted as bitter.

5. Conclusions

There are many sweet and bitter molecules; evolution has responded to the need to sense them by developing different strategies for their receptors. The need for detecting potentially harmful substances has produced a large family of receptors, the T2Rs (Adler et al., 2000; Matsunami et al., 2000). On the contrary, acceptance of useful sweet tastants is regulated, for mammals, by a single receptor (T1R2–T1R3; Li et al., 2002) endowed by a remarkable variety of active sites and related mechanisms (Morini et al., 2005). Only one receptor seems to be sufficient to explain the sweet taste elicited by small and large size sweet molecules. Sweet proteins represent an outstanding class among the many sweet molecules, partly because they have molecular volumes much larger than those of all other sweet molecules but also their sweetness is intrinsically very high. The only attempt to explain the interaction of these proteins with the sweet receptor is the wedge model (Tancredi et al., 2004) first proposed by Temussi (2002). Docking calculations of three well-characterized sweet proteins (brazzein, monellin, and thaumatin) suggested that the equilibrium between resting and active forms of the receptor can indeed be shifted by complexation of a protein on an external cavity on the surface of the active conformation. To validate the model using all the information accumulated in more recent years, I investigated the possibility of obtaining quantitative models of the complexes of sweet proteins with the T1R2–T1R3 receptor on the basis of the wedge model. I have shown that it is possible to refine the coarse complexes yielded by low-resolution docking and increase the resolution by yoking the best complexes to accurate locations on the sweet protein surface furnished by mutagenesis data (Temussi, 2011). It is also important to note the subtle relationship existing between bitter and sweet taste, exemplified

by the existence of pairs of optical isomers with partners eliciting "opposite" taste (Mazur et al., 1969; Shallenberger et al., 1969; Solms, 1969). It has been proposed that the link between bitter and sweet is furnished by the third partner of the taste modalities linked to food acceptance, that is, the umami receptor. The paradox of how sweet molecules become bitter through the inversion of a single chirality center can be explained by assuming that, in these cases, the receptor stimulated by the "bitter partner" of pairs of optical isomers is the T1R1–T1R3 (umami) receptor, already known as the receptor for L-aminoacids (Chandrashekar et al., 2006; Li et al., 2002). This view is consistent with the complexity of taste as perceived subjectively by humans, and it is not in contrast with the code in which taste cells are labeled to a single taste (Chandrashekar et al., 2006).

ACKNOWLEDGMENT

I wish to thank Annalisa Pastore (NIMR, MRC, London, UK) for constant encouragement and enlightening discussions.

REFERENCES

Adler, E., Hoon, M.A., Mueller, K.L., Chandrashekar, J., Ryba, N.J., Zuker, C.S., 2000. A novel family of mammalian taste receptors. Cell 100, 693–702.

Ariyoshi, Y., Kohmura, M., 1994. Solid-phase synthesis and structure-activity relationships of analogs of the sweet protein monellin. J. Soc. Synth. Org. Chem. Jpn. 52, 359–369.

Assadi-Porter, F.M., Maillet, E.L., Radek, J.T., Quijada, J., Markley, J.L., Max, M., 2010. Key amino acid residues involved in multi-point binding interactions between brazzein a sweet protein and the T1R2–T1R3 human sweet receptor. J. Mol. Biol. 398, 584–599.

Attwood, T.K., Findlay, J.B., 1994. Fingerprinting G-protein-coupled receptors. Protein Eng. 7, 195–203.

Bachmanov, A., Reed, D.R., Ninomiya, Y., Inoue, M., Tordoff, M.G., Price, R.A., et al., 1997. Sucrose consumption in mice, major influence of two genetic loci affecting peripheral sensory responses. Mamm. Genome 8, 545–548.

Bachmanov, A.A., Li, X., Reed, D.R., Ohmen, J.D., Li, S., Chen, Z., et al., 2001. Positional cloning of the mouse saccharin preference (Sac) locus. Chem. Senses 26, 925–933.

Bassoli, A., Drew, M.G.B., Merlini, L., Morini, G., 2002a. A general pseudoreceptor model for sweet compounds, a semi-quantitative prediction of binding affinity for sweet tasting molecules. J. Med. Chem. 45, 4402–4409.

Bassoli, A., Merlini, L., Morini, G., 2002b. Isovanillyl sweeteners. From molecules to receptors. Pure Appl. Chem. 74, 1181–1187.

Behrens, M., Meyerhof, W., 2006. Bitter taste receptors and human bitter taste perception. Cell. Mol. Life Sci. 63, 1501–1509.

Beidler, L.M., Gross, G.W., 1971. The nature of taste receptor sites. In: Neff, W.D. (Ed.), Contributions to Sensory Physiology, vol. 5. Academic Press, New York, NY, pp. 97–127.

Birch, G.G., Mylvaganam, A.R., 1976. Evidence for the proximity of sweet and bitter receptor sites. Nature 260, 632–634.

Blake, J.D., Cohen, F.E., 2001. Pairwise sequence alignment below the twilight zone. J. Mol. Biol. 307, 721–735.
Blizard, D., Kotlus, B., Frank, M., 1999. Quantitative trait loci associated with short-term intake of sucrose saccharin and quinine solutions in laboratory mice. Chem. Senses 24, 373–385.
Bohak, Z., Li, S.L., 1976. The structure of monellin and its relation to the sweetness of the protein. Biochim. Biophys. Acta 427, 153–170.
Bridel, M., Lavieille, R., 1931. The sweet principle of the leaves of Khaa-he-e (*Stevia Rebaudiana Bertoni*). C. R. Acad. Sci. 192, 1123–1125.
Caldwell, J.E., Abildgaard, F., Dzakula, Z., Ming, D., Hellekant, G., Markley, J.L., 1998. Solution structure of the thermostable sweet-tasting protein brazzein. Nat. Struct. Biol. 5, 427–431.
Capeless, C., Whitney, G., 1995. The genetic basis of preference for sweet substances among inbred strains of mice preference ratio phenotypes and the alleles of the sac and dpa loci. Chem. Senses 20, 291–298.
Castiglione-Morelli, M.A., Lelj, F., Naider, F., Tallon, M., Tancredi, T., Temussi, P.A., 1990. Conformation activity relationship of sweet molecules. Comparison of aspartame and naphtimidazole-sulfonic acids. J. Med. Chem. 33, 514–520.
Chandrashekar, J., Hoon, M.A., Ryba, N.J., Zuker, C.S., 2006. The receptors and cells for mammalian taste. Nature 444, 288–294.
Chandrashekar, J., Mueller, K.L., Hoon, M.A., Adler, E., Feng, L., Guo, W., et al., 2000. T2Rs function as bitter taste receptors. Cell 100, 703–711.
Chaudhari, N., Landin, A.M., Roper, S.D., 2000. A metabotropic glutamate receptor variant functions as a taste receptor. Nat. Neurosci. 3, 113–119.
Cline, D.B., 1996. Physical Origin of Homochirality in Life. AIP Press, Woodbury, New York, NY.
Cui, M., Jiang, P., Maillet, E., Max, M., Margolskee, R.F., Osman, R., 2006. The heterodimeric sweet taste receptor has multiple potential ligand binding sites. Curr. Pharm. Des. 12, 4591–4600.
De Simone, A., Spadaccini, R., Temussi, P.A., Fraternali, F., 2006. MD calculations of MNEI a sweet protein: hot spots from hydration sites are consistent with key mutations and receptor interaction derived from docking calculations. Biophys. J. 90, 3052–3061.
de Vos, A.M., Hatada, M., van der Wel, H., Krabbendam, H., Peerdeman, A.F., Kim, S.H., 1985. Three-dimensional structure of thaumatin I, an intensely sweet protein. Proc. Natl. Acad. Sci. USA 82, 1406–1409.
Delwiche, J., 1996. Are there basic tastes? Trends Food Sci. Technol. 7, 411–415.
DuBois, G.E., Crosby, G.A., Stephenson, R.A., 1981. Dihydrochalcone sweeteners. A study of the atypical temporal phenomena. J. Med. Chem. 24, 408–428.
Esposito, V., Gallucci, R., Picone, D., Tancredi, T., Temussi, P.A., 2006. The importance of electrostatic potential in the interaction of sweet proteins with the sweet taste receptor. J. Mol. Biol. 360, 448–456.
Firestein, S., 2000. Neurobiology, the good taste of genomics. Nature 404, 552–553.
Floriano, W.B., Hall, S., Vaidehi, N., Kim, U., Drayna, D., Goddard 3rd, W.A., 2006. Modeling the human PTC bitter-taste receptor interactions with bitter tastants. J. Mol. Model. 12, 931–941.
Fuller, J., 1974. Single-locus control of saccharin preference in mice. J. Hered. 65, 33–36.
Gibbs, B.F., Alli, I., Mulligan, C., 1996. Sweet and taste-modifying proteins, a review. Nutr. Res. 16, 1619–1630.
Gilbertson, T., Damak, S., Margolskee, R., 2000. The molecular physiology of taste transduction. Curr. Opin. Neurobiol. 10, 519–527.
Gokulan, K., Khare, S., Ronning, D.R., Linthicum, S.D., Sacchettini, J.C., Rupp, B., 2005. Cocrystal structures of NC68 Fab identify key interactions for high potency sweetener

recognition, implications for the design of synthetic sweeteners. Biochemistry 44, 9889–9898.
Goodman, M., Zhu, Q., Kent, D.R., Amino, Y., Iacovino, R., Benedetti, E., et al., 1997. Conformational analysis of the dipeptide taste ligand L-aspartyl-D-2-aminobutyric acid-(S)-alpha-ethylbenzylamide and its analogues by NMR spectroscopy, computer simulations and X-ray diffraction studies. J. Pept. Sci. 3, 231–241.
Hall, M.J., Bartoshuk, L.M., Cain, W.S., Stevens, J.C., 1975. PTC taste blindness and the taste of caffeine. Nature 253, 442–443.
Hatada, M., Jancarik, J., Graves, B., Kim, S.-H., 1985. Crystal structure of aspartame, a peptide sweetener. J. Am. Chem. Soc. 107, 4279–4282.
Holm, L., Sander, C., 1995. Dali, a network tool for protein structure comparison. Trends Biochem. Sci. 20, 478–480.
Hu, Z., Min, H., 1983. Studies on mabinlin, a sweet protein from the seeds of *Capparis masaikai* levl. I. Extraction, purification and certain characteristics. Acta Bot. Yunnan. 5, 207–212.
Huang, A.L., Chen, X., Hoon, M.A., Chandrashekar, J., Guo, W., Traenkner, D., et al., 2006. The cells and logic for mammalian sour taste detection. Nature 442, 934–938.
Hung, L.W., Kohmura, M., Ariyoshi, Y., Kim, S.H., 1999. Structural differences in D and L-monellin in the crystals of racemic mixture. J. Mol. Biol. 285, 311–321.
Ikeda, K., 2002. New seasonings. Chem. Senses 27, 847–849.
Inglett, G.E., May, J.F., 1968. Tropical plants with unusual taste properties. Econ. Bot. 22, 326–331.
Inglett, G.E., May, J.F., 1969. Serendipity berries source of a new intense sweetener. J. Food Sci. 34, 408–411.
Iyengar, R.B., Smits, P., van der Ouderaa, F., van der Wel, H., van Brouwershaven, J., Ravestein, P., et al., 1979. The complete amino-acid sequence of the sweet protein thaumatin I. Eur. J. Biochem. 96, 193–204.
Jiang, P., Ji, Q., Liu, Z., Snyder, L.A., Benard, L.M., Margolskee, R.F., et al., 2004. The cysteine-rich region of T1R3 determines responses to intensely sweet proteins. J. Biol. Chem. 279, 45068–45075.
Kamphuis, J., Lelj, F., Tancredi, T., Toniolo, C., Temussi, P.A., 1992. SAR of sweet molecules, conformational analysis of two hypersweet and two conformationally restricted aspartame analogues. QSAR 11, 486–491.
Kaneko, R., Kitabatake, N., 2001. Structure-sweetness relationship in thaumatin, importance of lysine residues. Chem. Senses 26, 167–177.
Kim, S.H., Kang, C.-H., Kim, R., Cho, J.M., Lee, Y.-B., Lee, T.-K., 1989. Redesigning a sweet protein, increased stability and renaturability. Protein Eng. 2, 571–575.
Kim, S.H., Kang, C.-H., Cho, J.M., 1991. Sweet proteins, biochemical studies and genetic engineering. In: Walters, D.E., Orthofer, F.T., DuBois, G.E. (Eds.), Sweeteners, Discovery, Molecular Design and Chemoreception, vol. 450. ACS Symposium Series, ACS, Washington, DC, pp. 28–40.
Kinnamon, S.C., 2000. A plethora of taste receptors. Neuron 25, 507–510.
Kitagawa, M., Kusakabe, Y., Miura, H., Ninomiya, Y., Hino, A., 2001. Molecular genetic identification of a candidate receptor gene for sweet taste. Biochem. Biophys. Res. Commun. 283, 236–242.
Kohmura, M., Nio, N., Ariyoshi, Y., 1992. Highly probable active site of the sweet protein monellin. Biosci. Biotechnol. Biochem. 56, 1937–1942.
Koradi, R., Billeter, M., Wuethrich, K., 1996. MOLMOL, a program for display and analysis of macromolecular structure. J. Mol. Graph. 14, 51–55.
Kunishima, N., Shimada, Y., Tsuji, Y., Sato, T., Yamamoto, M., Kumasaka, T., et al., 2000. Structural basis of glutamate recognition by a dimeric metabotropic glutamate receptor. Nature 407, 971–977.

Kurihara, K., Beidler, L.M., 1969. Taste-modifying protein from miracle fruit. Science 161, 1241–1243.
Kurihara, K., Kashiwayanagi, M., 2000. Physiological studies on umami taste. J. Nutr. 130, 931S–934S.
Lee, S.Y., Lee, J.H., Chang, H.J., Cho, J.M., Jung, J.W., Lee, W., 1999. Solution structure of a sweet protein single-chain monellin determined by nuclear magnetic resonance and dynamical simulated annealing calculations. Biochemistry 38, 2340–2346.
Lelj, F., Tancredi, T., Temussi, P.A., Toniolo, C., 1976. Interaction of alpha-L-aspartyl-L-phenylalanine methyl ester with the receptor site of the sweet taste bud. J. Am. Chem. Soc. 98, 6669–6675.
Lesk, A.M., Chothia, C., 1980. How different amino acid sequences determine similar protein structures: the structure and evolutionary dynamics of the globins. J. Mol. Biol. 136, 225–270.
Li, X., Inoue, M., Reed, D.R., Hunque, T., Puchalski, R.B., Tordoff, M.G., et al., 2001. High-resolution genetic mapping of the saccharin preference locus (Sac) and the putative sweet taste receptor (T1R1) gene (Gpr70) to mouse distal Chromosome 4. Mamm. Genome 12, 13–16.
Li, X., Staszewski, L., Xu, H., Durick, K., Zoller, M., Adler, E., 2002. Human receptors for sweet and umami taste. Proc. Natl. Acad. Sci. USA 99, 4692–4696.
Li, D.F., Jiang, P., Zhu, D.Y., Hu, Y., Max, M., Wang, D.C., 2008. Crystal structure of Mabinlin II: a novel structural type of sweet proteins and the main structural basis for its sweetness. J. Struct. Biol. 162, 50–62.
Lindemann, B., 1996. Taste reception. Physiol. Rev. 76, 718–766.
Lindemann, B., 1999. Receptor seeks ligand, on the way to cloning the molecular receptors for sweet and bitter taste. Nat. Med. 5, 381–382.
Lindemann, B., 2001. Receptors and transduction in taste. Nature 413, 219–225.
Liu, X., Maeda, S., Hu, Z., Aiuchi, T., Nakaya, K., Kurihara, Y., 1993. Purification, complete amino acid sequence and structural characterization of the heat-stable sweet protein, mabinlin II. Eur. J. Biochem. 211, 281–287.
Lush, I., 1989. The genetics of tasting in mice, VI. Saccharin, acesulfame, dulcin and sucrose. Genet. Res. 53, 95–99.
Lush, I., Hornigold, N., King, P., Stoye, J., 1995. The genetics of tasting in mice. VII. Glycine revisited, and the chromosomal location of Sac and Soa. Genet. Res. 66, 167–174.
Lyall, V., Heck, G.L., Vinnikova, A.K., Ghosh, S., Phan, T.H., Alam, R.I., et al., 2004. The mammalian amiloride-insensitive non-specific salt taste receptor is a vanilloid receptor-1 variant. J. Physiol. 558, 147–159.
Masuda, T., Ide, N., Kitabatake, N., 2005. Structure-sweetness relationship in egg white lysozyme, role of lysine and arginine residues on the elicitation of lysozyme sweetness. Chem. Senses 30, 667–681.
Matsunami, H., Montmayeur, J.P., Buck, L.B., 2000. A family of candidate taste receptors in human and mouse. Nature 404, 601–604.
Max, M., Shanker, Y.G., Huang, L., Rong, M., Liu, Z., Campagne, F., et al., 2001. Tas1r3, encoding a new candidate taste receptor, is allelic to the sweet responsiveness locus Sac. Nat. Genet. 28, 58–63.
May, L.T., Christopoulos, A., 2003. Allosteric modulators of G-protein-coupled receptors. Curr. Opin. Pharmacol. 3, 551–556.
Mazur, R.H., Schlatter, J.M., Goldkamp, A.H., 1969. Structure-taste relationships of some dipeptides. J. Am. Chem. Soc. 91, 2684–2691.
McLaughlin, S.K., McKinnon, P.J., Margolskee, R.F., 1992. Gustducin is a tastecell-specific G protein closely related to the transducins. Nature 357, 563–569.

McLaughlin, S.K., McKinnon, P.J., Spickofsky, N., Danho, W., Margolskee, R.F., 1994. Molecular cloning of G proteins and phosphodiesterases from rat taste cells. Physiol. Behav. 56, 1157–1164.
Miguet, L., Zhang, Z., Grigorov, M.G., 2006. Computational studies of ligand-receptor interactions in bitter taste receptors. J. Recept. Signal Transduct. Res. 26, 611–630.
Ming, D., Hellekant, G., 1994. Brazzein, a new high-potency thermostable sweet protein from Pentadiplandra brazzeana B. FEBS Lett. 355, 106–108.
Moncrieff, R.W., 1967. The Chemical Senses. Hill, London.
Montmayeur, J.P., Liberles, S.D., Matsunami, H., Buck, L.B.A., 2001. Candidate taste receptor gene near a sweet taste locus. Nat. Neurosci. 4, 492–498.
Morini, G., Temussi, P.A., 2005. Micro and macro models of the sweet receptor. Chem. Senses 30, 86–87.
Morini, G., Bassoli, A., Temussi, P.A., 2005. From small sweeteners to sweet proteins, anatomy of the binding sites of the human T1R2-T1R3 receptor. J. Med. Chem. 48, 5520–5529.
Morris, J.A., 1976. Sweetening agents from natural sources. Lloydia 39, 25–38.
Morris, J.A., Cagan, R.H., 1972. Purification of monellin, the sweet principle of *Dioscoreophyllum cumminsii*. Biochim. Biophys. Acta 261, 114–122.
Murzin, A.G., 1993. Sweet-tasting protein monellin is related to the cystatin family of thiol proteinase inhibitors. J. Mol. Biol. 230, 689–694.
Muto, T., Tsuchiya, D., Morikawa, K., Jingami, H., 2007. Structures of the extracellular regions of the group II/III metabotropic glutamate receptors. Proc. Natl. Acad. Sci. USA 104, 3759–3764.
Nelson, G., Hoon, M.A., Chandrashekar, J., Zhang, Y., Ryba, N.J., Zuker, C.S., 2001. Mammalian sweet taste receptors. Cell 106, 381–390.
Niccolai, N., Spadaccini, R., Scarselli, M., Bernini, A., Crescenzi, O., Spiga, F., et al., 2001. Probing the surface of a sweet protein, NMR study of MNEI with a paramagnetic probe. Protein Sci. 10, 1498–1507.
Nofre, C., Tinti, J.-M., Chatzopoulos-Ouar, F., 1988. Preparation of (phenylguanidino)- and [[1-(phenylamino)ethyl]amino]acetic acids as sweeteners. Eur. Pat. Appl. EP 241, 395, 1987, Chem. Abstr., 109, 190047k.
Ogata, C.M., Gordon, P.F., de Vos, A.M., Kim, S.H., 1992. Crystal structure of a sweet tasting protein thaumatin I, at 1.65 A resolution. J. Mol. Biol. 228, 893–908.
Ohta, K., Masuda, T., Ide, N., Kitabatake, N., 2008. Critical molecular regions for elicitation of the sweetness of the sweet-tasting protein thaumatin I. FEBS J. 275, 3644–3652.
Paladino, A., Colonna, G., Facchiano, A.M., Costantini, S., 2010. Functional hypothesis on miraculin' sweetness by a molecular dynamics approach. Biochem. Biophys. Res. Commun. 396, 726–730.
Pastore, A., Lesk, A.M., 1990. Comparison of the structures of globins and phycocyanins: evidence for evolutionary relationship. Proteins Struct. Funct. Genet. 8, 133–155.
Pin, J.P., Galvez, T., Prezeau, L., 2003. Evolution, structure, and activation mechanism of family 3/C G-protein-coupled receptors. Pharmacol. Ther. 98, 325–354.
Polinelli, S., Broxterman, Q.B., Schoemaker, H.E., Boesten, W.H.J., Crisma, M., Valle, G., et al., 1992. New aspartame-like sweeteners containing L-(Me)Phe. Bioorg. Med. Chem. Lett. 2, 453–456.
Sainz, E., Korley, J.N., Battey, J.F., Sullivan, S.L., 2001. Identification of a novel member of the T1R family of putative taste receptors. J. Neurochem. 77, 896–903.
Sali, A., Blundell, T.L., 1993. Comparative protein modeling by satisfaction of spatial restraints. J. Mol. Biol. 234, 779–815.
San Gabriel, A., Uneyama, H., Yoshie, S., Torii, K., 2005. Cloning and characterization of a novel mGluR1 variant from vallate papillae that functions as a receptor for L-glutamate stimuli. Chem. Senses 30, i25–i26.
Schiffman, S.S., Reilly, D.A., Clark 3rd, T.B., 1979. Qualitative differences among sweeteners. Physiol. Behav. 23, 1–9.

Servant, G., Tachdjian, C., Tang, X.Q., Werner, S., Zhang, F., Li, X., et al., 2010. Positive allosteric modulators of the human sweet taste receptor enhance sweet taste. Proc. Natl. Acad. Sci. USA 107, 4746–4751.

Shallenberger, R.S., Acree, T., 1967. Molecular theory of sweet taste. Nature 216, 480–482.

Shallenberger, R.S., Acree, T.E., Lee, C.Y., 1969. Sweet taste of D and L-sugars and amino-acids and the steric nature of their chemo-receptor site. Nature 221, 555–556.

Shin, W., Kim, S.J., Shin, J.M., Kim, S.H., 1995. Structure-taste correlations in sweet dihydrochalcone, sweet dihydroisocoumarin, and bitter flavone compounds. J. Med. Chem. 38, 4325–4331.

Shirasuka, Y., Nakajima, K., Asakura, T., Yamashita, H., Yamamoto, A., Hata, S., et al., 2004. Neoculin as a new taste-modifying protein occurring in the fruit of *Curculigo latifolia*. Biosci. Biotechnol. Biochem. 68, 1403–1407.

Solms, J., 1969. The taste of amino acids, peptides, and proteins. J. Agric. Food Chem. 17, 686–688.

Solms, J., Vuataz, L., Egli, R.H., 1965. The taste of L- and D-amino acids. Experientia 21, 692–694.

Somoza, J.R., Cho, J.M., Kim, S.H., 1995. The taste-active regions of monellin, a potently sweet protein. Chem. Senses 20, 61–68.

Spadaccini, R., Crescenzi, O., Tancredi, T., De Casamassimi, N., Saviano, G., Scognamiglio, R., et al., 2001. Solution structure of a sweet protein, NMR study of MNEI, a single chain monellin. J. Mol. Biol. 305, 505–514.

Spadaccini, R., Trabucco, F., Saviano, G., Picone, D., Crescenzi, O., Tancredi, T., et al., 2003. The mechanism of interaction of sweet proteins with the T1R2-T1R3 receptor, evidence from the solution structure of G16A-MNEI. J. Mol. Biol. 328, 683–692.

Sung, Y.H., Shin, J., Chang, H.J., Cho, J.M., Lee, W., 2001. Solution structure, backbone dynamics, and stability of a double mutant single-chain monellin. structural origin of sweetness. J. Biol. Chem. 276, 19624–19630.

Suzuki, M., Kurimoto, E., Nirasawa, S., Masuda, Y., Hori, K., Kurihara, Y., et al., 2004. Recombinant curculin heterodimer exhibits taste-modifying and sweet-tasting activities. FEBS Lett. 573, 135–138.

Tancredi, T.T., Lelj, F., Temussi, P.A., 1979. Three-dimensional mapping of the bitter taste receptor site. Chem. Senses Flav. 4, 259–264.

Tancredi, T., Iijima, H., Saviano, G., Amodeo, P., Temussi, P.A., 1992. Structural determination of the active site of a sweet protein, a ^{1}H NMR investigation of MNEI. FEBS Lett. 310, 27–30.

Tancredi, T., Pastore, A., Salvatori, S., Esposito, V., Temussi, P.A., 2004. Interaction of sweet proteins with their receptor. A conformational study of peptides corresponding to loops of brazzein, monellin and thaumatin. Eur. J. Biochem. 271, 2231–2240.

Temussi, P.A., 2002. Why are sweet proteins sweet? Interaction of brazzein, monellin and thaumatin with the T1R2-T1R3 receptor. FEBS Lett. 526, 1–3.

Temussi, P.A., 2006. Natural sweet macromolecules: how sweet proteins work. Cell. Mol. Life Sci. 63, 1876–1888.

Temussi, P.A., 2007. The sweet taste receptor: a single receptor with multiple sites and modes of interaction. Adv. Food Nutr. Res 53, 199–239.

Temussi, P.A., 2009. Sweet, bitter and umami receptors: a complex relationship. Trends Biochem. Sci. 34, 296–302.

Temussi, P.A., 2011. Determinants of sweetness in proteins: a topological approach. J. Mol. Recogn. in press.

Temussi, P.A., Lelj, F., Tancredi, T., 1978. Three-dimensional mapping of the sweet taste receptor site. J. Med. Chem. 21, 1154–1158.

Temussi, P.A., Lelj, F., Tancredi, T., Castiglione-Morelli, M.A., Pastore, A., 1984. Soft agonist-receptor interactions, theoretical and experimental simulation of the active site of the receptor site of sweet molecules. Int. J. Quantum Chem. 26, 889–906.

Theerasilp, S., Kurihara, Y., 1988. Complete purification and characterization of the taste-modifying protein, miraculin, from miracle fruit. J. Biol. Chem. 263, 11536–11539.
Theerasilp, S., Hitotsuya, H., Nakajo, S., Nakaya, K., Nakamura, Y., Kurihara, Y., 1989. Complete amino acid sequence and structure characterization of the taste-modifying protein, miraculin. J. Biol. Chem. 264, 6655–6659.
Thompson, J.D., Higgins, D.G., Gibson, T.J., 1994. CLUSTAL_W: improving the sensitivity of progressive multiple sequence alignment through sequence weighting, position-specific gap penalties and weight matrix choice. Nucleic Acids Res. 22, 4673–4680.
Thompson, J.D., Gibson, T.J., Plewniak, F., Jeanmougin, F., Higgins, D.G., 1997. The CLUSTAL_X windows interface, flexible strategies for multiple sequence alignment aided by quality analysis tools. Nucleic Acids Res. 24, 4876–4882.
Tinti, J.M., Nofre, C., 1991. Why does a sweetener taste sweet? A new model. In: Walters, D.E., Orthofer, F.T., DuBois, G.E. (Eds.), Sweeteners, Discovery, Molecular Design and Chemoreception, vol. 450. ACS Symposium Series, ACS, Washington, DC, pp. 88–99.
Tomchik, S.M., Berg, S., Kim, J.W., Chaudhari, N., Roper, S.D., 2007. Breadth of tuning and taste coding in mammalian taste buds. J. Neurosci. 27, 10840–10848.
Tsuchiya, D., Kunishima, N., Kamiya, N., Jingami, H., Morikawa, K., 2002. Structural views of the ligand-binding cores of a metabotropic glutamate receptor complexed with an antagonist and both glutamate and Gd3+. Proc. Natl. Acad. Sci. USA 99, 2660–2665.
Vakser, I.A., 1995. Protein docking for low-resolution structures. Protein Eng. 8, 371–377.
Vakser, I.A., Matar, O.G., Lam, C.F., 1999. A systematic study of low-resolution recognition in protein-protein complexes. Proc. Natl. Acad. Sci. USA 96, 8477–8482.
van der Wel, H., Loeve, K., 1972. Isolation and characterization of thaumatin I and II, the sweet-tasting proteins from *Thaumatococcus daniellii* Benth. Eur. J. Biochem. 31, 221–225.
Vedani, A., Zbinden, P., Snyder, J.P., Greenidge, P.A., 1995. Pseudoreceptor modelling, the construction of three dimensional receptor surrogates. J. Am. Chem. Soc. 117, 4987–4994.
Verkade, P.E., 1967. On organic compounds with a sweet and/or a bitter taste Il Farmaco. Farmaco. Sci. 23, 248–291.
Walters, D.E., 1995. Using models to understand and design sweeteners. J. Chem. Educ. 72, 680–683.
Walters, D.E., 2002. Homology-based model of the extracellular domain of the taste receptor T1R3. Pure Appl. Chem. 74, 1117–1123.
Walters, D.E., Hellekant, G., 2006. Interactions of the sweet protein brazzein with the sweet taste receptor. J. Agric. Food Chem. 54, 10129–10133.
Walters, D.E., Pearlstein, R.A., Krimmel, C.P., 1986. A procedure for preparing models of receptor sites. J. Chem. Educ. 63, 869–872.
Williams, A.H., 1964. Dihydrochalcones; their occurrence and use as indicators in chemical plant taxonomy. Nature 202, 824–825.
Yamashita, H., Theerasilp, S., Aiuchi, T., Nakaya, K., Nakamura, Y., Kurihara, Y., 1990. Purification and complete amino acid sequence of a new type of sweet protein taste-modifying activity, curculin. J. Biol. Chem. 265, 15770–15775.
Zhang, F., Klebansky, B., Fine, R.M., Xu, H., Pronin, A., Liu, H., et al., 2008. Molecular mechanism for the umami taste synergism. Proc. Natl. Acad. Sci. USA 105, 20930–20934.

CHAPTER SEVEN

Cell-Cycle Control and Plant Development

Soichi Inagaki *and* Masaaki Umeda

Contents

Abstract

The cell cycle is driven by the activity of cyclin-dependent kinase (CDK)–cyclin complexes. Therefore, internal and external signals converge on the regulation of CDK–cyclin activity to modulate cell proliferation in specific developmental processes and under various environmental conditions. CDK–cyclin activity is fine-tuned by multiple mechanisms, for example, transcriptional control, protein degradation, phosphorylation, and binding to CDK inhibitor. These molecular mechanisms underlie the regulation of the entry into or the exit from the cell cycle, the rate of cell cycle, or the transition from the mitotic cell cycle to the

Graduate School of Biological Sciences, Nara Institute of Science and Technology, Takayama, Ikoma, Nara, Japan

International Review of Cell and Molecular Biology, Volume 291
ISSN 1937-6448, DOI: 10.1016/B978-0-12-386035-4.00007-0

endocycle. The multiple mechanisms regulating CDK–cyclin activity coordinately enable the elaborate control of cell cycle by various upstream signals. Here, we review the molecular mechanisms that regulate the cell cycle and the endocycle in plants. We also introduce the recent progress in elucidating the regulatory mechanisms underlying plant development and the stress response in terms of cell-cycle control.

Key Words: Cell cycle, Endocycle, Phytohormone, DNA damage checkpoint, CDK.

1. Introduction

Higher plants continuously develop organs throughout their life cycle, and this process is dependent on the flexible control of cell division and cell expansion. As plant cells do not move within their organs and plants form their body by laying cells like building blocks, the spatiotemporally optimized control of cell division and expansion plays a central role in the highly elaborate morphogenesis and differentiation of each organ. Studies on cell-division control in plants have benefited from genetic analyses using the model plant *Arabidopsis thaliana*. The genome sequence of *A. thaliana* has revealed that there are many cell-cycle-related genes with counterparts in yeast and animals, and most of the cell-cycle regulators are encoded by multiple loci. They have specific or redundant functions in cell-cycle regulation; however, it has been difficult to identify the particular function(s) of each gene. Functional analysis of these regulators has suffered from the fact that cell-cycle progression is a fundamental process in plant development; thus, a deficiency in the regulatory mechanisms is predicted to cause a lethal phenotype. However, recent advances in high-throughput analyses and the accumulation of useful genetic material have enabled us to tackle the challenging questions: How do cells "know" when and where to divide, terminate, or expand in a specific developmental context? How do plants adjust cell division and expansion in response to growth conditions and environmental stress? How is the transition from the mitotic cycle to endocycle controlled?

To solve these questions, it is essential to understand the fundamental mechanisms that control cell-cycle progression. Here, we introduce the underlying genetic mechanisms of cell-cycle control in plants, which have been revealed by biochemical and genetic analyses within the past 20 years. We also discuss our understanding of the regulatory mechanisms governing the endocycle, an alternate version of the cell cycle. Finally, we illustrate the elaborate regulation of cell-cycle progression by external stimuli and developmental signals. The integration of a wide range of knowledge will be

useful to understand plant-specific strategies for their continuous development and adaptation to the environment.

2. Basic Regulatory Mechanisms of the Cell Cycle

2.1. Cyclin-dependent kinases

As in yeast and animals, cyclin-dependent kinases (CDKs) are the central regulators of the cell cycle in plants. The one-way progression of the cell cycle is established by regularly alternating the activity of CDKs. CDK activity becomes higher at the G1/S and G2/M boundaries and is associated with the phosphorylation of a large number of proteins, leading to the onset of DNA replication and mitosis, respectively. The modification of CDK activity by transcriptional control, protein–protein interactions, posttranslational modifications, or protein degradation is the eventual convergence point that governs cell-cycle progression (Fig. 7.1). Whereas eight classes of CDKs (CDKA to CDKG, and CDK-like kinases—CKLs) have been identified in *A. thaliana*, CDKA and CDKB are the only CDKs that directly regulate cell-cycle progression (Menges et al., 2005; Vandepoele et al., 2002). CDKC and CDKE are presumed to regulate transcription, as deduced from the function of their mammalian homologs CDK9 and CDK8, respectively. CDKD and CDKF are CDK-activating kinases (CAKs; see below). CDKGs and CKLs are recently identified classes that consist of 2 and 15 genes, respectively, and the latter constitute a distant and distinct phylogenetic clade from the other CDKs (Menges et al., 2005).

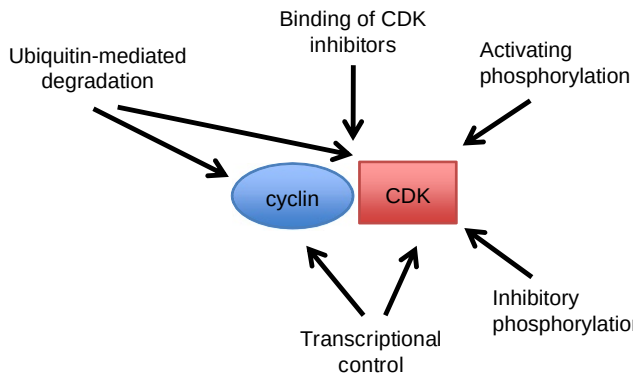

Figure 7.1 Multiple levels of regulation of CDK activity. See Sections 2.3–2.6 for details.

Although CKLs show high sequence similarities among members, suggesting their recent divergence, their functions have not yet been identified.

CDKA is encoded by a single copy gene (*CDKA;1*) in *A. thaliana* and contains a conserved PSTAIRE motif in its cyclin-binding domain. CDKA;1 is the only CDK identified so far in *A. thaliana* that can complement the temperature-sensitive *cdc2* mutant of *Schizosaccharomyces pombe* (Ferreira et al., 1991). Overexpression of dominant-negative *CDKA;1* abolishes cell division (Hemerly et al., 1995), suggesting that CDKA;1 is essential for cell-cycle progression in plants. Null mutations in *CDKA;1* impair the division of male gametophytes into two sperm cells, whereas *cdka;1* female gametophytes develop normally; thus, pollen carrying the *cdka;1* mutation cannot undergo double fertilization (Iwakawa et al., 2006; Nowack et al., 2006).

CDKB can be grouped into the CDKB1 and CDKB2 subfamilies, which are both encoded by two genes in *A. thaliana* (*CDKB1;1* and *CDKB1;2* for CDKB1; *CDKB2;1* and *CDKB2;2* for CDKB2). CDKBs are specific to plants (Boudolf et al., 2001; Hirayama et al., 1991; Joubès et al., 2000). The PSTAIRE motif in CDKA is replaced with PPTALRE and P(P/S)TTLRE in CDKB1 and CDKB2, respectively (Vandepoele et al., 2002). CDKBs have the unique feature that their expression is differentially regulated during the cell cycle; the *CDKB1* transcript accumulates from the late S phase to the M phase, whereas *CDKB2* is expressed in a more restricted period from the G2 to M phase (Breyne et al., 2002; Menges et al., 2002, 2003, 2005; Porceddu et al., 2001; Segers et al., 1996; Umeda et al., 1999). In addition to transcriptional control, CDKB2 expression was shown to be regulated by protein degradation because a translational fusion of CDKB2;1 with β-glucuronidase (GUS), but not a *CDKB2;1* promoter–GUS fusion, showed a patchy expression pattern in the *A. thaliana* root meristem. Indeed, CDKB2;1 and CDKB2;2 have possible PEST motifs, which are signals for proteolytic degradation (Adachi et al., 2006). Treatment of CDKB2:GUS roots with the proteasome inhibitor MG132 increases the expression of GUS, suggesting that proteasome-mediated proteolysis regulates CDKB2 expression. However, the molecular mechanism underlying the degradation of CDKB2 protein has not been identified.

As predicted from its expression pattern, CDKB1 controls G2/M progression (Boudolf et al., 2004a; Porceddu et al., 2001). Although the detailed function of CDKB2 in cell-cycle progression has not been elucidated, the two *A. thaliana CDKB2* genes are expressed in meristematic cells and are required for cell proliferation and the execution of genetic programs in the meristem (Andersen et al., 2008).

2.2. Cyclin

The cell-cycle phase-specific expression of cyclins activates CDKs in a time-controlled manner by directly interacting with CDKs. Different CDK–cyclin pairs form complexes and regulate different stages of the cell cycle.

In *A. thaliana*, ~50 genes encode cyclin-related proteins, in which 32 cyclins have putative functions in cell-cycle regulation: 10 A-type, 11 B-type, 10 D-type, and 1 H-type cyclins (Menges et al., 2005).

Each cyclin gene shows a specific expression pattern during the cell cycle. The function of individual cyclins has been suggested from their expression patterns, interacting partners, and the effect caused by altering their expression. Generally, A-type cyclins (CYCAs) control S-to-M phase progression, and CYCBs control the G2/M transition and M phase progression (Inzé and De Veylder, 2006). CYCDs control the G1/S transition and cell proliferation in response to external signals, for example, phytohormones and nutrient availability. However, the expression of CYCD genes is not specific to the G1/S phase, and some are expressed at the G2/M phase (Menges et al., 2005; Sorrell et al., 1999).

The 10 genes that encode CYCAs are divided into the *CYCA1*, *CYCA2*, and *CYCA3* subfamilies, which include two, four, and four genes, respectively, in *A. thaliana* (Vandepoele et al., 2002; Wang et al., 2004a). *CYCA1* and *CYCA2* show a peak of expression at the G2/M phase, whereas *CYCA3* is expressed during the G1/S transition phase and S phase in synchronized *A. thaliana* suspension cells (Menges et al., 2005). A number of CYCA proteins can bind to CDKB and CDKA proteins (Boruc et al., 2010; Van Leene et al., 2010). Functional genetic analyses have revealed some putative functions of the CYCA proteins. CYCA2;3 was shown to form a complex with CDKB1;1 and promote the mitotic cell cycle (Boudolf et al., 2009). CYCA2;3 was shown to interact with CDKA;1 and repress endocycle progression (Imai et al., 2006). CYCA1;2 (also known as TAM) is required for meiosis in male gametophytes (d'Erfurth et al., 2010; Wang et al., 2004b). Recently, we revealed that the CYCA3;1–CDKA;1 complex phosphorylates histone H1 and retinoblastoma-related (RBR) protein *in vitro* (Takahashi et al., 2010a), suggesting that CYCA3 can act as a G1/S cyclin to promote entry into the S phase.

Eleven genes encode CYCBs in *A. thaliana*: five for *CYCB1*, five for *CYCB2*, and one for *CYCB3* (Vandepoele et al., 2002; Wang et al., 2004a). All of them have expression peaks at the G2/M transition phase (Menges et al., 2002, 2005). They can interact with CDKA, CDKB1, and CDKB2 (Boruc et al., 2010; Van Leene et al., 2010), although the function of these complexes in cell-cycle progression is largely unexplored. The ectopic expression of *CYCB1;1* under the control of the *CDKA;1* promoter promotes root growth without altering organ morphology, suggesting that the increased expression of *CYCB1;1* accelerates cell-cycle progression and, thus, meristem activity (Doerner et al., 1996). The induction of cell division was demonstrated by the ectopic expression of *CYCB1;2* in differentiating trichomes (unicellular hairs on leaves), resulting in the formation of multicellular trichomes (Schnittger et al., 2002). CYCB2s from rice (*Oryza sativa*) form complexes with CDKB2 and activate histone H1 kinase

activity *in vitro* (Lee et al., 2003). *CYCB2;2* overexpression in rice enhances root growth by increasing the cell number, indicating that CYCB2 can stimulate cell division.

Ten genes encoding CYCDs have been identified in *A. thaliana*, and they are classified into seven subfamilies (CYCD1 to CYCD7): CYCD3 is encoded by three genes, CYCD4 by two genes, and the other five CYCDs are each encoded by a single gene (Vandepoele et al., 2002). *CYCD1;1*, *CYCD2;1*, and *CYCD3;1* were originally identified by screening for *A. thaliana* genes that can complement a yeast G1 cyclin mutant (Soni et al., 1995). The majority of CYCD proteins can interact with CDKA;1 (Boruc et al., 2010; Van Leene et al., 2010), and the overexpression of some CYCD genes accelerates the entry of the cell into the S phase (Cockcroft et al., 2000; Dewitte et al., 2003; Kono et al., 2007; Koroleva et al., 2004; Masubelele et al., 2005, Menges et al., 2006), suggesting that CDKA–CYCD complexes regulate the G1/S transition. In fact, the overexpression of *A. thaliana* CYCD2;1 in *Nicotiana tabacum* increased the overall growth rate of shoots, but the final size of each organ was the same as in wild-type plants (Cockcroft et al., 2000).

2.3. CDK inhibitors

In contrast to cyclins, CDK inhibitors negatively regulate the activity of CDKs by directly binding to CDKs (Morgan, 1997; Nakayama and Nakayama, 1998). A plant CDK inhibitor was first identified by screening for proteins that can interact with CDKA (Lui et al., 2000; Wang et al., 1997). Seven genes encode the CDK inhibitor Kip-related protein (KRP) family in *A. thaliana*: ICK1/KRP1, ICK2/KRP2, and KRP3 to KRP7 (De Veylder et al., 2001). ICK1/KRP1, ICK2/KRP2, or KRP6 overexpression strongly inhibit growth and affect organ morphology (De Veylder et al., 2001; Wang et al., 2000; Zhou et al., 2003). All KRPs, except KRP5, bind to CDKA;1 but not to CDKB1;1 in the yeast two-hybrid system (De Veylder et al., 2001). Interestingly, all KRPs can interact with D-type cyclins, for example, CYCD1;1, CYCD2;1, and CYCD3;1 (Wang et al., 1998; Zhou et al., 2003), suggesting that KRPs inhibit the activity of CYCD–CDKA complexes. KRPs are small proteins with a C-terminal domain (CTD) that is required for CDK- or cyclin-binding and their inhibitory function (De Clercq and Inzé, 2006; De Veylder et al., 2001). Although KRPs and animal CDK inhibitors, for example, $p21^{Cip1}$, $p27^{Kip1}$, and $p57^{Kip2}$, show limited sequence similarities in their CDK/cyclin-binding domains, their overall structures are sufficiently different that the functions and regulatory mechanisms of KRPs are suggested to differ from those of animal CDK inhibitors (De Clercq and Inzé, 2006).

A second class of CDK inhibitors was identified in *A. thaliana*, named SIAMESE (SIM) and SIM-related (SMR) proteins (Churchman et al., 2006).

SIM and SMR proteins are only found in plants, including rice, maize, tomato, and poplar, and show localized sequence similarity to KRPs within the C-terminal cyclin-binding domain (Churchman et al., 2006; Peres et al., 2007). The founder member, SIM, represses the mitotic cell cycle in endoreduplicating trichomes (Walker et al., 2000). SIM overexpression significantly reduces growth and generates enlarged cells with increased nuclear content, suggesting that SIM inhibits the activity of CDK at G2/M and promotes endoreduplication (Churchman et al., 2006). Fluorescence resonance energy transfer (FRET) analysis demonstrated that SIM and the rice SMR protein EL2 specifically interact with CDKA;1 and CYCD proteins but not with CDKB proteins in the nucleus (Churchman et al., 2006; Peres et al., 2007). Further, EL2 was shown to inhibit the activity of CDKA;1 *in vitro* (Peres et al., 2007). However, recent interatomic analyses using tandem affinity purification (TAP) and mass spectrometry in *A. thaliana* cell suspension culture showed that SIM, SMR1, and SMR2 were copurified with CDKB1;1 but not with CDKA;1, whereas SMR3–6 and SMR8 were associated with CDKA;1 (Van Leene et al., 2010). Interestingly, the expression of many *SMR* genes differentially responds to several stress conditions (Peres et al., 2007; see below), suggesting that *SMRs* are involved in altering cell-cycle progression in response to external stress.

2.4. CDK phosphorylation

CDK activity is also regulated by phosphorylation. Phosphorylation of a conserved threonine residue (Thr-161 in *A. thaliana* CDKA;1) in the T-loop region is required for the recognition of substrates and the full activity of CDK (Draetta, 1997; Nigg, 1996). CAKs catalyze this activating phosphorylation of CDKs. In plants, two classes of CAKs have been identified: CDKD and CDKF (Umeda et al., 2005). The CDKD class is structurally related to the vertebrate CAK, CDK7, which phosphorylates the CTD of the largest subunit of RNA polymerase II in addition to CDK (Serizawa et al., 1995; Shiekhattar et al., 1995). In *A. thaliana*, three *CDKD* genes have been identified: *CDKD;1*, *CDKD;2*, and *CDKD;3* (originally named *CAK3At*, *CAK4At*, and *CAK2At*, respectively; Shimotohno et al., 2003; Umeda et al., 2005). CDKD;2 and CDKD;3 phosphorylate human CDK2 and *A. thaliana* CTD *in vitro* (Shimotohno et al., 2003). The kinase activity of CDKD;3 on CDK2 was higher than that of CDKD;2, but the kinase activity on CTD is much higher with CDKD;2 than CDKD;3, suggesting that multiple CAKs differently regulate the cell cycle and transcription (Shimotohno et al., 2003). The kinase activity of CDKD;1 on CDK and CTD was not detected *in vitro* (Shimotohno et al., 2004).

CDKF (originally named CAK1At) is another CAK and plant-specific protein that is encoded by a single gene, *CDKF;1*, in *A. thaliana* (Shimotohno

et al., 2004, 2006; Umeda et al., 1998). CDKF;1 can phosphorylate human CDK2 *in vitro* and CDKA;1 in *A. thaliana* root protoplasts (Shimotohno et al., 2006; Umeda et al., 1998). CDKF;1 also phosphorylates CDKD;2 and CDKD;3, thereby activating the CTD kinase activity of CDKD;2 (Shimotohno et al., 2004). These results suggest that the kinase cascade is mediated by multiple CAKs that coordinately regulate basal transcription and cell-cycle progression during plant development (Umeda et al., 2005).

A null mutation of *CDKF;1* does not affect the activity of CDKA, CDKB1, or CDKB2; however, it strongly impaired cell proliferation and cell expansion during postembryonic development (Takatsuka et al., 2009). Protein stability and the CTD kinase activity of CDKD;2 are decreased in this *cdkf;1* mutant, suggesting that defective basal transcription might cause these defects (Takatsuka et al., 2009). Therefore, it is inferred that CDKDs are mainly involved in CDK activation during postembryonic development. Although loss-of-function mutants for *CDKD;1* or *CDKD;3* do not show any growth defects (Shimotohno et al., 2006), further studies with multiple combinations of *cdkd* mutants will reveal the *in vivo* functions of each CDKD in plant tissues.

As expected from the importance of T-loop phosphorylation, a mutant CDKA;1 with a nonphosphorylatable Val at Thr-161 does not rescue the *cdka;1* mutant from the male gametophytic defect (Dissmeyer et al., 2007). A phospho-mimicry version of CDKA;1 with Asp at Thr-161 can rescue *cdka;1* mutants, but it shows significantly reduced kinase activity; thus, the rescued plant exhibits strongly reduced vegetative growth and sterility due to the meiotic defect (Dissmeyer et al., 2007). These results indicate that the proper regulation of T-loop phosphorylation is a prerequisite for the full activity of CDKA;1 and normal plant development.

CDK activity is modulated by the inhibitory phosphorylation of Tyr and Thr in its N-terminal ATP-binding domain. In yeast and animals, WEE1 kinase and CDC25 phosphatase regulate the phosphorylation status of these residues, thereby controlling cell-cycle progression. *A. thaliana* WEE1 can phosphorylate CDKA;1 at Tyr-15 *in vitro* (Shimotohno et al., 2006). The expression of CDKA;1 in which Thr-14 and Tyr-15 are substituted with phospho-mimic Asp and Glu, respectively, results in strongly reduced cell proliferation, and does not fully complement the generative cell division defect in the *cdka;1* mutant, demonstrating that inhibitory phosphorylation also controls the activity of plant CDKA (Dissmeyer et al., 2009). However, a *wee1* mutant and *cdka;1* expressing nonphosphorylatable CDKA;1 (with Val and Phe, instead of Thr-14 and Tyr-15, respectively) behave differently in terms of the DNA damage response (see below), and the functional homolog of CDC25 has not been identified in higher plants (Boudolf et al., 2006; Dissmeyer et al., 2009). Therefore, the functional significance of inhibitory phosphorylation in plant development and the genotoxic stress response is currently unknown.

2.5. Protein degradation

Controlled protein degradation of cell-cycle regulators is one of the key mechanisms that ensures the one-way progression of the eukaryotic cell cycle (Frescas and Pagano, 2008; Marrocco et al., 2010; Pesin and Orr-Weaver, 2008). The levels of many cell-cycle regulators with either positive or negative functions in cell-cycle progression are regulated by protein degradation in a cell-cycle phase-dependent manner or in response to internal or external stimuli (Marrocco et al., 2010). Proteins for degradation are selectively labeled with polyubiquitin by specific E3 ubiquitin ligases (Pickart, 2001). Anaphase-promoting complex/cyclosome (APC/C) and Skp1/Cullin/F-box (SCF) are the major E3 ubiquitin ligase classes involved in cell-cycle control (Vodermaier, 2004).

As the levels of cyclin proteins are the major determinant of CDK activity, cyclin degradation is an important mechanism in cell-cycle control. Plant A- and B-type cyclins contain the destruction box motif that is required for proteasome-mediated degradation (Colon-Carmona et al., 1999; Criqui et al., 2000; Genschik et al., 1998; Weingartner et al., 2004). The significance of the protein degradation of cyclins was demonstrated by the overexpression of CYCB1 with a mutation in its destruction box in *N. tabacum* plants and suspension-cultured BY-2 cells (Weingartner et al., 2004). The expression of mutated CYCB1 impairs M phase progression after anaphase, resulting in a large proportion of polyploid nuclei and abnormal organ development. Ubiquitination of CYCA and CYCB is probably mediated by APC/C, as knockout or knockdown of APC/C subunit genes causes the accumulation of CYCA or CYCB fused with a GUS reporter (Capron et al., 2003; Kwee and Sundaresan, 2003; Marrocco et al., 2009; Pérez-Pérez et al., 2008).

CYCD3 expression is also regulated by proteolysis (Planchais et al., 2004). *A. thaliana* CYCD3;1 is a highly unstable protein, and its levels rapidly decrease upon sucrose depletion, which is associated with cell-cycle arrest at the G1 phase. In fact, CYCD3;1 levels are significantly decreased by treatment with a protein synthesis inhibitor, cycloheximide, while they are increased by treatment with MG132 in proliferating and sucrose-starved cells (Planchais et al., 2004). These results indicate the dynamic regulation of CYCD3 levels by controlled proteolysis in response to nutrient conditions.

In addition to positive regulators of the cell cycle, the levels of negative regulators are also controlled via protein degradation. In yeast and metazoans, CDK inhibitors are degraded at the G1/S transition through SCF-type E3 ligase-mediated ubiquitination; thus, CDK is activated, resulting in S phase entry (Frescas and Pagano, 2008; Schwob et al., 1994). In plants, several KRPs, such as ICK1/KRP1 and ICK2/KRP2, were suggested to be degraded by the proteasome (Jakoby et al., 2006; Ren et al., 2008; Verkest

et al., 2005). Recently, the importance of KRP protein degradation in gametophytic cell division was demonstrated. The RHF1a and RHF2a RING-finger proteins, which are components of the RING-type E3 ligase complex, were shown to be involved in KRP6 turnover during gametogenesis (Liu et al., 2008). A double mutant for *RHF1a* and *RHF2a* showed defective gametophytic cell division, and this phenotype was rescued by reducing KRP6 expression, indicating the functional relevance of KRP6 degradation. It was also shown that the FBL17 F-box protein is involved in male gametogenesis through its targeting of KRP6 and KRP7 (Gusti et al., 2009; Kim et al., 2008). FBL17 is a component of an SCF complex and is specifically expressed in developing pollen before generative cell division. An *fbl17* mutant is defective for generative cell division in developing pollen, which is very similar to the phenotype observed in the *cdka;1* mutant, suggesting that FBL17 enables generative cell division by activating CDKA;1 via the degradation of KRP6 and KRP7 (Gusti et al., 2009; Kim et al., 2008).

Two types of E3 ubiquitin ligases are implicated in the control of KRP1 degradation: the SCF-type complex containing F-box proteins SKP2A and SKP2B, which are homologs of mammalian SKP2, and RING E3 with RING-finger protein RKP, the homolog of mammalian KPC1. In mammals, SKP2 and KPC1 are independently involved in the degradation of the $p27^{Kip1}$ CDK inhibitor (Frescas and Pagano, 2008; Kamura et al., 2004). Whereas the overall sequences of SKP2s and RKP are very different from their mammalian counterparts, some functional conservation has been demonstrated. The overexpression of *SKP2B* or *RKP* inhibits the accumulation of KRP1 and suppresses the phenotypes of *KRP1*-overexpressing plants, for example, leaf serration (Ren et al., 2008). However, triple loss-of-function *skp2a skp2b rkp* plants show normal morphology, regardless of the high accumulation of KRP1. Therefore, unlike gametophytic cell division, the importance of CDK inhibitor degradation during vegetative development has not been clearly demonstrated.

2.6. Transcriptional control

The transcriptional control of cell-cycle regulators is largely unknown in plants, although the expression of many cell-cycle-related genes is differently regulated during the cell cycle (Menges et al., 2003). Many genes with a peak of expression at the G2/M phase, including the genes for A- and B-type cyclins, kinesin-like proteins (NACKs), and the cytokinesis-specific syntaxin KNOLLE (KN), have mitosis-specific activator (MSA) elements in their promoter regions (Ito, 2000; Ito et al., 1998; Menges et al., 2005). MSA elements are necessary and sufficient for G2/M-specific expression (Ito et al., 1998). Three Myb repeat (MYB3R) transcription factors that recognize MSA elements were first identified in tobacco (NtMYBA1,

NtMYBA2, and NtMYBB; Ito et al., 2001). NtMYBA1 and NtMYBA2 are specifically expressed from G2 to the early M phase and can transactivate MSA-containing promoters. However, NtMYBB is expressed throughout the cell cycle and has a repressive function toward MSA elements (Ito et al., 2001). NtMYBA2 was shown to be phosphorylated and activated by CDK–CYCA or CDK–CYCB complexes, suggesting a positive feedback loop in G2/M-specific transcriptional control where MYB promotes the transcription of CYCA and CYCB, and then CDK–CYCA/B activates MYB (Araki et al., 2004). In addition, the promoters of *NtMYBA1* and *NtMYBA2* contain MSA elements and are possibly activated by their own products (Kato et al., 2009). These mechanisms are suggested to cause a burst of CDK activity and consequent entry into the M phase.

A. thaliana has five MYB3R proteins, MYB3R1 to MYB3R5, in which MYB3R1 and MYB3R4 are highly similar to NtMYBA1 and NtMYBA2 (Haga et al., 2007). A double mutant for *MYB3R1* and *MYB3R4* shows a defect in cytokinesis and decreased expression of some G2/M-specific genes, for example, *CYCB2* and *KN*. Interestingly, the transcript level of *MYB3R1* does not change throughout the cell cycle, whereas *MYB3R4* has a peak of expression at G2/M (Haga et al., 2007), suggesting that the posttranslational regulation of MYB3R1 may be associated with the G2/M-specific transcription of target genes, for example, MYB3R1 may be phosphorylated and activated by CDK, as in the case of NtMYBA2. However, even in an *myb3r1 myb3r4* double mutant, many mitotic genes carrying MSA elements within their promoters still display a G2/M-biased expression pattern, suggesting that other MYB3R factors and/or unidentified transcription factors are also involved in the control of their G2/M phase-specific expression. A possible candidate is another MYB protein, CDC5, which is implicated in cell-cycle control in yeast and animals (Bernstein and Coughlin, 1998; Ohi et al., 1998). A homozygous *cdc5* mutant of *A. thaliana* is embryonic lethal, and *CDC5* knockdown led to defects in meristem activity and the decreased expression of *CDKB1;1* (Lin et al., 2007).

In addition to G2/M-specific regulation via the MSA-elements, *CYCB1;1* expression is quantitatively controlled through GCCCR (R is A or G) motifs in its promoter (Li et al., 2005). Class I teosinte-branched, cycloidea, PCNA factor (TCP) transcription factors bind to GGNCCCAC consensus sequences; indeed, TCP20 binds to the *CYCB1;1* promoter in a chromatin immunoprecipitation (ChIP) assay. Interestingly, GCCCR motifs are also required for the high-level expression of ribosomal protein genes in rapidly growing cells, and TCP20 also binds to their promoters, suggesting that TCP proteins may coordinate growth and division in proliferating cells (Li et al., 2005).

A. thaliana CDKA;1 is expressed not only in the dividing cells of the embryo and meristem but also in the differentiated tissues of the root, leaf,

and flower (Adachi et al., 2009). Detailed promoter analyses revealed that distinct *cis*-elements independently regulate the quantitative and cell type-specific expression of *CDKA;1*. Expression in the epidermis on the abaxial side (underside) of leaves is regulated by a promoter region that is distinct from the other regulatory elements controlling its expression in the inner layers of leaves and shoot apical meristem, including the outermost L1 layer (Adachi et al., 2009). Such cell type-specific transcriptional control of cell-cycle regulators may underpin the highly organized morphogenesis of organs.

2.7. E2F-RBR pathway

E2F transcription factors are involved in control of the G1/S transition in animals and plants by mediating the transcriptional activation of many genes required for cell-cycle progression and DNA replication (Inzé and De Veylder, 2006; van den Heuvel and Dyson, 2008). E2F and dimerization partner (DP) proteins form a heterodimer and bind to the E2F-binding sites in target promoters. The *A. thaliana* genome encodes three canonical E2F proteins (E2Fa, E2Fb, and E2Fc) and two DP proteins (DPa and DPb). E2Fa and E2Fb function as transcriptional activators, and the overexpression of E2Fa or E2Fb with DPa induced cell proliferation in differentiated tissues and tobacco BY-2 cells (De Veylder et al., 2002; Magyar et al., 2005; Rossignol et al., 2002; Sozzani et al., 2006). However, the E2Fc–DPb complex acts as a repressor and has a negative effect on cell proliferation and the expression of a DNA replication-related gene (del Pozo et al., 2002, 2006). The E2F-targets include many genes involved in the initiation and progression of DNA replication, DNA repair, and chromatin regulation (Ramirez-Parra et al., 2003; Takahashi et al., 2008, 2010b; Vandepoele et al., 2005).

The temporal regulation of E2F-DP activity is controlled by its interactions with a negative regulator, the retinoblastoma (Rb) protein (RBR in plants). CDK-mediated hyperphosphorylation of Rb during the G1 phase releases a functional E2F-DP heterodimer that activates target genes and promotes S phase entry (Attwooll et al., 2004; Dyson, 1998; Shen, 2002). Plant RBR proteins interact with CYCDs and are phosphorylated by CYCD–CDKA complexes (Boniotti and Gutierrez, 2001; Nakagami et al., 1999, 2002). The functional significance of plant RBR proteins was demonstrated by genetic analysis in *A. thaliana*, which encodes only one RBR protein. Knockout or knockdown of the *RBR* gene causes excessive cell proliferation and defects in cell differentiation during megagametogenesis and in the root and shoot (Borghi et al., 2010; Chen et al., 2009; Ebel et al., 2004; Wildwater et al., 2005). Interestingly, loss of *RBR* or the simultaneous overexpression of E2Fa and DPa in root stem cells leads to

an increase of the stem cell pool, implying that the stem cell state is maintained by the E2F–RBR pathway (Wildwater et al., 2005).

In addition to the canonical E2F proteins, plants and mammals have atypical E2F factors (Lammens et al., 2009). In *A. thaliana*, three atypical E2F factors have been identified, E2Fd/DEL2, E2Fe/DEL1, and E2Ff/DEL3 (DEL stands for DP-E2F-like), which have characteristics of E2F and DP (Vandepoele et al., 2002). Unlike canonical E2Fs, atypical E2Fs can bind to target DNA without forming heterodimers with DP proteins, probably because atypical E2Fs have a duplicated DNA-binding domain; one is similar to that in canonical E2Fs and the other is similar to that in DPs (Kosugi and Ohashi, 2002; Lammens et al., 2009; Mariconti et al., 2002). It is unlikely that the atypical E2Fs are regulated by the RBR protein because they do not have an Rb-binding domain (Lammens et al., 2009). Although atypical E2Fs competitively inhibit the transcription of genes controlled by canonical E2Fs (Kosugi and Ohashi, 2002; Mariconti et al., 2002), the biological functions of atypical E2Fs do not seem to be directly related to the G1/S transition (Lammens et al., 2008; Ramirez-Parra et al., 2004; Vlieghe et al., 2005). By using a ChIP assay, E2Ff/DEL3 was shown to bind to the promoters of genes for cell wall biogenesis and expansion, which contain putative E2F-binding sites, but not to those of DNA replication genes. As a consequence, the loss of function or overexpression of *E2Ff/DEL3* affects cell elongation without influencing the cell cycle (Ramirez-Parra et al., 2004). E2Fe/DEL1 represses endoreduplication in proliferating cells, likely through the repression of the CCS52A2 APC activator gene (Lammens et al., 2008; Vlieghe et al., 2005; see below). Recently, the altered expression of E2Fd/DEL2 was shown to cause changes in cell division and elongation in the root meristem and the expression of several cell-cycle regulators, including *E2Fa*, *E2Fb*, and *E2Fe/DEL1* (Sozzani et al., 2010b). Although the direct targets of E2Fd/DEL2 have not been identified, this result implies that genetic interactions among E2Fs may be involved in the proper control of cell proliferation during organ formation and tissue development.

3. Endocycle

The endocycle is an alternate version of the cell cycle that leads to endoreduplication, in which cells multiply their nuclear DNA content (ploidy) by repeating DNA replication without an intervening mitosis. Endoreduplication is often associated with cell expansion and cell differentiation; thus, the switch from the mitotic cell cycle to the endocycle is correlated with a phase change from cell proliferation to cell differentiation. The extent and relevance of endoreduplication differ among species and

cell types. In *A. thaliana*, endoreduplication occurs in most organs and tissues, for example, root, hypocotyl, leaf, and sepal; however, endoreduplication is rarely observed in tobacco and rice. Although increased ploidy probably contributes to cell growth and expansion, cell size is not strictly correlated with the ploidy level in different tissues, species, or intraspecific variants (Sugimoto-Shirasu and Roberts, 2003). Therefore, the functional significance of endoreduplication during organ development is currently enigmatic, but many efforts toward understanding the molecular mechanisms controlling the switch from the mitotic cycle to the endocycle and endocycle progression have been made in the past decade (Breuer et al., 2010).

3.1. Endocycle machinery

To operate the endocycle, cells need to skip the entire mitotic stage, including chromosome compaction, separation, and cytokinesis. To achieve this, the activity of mitotic cyclin–CDK complexes needs to be repressed to inhibit G2-to-M progression. Further, rereplication without passing through the mitotic events requires specialized mechanisms because normal mitotic cells have a regulatory system that prevents rereplication until mitosis is completed. During the mitotic cell cycle, components of the prereplication complex (pre-RC) dissociate from chromatin after the initiation of DNA replication, thereby preventing rereplication until the end of the M phase. Lowering CDK activity at the end of the M phase through the action of APC enables the pre-RC components to associate with chromatin (Wuarin et al., 2002). Therefore, one can speculate that the specific reduction of mitotic CDK activity inhibits entry to mitosis and facilitates rereplication. In addition, studies of the endocycle in *Drosophila melanogaster* suggested that the APC is also involved in DNA replication in endocycling cells through the degradation of geminin, an inhibitor of pre-RC formation (Zielke et al., 2008). Therefore, endocycling cells share most of the same regulatory components as mitotic cells to achieve cyclical and repetitive DNA replication, but some triggers that cause quantitative changes of these components are required for endocycle induction (Fig. 7.2).

CDKB1 and CDKB2 are possible CDK candidates whose activity is repressed at the onset of the endocycle, as they show a biased expression at G2/M in dividing cells (Andersen et al., 2008; Boudolf et al., 2004b). The overexpression of dominant-negative (kinase-dead) CDKB1;1 in *A. thaliana* causes the accelerated onset of the endocycle (Boudolf et al., 2004b). Conversely, the simultaneous overexpression of CDKB1;1 and its interacting partner CYCA2;3 induces ectopic cell division and strongly reduces the ploidy level (Boudolf et al., 2009). These results indicate that the downregulation of CDKB1;1–CYCA2;3 activity is one of the mechanisms that controls the transition from mitosis to the endocycle.

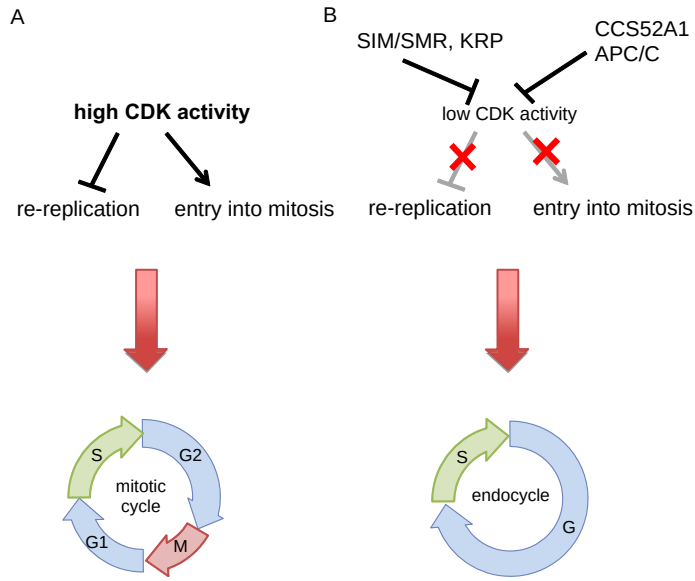

Figure 7.2 Control of the mitotic cycle and endocycle. (A) In the mitotic cell cycle, a high level of CDK activity triggers entry into M phase and inhibits S phase entry by preventing pre-RC formation. At the end of mitosis, APC/C induces cyclin degradation and thus lowers CDK activity, leading to pre-RC formation on chromatin. (B) In endoreduplicating cells, CDK activity is lowered by the action of CCS52A1-APC/C and the CDK inhibitors SIM/SMR and KRP. Low CDK activity leads to the inhibition of M phase entry and the activation of rereplication.

The level of CYCA2;3 was shown to be regulated by the APC/C activator CCS52A1. CCS52A1 is a member of the CDH1/FZR/CCS52-like APC/C activator family, which brings the substrate to the APC/C. *A. thaliana* expresses three *CCS52* genes: *CCS52A1*, *CCS52A2*, and *CCS52B*. In a *ccs52a1* mutant, CYCA2;3-GFP is stabilized in a zone where cells exit from the mitotic cycle and enter the endocycle, indicating that CCS52A1 downregulates CYCA2;3 directly or indirectly (Boudolf et al., 2009). Loss-of-function and overexpression studies showed that CCS52A1 positively regulates entry into the endocycle in roots, trichomes, and leaves (Kasili et al., 2010; Larson-Rabin et al., 2009; Vanstraelen et al., 2009). The expression of *CCS52A1* in roots starts in cells that shift from the mitotic cycle to the endocycle; thus, it may determine the timing of this switch.

CDKB1;1 has been proposed to control the transition to the endocycle by modulating CDKA;1 activity through the regulation of the levels of the KRP2 CDK inhibitor (Verkest et al., 2005). Moderate overexpression of KRP2 decreases CDKA;1 activity in mitotically active tissue, but not in

endoreduplicating tissue, and promotes endoreduplication. The weak inhibition of CDKA;1 is supposed to cause a specific inhibition of the mitotic activity of CDK, thus leading to endoreduplication. CDKB1;1 phosphorylates KRP2, leading to its proteasome-mediated degradation (Verkest et al., 2005). CDKB1;1 mRNA and protein levels are higher in mitotically active tissue than in endoreduplicating tissue, suggesting that CDKB1;1 promotes KRP2 degradation and inhibits entry into the endocycle by maintaining CDKA;1 activity. This hypothesis offers a new mechanism by which the fine-tuning of phase-specific CDK activity is controlled through the interaction of different CDK proteins.

CDKB2 was also shown to repress entry into the endocycle (Andersen et al., 2008). *CDKB2;1* and *CDKB2;2* are specifically expressed in meristems. The expression of artificial microRNA for *CDKB2;1* and *CDKB2;2* leads to early entry into the endocycle; however, a similar result was also obtained by overexpressing *CDKB2;1*, suggesting that strict control of CDKB2 levels is crucial to maintain meristem activity and the pool of dividing cells.

The SIM and SMR family of CDK inhibitors provide another parallel mechanism that regulates CDK activity at the onset of the endocycle. A *sim* mutant develops multicellular trichomes with decreased ploidy levels (Walker et al., 2000). Conversely, the overexpression of *SIM* generates greatly enlarged cells and increased ploidy levels (Churchman et al., 2006). The *sim* mutant ectopically expresses *CYCB1;2* in trichomes, and the expression of *CYCB1;2* under the control of a trichome-specific promoter induces multicellular trichomes, as observed in the *sim* mutant (Schnittger et al., 2002). These results suggest that SIM promotes the onset of the endocycle by reducing mitotic CDK activity during trichome development.

SMR1/LOSS OF GIANT CELLS FROM ORGANS (LGO) regulates the endocycle in sepal epidermal cells. The *A. thaliana* sepal epidermis is composed of cells of strikingly varied sizes with ploidy levels from 2C to 16C, where cell size is highly correlated with the ploidy level (Roeder et al., 2010). This endocycle-associated cell expansion is dependent on the function of SMR1/LGO, as an SMR1/LGO loss-of-function mutation resulted in the loss of giant cells in the sepal epidermis, which was accompanied by a decreased level of DNA ploidy. The endoreduplication level and the morphology of trichomes are normal in the *smr1/lgo* mutant, indicating that each SIM-related CDK inhibitor may control endoreduplication in a particular developmental context.

Maize (*Zea mays*) endosperm and tomato (*Solanum lycopersicon*) fruit have been used as model tissues to investigate endocycle control. Individual nuclei in maize endosperm increase their DNA ploidy from 3C to more than 96C (Kowles and Phillips, 1985), and the progression of endoreduplication is associated with a decrease of M phase-promoting CDK activity

(Grafi and Larkins, 1995). Although the mechanism that specifically down-regulates M phase-promoting CDK activity in developing endosperm is currently unknown, it might involve phosphorylation by WEE1 (Sun et al., 1999) or binding to KRPs (Coelho et al., 2005). In the pericarp of tomato fruit, the ploidy reaches up to 256C (Joubès et al., 1999), and the level of ploidy is well correlated with cell size and fruit weight in various tomato strains (Cheniclet et al., 2005). Knockdown of either *WEE1* or *CCS52A* decreased the ploidy level, cell size, and fruit weight, suggesting that WEE1 and CCS52A are involved in the mitosis-to-endocycle transition and/or endocycle progression (Gonzalez et al., 2007; Mathieu-Rivet et al., 2010). The molecular mechanisms that control the expression and activity of these endocycle-promoting factors will be important in the tissue-specific regulation of cell division and cell expansion.

3.2. Developmental regulation of the endocycle

The spatiotemporally regulated transition from the mitotic cycle to the endocycle is critical for proper organ development. To control the machinery that drives the mitotic cycle and the endocycle, developmental signals, for example, plant hormones and growth factors, are inferred to play key roles. It is easy to follow the transition from the mitotic cycle to the endocycle in *A. thaliana* roots because the root cells significantly increase their volume at the onset of the endocycle. The distribution of auxin has been shown to be critical for the regulation of cell proliferation and cell expansion in a concentration-dependent manner in the root meristem, that is, a high concentration of auxin promotes cell proliferation in the apical region and a lower concentration allows cells to expand and differentiate in the basal region (Blilou et al., 2005; Galinha et al., 2007). Recently, it was reported that auxin guides the transition from the mitotic cycle to the endocycle by modulating the expression of cell-cycle regulators (Ishida et al., 2010). Mutations in genes for auxin biosynthesis, transport, and signaling or treatment with auxin antagonists led to an increase in DNA ploidy. In auxin signaling-deficient roots, cells enter the endocycle in a more apical part compared to wild type or nontreated plants, suggesting that auxin represses entry into the endocycle. Since this early onset of the endocycle was partially suppressed by the overexpression of CYCA2;3, auxin appears to maintain the mitotic state of cells by upregulating CDK activity.

A SUMO E3 ligase, HIGH PLOIDY2 (HPY2), is expressed in the root meristem, and its expression gradually decreases as cells leave the mitotic cycle and enter the endocycle (Ishida et al., 2009). An *hpy2* mutant shows the early onset of the endocycle and expresses very low levels of CDKB1 and CDKB2. These results demonstrate that HPY2-mediated protein SUMOylation is important in maintaining the mitotic state of cells and in

repressing the endocycle. A graded distribution of auxin and the auxin-inducible AP2 transcription factor PLETHORA (PLT) may define the expression domain of HPY2 and repress premature entry into the endocycle (Galinha et al., 2007; Ishida et al., 2009).

In addition to auxin, other plant hormones, for example, cytokinin and gibberellin (GA), also coordinate cell division and cell differentiation in the root meristem (Achard et al., 2009; Dello Ioio et al., 2008; Ubeda-Tomás et al., 2009). Since the actions of these plant hormones cross talk with the signaling mechanisms underlying the auxin response (Dello Ioio et al., 2008; Fu and Harberd, 2003; Moubayidin et al., 2010; Ruzicka et al., 2009), they also affect the transition into the endocycle (Ishida et al., 2010). Further, recently identified secreted small peptides, root meristem growth factors (RGFs), could be additional important regulators because they show a graded expression pattern in the root meristem with maxima in the stem cell region; in addition, they positively regulate the meristematic cell population by promoting the expression of PLT (Matsuzaki et al., 2010).

4. Regulation of the Cell Cycle by Internal and External Stimuli

4.1. DNA damage checkpoint

Because of their sessile lifestyle and their dependence on sunlight for photosynthesis, plants cannot evade genotoxic ultraviolet (UV) radiation or other threats to the integrity of their genomes. DNA damage can be induced not only by exposure to environmental stress, for example, UV radiation and genotoxic compounds but also by endogenous factors, for example, replication errors and reactive oxygen intermediates (Ciccia and Elledge, 2010). Therefore, all organisms deploy defense mechanisms to operate signal transduction pathways that enable damaged cells to repair their DNA and to recover from the emergent state. To faithfully repair damaged DNA, cells must coordinate DNA repair with cell-cycle progression by delaying or even arresting the cell cycle until the damage is completely repaired. This is called the DNA damage checkpoint (Fig. 7.3).

4.1.1. ATM, ATR, and SOG1

The DNA damage checkpoint in plants is largely unexplored. Although some factors that sense DNA damage are conserved among fungi, animals, and plants, most of the signal transducers identified in fungi and animals are not conserved in plants (Cools and De Veylder, 2009). This leads to the hypothesis that plants have specific DNA damage checkpoint mechanisms that support their different lifestyle and cellular events.

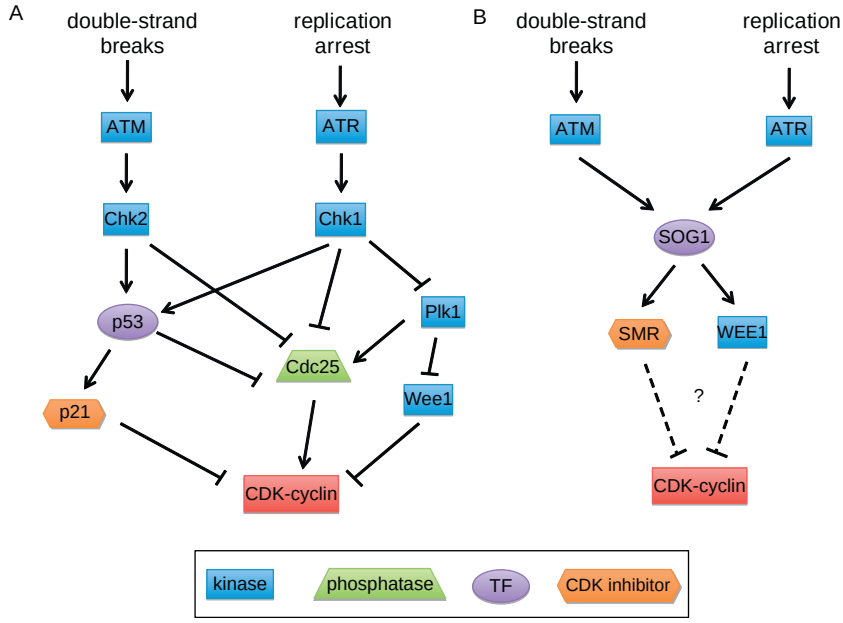

Figure 7.3 DNA damage checkpoint pathways in mammals and plants. (A) DNA damage checkpoint mechanism in mammals. (B) DNA damage checkpoint mechanism in *A. thaliana*. Orthologs of Chk1, Chk2, and Cdc25 have not been identified in plants.

The conserved protein kinases ataxia telangiectasia mutated (ATM) and ATM and Rad3-related (ATR) transmit DNA damage signals to cellular events by phosphorylating several key proteins. Generally, DNA double-strand breaks (DSBs) activate ATM, whereas ATR is activated in response to single stranded DNA, which is generated as a repair intermediate or by replication arrest. An *A. thaliana atm* mutant shows hypersensitivity to gamma irradiation and the DNA-alkylating agent methyl methanesulfonate and defects in meiosis (Garcia et al., 2003). However, an *atr* mutant is hypersensitive to hydroxyurea (HU), aphidicolin, and UV-B, which block DNA replication, whereas it shows only mild sensitivity to gamma irradiation (Culligan et al., 2004). These results indicate that the functional differentiation of ATM and ATR are essentially conserved between animals and plants.

In animals, the p53 transcription factor governs most of the molecular events in the DNA damage response. After DNA damage, activated ATM and ATR phosphorylate and activate Chk2 and Chk1 kinases, respectively, and these active kinases then phosphorylate p53, leading to its stabilization and nuclear accumulation (Rozan and El-Deiry, 2007). As a

consequence, p53 actively transcribes many genes that regulate DNA repair, cell-cycle delay, and apoptosis.

Although phosphorylation targets of ATM and ATR, for example, Chk1, Chk2, and p53 homologs, have not been identified in plants, the participation of a central regulator in the DNA damage checkpoint was uncovered by the identification of the NAC-domain-containing transcription factor SOG1 (Yoshiyama et al., 2009). After gamma irradiation, the transcript levels of hundreds of genes (for DNA repair- and cell-cycle-related proteins) are rapidly elevated, and this upregulation is mostly dependent on *ATM* and *SOG1* but not on *ATR* (Culligan et al., 2006). A *sog1* mutant fails to arrest leaf development after gamma irradiation, which emerges in DNA repair-deficient *xpf* mutant backgrounds, and this phenotype is shared with an *atr* mutant, but not with an *atm* mutant. These results suggest that SOG1 has a role in ATM- and ATR-dependent pathways; therefore, it may be a functional homolog of p53 and controls a broad transcriptional response to DNA damage.

4.1.2. Cell-cycle regulators

To delay or arrest the cell cycle upon DNA damage, CDK activity needs to be downregulated. In animals, the ATM-Chk2 and ATR-Chk1 pathways phosphorylate Cdc25 phosphatase, leading to its degradation or sequestration from the nucleus. In addition, ATM and ATR prevent the degradation of Wee1 kinase until DNA repair is completed; thus, CDKs are inactivated by inhibitory phosphorylation (Harper and Elledge, 2007). However, this mechanism is unlikely to function in plants because Chk1, Chk2, and Cdc25 homologs have not been identified.

WEE1 is rapidly transcriptionally upregulated after DNA damage treatment in *A. thaliana* (De Schutter et al., 2007). The upregulation of *WEE1* mRNA levels in response to gamma irradiation is dependent on *ATM*, whereas it is *ATR*-dependent during DNA replication stress. A loss-of-function *wee1* mutant is hypersensitive to HU and aphidicolin, which impair DNA replication. In addition, a double mutant for *wee1* and DNA replication-deficient *e2f target gene 1* (*etg1*) exhibits severely retarded growth, which is nearly identical to the phenotype of an *atr etg1* double mutant (Takahashi et al., 2008). These results suggest that WEE1 functions in response to DNA replication stress downstream of ATR. However, a *wee1* mutant and a nonphosphorylatable *cdka;1* (T14V, Y15F) mutant show different responses to HU; namely, the sensitivity of *cdka;1* (T14V, Y15F) to HU is the same as that of the wild type (Dissmeyer et al., 2009). Therefore, WEE1 seems to confer tolerance to DNA replication stress independently of the inhibitory phosphorylation of CDKA;1. It is possible that WEE1 phosphorylates proteins other than CDKA;1 to preserve cellular and meristem integrity after DNA replication stress.

Some genes encoding the SIM and SMR CDK-inhibitor families are strongly upregulated by gamma irradiation (Adachi et al., 2011; Culligan et al., 2006). This rapid and strong upregulation is dependent on ATM. Although a role for this group of CDK inhibitors in the cell-cycle checkpoint has not been demonstrated, it might have an inhibitory function on CDKs in response to DNA damage.

Although the expression levels of several mitotic cyclin or CDK genes is decreased after DNA damage treatment (Adachi et al., 2011), *CYCB1;1* expression is rapidly and strongly upregulated after gamma irradiation (Culligan et al., 2006; Ricaud et al., 2007). This upregulation is due to transcriptional activation and posttranslational stabilization, which are mainly dependent on ATM and ATR, respectively (Culligan et al., 2006). The increased expression of *CYCB1;1* was also observed in several *A. thaliana* mutants that constitutively accumulate DNA damage, even in nondividing cells (Breuer et al., 2007; Inagaki et al., 2006; Kirik et al., 2007; Suzuki et al., 2005; Takahashi et al., 2008). However, these mutants vary in their cell-cycle-related phenotypes, for example, some promoted entry into the endocycle, and others had reduced DNA ploidy levels. Therefore, the role of *CYCB1;1* in the DNA damage response is currently enigmatic. It might act as a counterpoise against the downregulation of other mitotic genes and participate in the control of cell-cycle restart after the completion of DNA repair.

4.2. Phytohormones and the cell cycle

Plant development is highly adaptive to environmental conditions, for example, light, nutrient or water availability, temperature, and other stresses. Several phytohormones control plant growth and development in response to external signals by regulating cell proliferation and expansion. Some of them control meristem function and organogenesis, which involve the regulation of cell division. Considerable progress has been made on characterizing the molecular mechanisms that underlie the modulation of hormone levels or distribution in response to developmental or environmental cues and the cross talk between different hormonal signals (Wolters and Jürgens, 2009). However, it is largely unknown how these hormones regulate cell-cycle progression at the molecular level.

Auxin, cytokinin, GA, and brassinosteroid are the phytohormones that regulate plant growth and development. Among them, auxin and cytokinin were classically identified as hormones that stimulate cell proliferation; the exogenous application of auxin and cytokinin is essential for callus formation in explants (Skoog and Miller, 1957). Recently, it was shown that the localized accumulation of endogenous auxin and cytokinin is crucial for controlled cell proliferation in root and shoot apical meristems, respectively (Blilou et al., 2005; Miyawaki et al., 2006).

Auxin is required for the culture of tobacco BY-2 cells. It was shown that the addition of auxin stabilizes the E2Fb protein (Magyar et al., 2005), while coexpression of E2Fb with DPa can stimulate cell proliferation and inhibit cell expansion in the absence of auxin by promoting entry into the S and M phases. These results suggest that auxin regulates cell division by controlling the protein level of E2Fb.

During lateral root development, mitotically silent pericycle cells initiate cell division after receiving auxin signals. Successive treatments with an auxin transport inhibitor and auxin synchronously induce lateral root formation (Himanen et al., 2002). In this system, the expression of many cell-cycle regulators is differently regulated after auxin treatment. A number of G2/M genes are upregulated at 6 h after auxin treatment, indicating that auxin stimulates cell-cycle reentry in pericycle cells. Interestingly, within 1.5 h of auxin treatment, the expression of KRP2 is strongly reduced. The overexpression of *KRP2* reduces the number of lateral roots (Himanen et al., 2002), and a loss-of-function *krp2* mutant has increased lateral root density (Sanz et al., 2011). Therefore, the downregulation of KRP2 and possibly other KRPs may promote lateral root initiation, suggesting a role for KRPs in connecting the auxin signal with cell-cycle control.

Although the application of exogenous auxin and cytokinin at appropriate concentrations induces callus formation in plant tissues, a *proporz1* (*prz1*) mutant for the transcriptional adaptor protein PRZ1/AtADA2b forms callus-like tissue in the presence of either auxin or cytokinin (Sieberer et al., 2003). Upon callus formation, this *prz1* mutant shows altered expression of a number of cell-cycle-related genes, for example, *KRP2*, *KRP3*, and *KRP7* expressions are decreased as compared to wild type (Sieberer et al., 2003). Interestingly, the overexpression of *KRP7* partially rescues the developmental phenotype of *prz1* (Anzola et al., 2010). Conversely, antisense suppression of multiple *KRP* genes, including *KRP2*, *KRP3*, and *KRP7*, in wild-type plants leads to abnormal plant development and the generation of callus-like tissue in the absence of exogenous phytohormones. As the yeast homolog of PRZ1/AtADA2b is a subunit of Spt-Ada-Gcn5-acetyltransferase (SAGA), which controls histone acetylation, PRZ1/AtADA2b may control the expression of cell-cycle regulators, for example, *KRPs*, by regulating the histone acetylation of target loci, thereby regulating cell proliferation.

Cytokinin elevates the expression of *CYCD3;1* in cultured cells and *A. thaliana* plants, and its overexpression induces callus formation in explants in the absence of cytokinin (Riou-Khamlichi et al., 1999). Therefore, cytokinin is suggested to stimulate dedifferentiation and cell-cycle entry through the transcriptional induction of *CYCD3*. A triple mutant for *CYCD3;1–CYCD3;3* had reduced cell numbers and increased cell size in the lateral organs of the shoot (Dewitte et al., 2007). This *CYCD3* triple mutant generates shoot apical meristem with a reduced cell number as

compared with wild type and shows a reduced number of branching and axillary shoots, which are remarkably similar phenotypes to those observed in plants with reduced cytokinin levels (Dewitte et al., 2007; Werner et al., 2003). The endogenous cytokinin level is normal, but the cytokinin response in callus formation is impaired in *cycd3;1–3*, suggesting that the *CYCD3* genes are the key targets of cytokinin that promote cell division. *CYCD3* expression was also upregulated by brassinosteroid (Hu et al., 2000), but its physiological relevance has not yet been uncovered.

The AP2 family transcription factor AINTEGUMENTA (ANT) also coordinates cell proliferation and phytohormone signals. The overexpression of *ANT* produces larger organs in shoots by extending the period of cell proliferation and organ growth (Mizukami and Fischer, 2000). The expression of *ANT* is higher in proliferating organs, and *ANT*-overexpressing plants continue to express *CYCD3;1*, even in mature leaves, suggesting that ANT maintains cell division in growing organs (Elliott et al., 1996; Mizukami and Fischer, 2000). The auxin-inducible gene *AUXIN-REGULATED GENE INVOLVED IN ORGAN SIZE* (*ARGOS*) acts upstream of *ANT* and positively controls cell number and organ size (Hu et al., 2003), indicating a role for CYCD3 as a molecular link between auxin and cytokinin signaling in the regulation of cell proliferation and organ development.

GA regulates cell proliferation and cell expansion in response to environmental changes (Achard et al., 2006). GA acts by promoting the destruction of DELLA proteins, which restrain cell proliferation and expansion (Itoh et al., 2008). In a GA-deficient *ga1* mutant, the rate of cell production is decreased in the leaves and roots, and this phenotype is suppressed by the quadruple loss-of-function mutations in the DELLA proteins (*gai*, *rga*, *rgl1*, and *rgl2*; Achard et al., 2009; Ubeda-Tomás et al., 2009). The expression of *KRP2*, *SIM*, *SMR1*, and *SMR2* is elevated in *ga1* plants, and this is suppressed by the quadruple-DELLA mutant (Achard et al., 2009), suggesting that these CDK inhibitors might regulate the cell division rate under the control of the GA-DELLA module. Interestingly, auxin was shown to be necessary for the GA-mediated degradation of the DELLA proteins (Fu and Harberd, 2003), suggesting another pathway by which auxin promotes cell proliferation.

4.3. Developmental control of the cell cycle

Cell division and differentiation need to be fine-tuned in the developmental context to accomplish highly ordered morphogenesis. The understanding of the molecular mechanisms that control plant cell-cycle progression in a particular developmental process has been advanced in the past few years. The existence of exceptionally large numbers of cell-cycle-related genes implies that many of them act as "specialists" in each process.

Germination is the process in which the dormant embryo starts to grow by cell expansion and cell division. During germination, cells shift from the

quiescent state (at G1 in *A. thaliana*) to the proliferative state by the concomitant upregulation of many cell-cycle regulators in a highly ordered manner (Masubelele et al., 2005). Among them, 9 of the 10 *CYCD* genes are differentially upregulated. Loss-of-function mutants for *CYCD1;1* and *CYCD4;1* exhibit a delay in starting cell proliferation in the germinating root meristem, but the extent of the delay is different between these two mutants, suggesting nonredundant functions of these CYCDs in cell-cycle entry during germination.

In the root apical meristem, the well-characterized transcription factors SHOOTROOT (SHR) and SCARECROW (SCR) regulate the formative asymmetric division of ground tissue stem cells, which generates cortex and endodermis cells (Heidstra et al., 2004; Helariutta et al., 2000). Using cell type-specific transcriptomic analysis and ChIP-chip analysis, *CYCD6;1* was identified as a direct target of SHR and SCR (Sozzani et al., 2010a). The expression of *CYCD6;1* is specific to ground tissue stem cells, and its loss-of-function mutant exhibits defects in their formative division. Since the SHR/SCR-independent expression of *CYCD6;1* in ground tissue cells can induce their formative division in an *shr* mutant, SHR and SCR are suggested to regulate the specific asymmetric cell division, at least in part, by upregulating *CYCD6;1* (Sozzani et al., 2010a).

During postembryonic root development, the expression of *CYCD4;1* is specific to the pericycle cells adjacent to the xylem poles in the meristematic region, which later initiate lateral root formation (Nieuwland et al., 2009). A *cycd4;1* mutant has low cell division activity in the pericycle, leading to a decrease in lateral root density, but this does not affect cell division in the other cell files. It was also revealed that sucrose enhances lateral root formation, in part, by upregulating *CYCD4;1* expression. Although it is currently unknown how cell division in meristematic pericycle cells controls the frequency of lateral root formation, it is intriguing that nutrient-controlled lateral root density is mediated by the control of a specific cell-cycle regulator.

During leaf formation, a pair of guard cells is generated through a well-coordinated pattern of cell division in the stomatal lineage. The expression of *CDKB1;1* in cotyledons is specific to the stomatal lineage. The overexpression of dominant-negative CDKB1;1 (N161) resulted in a decrease of the total cell number and proportion of guard cells in cotyledons and leaves (Boudolf et al., 2004a). Although guard cells usually have a DNA ploidy of 2C, ~50% of the stomata in cotyledons of CDKB1;1 (N161) plants have an aberrant morphology with 4C nuclei as a result of the failure in the symmetric division of the guard mother cell. A recent report demonstrated that stomatal cell division is terminated via the negative regulation of CDKB1;1 by the two MYB transcription factors FOUR LIPS (FLP) and MYB88 (Xie et al., 2010). Therefore, *CDKB1;1* may have a specific role in controlling the symmetric division of guard mother cell at the final step of the stomatal developmental pathway.

Both *cycd4;1* and *cycd4;2* mutants show reduced number of nonprotruding cells in hypocotyls (Kono et al., 2007). Stomata are formed in the nonprotruding cell file; thus, the number of stomata was decreased in the mutant hypocotyls. Conversely, their overexpression increased the number of nonprotruding cells and stomata. However, in leaves, single and double mutants for *CYCD4;1* and *CYCD4;2* or their overexpression do not significantly affect cell division in the stomatal lineage, suggesting that different mechanisms control stomatal cell division between the leaves and hypocotyls.

5. Concluding Remarks

Considerable efforts have been made to understand the control of cell division in plant development; however, we are still far from a comprehensive understanding of the highly plastic regulation of plant development. Recent highlights are the demonstration of the direct control of cell-cycle-related genes by transcription factors, for example, SHR–SCR and FLP–MYB88, which play a major role in cell fate determination and cell differentiation. Although the spatiotemporal regulation of the cell cycle is not solely dependent on transcriptional control, the future identification of upstream transcriptional factors acting on the promoters of cell-cycle-related genes would provide further insights into the developmental control of the cell cycle. An understanding of the mechanisms underlying the transition from the mitotic cell cycle to the endocycle is also important to reveal the processes for cell differentiation and the control of organ size. Future studies will reveal how internal and external signals control cell-cycle progression and how plants maintain proper organ development under various environmental stresses.

ACKNOWLEDGMENTS

We thank Naoki Takahashi for comments on this chapter. S. I. is supported by Grants-in-Aid for Scientific Research on Innovative Areas (Grant No. 22119009) from the Ministry of Education, Culture, Sports, Science and Technology of Japan.

REFERENCES

Achard, P., Cheng, H., De Grauwe, L., Decat, J., Schoutteten, H., Moritz, T., et al., 2006. Integration of plant responses to environmentally activated phytohormonal signals. Science 311, 91–94.

Achard, P., Gusti, A., Cheminant, S., Alioua, M., Dhondt, S., Coppens, F., et al., 2009. Gibberellin signaling controls cell proliferation rate in Arabidopsis. Curr. Biol. 19, 1188–1193.

Adachi, S., Uchimiya, H., Umeda, M., 2006. Expression of B2-type cyclin-dependent kinase is controlled by protein degradation in *Arabidopsis thaliana*. Plant Cell Physiol. 47, 1683–1686.

Adachi, S., Nobusawa, T., Umeda, M., 2009. Quantitative and cell type-specific transcriptional regulation of A-type cyclin-dependent kinase in *Arabidopsis thaliana*. Dev. Biol. 329, 306–314.

Adachi, S., Minamisawa, K., Okushima, Y., Inagaki, S., Yoshiyama, K., Kondou, Y., et al., 2011. Programmed induction of endoreduplication by DNA double-strand breaks in Arabidopsis. Proc. Natl. Acad. Sci. USA 108, 10004–10009.

Andersen, S.U., Buechel, S., Zhao, Z., Ljung, K., Novák, O., Busch, W., et al., 2008. Requirement of B2-type cyclin-dependent kinases for meristem integrity in *Arabidopsis thaliana*. Plant Cell 20, 8088–8100.

Anzola, J.M., Sieberer, T., Ortbauer, M., Butt, H., Korbei, B., Weinhofer, I., et al., 2010. Putative Arabidopsis transcriptional adaptor protein (PROPORZ1) is required to modulate histone acetylation in response to auxin. Proc. Natl. Acad. Sci. USA 107, 10308–10313.

Araki, S., Ito, M., Soyano, T., Nishihama, R., Machida, Y., 2004. Mitotic cyclins stimulate the activity of c-Myb-like factors for transactivation of G2/M phase-specific genes in tobacco. J. Biol. Chem. 279, 32979–32988.

Attwooll, C., Lazzerini Denchi, E., Helin, K., 2004. The E2F family: specific functions and overlapping interests. EMBO J. 23, 4709–4716.

Bernstein, H.S., Coughlin, S.R., 1998. A mammalian homolog of fission yeast Cdc5 regulates G2 progression and mitotic entry. J. Biol. Chem. 273, 4666–4671.

Blilou, I., Xu, J., Wildwater, M., Willemsen, V., Paponov, I., Friml, J., et al., 2005. The PIN auxin efflux facilitator network controls growth and patterning in Arabidopsis roots. Nature 433, 39–44.

Boniotti, M.B., Gutierrez, C., 2001. A cell-cycle-regulated kinase activity phosphorylates plant retinoblastoma protein and contains, in Arabidopsis, a CDKA/cyclin D complex. Plant J. 28, 341–350.

Borghi, L., Gutzat, R., Fütterer, J., Laizet, Y., Hennig, L., Gruissem, W., 2010. Arabidopsis RETINOBLASTOMA-RELATED is required for stem cell maintenance, cell differentiation, and lateral organ production. Plant Cell 22, 1792–1811.

Boruc, J., Van den Daele, H., Hollunder, J., Rombauts, S., Mylle, E., Hilson, P., et al., 2010. Functional modules in the Arabidopsis core cell cycle binary protein–protein interaction network. Plant Cell 22, 1264–1280.

Boudolf, V., Rombauts, S., Naudts, M., Inzé, D., De Veylder, L., 2001. Identification of novel cyclin-dependent kinases interacting with the CKS1 protein of Arabidopsis. J. Exp. Bot. 52, 1381–1382.

Boudolf, V., Barroco, R., Engler Jde, A., Verkest, A., Beeckman, T., Naudts, M., et al., 2004a. B1-type cyclin-dependent kinases are essential for the formation of stomatal complexes in *Arabidopsis thaliana*. Plant Cell 16, 945–955.

Boudolf, V., Vlieghe, K., Beemster, G.T., Magyar, Z., Torres Acosta, J.A., Maes, S., et al., 2004b. The plant-specific cyclin-dependent kinase CDKB1;1 and transcription factor E2Fa-DPa control the balance of mitotically dividing and endoreduplicating cells in Arabidopsis. Plant Cell 16, 2683–2692.

Boudolf, V., Inzé, D., De Veylder, L., 2006. What if higher plants lack a CDC25 phosphatase? Trends Plant Sci. 11, 474–479.

Boudolf, V., Lammens, T., Boruc, J., Van Leene, J., Van Den Daele, H., Maes, S., et al., 2009. CDKB1;1 forms a functional complex with CYCA2;3 to suppress endocycle onset. Plant Physiol. 150, 1482–1493.

Breuer, C., Stacey, N.J., West, C.E., Zhao, Y., Chory, J., Tsukaya, H., et al., 2007. BIN4, a novel component of the plant DNA topoisomerase VI complex, is required for endoreduplication in Arabidopsis. Plant Cell 19, 3655–3668.

Breuer, C., Ishida, T., Sugimoto, K., 2010. Developmental control of endocycles and cell growth in plants. Curr. Opin. Plant Biol. 13, 654–660.
Breyne, P., Dreesen, R., Vandepoele, K., De Veylder, L., Van Breusegem, F., Callewaert, L., et al., 2002. Transcriptome analysis during cell division in plants. Proc. Natl. Acad. Sci. USA 99, 14825–14830.
Capron, A., Serralbo, O., Fülöp, K., Frugier, F., Parmentier, Y., Dong, A., et al., 2003. The Arabidopsis anaphase-promoting complex or cyclosome: molecular and genetic characterization of the APC2 subunit. Plant Cell 15, 2370–2382.
Chen, Z., Hafidh, S., Poh, S.H., Twell, D., Berger, F., 2009. Proliferation and cell fate establishment during Arabidopsis male gametogenesis depends on the Retinoblastoma protein. Proc. Natl. Acad. Sci. USA 106, 7257–7262.
Cheniclet, C., Rong, W.Y., Causse, M., Frangne, N., Bolling, L., Carde, J.P., et al., 2005. Cell expansion and endoreduplication show a large genetic variability in pericarp and contribute strongly to tomato fruit growth. Plant Physiol. 139, 1984–1994.
Churchman, M.L., Brown, M.L., Kato, N., Kirik, V., Hülskamp, M., Inzé, D., et al., 2006. SIAMESE, a plant-specific cell cycle regulator, controls endoreplication onset in *Arabidopsis thaliana*. Plant Cell 18, 3145–3157.
Ciccia, A., Elledge, S.J., 2010. The DNA damage response: making it safe to play with knives. Mol. Cell 40, 179–204.
Cockcroft, C.E., den Boer, B.G., Healy, J.M., Murray, J.A., 2000. Cyclin D control of growth rate in plants. Nature 405, 575–579.
Coelho, C.M., Dante, R.A., Sabelli, P.A., Sun, Y., Dilkes, B.P., Gordon-Kamm, W.J., et al., 2005. Cyclin-dependent kinase inhibitors in maize endosperm and their potential role in endoreduplication. Plant Physiol. 138, 2323–2336.
Colon-Carmona, A., You, R., Haimovitch-Gal, T., Doerner, P., 1999. Technical advance: spatio-temporal analysis of mitotic activity with a labile cyclin–GUS fusion protein. Plant J. 20, 503–508.
Cools, T., De Veylder, L., 2009. DNA stress checkpoint control and plant development. Curr. Opin. Plant Biol. 12, 23–28.
Criqui, M.C., Parmentier, Y., Derevier, A., Shen, W.H., Dong, A., Genschik, P., 2000. Cell cycle-dependent proteolysis and ectopic overexpression of cyclin B1 in tobacco BY2 cells. Plant J. 24, 763–773.
Culligan, K., Tissier, A., Britt, A., 2004. ATR regulates a G2-phase cell-cycle checkpoint in *Arabidopsis thaliana*. Plant Cell 16, 1091–1104.
Culligan, K.M., Robertson, C.E., Foreman, J., Doerner, P., Britt, A.B., 2006. ATR and ATM play both distinct and additive roles in response to ionizing radiation. Plant J. 48, 947–961.
D'Erfurth, I., Cromer, L., Jolivet, S., Girard, C., Horlow, C., Sun, Y., et al., 2010. The cyclin-A CYCA1;2/TAM is required for the meiosis I to meiosis II transition and cooperates with OSD1 for the prophase to first meiotic division transition. PLoS Genet. 6, e1000989.
De Clercq, A., Inzé, D., 2006. Cyclin-dependent kinase inhibitors in yeast, animals, and plants: a functional comparison. Crit. Rev. Biochem. Mol. Biol. 41, 293–313.
De Schutter, K., Joubès, J., Cools, T., Verkest, A., Corellou, F., Babiychuk, E., et al., 2007. Arabidopsis WEE1 kinase controls cell cycle arrest in response to activation of the DNA integrity checkpoint. Plant Cell 19, 211–225.
De Veylder, L., Beeckman, T., Beemster, G.T., Krols, L., Terras, F., Landrieu, I., et al., 2001. Functional analysis of cyclin-dependent kinase inhibitors of Arabidopsis. Plant Cell 13, 1653–1668.
De Veylder, L., Beeckman, T., Beemster, G.T., de Almeida Engler, J., Ormenese, S., Maes, S., et al., 2002. Control of proliferation, endoreduplication and differentiation by the Arabidopsis E2Fa-DPa transcription factor. EMBO J. 21, 1360–1368.

del Pozo, J.C., Boniotti, M.B., Gutierrez, C., 2002. Arabidopsis E2Fc functions in cell division and is degraded by the ubiquitin-SCF(AtSKP2) pathway in response to light. Plant Cell 14, 3057–3071.

del Pozo, J.C., Diaz-Trivino, S., Cisneros, N., Gutierrez, C., 2006. The balance between cell division and endoreplication depends on E2FC-DPB, transcription factors regulated by the ubiquitin-SCFSKP2A pathway in Arabidopsis. Plant Cell 18, 2224–2235.

Dello Ioio, R., Nakamura, K., Moubayidin, L., Perilli, S., Taniguchi, M., Morita, M.T., et al., 2008. A genetic framework for the control of cell division and differentiation in the root meristem. Science 322, 1380–1384.

Dewitte, W., Riou-Khamlichi, C., Scofield, S., Healy, J.M., Jacqmard, A., Kilby, N.J., et al., 2003. Altered cell cycle distribution, hyperplasia, and inhibited differentiation in Arabidopsis caused by the D-type cyclin CYCD3. Plant Cell 15, 79–92.

Dewitte, W., Scofield, S., Alcasabas, A.A., Maughan, S.C., Menges, M., Braun, N., et al., 2007. Arabidopsis CYCD3 D-type cyclins link cell proliferation and endocycles and are rate-limiting for cytokinin responses. Proc. Natl. Acad. Sci. USA 104, 14537–14542.

Dissmeyer, N., Nowack, M.K., Pusch, S., Stals, H., Inzé, D., Grini, P.E., et al., 2007. T-loop phosphorylation of Arabidopsis CDKA;1 is required for its function and can be partially substituted by an aspartate residue. Plant Cell 19, 972–985.

Dissmeyer, N., Weimer, A.K., Pusch, S., De Schutter, K., Kamei, C.L., Nowack, M.K., et al., 2009. Control of cell proliferation, organ growth, and DNA damage response operate independently of dephosphorylation of the Arabidopsis Cdk1 homolog CDKA;1. Plant Cell 21, 3641–3654.

Doerner, P., Jorgensen, J.E., You, R., Steppuhn, J., Lamb, C., 1996. Control of root growth and development by cyclin expression. Nature 380, 520–523.

Draetta, G.F., 1997. Cell cycle: will the real Cdk-activating kinase please stand up. Curr. Biol. 7, R50–R52.

Dyson, N., 1998. The regulation of E2F by pRB-family proteins. Genes Dev. 12, 2245–2262.

Ebel, C., Mariconti, L., Gruissem, W., 2004. Plant retinoblastoma homologues control nuclear proliferation in the female gametophyte. Nature 429, 776–780.

Elliott, R.C., Betzner, A.S., Huttner, E., Oakes, M.P., Tucker, W.Q., Gerentes, D., et al., 1996. AINTEGUMENTA, an APETALA2-like gene of Arabidopsis with pleiotropic roles in ovule development and floral organ growth. Plant Cell 8, 155–168.

Ferreira, P.C., Hemerly, A.S., Villarroel, R., Van Montagu, M., Inzé, D., 1991. The Arabidopsis functional homolog of the p34cdc2 protein kinase. Plant Cell 3, 531–540.

Frescas, D., Pagano, M., 2008. Deregulated proteolysis by the F-box proteins SKP2 and beta-TrCP: tipping the scales of cancer. Nat. Rev. Cancer 8, 438–449.

Fu, X., Harberd, N.P., 2003. Auxin promotes Arabidopsis root growth by modulating gibberellin response. Nature 421, 740–743.

Galinha, C., Hofhuis, H., Luijten, M., Willemsen, V., Blilou, I., Heidstra, R., et al., 2007. PLETHORA proteins as dose-dependent master regulators of Arabidopsis root development. Nature 449, 1053–1057.

Garcia, V., Bruchet, H., Camescasse, D., Granier, F., Bouchez, D., Tissier, A., 2003. AtATM is essential for meiosis and the somatic response to DNA damage in plants. Plant Cell 15, 119–132.

Genschik, P., Criqui, M.C., Parmentier, Y., Derevier, A., Fleck, J., 1998. Cell cycle-dependent proteolysis in plants. Identification of the destruction box pathway and metaphase arrest produced by the proteasome inhibitor mg132. Plant Cell 10, 2063–2076.

Gonzalez, N., Gévaudant, F., Hernould, M., Chevalier, C., Mouras, A., 2007. The cell cycle-associated protein kinase WEE1 regulates cell size in relation to endoreduplication in developing tomato fruit. Plant J. 51, 642–655.

Grafi, G., Larkins, B.A., 1995. Endoreduplication in maize endosperm: involvement of m phase-promoting factor inhibition and induction of s phase-related kinases. Science 269, 1262–1264.

Gusti, A., Baumberger, N., Nowack, M., Pusch, S., Eisler, H., Potuschak, T., et al., 2009. The *Arabidopsis thaliana* F-box protein FBL17 is essential for progression through the second mitosis during pollen development. PLoS One 4, e4780.

Haga, N., Kato, K., Murase, M., Araki, S., Kubo, M., Demura, T., et al., 2007. R1R2R3-Myb proteins positively regulate cytokinesis through activation of KNOLLE transcription in *Arabidopsis thaliana*. Development 134, 1101–1110.

Harper, J.W., Elledge, S.J., 2007. The DNA damage response: ten years after. Mol. Cell 28, 739–745.

Heidstra, R., Welch, D., Scheres, B., 2004. Mosaic analyses using marked activation and deletion clones dissect Arabidopsis SCARECROW action in asymmetric cell division. Genes Dev. 18, 1964–1969.

Helariutta, Y., Fukaki, H., Wysocka-Diller, J., Nakajima, K., Jung, J., Sena, G., et al., 2000. The SHORT-ROOT gene controls radial patterning of the Arabidopsis root through radial signaling. Cell 101, 555–567.

Hemerly, A., Engler J de, A., Bergounioux, C., Van Montagu, M., Engler, G., Inze, D., et al., 1995. Dominant negative mutants of the Cdc2 kinase uncouple cell division from iterative plant development. EMBO J. 14, 3925–3936.

Himanen, K., Boucheron, E., Vanneste, S., de Almeida Engler, J., Inzé, D., Beeckman, T., 2002. Auxin-mediated cell cycle activation during early lateral root initiation. Plant Cell 14, 2339–2351.

Hirayama, T., Imajuku, Y., Anai, T., Matsui, M., Oka, A., 1991. Identification of two cell-cycle-controlling cdc2 gene homologs in *Arabidopsis thaliana*. Gene 105, 159–165.

Hu, Y., Bao, F., Li, J., 2000. Promotive effect of brassinosteroids on cell division involves a distinct CycD3-induction pathway in Arabidopsis. Plant J. 24, 693–701.

Hu, Y., Xie, Q., Chua, N.H., 2003. The Arabidopsis auxin-inducible gene ARGOS controls lateral organ size. Plant Cell 15, 1951–1961.

Imai, K.K., Ohashi, Y., Tsuge, T., Yoshizumi, T., Matsui, M., Oka, A., et al., 2006. The A-type cyclin CYCA2;3 is a key regulator of ploidy levels in Arabidopsis endoreduplication. Plant Cell 18, 382–396.

Inagaki, S., Suzuki, T., Ohto, M.A., Urawa, H., Horiuchi, T., Nakamura, K., et al., 2006. Arabidopsis TEBICHI, with helicase and DNA polymerase domains, is required for regulated cell division and differentiation in meristems. Plant Cell 18, 879–892.

Inzé, D., De Veylder, L., 2006. Cell cycle regulation in plant development. Annu. Rev. Genet. 40, 77–7105.

Ishida, T., Fujiwara, S., Miura, K., Stacey, N., Yoshimura, M., Schneider, K., et al., 2009. SUMO E3 ligase HIGH PLOIDY2 regulates endocycle onset and meristem maintenance in Arabidopsis. Plant Cell 21, 2284–2297.

Ishida, T., Adachi, S., Yoshimura, M., Shimizu, K., Umeda, M., Sugimoto, K., 2010. Auxin modulates the transition from the mitotic cycle to the endocycle in Arabidopsis. Development 137, 63–71.

Ito, M., 2000. Factors controlling cyclin B expression. Plant Mol. Biol. 43, 677–690.

Ito, M., Iwase, M., Kodama, H., Lavisse, P., Komamine, A., Nishihama, R., et al., 1998. A novel *cis*-acting element in promoters of plant B-type cyclin genes activates M phase-specific transcription. Plant Cell 10, 331–341.

Ito, M., Araki, S., Matsunaga, S., Itoh, T., Nishihama, R., Machida, Y., et al., 2001. G2/M-phase-specific transcription during the plant cell cycle is mediated by c-Myb-like transcription factors. Plant Cell 13, 1891–1905.

Itoh, H., Ueguchi-Tanaka, M., Matsuoka, M., 2008. Molecular biology of gibberellins signaling in higher plants. Int. Rev. Cell Mol. Biol. 268, 191–221.

Iwakawa, H., Shinmyo, A., Sekine, M., 2006. Arabidopsis CDKA;1, a cdc2 homologue, controls proliferation of generative cells in male gametogenesis. Plant J. 45, 819–831.

Jakoby, M.J., Weinl, C., Pusch, S., Kuijt, S.J., Merkle, T., Dissmeyer, N., et al., 2006. Analysis of the subcellular localization, function, and proteolytic control of the Arabidopsis cyclin-dependent kinase inhibitor ICK1/KRP1. Plant Physiol. 141, 1293–1305.

Joubès, J., Phan, T.H., Just, D., Rothan, C., Bergounioux, C., Raymond, P., et al., 1999. Molecular and biochemical characterization of the involvement of cyclin-dependent kinase A during the early development of tomato fruit. Plant Physiol. 121, 857–869.

Joubès, J., Chevalier, C., Dudits, D., Heberle-Bors, E., Inze, D., Umeda, M., et al., 2000. CDK-related protein kinases in plants. Plant Mol. Biol. 43, 607–620.

Kamura, T., Hara, T., Matsumoto, M., Ishida, N., Okumura, F., Hatakeyama, S., et al., 2004. Cytoplasmic ubiquitin ligase KPC regulates proteolysis of p27(Kip1) at G1 phase. Nat. Cell Biol. 6, 1229–1235.

Kasili, R., Walker, J.D., Simmons, L.A., Zhou, J., De Veylder, L., Larkin, J.C., 2010. SIAMESE cooperates with the CDH1-like protein CCS52A1 to establish endoreplication in *Arabidopsis thaliana* trichomes. Genetics 185, 257–268.

Kato, K., Gális, I., Suzuki, S., Araki, S., Demura, T., Criqui, M.C., et al., 2009. Preferential up-regulation of G2/M phase-specific genes by overexpression of the hyperactive form of NtmybA2 lacking its negative regulation domain in tobacco BY-2 cells. Plant Physiol. 149, 1945–1957.

Kim, H.J., Oh, S.A., Brownfield, L., Hong, S.H., Ryu, H., Hwang, I., et al., 2008. Control of plant germline proliferation by SCF(FBL17) degradation of cell cycle inhibitors. Nature 455, 1134–1137.

Kirik, V., Schrader, A., Uhrig, J.F., Hulskamp, M., 2007. MIDGET unravels functions of the Arabidopsis topoisomerase VI complex in DNA endoreduplication, chromatin condensation, and transcriptional silencing. Plant Cell 19, 3100–3110.

Kono, A., Umeda-Hara, C., Adachi, S., Nagata, N., Konomi, M., Nakagawa, T., et al., 2007. The Arabidopsis D-type cyclin CYCD4 controls cell division in the stomatal lineage of the hypocotyl epidermis. Plant Cell 19, 1265–1277.

Koroleva, O.A., Tomlinson, M., Parinyapong, P., Sakvarelidze, L., Leader, D., Shaw, P., et al., 2004. CycD1, a putative G1 cyclin from *Antirrhinum majus*, accelerates the cell cycle in cultured tobacco BY-2 cells by enhancing both G1/S entry and progression through S and G2 phases. Plant Cell 16, 2364–2379.

Kosugi, S., Ohashi, Y., 2002. E2Ls, E2F-like repressors of Arabidopsis that bind to E2F sites in a monomeric form. J. Biol. Chem. 277, 16553–16558.

Kowles, R.V., Phillips, R.L., 1985. DNA amplification patterns in maize endosperm nuclei during kernel development. Proc. Natl. Acad. Sci. USA 82, 7010–7014.

Kwee, H.S., Sundaresan, V., 2003. The NOMEGA gene required for female gametophyte development encodes the putative APC6/CDC16 component of the anaphase promoting complex in Arabidopsis. Plant J. 36, 853–866.

Lammens, T., Boudolf, V., Kheibarshekan, L., Zalmas, L.P., Gaamouche, T., Maes, S., et al., 2008. Atypical E2F activity restrains APC/CCCS52A2 function obligatory for endocycle onset. Proc. Natl. Acad. Sci. USA 105, 14721–14726.

Lammens, T., Li, J., Leone, G., De Veylder, L., 2009. Atypical E2Fs: new players in the E2F transcription factor family. Trends Cell Biol. 19, 111–118.

Larson-Rabin, Z., Li, Z., Masson, P.H., Day, C.D., 2009. FZR2/CCS52A1 expression is a determinant of endoreduplication and cell expansion in Arabidopsis. Plant Physiol. 149, 874–884.

Lee, J., Das, A., Yamaguchi, M., Hashimoto, J., Tsutsumi, N., Uchimiya, H., et al., 2003. Cell cycle function of a rice B2-type cyclin interacting with a B-type cyclin-dependent kinase. Plant J. 34, 417–425.

Li, C., Potuschak, T., Colon-Carmona, A., Gutierrez, R.A., Doerner, P., 2005. Arabidopsis TCP20 links regulation of growth and cell division control pathways. Proc. Natl. Acad. Sci. USA 102, 12978–12983.

Lin, Z., Yin, K., Zhu, D., Chen, Z., Gu, H., Qu, L.J., 2007. AtCDC5 regulates the G2 to M transition of the cell cycle and is critical for the function of Arabidopsis shoot apical meristem. Cell Res. 17, 815–828.

Liu, J., Zhang, Y., Qin, G., Tsuge, T., Sakaguchi, N., Luo, G., et al., 2008. Targeted degradation of the cyclin-dependent kinase inhibitor ICK4/KRP6 by RING-type E3 ligases is essential for mitotic cell cycle progression during Arabidopsis gametogenesis. Plant Cell 20, 1538–1554.

Lui, H., Wang, H., Delong, C., Fowke, L.C., Crosby, W.L., Fobert, P.R., 2000. The Arabidopsis Cdc2a-interacting protein ICK2 is structurally related to ICK1 and is a potent inhibitor of cyclin-dependent kinase activity in vitro. Plant J. 21, 379–385.

Magyar, Z., De Veylder, L., Atanassova, A., Bakó, L., Inzé, D., Bögre, L., 2005. The role of the Arabidopsis E2FB transcription factor in regulating auxin-dependent cell division. Plant Cell 17, 2527–2541.

Mariconti, L., Pellegrini, B., Cantoni, R., Stevens, R., Bergounioux, C., Cella, R., et al., 2002. The E2F family of transcription factors from *Arabidopsis thaliana*. Novel and conserved components of the retinoblastoma/E2F pathway in plants. J. Biol. Chem. 277, 9911–9919.

Marrocco, K., Thomann, A., Parmentier, Y., Genschik, P., Criqui, M.C., 2009. The APC/C E3 ligase remains active in most post-mitotic Arabidopsis cells and is required for proper vasculature development and organization. Development 136, 1475–1485.

Marrocco, K., Bergdoll, M., Achard, P., Criqui, M.C., Genschik, P., 2010. Selective proteolysis sets the tempo of the cell cycle. Curr. Opin. Plant Biol. 13, 631–639.

Masubelele, N.H., Dewitte, W., Menges, M., Maughan, S., Collins, C., Huntley, R., et al., 2005. D-type cyclins activate division in the root apex to promote seed germination in Arabidopsis. Proc. Natl. Acad. Sci. USA 102, 15694–15699.

Mathieu-Rivet, E., Gévaudant, F., Sicard, A., Salar, S., Do, P.T., Mouras, A., et al., 2010. Functional analysis of the anaphase promoting complex activator CCS52A highlights the crucial role of endo-reduplication for fruit growth in tomato. Plant J. Cell Mol. Biol. 62, 727–741.

Matsuzaki, Y., Ogawa-Ohnishi, M., Mori, A., Matsubayashi, Y., 2010. Secreted peptide signals required for maintenance of root stem cell niche in Arabidopsis. Science 329, 1065–1067.

Menges, M., Hennig, L., Gruissem, W., Murray, J.A., 2002. Cell cycle-regulated gene expression in Arabidopsis. J. Biol. Chem. 277, 41987–42002.

Menges, M., Hennig, L., Gruissem, W., Murray, J.A., 2003. Genome-wide gene expression in an Arabidopsis cell suspension. Plant Mol. Biol. 53, 423–442.

Menges, M., de Jager, S.M., Gruissem, W., Murray, J.A., 2005. Global analysis of the core cell cycle regulators of Arabidopsis identifies novel genes, reveals multiple and highly specific profiles of expression and provides a coherent model for plant cell cycle control. Plant J. 41, 546–566.

Menges, M., Samland, A.K., Planchais, S., Murray, J.A., 2006. The D-type cyclin CYCD3;1 is limiting for the G1-to-S-phase transition in Arabidopsis. Plant Cell 18, 893–906.

Miyawaki, K., Tarkowski, P., Matsumoto-Kitano, M., Kato, T., Sato, S., Tarkowska, D., et al., 2006. Roles of Arabidopsis ATP/ADP isopentenyltransferases and tRNA isopentenyltransferases in cytokinin biosynthesis. Proc. Natl. Acad. Sci. USA 103, 16598–16603.

Mizukami, Y., Fischer, R.L., 2000. Plant organ size control: AINTEGUMENTA regulates growth and cell numbers during organogenesis. Proc. Natl. Acad. Sci. USA 97, 942–947.

Morgan, D.O., 1997. Cyclin-dependent kinases: engines, clocks, and microprocessors. Annu. Rev. Cell Dev. Biol. 13, 261–291.

Moubayidin, L., Perilli, S., Dello Ioio, R., Di Mambro, R., Costantino, P., Sabatini, S., 2010. The rate of cell differentiation controls the Arabidopsis root meristem growth phase. Curr. Biol. 20, 1138–1143.

Nakagami, H., Sekine, M., Murakami, H., Shinmyo, A., 1999. Tobacco retinoblastoma-related protein phosphorylated by a distinct cyclin-dependent kinase complex with Cdc2/cyclin D in vitro. Plant J. 18, 243–252.

Nakagami, H., Kawamura, K., Sugisaka, K., Sekine, M., Shinmyo, A., 2002. Phosphorylation of retinoblastoma-related protein by the cyclin D/cyclin-dependent kinase complex is activated at the G1/S-phase transition in tobacco. Plant Cell 14, 1847–1857.

Nakayama, K., Nakayama, K., 1998. Cip/Kip cyclin-dependent kinase inhibitors: brakes of the cell cycle engine during development. Bioessays 20, 1020–1029.

Nieuwland, J., Maughan, S., Dewitte, W., Scofield, S., Sanz, L., Murray, J.A., 2009. The D-type cyclin CYCD4;1 modulates lateral root density in Arabidopsis by affecting the basal meristem region. Proc. Natl. Acad. Sci. USA 106, 22528–22533.

Nigg, E.A., 1996. Cyclin-dependent kinase 7: at the cross-roads of transcription, DNA repair and cell cycle control? Curr. Opin. Cell Biol. 8, 312–317.

Nowack, M.K., Grini, P.E., Jakoby, M.J., Lafos, M., Koncz, C., Schnittger, A., 2006. A positive signal from the fertilization of the egg cell sets off endosperm proliferation in angiosperm embryogenesis. Nat. Genet. 38, 63–67.

Ohi, R., Feoktistova, A., McCann, S., Valentine, V., Look, A.T., Lipsick, J.S., et al., 1998. Myb-related Schizosaccharomyces pombe cdc5p is structurally and functionally conserved in eukaryotes. Mol. Cell. Biol. 18, 4097–4108.

Peres, A., Churchman, M.L., Hariharan, S., Himanen, K., Verkest, A., Vandepoele, K., et al., 2007. Novel plant-specific cyclin-dependent kinase inhibitors induced by biotic and abiotic stresses. J. Biol. Chem. 282, 25588–25596.

Pérez-Pérez, J.M., Serralbo, O., Vanstraelen, M., González, C., Criqui, M.C., Genschik, P., et al., 2008. Specialization of CDC27 function in the *Arabidopsis thaliana* anaphase-promoting complex (APC/C). Plant J. 53, 78–89.

Pesin, J.A., Orr-Weaver, T.L., 2008. Regulation of APC/C activators in mitosis and meiosis. Annu. Rev. Cell Dev. Biol. 24, 475–499.

Pickart, C.M., 2001. Mechanisms underlying ubiquitination. Annu. Rev. Biochem. 70, 503–533.

Planchais, S., Samland, A.K., Murray, J.A., 2004. Differential stability of Arabidopsis D-type cyclins: CYCD3;1 is a highly unstable protein degraded by a proteasome-dependent mechanism. Plant J. 38, 616–625.

Porceddu, A., Stals, H., Reichheld, J.P., Segers, G., De Veylder, L., Barroco, R.P., et al., 2001. A plant-specific cyclin-dependent kinase is involved in the control of G2/M progression in plants. J. Biol. Chem. 276, 36354–36360.

Ramirez-Parra, E., Frundt, C., Gutierrez, C., 2003. A genome-wide identification of E2F-regulated genes in Arabidopsis. Plant J. 33, 801–811.

Ramirez-Parra, E., Lopez-Matas, M.A., Frundt, C., Gutierrez, C., 2004. Role of an atypical E2F transcription factor in the control of Arabidopsis cell growth and differentiation. Plant Cell 16, 2350–2363.

Ren, H., Santner, A., del Pozo, J.C., Murray, J.A., Estelle, M., 2008. Degradation of the cyclin-dependent kinase inhibitor KRP1 is regulated by two different ubiquitin E3 ligases. Plant J. 53, 705–716.

Ricaud, L., Proux, C., Renou, J.P., Pichon, O., Fochesato, S., Ortet, P., et al., 2007. ATM-mediated transcriptional and developmental responses to gamma-rays in Arabidopsis. PLoS One 2, e430.

Riou-Khamlichi, C., Huntley, R., Jacqmard, A., Murray, J.A., 1999. Cytokinin activation of Arabidopsis cell division through a D-type cyclin. Science 283, 1541–1544.
Roeder, A.H., Chickarmane, V., Cunha, A., Obara, B., Manjunath, B.S., Meyerowitz, E. M., 2010. Variability in the control of cell division underlies sepal epidermal patterning in *Arabidopsis thaliana*. PLoS Biol. 8, e1000367.
Rossignol, P., Stevens, R., Perennes, C., Jasinski, S., Cella, R., Tremousaygue, D., et al., 2002. AtE2F-a and AtDP-a, members of the E2F family of transcription factors, induce Arabidopsis leaf cells to re-enter S phase. Mol. Genet. Genomics 266, 995–1003.
Rozan, L.M., El-Deiry, W.S., 2007. p53 downstream target genes and tumor suppression: a classical view in evolution. Cell Death Differ. 14, 3–9.
Ruzicka, K., Simásková, M., Duclercq, J., Petrásek, J., Zazímalová, E., Simon, S., et al., 2009. Cytokinin regulates root meristem activity via modulation of the polar auxin transport. Proc. Natl. Acad. Sci. USA 106, 4284–4289.
Sanz, L., Dewitte, W., Forzani, C., Patell, F., Nieuwland, J., Wen, B., et al., 2011. The Arabidopsis D-type cyclin CYCD2;1 and the inhibitor ICK2/KRP2 modulate auxin-induced lateral root formation. Plant Cell 23, 641–660.
Schnittger, A., Schobinger, U., Stierhof, Y.D., Hulskamp, M., 2002. Ectopic B-type cyclin expression induces mitotic cycles in endoreduplicating Arabidopsis trichomes. Curr. Biol. 12, 415–420.
Schwob, E., Böhm, T., Mendenhall, M.D., Nasmyth, K., 1994. The B-type cyclin kinase inhibitor p40SIC1 controls the G1 to S transition in *S. cerevisiae*. Cell 79, 233–244.
Segers, G., Gadisseur, I., Bergounioux, C., de Almeida Engler, J., Jacqmard, A., Van Montagu, M., et al., 1996. The Arabidopsis cyclin-dependent kinase gene cdc2bAt is preferentially expressed during S and G2 phases of the cell cycle. Plant J. 10, 601–612.
Serizawa, H., Mäkelä, T.P., Conaway, J.W., Conaway, R.C., Weinberg, R.A., Young, R.A., 1995. Association of Cdk-activating kinase subunits with transcription factor TFIIH. Nature 374, 280–282.
Shen, W.H., 2002. The plant E2F-Rb pathway and epigenetic control. Trends Plant Sci. 7, 505–511.
Shiekhattar, R., Mermelstein, F., Fisher, R.P., Drapkin, R., Dynlacht, B., Wessling, H.C., et al., 1995. Cdk-activating kinase complex is a component of human transcription factor TFIIH. Nature 374, 283–287.
Shimotohno, A., Matsubayashi, S., Yamaguchi, M., Uchimiya, H., Umeda, M., 2003. Differential phosphorylation activities of CDK-activating kinases in *Arabidopsis thaliana*. FEBS Lett. 534, 69–74.
Shimotohno, A., Umeda-Hara, C., Bisova, K., Uchimiya, H., Umeda, M., 2004. The plant-specific kinase CDKF;1 is involved in activating phosphorylation of cyclin-dependent kinase-activating kinases in Arabidopsis. Plant Cell 16, 2954–2966.
Shimotohno, A., Ohno, R., Bisova, K., Sakaguchi, N., Huang, J., Koncz, C., et al., 2006. Diverse phosphoregulatory mechanisms controlling cyclin-dependent kinase-activating kinases in Arabidopsis. Plant J. 47, 701–710.
Sieberer, T., Hauser, M.T., Seifert, G.J., Luschnig, C., 2003. PROPORZ1, a putative Arabidopsis transcriptional adaptor protein, mediates auxin and cytokinin signals in the control of cell proliferation. Curr. Biol. 13, 837–842.
Skoog, F., Miller, C.O., 1957. Chemical regulation of growth and organ formation in plant tissues cultured in vitro. Symp. Soc. Exp. Biol. 11, 118–130.
Soni, R., Carmichael, J.P., Shah, Z.H., Murray, J.A., 1995. A family of cyclin D homologs from plants differentially controlled by growth regulators and containing the conserved retinoblastoma protein interaction motif. Plant Cell 7, 85–103.
Sorrell, D.A., Combettes, B., Chaubet-Gigot, N., Gigot, C., Murray, J.A., 1999. Distinct cyclin D genes show mitotic accumulation or constant levels of transcripts in tobacco bright yellow-2 cells. Plant Physiol. 119, 343–352.

Sozzani, R., Maggio, C., Varotto, S., Canova, S., Bergounioux, C., Albani, D., et al., 2006. Interplay between Arabidopsis activating factors E2Fb and E2Fa in cell cycle progression and development. Plant Physiol. 140, 1355–1366.

Sozzani, R., Cui, H., Moreno-Risueno, M.A., Busch, W., Van Norman, J.M., Vernoux, T., et al., 2010a. Spatiotemporal regulation of cell-cycle genes by SHORTROOT links patterning and growth. Nature 466, 128–132.

Sozzani, R., Maggio, C., Giordo, R., Umana, E., Ascencio-Ibañez, J.T., Hanley-Bowdoin, L., et al., 2010b. The E2FD/DEL2 factor is a component of a regulatory network controlling cell proliferation and development in Arabidopsis. Plant Mol. Biol. 72, 381–395.

Sugimoto-Shirasu, K., Roberts, K., 2003. "Big it up": endoreduplication and cell-size control in plants. Curr. Opin. Plant Biol. 6, 544–553.

Sun, Y., Dilkes, B.P., Zhang, C., Dante, R.A., Carneiro, N.P., Lowe, K.S., et al., 1999. Characterization of maize (*Zea mays* L.) Wee1 and its activity in developing endosperm. Proc. Natl. Acad. Sci. USA 96, 4180–4185.

Suzuki, T., Nakajima, S., Inagaki, S., Hirano-Nakakita, M., Matsuoka, K., Demura, T., et al., 2005. *TONSOKU* is expressed in S phase of the cell cycle and its defect delays cell cycle progression in *Arabidopsis*. Plant Cell Physiol. 46, 736–742.

Takahashi, N., Lammens, T., Boudolf, V., Maes, S., Yoshizumi, T., De Jaeger, G., et al., 2008. The DNA replication checkpoint aids survival of plants deficient in the novel replisome factor ETG1. EMBO J. 27, 1840–1851.

Takahashi, I., Kojima, S., Sakaguchi, N., Umeda-Hara, C., Umeda, M., 2010a. Two Arabidopsis cyclin A3s possess G1 cyclin-like features. Plant Cell Rep. 29, 307–315.

Takahashi, N., Quimbaya, M., Schubert, V., Lammens, T., Vandepoele, K., Schubert, I., et al., 2010b. The MCM-binding protein ETG1 aids sister chromatid cohesion required for postreplicative homologous recombination repair. PLoS Genet. 6, e1000817.

Takatsuka, H., Ohno, R., Umeda, M., 2009. The Arabidopsis cyclin-dependent kinase-activating kinase CDKF;1 is a major regulator of cell proliferation and cell expansion but is dispensable for CDKA activation. Plant J. 59, 475–487.

Ubeda-Tomás, S., Federici, F., Casimiro, I., Beemster, G.T., Bhalerao, R., Swarup, R., et al., 2009. Gibberellin signaling in the endodermis controls Arabidopsis root meristem size. Curr. Biol. 19, 1194–1199.

Umeda, M., Bhalerao, R.P., Schell, J., Uchimiya, H., Koncz, C., 1998. A distinct cyclin-dependent kinase-activating kinase of *Arabidopsis thaliana*. Proc. Natl. Acad. Sci. USA 95, 5021–5026.

Umeda, M., Umeda-Hara, C., Yamaguchi, M., Hashimoto, J., Uchimiya, H., 1999. Differential expression of genes for cyclin-dependent protein kinases in rice plants. Plant Physiol. 119, 31–40.

Umeda, M., Shimotohno, A., Yamaguchi, M., 2005. Control of cell division and transcription by cyclin-dependent kinase-activating kinases in plants. Plant Cell Physiol. 46, 1437–1442.

van den Heuvel, S., Dyson, N.J., 2008. Conserved functions of the pRB and E2F families. Nat. Rev. Mol. Cell Biol. 9, 713–724.

Van Leene, J., Hollunder, J., Eeckhout, D., Persiau, G., Van De Slijke, E., Stals, H., et al., 2010. Targeted interactomics reveals a complex core cell cycle machinery in *Arabidopsis thaliana*. Mol. Syst. Biol. 6, 397.

Vandepoele, K., Raes, J., De Veylder, L., Rouzé, P., Rombauts, S., Inzé, D., 2002. Genome-wide analysis of core cell cycle genes in Arabidopsis. Plant Cell 14, 903–916.

Vandepoele, K., Vlieghe, K., Florquin, K., Hennig, L., Beemster, G.T., Gruissem, W., et al., 2005. Genome-wide identification of potential plant E2F target genes. Plant Physiol. 139, 316–328.

Vanstraelen, M., Baloban, M., Da Ines, O., Cultrone, A., Lammens, T., Boudolf, V., et al., 2009. APC/CCCS52A complexes control meristem maintenance in the Arabidopsis root. Proc. Natl. Acad. Sci. USA 106, 11806–11811.

Verkest, A., Manes, C.L., Vercruysse, S., Maes, S., Van Der Schueren, E., Beeckman, T., et al., 2005. The cyclin-dependent kinase inhibitor KRP2 controls the onset of the endoreduplication cycle during Arabidopsis leaf development through inhibition of mitotic CDKA;1 kinase complexes. Plant Cell 17, 1723–1736.

Vlieghe, K., Boudolf, V., Beemster, G.T., Maes, S., Magyar, Z., Atanassova, A., et al., 2005. The DP-E2F-like gene DEL1 controls the endocycle in *Arabidopsis thaliana*. Curr. Biol. 15, 59–63.

Vodermaier, H.C., 2004. APC/C and SCF: controlling each other and the cell cycle. Curr. Biol. 14, R787–R796.

Walker, J.D., Oppenheimer, D.G., Concienne, J., Larkin, J.C., 2000. SIAMESE, a gene controlling the endoreduplication cell cycle in *Arabidopsis thaliana* trichomes. Development 127, 3931–3940.

Wang, H., Fowke, L.C., Crosby, W.L., 1997. A plant cyclin-dependent kinase inhibitor gene. Nature 386, 451–452.

Wang, H., Qi, Q., Schorr, P., Cutler, A.J., Crosby, W.L., Fowke, L.C., 1998. ICK1, a cyclin-dependent protein kinase inhibitor from *Arabidopsis thaliana* interacts with both Cdc2a and CycD3, and its expression is induced by abscisic acid. Plant J. 15, 501–510.

Wang, H., Zhou, Y., Gilmer, S., Whitwill, S., Fowke, L.C., 2000. Expression of the plant cyclin-dependent kinase inhibitor ICK1 affects cell division, plant growth and morphology. Plant J. 24, 613–623.

Wang, G., Kong, H., Sun, Y., Zhang, X., Zhang, W., Altman, N., et al., 2004a. Genome-wide analysis of the cyclin family in Arabidopsis and comparative phylogenetic analysis of plant cyclin-like proteins. Plant Physiol. 135, 1084–1099.

Wang, Y., Magnard, J.L., McCormick, S., Yang, M., 2004b. Progression through meiosis I and meiosis II in Arabidopsis anthers is regulated by an A-type cyclin predominately expressed in prophase I. Plant Physiol. 136, 4127–4135.

Weingartner, M., Criqui, M.C., Meszaros, T., Binarova, P., Schmit, A.C., Helfer, A., et al., 2004. Expression of a nondegradable cyclin B1 affects plant development and leads to endomitosis by inhibiting the formation of a phragmoplast. Plant Cell 16, 643–657.

Werner, T., Motyka, V., Laucou, V., Smets, R., Van Onckelen, H., Schmülling, T., 2003. Cytokinin-deficient transgenic Arabidopsis plants show multiple developmental alterations indicating opposite functions of cytokinins in the regulation of shoot and root meristem activity. Plant Cell 15, 2532–2550.

Wildwater, M., Campilho, A., Perez-Perez, J.M., Heidstra, R., Blilou, I., Korthout, H., et al., 2005. The RETINOBLASTOMA-RELATED gene regulates stem cell maintenance in Arabidopsis roots. Cell 123, 1337–1349.

Wolters, H., Jürgens, G., 2009. Survival of the flexible: hormonal growth control and adaptation in plant development. Nat. Rev. Genet. 10, 305–317.

Wuarin, J., Buck, V., Nurse, P., Millar, J.B., 2002. Stable association of mitotic cyclin B/Cdc2 to replication origins prevents endoreduplication. Cell 111, 419–431.

Xie, Z., Lee, E., Lucas, J.R., Morohashi, K., Li, D., Murray, J.A., et al., 2010. Regulation of cell proliferation in the stomatal lineage by the Arabidopsis MYB FOUR LIPS via direct targeting of core cell cycle genes. Plant Cell 22, 2306–2321.

Yoshiyama, K., Conklin, P.A., Huefner, N.D., Britt, A.B., 2009. Suppressor of gamma response 1 (SOG1) encodes a putative transcription factor governing multiple responses to DNA damage. Proc. Natl. Acad. Sci. USA 106, 12843–12848.

Zhou, Y., Wang, H., Gilmer, S., Whitwill, S., Fowke, L.C., 2003. Effects of co-expressing the plant CDK inhibitor ICK1 and D-type cyclin genes on plant growth, cell size and ploidy in *Arabidopsis thaliana*. Planta 216, 604–613.

Zielke, N., Querings, S., Rottig, C., Lehner, C., Sprenger, F., 2008. The anaphase-promoting complex/cyclosome (APC/C) is required for rereplication control in endoreplication cycles. Genes Dev. 22, 1690–1703.

Index

P